AD NUMBER

ADB955509

NEW LIMITATION CHANGE

TO

Approved for public release, distribution unlimited

FROM

Distribution limited to DoD only; Critical Technology; 26 Mar 84. Other requests must be referred to Naval Research Lab., Code 1221. Washington, DC 20375.

AUTHORITY

Naval Research Laboratory, Technical Library, Research Reports Section Notice, dtd October 20, 2000.

NRL REPORT R-3171

UPPER ATMOSPHERE RESEARCH REPORT NO. IV

★

NAVAL RESEARCH LABORATORY
COMMODORE H. A. SCHADE, USN, DIRECTOR
WASHINGTON, D.C.

NRL REPORT R-3171

UPPER ATMOSPHERE RESEARCH REPORT NO. IV

Compiled and Edited

by

H. E. Newell, Jr. and J. W. Siry

Problem Numbers

34N26-02, 34P26-04,
34R25-01, 34R25-02,
34R10-20, 34R10-21.

Approved by:

J. M. Miller, Superintendent, Radio Division I

October 1, 1947

NAVAL RESEARCH LABORATORY

COMMODORE H. A. SCHADE, USN, DIRECTOR

WASHINGTON, D.C.

DISTRIBUTION

	Copy No.
GMC Committee, RDB, Wash., D. C.	A (1)
Ch. of Staff, USAF, Attn: DCS/M, MRD-4, Pentagon	" (2-5)
CG, AMC, Wright Field, Dayton, Ohio, Attn: TSEON-2	" (6-30)
CG, Air Univ., Maxwell Field, Ala., Attn: Air Univ. Library	" (31)
BuAer, Wash., D. C., Attn: TD-4	" (32-37)
BuOrd, Wash., D. C., Attn: Re-9	" (38-41)
BuShips, Wash., D. C., Attn: Codes 633, 910A, and 343	" (42-44)
Ch/GMBranch, Technical Command, Army Chem. Center, Md.	" (45)
CG, APG, Md., Attn: Ballistic Res. Lab.	" (46)
CG, Eglin Field, Fla., Attn: First Exp., GM Group	" (47)
CG, AAS, Fort Bliss, Texas	" (48)
CO, Frankford Arsenal, Phila., Attn: Fire Control Design Div.	" (49)
Commander, NAMC, Phila.	" (50)
CO, NADS, Johnsville, Pa.	" (51)
CO, ONR, San Francisco	" (52)
CO, SCEL, Bradley Beach, N. J.	" (54-55)
CO, NAMTC, Pt. Mugu, Calif.	" (56)
CO, NOTS, Inyokern, Calif.	" (57)
CO, Alamorgodo Army Air Base, N. M.	" (58)
Dir., DTMB, Wash., 7, D. C., Attn: Aero. Mechanics Div.	" (59)
Dir., NACA, Wash., D. C., Attn: Mr. C. H. Helms	" (60-63)
Dir., NRL, Wash., 20, D. C.	" (64-66)
Dir., Spec. Devices Center, ONR, Sands Point, L. I., Attn: TID	" (67)
First Antiaircraft Artillery, GM Btn., White Sands Proving Ground	" (68)
Head, PG School, U. S. Naval Academy, Annapolis	" (69)
RDB, Attn: Library	" (72)
Dept of the Army, Office of the Ch. of Ord., Attn: ORDTU, Pentagon	" (73)
OinC, BOEU, Hydraulics Bldg., Nat'l BuStds., Wash., D. C.	" (74)
OinC, NOL, NavGun, Wash., D. C., Attn: Dr. R. J. Seeger	" (75-76)
OinC, Ord. Res. and Dev. Div. Suboffice (Rocket) Ft. Bliss, Texas	" (77)
CNO, Op-57	" (78)
Watson Labs., AMC, Eatontown, N. J.	" (79)
Watson Labs., AMC, Cambridge Field Station, Mass., Attn: Dr. M. O'Day	" (80)
CG, Army Ground Forces, Ft. Monroe, Va., Attn: Ch/Dev. Sect. GNDEV-9	" (81)
ONR, c/o Lib. of Congress, Tech. Info. Sect., Attn: J. Heald	" (82-84)
Ch/Res. and Eng. Div., Off. Ch. Chem. Corps, Army Chem. Center, Md.	" (85)
CO, NAOTS, Chincoteague, Va.	" (86)
AEC, Div. Mil. Applic., Wash., 25, D. C., Attn: Col. D. J. Keirn	B (1)
BAGR,-ED, NY Nav. Shipyard, Bldg. No. 3, Brooklyn 1, N. Y.	" (2)
BAGR,-CD, Wright Field, Dayton, Ohio, Attn: Lt. Col. J. A. Gerath	" (3)
BAGR,-WD, Los Angeles	" (4)
BuOrd, Wash., 25, D. C., Attn: Re-9	" (5-8)
CNO, Wash., 25, D. C., Attn: Op-34H, Op34H8, and Op-413	" (9-11)
Ch. of Staff, USAF, Attn: DCS/M, MRD; Pentagon	" (13)
CG, APG, Md., Attn: Lib. Sect.	" (15)
CG, AU, Maxwell Field, Attn: Lib. of AAFSSS, Craig Field, Ala.	" (16)
CG, AU, Maxwell Field, Attn: Lib. for AAFTS, Tyndall Field, Fla.	" (17)

		Copy No.
Comdt., Command and Staff College, Ft. Leavenworth, Kansas	"	(18)
Comdt., Mar. Corps., Wash., D. C.,Attn: G-3 (Special Weapons)	"	(19)
Comdt., Armed Forces Staff College, Norfolk 11, Va.	"	(20)
COM NATC, Patuxent River, Md., Attn: Dir. of Tests	"	(21)
CO, NAES, Phila., Attn: Supt. AEL	"	(22)
CO, Watertown Arsenal, Mass., Attn: Laboratory	"	(24)
ComOpDevFor, c/o Fleet Post Office, N. Y., N. Y.	"	(25-26)
Dir. Res. and Dev., War Dept. Gen Staff, Pentagon	"	(27)
Dir., Seacoast Service Test Sect. AFG Board No. 1, Ft. Baker, Calif.	"	(28)
Hd. Ord. and Gunnery, USNA, Annapolis	"	(29)
OCO, Ord. Res. and Dev. Serv., Ammunition Branch, Pentagon	"	(30)
OCSigO, Engr. and Tec. Serv., Engr. Div., Pentagon	"	(31)
Off. Sec. of War, Pentagon	"	(32)
Ord. Adv. Comm. on GM, General Radio Co., Cambridge 39, Attn: Dr. H. B. Richmond	"	(34)
Pres. Army Ground Forces Board No. 1, Ft. Bragg, N. C.	"	(35)
Pres. Army Ground Forces Board No. 4, Ft. Bliss, Texas	"	(36)
Prof. of Ord., U. S. Military Academy, West Point, N. Y.	"	(37)
Sec. Special Board, Comdt. of Marine Corps, Marine Corps School, Quantico	"	(38)
National War College, Wash., D. C.,Attn: Library	"	(39)
DCO for APL, JHU, Silver Spring, Md.	C	(1-3)
BAR, Buffalo, for BAC, Niagara Falls, Attn: Mr. R. H. Stanley and Mr. Hamlin	"	(4)
BTL, Whippany, N. J., Attn: Mr. W. C. Tinus	"	(5)
DCO for Bendix Av. Corp., Detroit, Mich., Attn: Dr. Harner Selvidge	"	(6)
Boeing Aircraft Corp., Seattle, Attn: Mr. R. H. Nelson	"	(7)
DCO for C-V Air. Corp., LSL, Daingerfield, Texas, Attn: Mr. Arnold	"	(8)
BAR, Consolidated-Vultee Air. Corp., San Diego, Attn: Mr. Ables	"	(9)
DCO for Cornell Aero. Lab., Buffalo, N. Y., Attn: Mr. W. M. Duke	"	(10)
BAR for Curtiss-Wright Corp., Columbus, Attn: Mr. B. Eaton	"	(11)
BAR for Douglas Aircraft Co., El Segundo, Calif., Attn: Mr. Heinemann	"	(12)
Douglas Air. Co., Santa Monica, Attn: Mr. A. E. Raymond, (Project Rand) and Mr. E. F. Burton	"	(13-14)
INSORD for Eastman Kodak Co., Rochester, N. Y., Attn: Dr. Trotter	"	(15)
Fairchild Eng. and Air. Corp., NEPA Div., Oak Ridge, Attn: Mr. Kalitinsky	"	(16)
RIC-BuAer for Fairchild Eng. and Air. Corp., Farmingdale, Attn: J. A. Slonin	"	(17)
CO, NADS for Franklin Inst. Labs., Phila., Attn: Mr. R. H. McClarren	"	(18)
ARLO for Gen. Elec. Co., Schenectady, N. Y., Project HERMES, Attn: Mr. C. K. Bauer	"	(19)
INSORD for DCO, G. E. Co., Schenectady, N. Y.	"	(20)
G. E. Co., Av. Div., Schenectady, Attn: Mr. S. A. Schuler, and Mr. P. Class	"	(21)
BAR for Glenn L. Martin Co., Balt., Attn: Mr. N. M. Voorhies	"	(22)
Glenn L. Martin, Balt., Attn: Mr. W. B. Bergen	"	(23)
INSMAT, Chicago for Globe Corp., Joliet, Ill., Attn: Mr. J. A. Weagle	"	(24)
BAR for Goodyear Aircraft Corp., Akron, Attn: Dr. Carl Arnstein	"	(25)
Goodyear Aircraft, Plant B, Akron, Attn: Mr. A. J. Peterson	"	(26)
BAR for Grumman Air. Engr. Corp., Bethpage, L. I., Attn: Mr. Schwendler	"	(27)
Hughes Aircraft Co., Culver City, Calif., Attn: Mr. D. H. Evans	"	(28)
OinC, Res. and Dev. Serv. Suboffice (Rocket) CIT, Pasadena	"	(29-30)
INSMAT for Kellex Corp., New York, N. Y.	"	(31)
DCO for M. W. Kellogg Co., Jersey City, N. J., Attn: Dr. G. H. Messerly	"	(32)
NORTLO for Chairman, MIT, GMC, Project Meteor Office, Cambridge, Attn: Guided Missiles Library	"	(33-34)

Distribution (Cont.)

		Copy No.
BAR for McDonnell Aircraft Corp., St. Louis, Attn: W. P. Montgomery	"	(35)
BAR for NAA, Inc., Los Angeles, Attn: Mr. D. H. Mason	"	(36)
Northrop Aircraft Inc., Hawthorne, Calif.	"	(37)
DCO for Princeton University, Attn: Mr. Harry Ashworth, Sr.	"	(38)
CO, ONR Branch Office, N. Y. for Princeton U., Attn: Proj. SQUID	"	(39-41)
INSMAT for Radio Corp. of America, Camden, N. J., Attn: Mr. T. T. Eaton	"	(42)
BAR for Radioplane Corp, Van Nuys, Calif., Attn: Mr. Ferris Smith	"	(43)
INSMAT, Boston, for Raytheon Mfgr. Co., Waltham, Attn: Mrs. H. L. Thomas	"	(44)
INSMAT, Brooklyn, for Reeves Instrument Corp., N. Y., N. Y.	"	(45)
Republic Aviation Corp., Farmingdale, L. I., Attn: Dr. Wm. O'Donnell	"	(46)
Ryan Aero. Co., Lindberg Field, San Diego 12, Calif., Attn: Mr. H. A. Sutton	"	(47)
INSMAT, Brooklyn, for Sperry Gyroscope Co, Great Neck, L. I.	"	(49)
BAR, U. A. Corp., Stratford, for U. A. Corp, Chance Vought Air. Div., Stratford, Conn., Attn: Mr. P. S. Baker	"	(50)
BAR, U. A. Corp., E. Hartford, for U. A. Corp., Research Dept., E. Hartford, Attn: Mr. J. G. Lee	"	(51)
Univ. of Mich., Aero. Res. Center, Willow Run Airport, Attn: R. F. May	"	(52)
BAR, Pasadena for USC, Naval Res. Proj., LA, Attn: Dr. R. T. DeVault	"	(53)
DCO, Univ. of Texas, Defense Res. Lab., Austin, Attn: Dr. C. P. Boner	"	(54)
Lockheed Aircraft Corp., Burbank, Calif., Attn: Mr. H. L. Hibbard	"	(56)
Calif. Inst. of Tech., JPL, Pasadena, Attn: Mr. L. G. Dunn	"	(57)
Univ. of Chicago, Ord. Res., Chicago 37, Illinois		(58)

Belmont Radio Corp., Chicago, Attn: Mr. H. C. Mattes	DG	(1)
BARR for Bendix Aviation Corp., Teteboro, N. Y., Attn: Mr. R. C. Sylvander	"	(2)
DCO, BAC for Bendix Aviation Corp., N. Hollywood, Attn: R. M. Russell	"	(3)
Bendix Aviation Radio Div., Balt., Md., Attn: Mr. A. C. Omberg	"	(4)
Buehler and Co., Chicago, Attn: Mr. Jack M. Roehn	"	(5)
CG, AAf, Pentagon, Attn: AC/AS-4, DRE-2F	"	(6)
BAR, San Diego, for Consolidated-Vultee, Attn: Mr. Breitwieser	"	(7)
Cornell Univ., Ithaca, N. Y., Attn: Mr. W. C. Ballard, Jr.	"	(8)
Dir., USNEL, San Diego, Calif.	"	(9)
Electro-Mechanical Research, Ridge Field, Conn., Attn: Mr. Chas. B. Aiken	"	(10)
DCO, INSMAT, Fort Wayne, for Farnsworth Television and Radio Co., Attn: Mr. J. D. Schantz	"	(11)
Federal Telephone and Radio Corp., Newark, N. J., Attn: Mr. E. N. Wendell	"	(12)
Galvin Mfg. Corp., Chicago, Attn: Mr. G. R. MacDonald	"	(13)
Gilfillan Corp., Los Angeles, Attn: Mr. G. H. Miles	"	(15)
INSMAT, N. Y. for Hillyer Eng. Co., Attn: Mr. Curtiss Hillyer	"	(16)
INSMAT, N. Y. for Kearfott Co., Inc.	"	(17)
Lear, Inc., Grand Rapids, Michigan, Attn: Mr. R. M. Mock	"	(18)
Mfg. Machine and Tool Co., Mt. Vernon, N. Y., Attn: Mr. J. Kloppinger	"	(19)
Minneapolis-Honeywell Mfg. Co., Minneapolis, Attn: Mr. W. J. McGoldrick	"	(20)
Ohio State Univ., Columbus, Attn: Mr. T. E. Davis, Staff Assistant	"	(21)
Haller, Raymond and Brown, State College, Pa., Attn: Dr. R. C. Raymond, Pres.	"	(22)
OCSigO, Eng. and Tech. Ser., Engr. Div., Pentagon, Wash., D. C.	"	(23)
Raytron, Inc., Jackson, Mich., Attn: Mr. J. R. Gelzer	"	(24)
L. N. Schwein Eng. Co., Los Angeles, Attn: L. N. Schwein	"	(25)
SNLO, USNEL, Sig. Corps. Engr. Lab., Ft. Monmouth, N. J.	"	(26)
INSMAT, N. Y. for Servo Corp. of Amer., Lindenhurst, L. I.	"	(27)
BAR, N. Y. for Square D. Co., Kollsman Instrument Div., Elmhurst, N. Y., Attn: Mr. V. E. Carbonara	"	(28)

		Copy No.
Stromberg-Carlson Co., Rochester, N. Y., Attn: Mr. L. L. Spencer	"	(29)
DCO, MIT, Cambridge, for Sub. Sig. Co., Boston, Attn: Mr. Edgar Horton	"	(30)
Summers Gyroscope Co., Santa Monica, Calif., Attn: Mr. T. Summers	"	(31)
INSMAT, N. Y., for Sylvania Elec. Products, Inc., Flushing, N. Y., Attn: Dr. Robert Bowie	"	(32)
Univ. of Ill., Urbana, Ill., Attn: Mr. H. E. Cunningham	"	(33)
Univ. of Pittsburgh, Attn: Mr. E. A. Holbrook	"	(35)
DCO, Univ. of Va. for Univ. of Va., Physics Dept., Charlottesville, Attn: Dr. J.W. Beams	"	(36)
Washington Univ., Clayton, Missouri, Attn: Dr. R. C. Spencer	"	(37)
Westinghouse Elec. Corp., Pittsburgh, Attn: Mr. F. W. Godsey	"	(38)
Dir. of Specialty Products Dev., Whippany Radio Lab., Whippany, N. J., Attn: Mr. M. H. Cook	"	(39)
Zenith Radio Corp., Chicago, Ill., Attn: Mr. Hugh Robertson	"	(40)
INSMAT, Syracuse, N. Y., for G. E. Co., N. Y., Attn: Mr. W. Hafstrom	"	(41)
INSMAT, Boston, for Doelcam Corp., West Newton, Mass., Attn: J. J. Wilson	"	(42)
Teleregister Corp., New York, N. Y., Attn: Mr. M. L. Haselton	"	(43)
Airborne Instruments Lab., Mineola, L. I., Attn: Mr. Walter Tolles	"	(44)
Fairchild Camera and Instruments Corp., Jamaica, N. Y., Attn: Mr. A. Lockner	"	(45)
BAR, Pasadena, for Aerojet Engr. Corp., Azuza, Attn: Mr. K. F. Mundt	DP	(1)
Armour Research Foundation, Chicago, Attn: Mr. W. A. Casler	"	(2)
Arthur D. Little, Inc., Cambridge, Attn: Mr. Helge Holst	"	(3)
Battelle Memorial Institute, Columbus, Attn: Dr. B. D. Thomas	"	(4)
DCO, for Bendix Aviation Corp., N. Hollywood, Attn: R. M. Russell	"	(5)
Bendix Products Div., Bendix Aviation Corp., S. Bend, Ind., Attn: F. C. Mock	"	(6)
CG, AAF, Pentagon, Attn: AC/AS-4, DRE-2E	"	(7)
CG, AMC, Wright Field, Attn: TSEPP-4B(2) TSEPP-4A(1) TSEPP-5C(1) TSORE(1) TSEPP-5A(1)	"	(8-13)
CO, Picatinny Arsenal, Dover, N. J., Attn: Technical Div.	"	(14)
CO, Watertown Arsenal, Watertown, Mass., Attn: Laboratory	"	(15)
BAR for Continental Av. and Engr. Corp., Detroit	"	(16)
Curtiss-Wright Corp., Prop. Div., Caldwell, N. J., Attn: Mr. C. W. Chillson	"	(17)
DCO for Experiment, Inc., Richmond, Va., Attn: Dr. J. W. Mullen, II	"	(18)
BAR, Bethpage, L. I., for Fairchild Air. and Eng. Co., Farmingdale, N. Y.	"	(19)
BAR for Gen. Motors Corp., Allison Div., Indianapolis, Attn: Ronald Hazen	"	(20)
G. M. Giannini and Co., Inc., Pasadena	"	(21)
INSMAT, New York for Hercules Powder Co., Port Ewen, N. Y.	"	(22)
BAR, Pasadena, for Marquardt Aircraft Co., Venice, Attn: Dr. R. E. Marquardt	"	(23)
Menasco Mfg. Co., Burbank, Calif., Attn: Robert R. Miller	"	(24)
INSMAT, N.Y. for N. Y. U., Applied Math. Center, N. Y., Attn: Dr. R. Courant	"	(25)
Dept. of the Army, Office of the Ch. of Ord., Attn: ORDTU, Pentagon	"	(26)
INSMAT, N. Y. for Polytechnic Inst., of Brooklyn, Attn: Mr. R. P. Harrington	"	(27)
INSMAT, Chicago for Purdue Univ., Attn: Mr. G. S. Meikel	"	(28)
BARR, Dover, for Reaction Motors, Inc., Dover, N. J.	"	(29)
Rensselaer Polytechnic Inst. Troy, Attn: Inst. of Naval Science	"	(30)
Solar Aircraft Co., San Diego, Attn: Dr. M. A. Williamson	"	(31)
INSMAT, N. J. for Standard Oil Co., Esso Lab., Elizabeth, N. J., Attn: W. J. Sweeney	"	(32)
DCO, Charlottesville, for U. of Va., Physics Dept., Attn: Dr. J. W. Beams	"	(33)
INSMAT, Chicago, for U. of Wisconsin, Attn: Dr. J. O. Hirschfelder	"	(34)
BARR, Westinghouse for Westinghouse Electric Co., Essington, Pa.	"	(35)
BAR, Woodridge, for Wright Aeronautical Corp., Woodridge, N. J.	"	(36)
Supt., Shipbuilding, USN, Quincy, for Bethlehem Steel Corp., Shipbuilding Div., Quincy, Attn: Mr. B. Fox	"	(37)
Ohio State University, Columbus, Attn: Dr. H. L. Johnson	"	(38)
DCO, APL, JHU, for Rocket Propellant Agency, APL, JHU, Attn: Dr. S. Githens	"	(39)

Distribution (Cont.)

	Copy No.
DCO, Albuquerque, for New Mex. Sch. Mines, Res. and Dev. Div., Attn: Dr. E. J. Workman	DA-1
DCO, Albuquerque, for New Mex. Sch. A and M Arts State College, Attn: Dr. George Gardiner	DA-2
INSMAT, N. Y. for N.Y.U. Appl. Math. Center, Attn: Mr. Richard Courant	DA-3
Office of Ch. of Ord., Ord. Res. and Dev. Div. R and M Br., Ballistics Sec.	DA-4
INSMAT, N. Y. for Polytechnic Inst., of Brooklyn, Attn: Mr. R. P. Harrington	DA-5
INSMAT, Milwaukee, for U. of Minnesota, Attn: Dr. Akerman	DA-6
BAR, Pasadena, for Aerojet Eng. Corp. Azuza, Attn: Mr. K. F. Mundt	DA-7
BAR, Pasadena for Marquardt Aircraft Co., Venice, Attn: Dr. R. E. Marquardt	DA-8
BAR, Pasadena, for Aerojet Eng. Corp. Azuza, Attn: Mr. K. F. Mundt	DL-1
BAR, Harrison, N. J. for McKiernan-Terry Corp., Harrison, N. J.	DL-2
Naval Aircraft Factory, Philadelphia, Attn: Ships Installations Div.	DL-3
BAR, Dover, for Reaction Motors, Inc., Dover, N. J.	DL-4
Supt. of Shipbuilding, USN, Quincy, for Bethlehem Steel Corp., Shipbldg. Div., Quincy, Mass., Attn: Mr. B. Fox	DL-5
DCO, Silver Spring, for APL, Rocket Prop. Ay., Attn: Dr. S. Githens	DL-6
DCO, Baltimore, for Johns Hopkins U. Rad. Lab., Attn: Dr. Joyce Bearden	DW-1
Office of the Ch. of Ord., Ord. Res. and Dev. Div. Ammunition Br., Pentagon	DW-2
DCO, Seattle for U. of Washington, Seattle, Attn: Dr. J. E. Henderson	DW-3
ONR-Planning Division; Program Subdivision: Armament and GM Section: Scientific Subdivision (4 copies): Geophysics Section: Electronics Section; Physics Section: Publication Liaison	E (1-12)
CNO-OP-05; OP-06; OP-03; OP-503; OP-601; OP-413; OP-413C; OP-04/06; OP-100F: CinCLantFlt:CinCpacFlt.	" (13-24)
BuAer-Aer-E18; Aer-E1; Aer-E1-35; Aer-SI-50DAS (2 copies): Aer-Pa.	" (25-31)
BuOrd-Adlf: Ple: Re: Rea:	" (32-36)
BuShips- Code 330: Code 900: Code 910: Code 918-L. C. Watson Labs; Code 920; Code 938 (2 copies)	" (37-43)
Naval Observatory	" (44)
NavGun, Washington	" (45)
MarCorps-Military Sec. G-3	" (46-48)
NORTLC-MIT	" (49-50)
NOTU-WSPG	" (51)
NPG-Dahlgren	" (52)
NRL Field Group - WSPG	" (53-56)
SNLO-USNELO-Ft., Monmouth	" (57)
AMC-Watson Labs, Electronics Subdivision TSESA-7, Wright Field	" (58-59)
NavOrdDev. U-APL	" (60-61)
Ch/CRD-Rocket Dev. Div: Sub Office (Rockets) CIT	" (62)
ESL-Belmar, N. J.	" (63)

		Copy No.
Air Tactical School, Air Un. -Tyndall Field, Fla.	"	(64)
JRDB:JRDB-GM Committee	"	(65-66)
SDC, ONR. Sands Point, Att: Technical Information Desk	"	(67)
Dev. Contract Officer, Cornell Aero. Lab-Att: Dr. C. C. Furnas	"	(68-69)
Dev. Contract Officer-APL, Johns Hopkins	"	(70-72)
U. of Mich-Att: Dr. Dow: Mr. M. B. Small:	"	(73-77)
State College Penna. -Att: Haller, Raymond and Brown	"	(78-80)
Princeton U-Att: Fr. H. D. Smyth	"	(81)
BAR, Pasadena, Cal. for Aerojet, Att: Dr. F. Zwicky: W. E. Zisch	"	(82-83)
BAR, Consolidated Vultee, Downey, Cal., Att: C. R. Irvine	"	(84-85)
Dev. Contract Officer for Gen. Elec. Co., Schenectady - Att: Mr. G. K. Megerian (2 copies) Dr. R. W. Porter (2 copies)	"	(86-89)
BAR-Lockheed Aircraft Corp.	"	(90-91)
NavGun-Optical Shop	F	(1)
OinC BOEU-NBS, Attn: Dr. J. H. Dellinger; Dr. I. O. Gardner; Dr. W. F. Meggers; Dr. Newbern Smith; Dr. H. Diamond, Dr. H. C. Dryden.	"	(2-7)
NORTLO-MIT, Attn: Dr. D. C. Stockbarger, Dr. G. R. Harrison, Dr. Z. Kopal	"	(8-10)
NavOrdDev. U-APL, Att: Dr. Hafstad; Dr. Van Allen; Dr. Tatel; Dr. Hopfield	"	(11-15)
AWS-R & D Div., Langley Field	"	(16)
WDSS-Res. & Dev. Div., Att: Col. Trichel	"	(17)
JRDB-Panel on the Upper Atmosphere, Att: Dr. Landsberg, Sec'y,	"	(18-37)
Weather Bureau	"	(38-39)
NACA-Langley Field	"	(40-42)
BAR, Pasadena, Cal. for UCLA, Att: Dr. Joseph Kaplan	"	(43-44)
Cal. Tech-Att: Dr. Millikan: Dr. Dunn: Prof. O. R. Wulf	"	(45-48)
U. of Cal., Berkeley	"	(49)
Carnegie Tech-Att: Mr. B. R. Teare	"	(50)
U. of Chicago - Att: Prof. Marcel Schein	"	(51)
University of Chicago, Yerkes Observatory, Williams Bay, Wisc., Att. Dr. Jesse L. Greenstein	"	(52)
Harvard Observatory - Climax, Att: Dr. Walter O. Roberts	"	(53)
Harvard Observatory - Cambridge, Att: Dr. Shapley; Dr. Menzel; Dr. Whipple	"	(54-56)
Harvard U - Att: Prof. Theo. Syman; Prof. H. R. Mimno	"	(57-58)
Johns Hopkins U - Att: Dr. G. H. Dieke; Dr. A. H. Pfund; Dr. John Strong; and Dr. R. W. Wood	"	(59-61)
U. of Mich. - Att: Dr. M. H. Nichols	"	(62)
Michigan Observatory, Ann Arbor, Mich., Att: Dr. Goldberg	"	(63)
Mt. Wilson Observatory - Att: Dr. H. D. Babcock	"	(64)
Ohio State U., - Att: Dr. George Sinclair	"	(65)
U. of Pitt., - Att: Dr. A. J. Worthing	"	(66)
Princeton U, Palmer Physical Lab., Att: Prof. R. Ladenburg	"	(67)
Princeton Observatory, Att: Dr. Spitzer; Dr. Russell	"	(68-69)
U. of Rochester - Att: Dr. Brian O'Brien	"	(70)
U. of Wisconsin - Att: Dr. Gregory Breit	"	(71)
AIL - Mineola, Att: Mr. Skifter	"	(72)
SINM, Boston, Mass., for Baird Assn., Cambridge	"	(73-75)
BAR - Douglas Aircraft - Att: Mr. R. L. McKay; Dr. Klemperer	"	(76-77)

Distribution (Cont.)

		Copy No.
NAMU, Johnsville, Pa., for Franklin Ins., Labs - Att: Mr. W. F. Gould	"	(78)
Dev. Contract Officer, Gen. Elec. Co., Schenectady, Att: Dr. D. F. Green, Dr. K. H. Kingdon	"	(79-80)
Carnegie Inst., - Att. Dr. Merle A. Tuve	"	(81)
Ord. Adv. Committee on GM - Gen'l. Radio Co., Cambridge, Att: Dr. H. B. Richmond	"	(82-83)
SIMN - Gen'l. Textile Mills - Att: Mr. L. P. Friedler	"	(84-85)
BAR - Glenn L. Martin Co., Att: Mr. Goddard; Mr. Vorhees; Mr. Routh	"	(86-88)
SINM - Harshaw Chemical Co., Att: Dr. H. O. Kremers	"	(89-90)
INM - Raytheon - Att: Dr. Edelfsen; Mr. H. T. Ashworth; Mr. H. Grant	"	(91-93)
INM - Sperry Gryoscope Co., Garden City, N. Y., Att: Mr. G. E. White	"	(94)

CONTENTS

CONTENTS (CONT'D)

ABSTRACT

This report gives an account of the Rocket-Sonde Research Program of the Naval Research Laboratory during the period of the third and fourth cycles of V-2 firings at White Sands in New Mexico. Three Naval Research Laboratory flights took place during these cycles on December 5, 1946, January 10, 1947 and March 7, 1947. Descriptions of these are provided, and the details of the instrumentation for the missiles are given. The results in cosmic ray research, high altitude spectroscopy, the investigation of the ionosphere, and atmospheric pressure and temperature studies are given. The vibration measurements which were made in the V-2 during the March 7 flight are described. Photography at very high altitudes is discussed. An analytical basis for determining the altitude of a spinning missile after fuel cutoff is presented. The report also includes further results, beyond those previously reported, of continuing analyses of spectrograms obtained on October 10, 1946. Finally, there are discussions of continued progress in telemetering, including a description of a new Naval Research Laboratory pulse matrix telemetering system.

STATUS OF THE PROBLEMS

This is an interim report on the problems listed on the title page; work on all these problems is continuing.

A photograph of the earth taken from the V-2 fired on March 7, 1947. When the picture was made, the rocket had an altitude of 162 kilometers (101 miles) and was within a quarter of a kilometer of the peak of its trajectory.

UPPER ATMOSPHERE RESEARCH

REPORT NO. IV

INTRODUCTION

After more than a year of research the Naval Research Laboratory's Upper Atmosphere Research Program can be viewed in perspective in a manner which was not possible initially. As a result, attention no longer focuses upon the few hundred seconds of a single V-2 flight, but rather upon the results of a number of flights. The results of past experiments now guide the planning of future research. Such effects are clearly reflected in the material of the present report.

The first chapter of the report provides a summary of the accomplishments of the Naval Research Laboratory's Rocket-Sonde Research Program through the fourth cycle of V-2 firings. This chapter is reproduced from a paper which was read before the Annual General Meeting of American Philosophical Society in 1947, and later published in the Proceedings of that institution.[1] The report as a whole deals principally with the results and methods associated with the Naval Research Laboratory flights in the third and fourth cycles. It also includes further reports on data from earlier flights, a discussion of the problem of determining missile aspect, and an account of the telemetering service which has been fundamental to the program.

A considerable number of new developments were associated with the three Naval Research Laboratory flights treated here. Circular polarization of the telemetering signal was first employed during the December 5, 1946 firing. For the first time, on January 10, 1947, an entire V-2 was devoted to a single phase of upper atmosphere research, namely: the study of the cosmic radiation. During the flight of March 7, 1947, and for the first time in history, the pressure and temperature of the atmosphere were measured to an altitude of 120 kilometers (75 miles), data on ion density were obtained from within the D and E regions of the ionosphere, a high-resolution spectrogram was made at 75 kilometers (47 miles) altitude, and photographs of the earth were taken from altitudes in excess of 160 kilometers (100 miles). The most widely known of the high altitude photographs appears in the Frontispiece. The March missile also carried the first of the series of redesigned research warheads now in use, a turnstile radiator for telemetering, and vibration measuring equipment.

---

[1]Ernst H. Krause, Proc. Amer. Philos. Soc. 91, (1947).

CHAPTER I

HIGH ALTITUDE RESEARCH WITH V-2 ROCKETS

by

Ernst H. Krause

The study of the heavens is an ancient science. It began with speculation about the movement and constitution of the sun; later it moved into the greater universe of the stars;[1] and more recently it expanded into that small but very interesting region of space represented by the earth's atmosphere.[2] It seems fitting that a review of the more modern aspects of this subject should be made here since Franklin himself, the founder of the American Philosophical Society, made some of his more important contributions to science in this field.[3]

The atmosphere of the earth is a very complex affair. Many things are known about it and yet the over-all picture is beclouded by lack of sufficient information of the various mechanisms involved to tie all of the observed phenomena into one unified picture. The presence of the lower atmosphere makes the study of phenomena in the upper atmosphere very difficult and in many cases impossible. Similarly, the existence of the atmosphere sets very definite limitations on studies in such fields as astrophysics and cosmic rays, while on the other hand the atmosphere provides us with many new phenomena to study, such as the ionosphere, the aurora, etc.

The answer to many of these difficulties is to study the phenomena within the atmosphere at those points where they occur and to make astrophysical and other studies from above the atmosphere. A step in this direction was the exploitation of the balloon as a vehicle. The balloon, however, has two serious shortcomings. First, it has a maximum ceiling between 30 and 40 km. Many observations have been made up to these altitudes by means of balloons, but a great deal of data is desired above these altitudes. Second, the payload capabilities of balloons are limited to the order of 100 pounds, unless one makes use of complicated balloon formations

---

[1]Shapley, H., and H. E. Howarth, A source book in astronomy, New York., McGraw-Hill, 1929.

[2]Hulburt, E. O., Upper atmosphere of the earth, J. Opt. Soc. Am. 37: 405, 1947

[3]Fleming, J. A., Terrestrial magnetism and electricity, 149, New York, McGraw-Hill, 1939.

or of very large balloons such as were used in the Explorer flights.[4,5] Both of these difficulties can be solved by the use of rockets which are not limited in ceiling, and, although there are payload limitations, the problem of carrying 1,000 pounds to altitudes of 200 km or more is perfectly feasible.

Although rockets themselves date back many centuries, the utilization of one which would carry sufficient weight to conduct an experiment did not seem practical up to the beginning of the last war. However, with the advent of the war, a tremendous impetus was given to rocketry because of its usefulness as a military device, so that several rocket-powered vehicles emerged from the war which could reach altitudes greatly in excess of any that had been reached before. Of these devices, the V-2, designed and built by the Germans, was well out in front. Not only did it reach altitudes much greater than any previously attained by rockets or by other means, but it also was sufficiently large that it could carry a payload much greater than any research worker had hoped for.

The work on the upper atmosphere utilizing the German V-2's in this country has been going on for a little more than one year. Even in so short a time it can be stated that the V-2 has already made important contributions to such fields as solar spectroscopy, cosmic rays, and the measurement of atmospheric pressures and temperatures.[6,7,8,9] To those

---

[4] O'Brien, B., Vertical distribution of ozone in the atmosphere, part one: Spectrographic results of the 1934 flight, N. G. S. Contrib. Tech. Papers, Stratosphere Series 2:49, 1936.

[5] O'Brien, B., F. L. Mohler, and H. S. Stewart, Jr., Vertical distribution of ozone in the atmosphere, part two: Spectrographic results of the 1935 flight, N. G. S. Contrib. Tech. Papers, Stratosphere Series 2:71, 1936.

[6] Upper atmosphere research report no. I, Naval Research Laboratory Report R-2955, 1946.

[7] Newell, H. E., and J. W. Siry, Upper atmosphere research report no. II, Naval Research Laboratory Report R-3030, 1946.

[8] Upper atmosphere research report no. III, Naval Research Laboratory Report R-3120, 1947.

[9] Upper atmosphere research report no. IV, Naval Research Laboratory Report R-3171, 1947.

of us in the field, it is somewhat surprising, but nevertheless gratifying, that the early experiments have proved so successful. We had anticipated that the complexities involved in perfecting the necessary new techniques could easily have consumed the first year's work.

First, I would like to say a few words about the organization of a project as large as this. There is no one organization that encompasses the entire project. The V-2's themselves are assembled, made ready to fire, and fired by the Army Ordnance Department with the aid of the General Electric Company under a special contract for this purpose. Once the V-2 has been fired, it is of course very important to know where it is at all times in its trajectory, so that data taken can be correlated against altitude, range, etc. The ballistics and the problem of tracking in general, involving many types of radio, radar, and optical methods, are the responsibility of the Ballistic Research Laboratories of the Aberdeen Proving Ground.

The actual upper atmosphere work is conducted by various institutions including the Air Material Command, involving the University of Michigan and Watson Laboratories, the Applied Physics Laboratory of The Johns Hopkins University, the Signal Corps, and the Naval Research Laboratory. In addition, there are numerous other contributing agencies, including Princeton University, the National Bureau of Standards, Harvard University, and California Institute of Technology. All of the work is coordinated through a V-2 Panel which consists of members from most of the above named institutions and agencies.

THE V-2

Just to refresh your memories I might point out a few of the characteristics of the V-2[10]. Figure 1 shows the V-2 on its launching platform. It stands about 46 feet high, has a total weight of 28,000 pounds when fueled and 9,000 pounds empty. The total weight of payload carried is about 2,000 pounds. Its diameter is 65 inches. Stabilization is accomplished by a set of carbon vanes placed in the jet, aided by a set of air vanes in the fins. Fixed gyroscope stabilization is maintained in azimuth, and a gyroscope program control feeds a predetermined tilt program to the fins. When the rocket motor is started, the rocket begins to rise slowly as soon as the acceleration due to the thrust exceeds 1 g. Since a rocket motor of this type is a constant thrust device and since the mass is constantly decreasing owing to fuel consumption, the acceleration gradually increases until after about 60 seconds it reaches a value of 6 g. At this point the fuel is completely consumed, the missile is out of the denser atmosphere and it proceeds on a trajectory which is a function only of its position and velocity at the time of fuel burnout. Up until the time of burnout it is, as previously pointed out, completely stabilized. Thereafter, since it is out of the atmosphere and since no more jet power is available, no further stabilization is obtained. The result is that any accidental angular momentum imparted during the fuel burnout period produces a roll, pitch, or yaw during the remainder of the free-space flight. Here we encounter the first objectionable feature of the V-2 rocket as a research vehicle. We find that, in general, there is a very definite roll about the rocket's longitudinal axis over most of the trajectory. In addition there have been cases where a definite yaw and pitch have been observed. The exact knowledge of the missile's attitude after burnout is not complete at present but is the subject of an intensive study.

---

[10]Smith, C. H., Jr., Upper atmosphere research report no. I, Chap. I. General description of the V-2 and the firing program of the Army Ordnance Department, Naval Research Laboratory Report R-2955: 7, 1946.

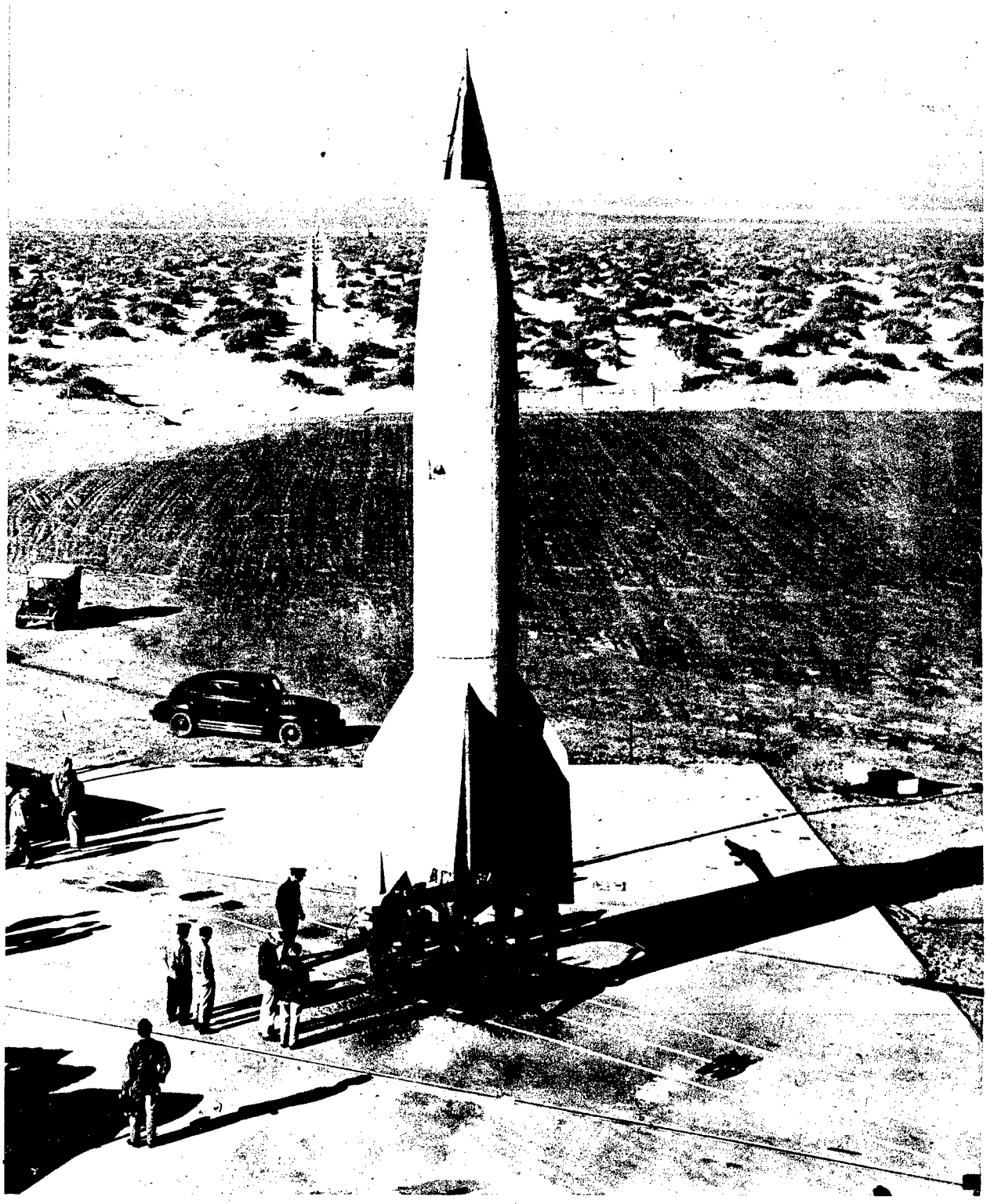

Fig. 1. V-2 on its launching platform. Note the camera opening in the midsection and also the special painting on the warhead to facilitate recovery.

Figure 2 shows the trajectory of the V-2 as it was plotted for a firing on March 7, 1947. A study of this trajectory brings out a second shortcoming of the rocket in general, that is the short time that it spends in free space. It can be seen, for example, that the time the rocket spends above 50 km is about 5 minutes. It is therefore necessary to complete all experiments in this limited time.

To conduct work in the V-2 it was necessary to design and build a special warhead with access doors for installing and adjusting the equipment. It is not a standard device but usually undergoes special modification for each flight, depending on the particular experiments involved.

DATA RECOVERY

Two general methods of data recovery are used. One involves telemetering (radio transmissions of data from the missile to the ground); the other involves direct recording of information on film or other recorders, followed by physical recovery of the equipment after impact.

Of these two general methods by far the more successful has been that of telemetering. The telemetering system which has been employed in all V-2 firings is a 23 channel pulse time modulated system designed at the Naval Research Laboratory.[11] The information is transmitted by means of a group of pulses such that the intelligence on any given channel is contained in the spacing between two adjacent pulses. Twenty-four such pulses constitute one group for a 23-channel system. The group repeats at a rate of approximately 200 cycles per second; hence each channel is sampled at this rate. Figure 3 shows the complete telemetering unit in its pressurized container together with the airborne antenna. Pressurization is, of course, necessary to avoid arc-over and corona at the lower pressures which the missile passes through. The system uses subminiature tubes, operates at a frequency of approximately 1,000 mc, and has a peak power output between one and two kw. The entire record of a flight is recorded on the ground by several different methods, the most important of which is a string oscillograph. A picture of a typical recording is shown in figure 4.

We have under development and should have in use within the next six months a 30-channel telemetering system using a 300-cycle sampling rate.[12]

---

[11] Heeren, V. L., C. H. Hoeppner, J. R. Kauke, S. W. Lichtman, and P. R. Shifflett, Telemetering from V-2 rockets, Electronics 20: 100-105, 1947.

[12] Upper atmosphere research report no. IV, Chap. XI, The Telemetering System, Naval Research Laboratory Report R-3171, 1947.

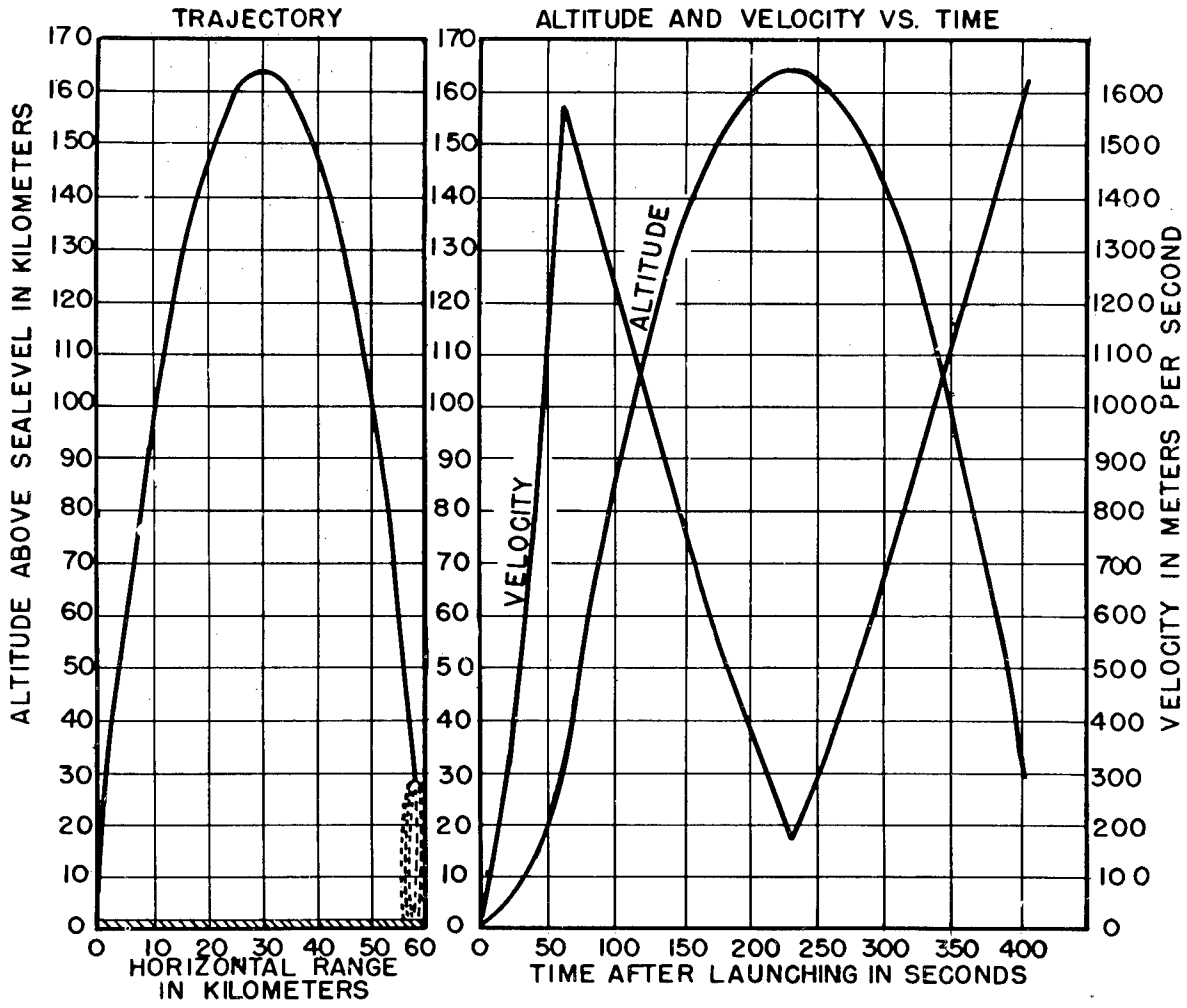

Fig. 2. Trajectory curves for 7 March 1947 flight

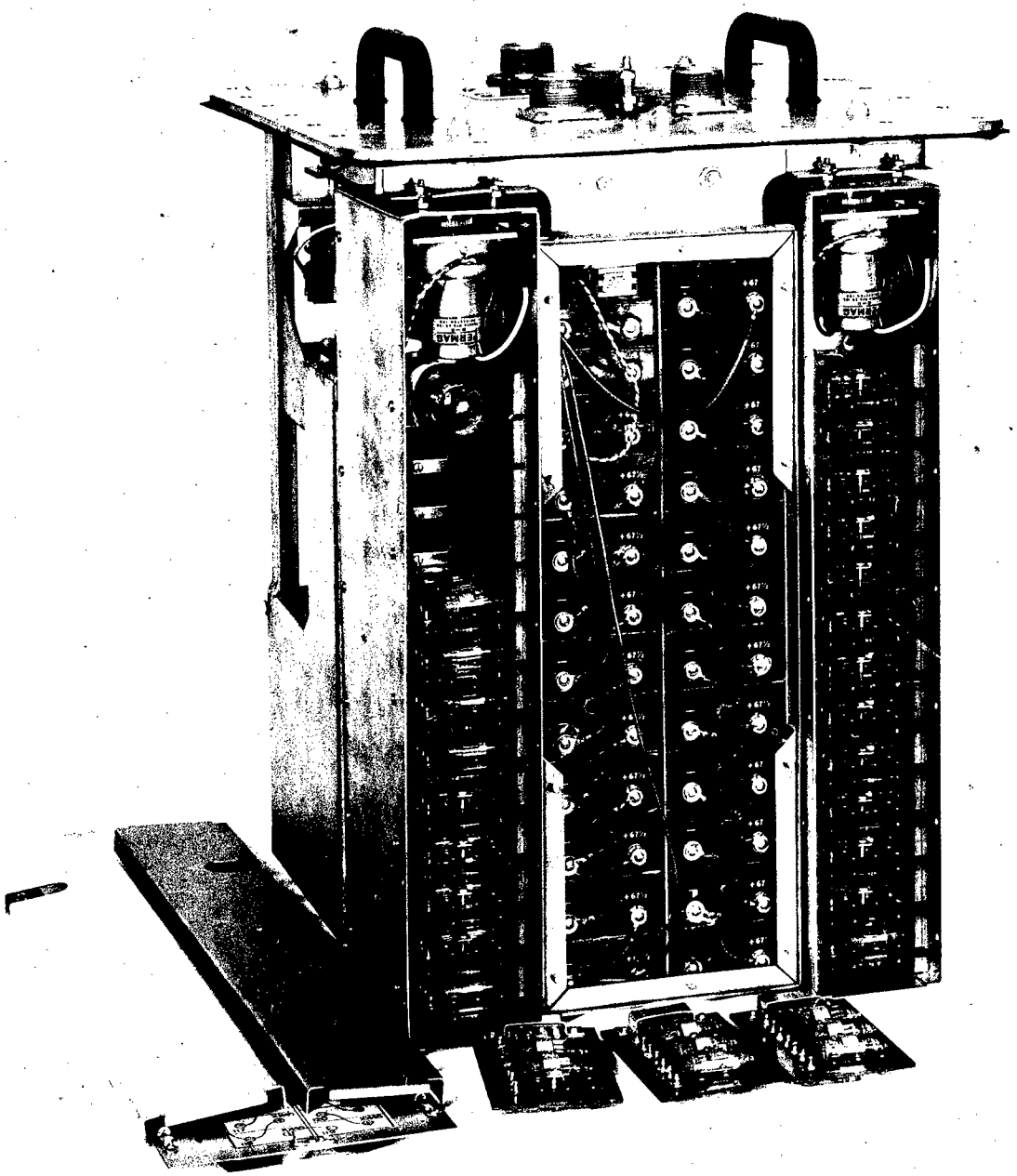

Fig. 3. Telemetering transmitter removed from its pressurized container. The circuitry for each of the 23 channels can be quickly unplugged for servicing. The two motors at the top are used for periodically transmitting calibrating voltages while in flight. Note the almost exclusive use of subminiature tubes

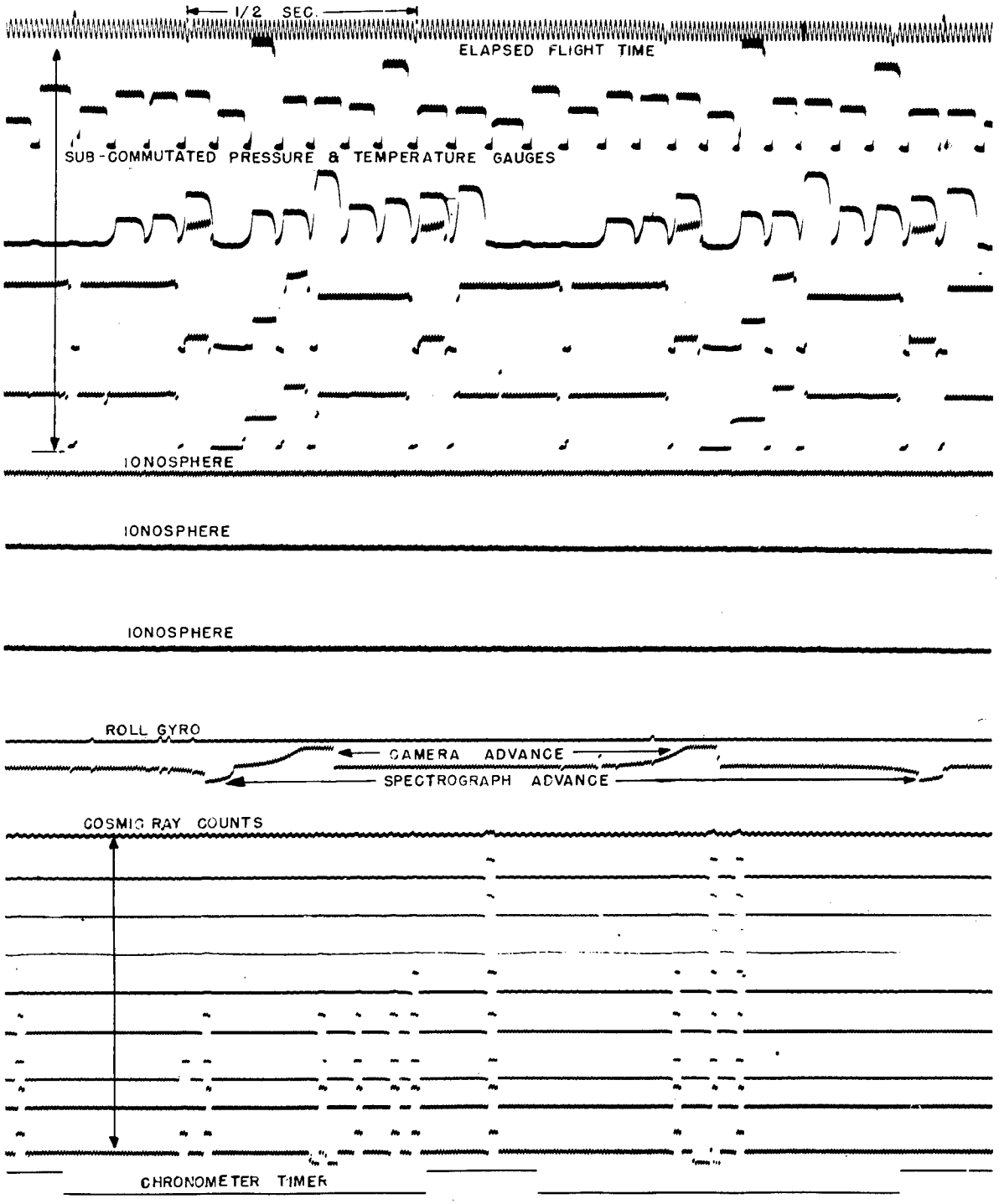

Fig.4. Typical section of telemetering record. Top and bottom of the record are timing signals. The subcommutated channels at the top of the record represent different types of pressure and temperature information, each individual deflection corresponding to a different guage. The ionosphere channels at this time in the record present essentially direct information. The roll gyroscope shows no roll since the missile is still in its stabilized period. The rest of the record is self-explanatory.

By means of a subcommutator we will be able to extend the number of channels to 450 using a sampling rate of approximately one per second.

The recovery of data by telemetering is not completely satisfactory in all cases. For example, the telemetering of spectrographic data, although possible, is not very satisfactory. Furthermore in all cases when the missile begins to gyrate severely, as it does occasionally, the telemetered data is not continuous because the antenna is at times completely shadowed by the missile. For these reasons other methods of data recovery are being studied. One of these methods is the use of drag mechanisms, including parachutes.

The use of drag mechanisms for recovery is probably feasible, but considerable development work still needs to be done. The present method of recovery involves breaking up the missile during its downward flight in such a way that each individual piece coming down has a high drag coefficient and very poor stability, the result being that the piece in question will tumble or float down. It has been found by this method that equipment even after very high flights will arrive at the earth in fair condition, and occasionally will be found completely intact. Thus, for example, on our October 10 flight, the spectrograph which was installed in a tail fin, was recovered in such a good condition that further calibration runs were made on it in the Laboratory without readjustment. The induced breakup had torn the fin loose and it had apparently floated back to the earth. Eight pounds of TNT tied to the beams supporting the warhead are usually used to produce blowoff. The correct time of detonation is obtained by means of a timer mechanism and also by means of radio such that the TNT is detonated by the appropriate one of these two methods at an altitude of about 60 km above the earth on the downward flight. A photograph of a V-2 after a 170 km high flight is shown in figure 5. By this means we have to date recovered four spectrographs (two in usable condition), three photographic recorders, four still picture cameras and ten motion picture cameras, most of which went to an altitude of 170 km. In all cases the films were in excellent condition, even though in some cases no precautions were taken to protect them on impact.

Our present program is concerned with four fields of high altitude research, namely, cosmic rays; the ionosphere; pressure, temperature, and composition measurements; and astrophysics involving primarily the spectrum of the sun. A typical layout of these various experiments in a V-2 is shown in the sketch of figure 6. A more detailed view of the installations in the warhead and control chamber is shown in figures 7, 8, and 9. Beginning at the extreme nose tip of the missile we have an installation for measuring ram pressures. Immediately behind this in the warhead is the cosmic-ray telescope with the necessary electronics below the telescope. The ionosphere transmitter is directly below the cosmic-ray electronics. Also in the warhead are a timer, remote control switching panel, accelerometers, telemetering commutator, batteries, and miscellaneous equipment. In the control chamber immediately behind the warhead are the telemetering transmitter, several distribution and testing panels, and the TNT for blowing off the warhead. In the midsection between the

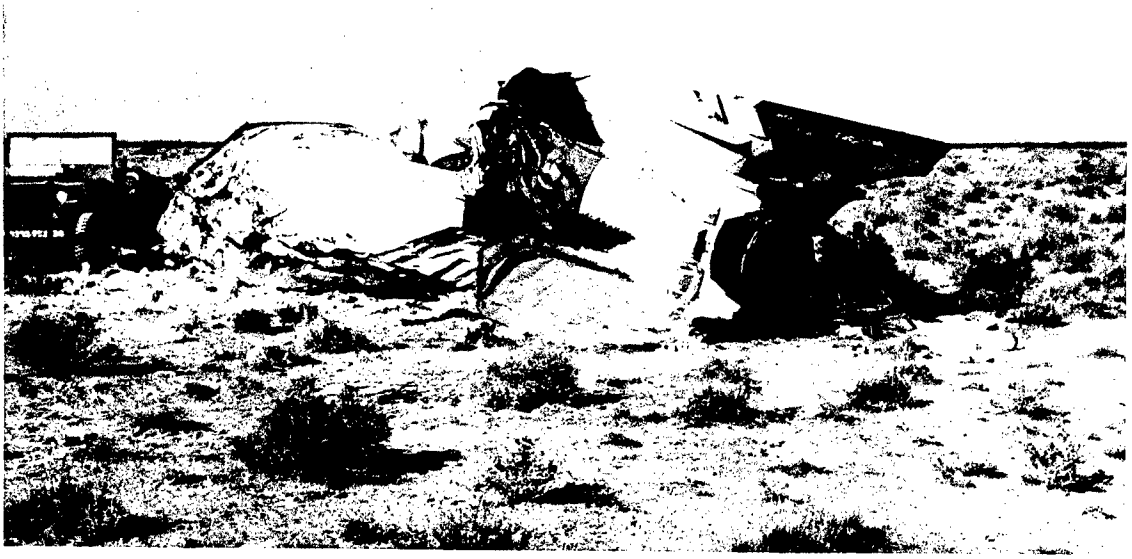

Fig. 5. V-2 after impact. The chances of recovery of film cartridges and other recorded data from the missile after impact are very good.

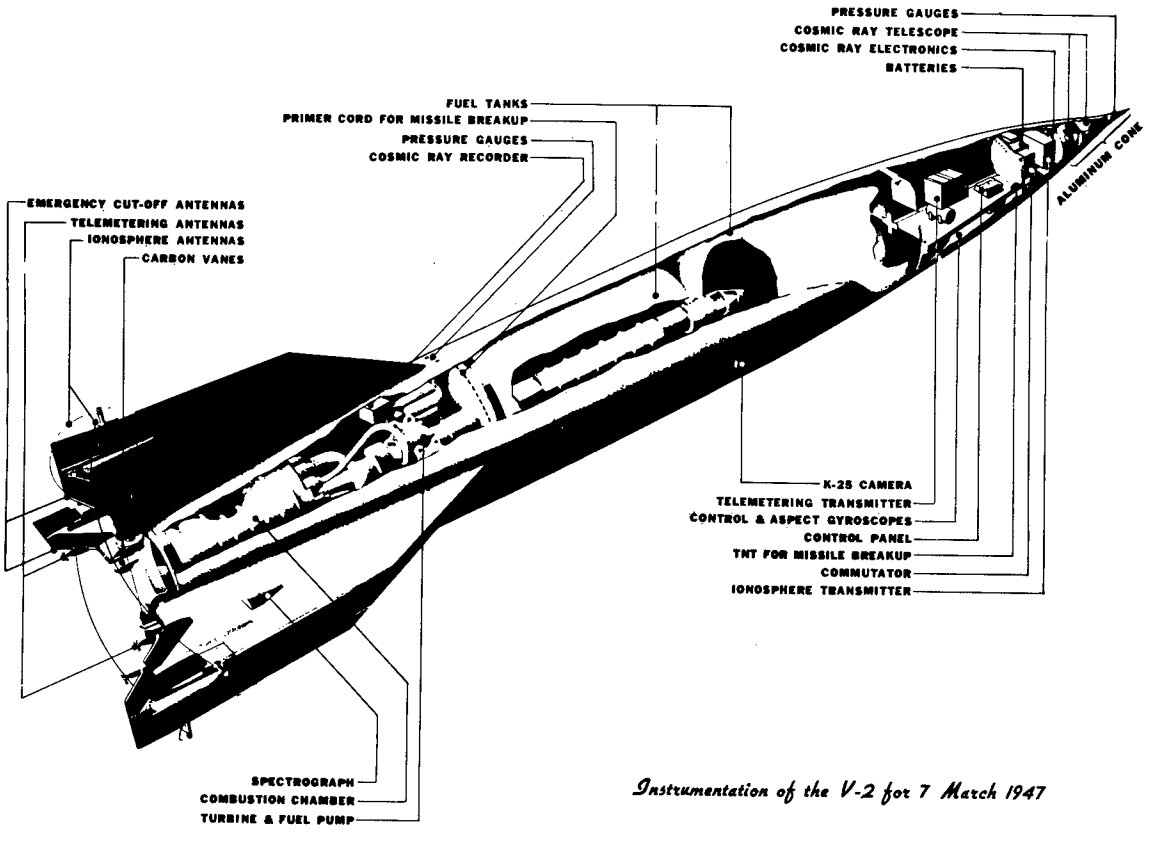

Fig. 6. Cutaway sketch of the V-2 as it is used for upper atmosphere research

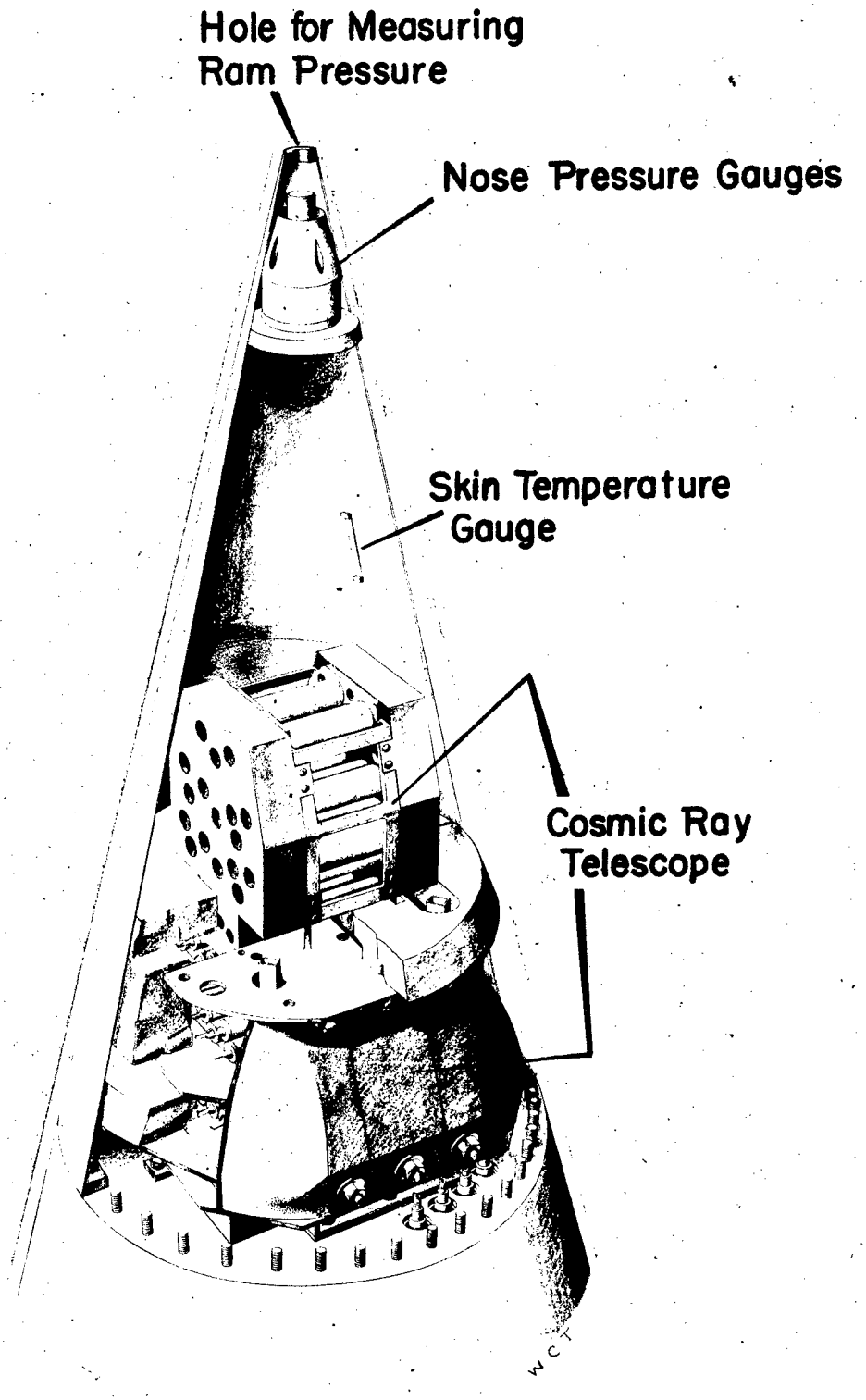

Fig. 7. Sketch showing the forward section of the warhead, including ram pressure gauges, skin temperature gauges, and cosmic-ray telescope

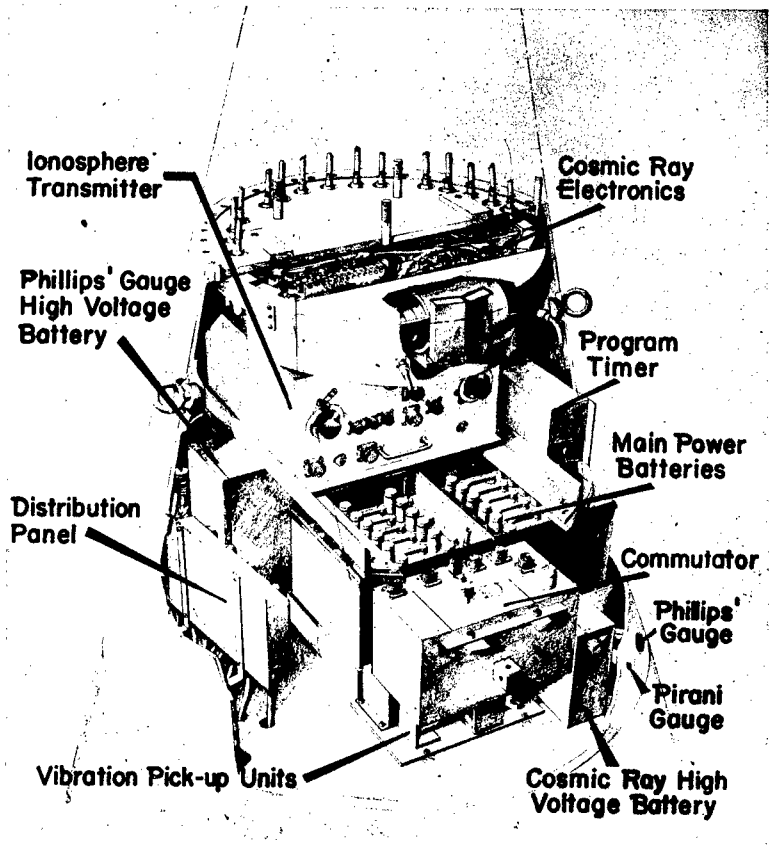

Fig. 8. Sketch showing bottom half of warhead, including cosmic-ray electronics, ionosphere transmitter, various pressure gauges, and miscellaneous equipment

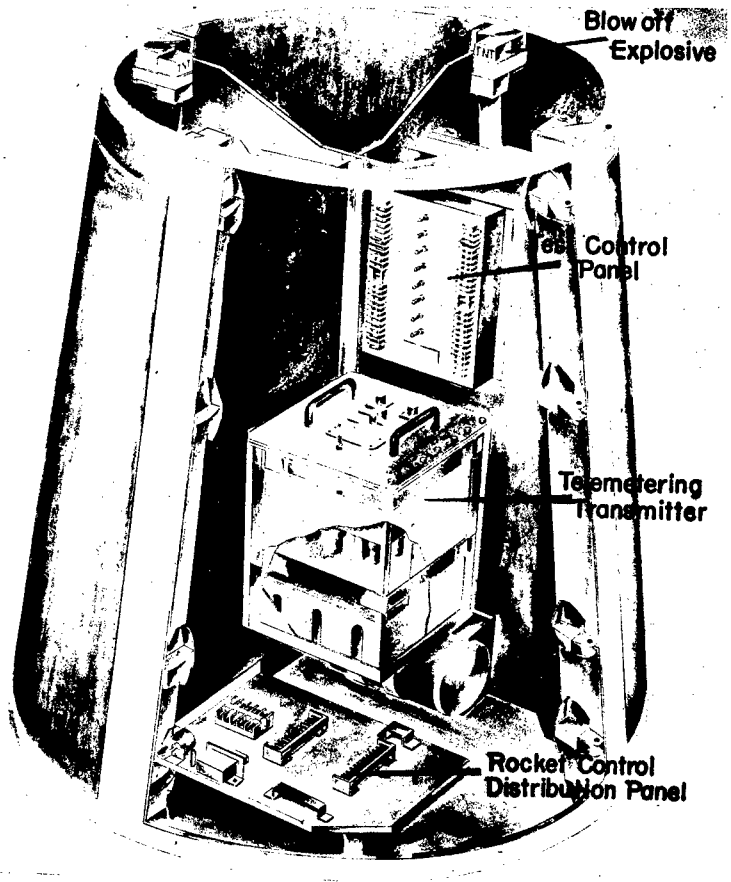

Fig. 9. Sketch showing chamber below warhead including telemetering transmitter and distribution panel

alcohol and oxygen tanks, two cameras are mounted for taking pictures at intervals on the way up. The cosmic-ray film-recording camera is mounted on one of the motor supports immediately below the oxygen tank. The spectrograph is mounted in one of the fins and is provided with a fairing to maintain the necessary streamlining of the fin. At the extreme tail end of the missile are mounted the various antennas for telemetering, ionosphere, and emergency cutoff equipment. I should now like to discuss each of the various experiments at greater length.

COSMIC RAYS

There are many cosmic-ray experiments that one can perform even in a rocket which spends only four or five minutes above the atmosphere. Of all the possibilities we felt that two stood out above all others, namely, (1) a determination of the nature of the primary radiation (heretofore the nature of the primaries could be inferred only from studies of the secondary or tertiary radiation within the atmosphere), and (2) a study of the fundamental reactions taking place as the primaries pass through the atmosphere.

Until the advent of the rocket, cosmic-ray experiments had been conducted in balloons up to an altitude of about 24 km, corresponding to an atmospheric pressure of 2 cm of mercury. These experiments [13], [14] had determined the distribution of the total as well as the "hard" cosmic radiation through the atmosphere, and they indicated that even at pressures as low as 2 cm of mercury the primary radiation had already reacted with air nuclei to produce a secondary radiation generally considered to be mesons. The V-2 was capable of reaching the region of the primaries (up to this time generally considered to be protons by most workers in the field[14, 15]) and also of passing through the very interesting region in which the ultranucleonic transformations, which result in meson production, take place. One of the latter was assumed to be the very important and fundamental proton-meson reaction about which very little is known, since it apparently occurs on earth only in the cosmic radiation at the top of the atmosphere.

---

[13] Bowen, I. S., R. A. Millikan, and H. V. Neher, New light on the nature and origin of the incoming cosmic rays, Phys. Rev. 53: 855-861, 1938.

[14] Schein, M., W. P. Jesse, and E. D. Wollan, The nature of the primary cosmic radiation and the origin of the mesotron, Phys. Rev. 56: 615, 1941.

[15] Johnson, T. H., Composition of cosmic rays. Evidence that protons are the primary particles of the hard component, Rev. Mod. Phys. 11: 208, 1939.

Four different cosmic-ray experiments have been successfully performed to date in four different flights.[16, 17, 18, 20, 21] At the present time three more experiments are in preparation for incorporation in flights during May and July 1947. The results of these experiments have given more insight into the nature of the cosmic radiation. The first two experiments established the fact that the greater portion of the primary radiation consists of "hard" particles (i.e. particles which will penetrate at least 12-15 cm of lead) and that about one out of every five such particles will produce a shower in 12 cm of lead. In addition it was found that large showers were produced by the primaries in the rather considerable mass of material in the warhead which surrounded the counter telescope. On the basis of this information the third and fourth experiments were performed which I should like to discuss in greater detail.

The third experiment[18] consisted of two parts. In the first part a cosmic-ray telescope was arranged to test the penetrating properties of the incoming ionizing radiation. It was found that (at a zenith angle of 45°) about 60 per cent of the radiation was absorbable in a large thickness of lead (14 cm). The other properties of the high altitude radiation were again verified, i.e., the large numbers of warhead showers, and the showers under 14 cm of lead (28 per cent in this measurement). The second part of the experiment, conducted in the same flight, tested for penetration through two successive lead plates each only 2 cm thick. It was then found that about 35 per cent of the high altitude rays were stopped in either the first plate or penetrated it and stopped in the second. This indicated that at least this component was not primary (if the improbable case is excluded that it consisted of nuclei of high atomic number). It has been suggested[19] that these are electrons which arise from the atmosphere below and are due to meson decay. The ones observed presumably originated above South America and spiraled around the earth's magnetic field lines to reach the point of observation. The remainder of the radiation (i.e. 65 per cent) was observed to penetrate the 4 cm of lead, some of it producing showers in either the first plate, the second plate, or both. An upper limit to the relative number of primary electrons is obtainable from these data. First, it cannot be greater than 65 per cent minus 40 per cent or 25 per cent of the total

---

[16]Golian, S. E., E. H. Krause, and G. J. Perlow, Cosmic radiation above forty miles, Phys. Rev. 70: 223, 1946.

[17]Golian, S. E., E. H. Krause, and G. J. Perlow, Additional cosmic-ray measurements with the V-2 rocket, Phys. Rev. 70: 776-777, 1946.

[18]Perlow, G. J., and J. D. Shipman, Jr., Non-primary cosmic-ray electrons above the earth's atmosphere, Phys. Rev. 71: 325, 1947.

[19]Wheeler, J. A., Private communication of August 26, 1946.

[20]Golian, S. E., and E. H. Krause, Phys. Rev. 71: 918, 1947.

[21]Howland, B., C. A. Schroeder, and J. D. Shipman, Jr., Electronics for cosmic-ray experiments, Rev. Sci. Inst. 18: 551, 1947.

radiation (including the non-primary electrons). Second, it must be less than the relative number of events in which showers were produced below 2 and 4 cm, since some of these are ascribed to particles of high penetrating power. This reduces the possible number of primary electrons to 9 per cent of the total or 18 per cent of the primary radiation.

The fourth experiment[20] consisted of a counter tube telescope arranged so that the percentage of particles penetrating 2 cm, 6 cm, and 12 cm of lead could be determined. The number of three-fold showers under these same thicknesses was also measured. The telescope was mounted vertically in a specially designed warhead so that it looked directly through the warhead nose as shown in figures 7, 10, and 11. The heavy lead shielding around the lower half of the telescope was introduced in an attempt to reduce the number of rocket showers found in previous experiments. This shielding, in conjunction with the absorbing lead plates, was sufficient to eliminate most of the registered rocket showers of primary or non-primary electronic origin. It was found that the number of rocket showers actually doubled over that of previous unshielded experiments. This would indicate that these showers must be of non-electronic origin. It was found that, above the atmosphere, 25 per cent of the total radiation present was absorbed in 6 cm of lead. Although this is somewhat less than that found in the first experiment, it is assumed to be the same type of non-primary electron component discussed above. The different percentages in the two experiments are attributed to the variation of this component with zenith angle. A total of 59 per cent of the particles penetrated 12 cm of lead. The remaining 16 per cent was absorbed in 12 cm. In all cases the larger portion did not produce showers under the lead. Thus, primary electrons would be ruled out since these would produce large showers under 2 and 4 cm. As a matter of fact it is difficult to understand how any of this component could be due to primary particles since the large energies associated with the primaries should produce some type of reaction below 12 cm of lead unless, of course, neutral particles are involved. If we assume that all of the radiation except that absorbed in 6 cm is primary, then we find that the electron component determined on the basis of shower production could not be more than a maximum of 14 per cent of the primary; the non-electronic component absorbed in 12 cm is 18 per cent of the primary and the non-electronic component penetrating 12 cm is 68 per cent of the primary. The ratio of the total radiation in free space to that at sea level was 11.5. The ratio of the hard component (that which penetrated 6 cm of lead) in free space to that at sea level was 9.0.

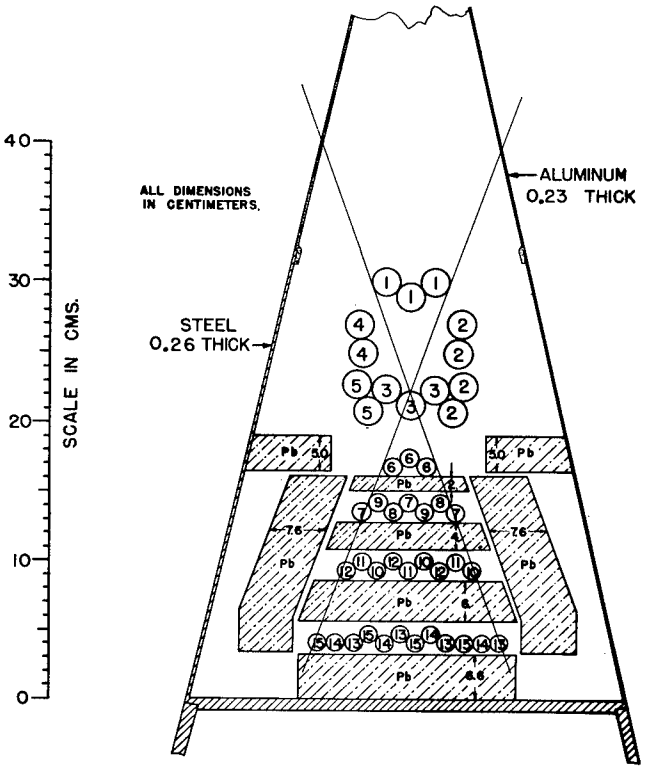

Fig. 10. Schematic of counter telescope arrangement in warhead for the 7 March 1947 missile

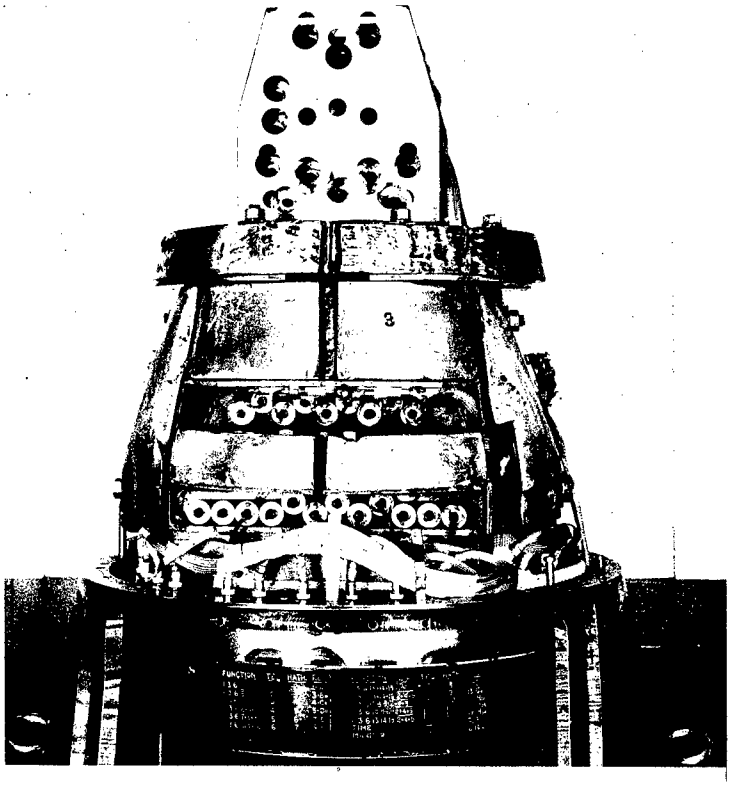

Fig. 11. Photograph of cosmic-ray telescope in 7 March 1947 missile

ASTROPHYSICS AND COMPOSITION

Because the earth's atmosphere had limited spectroscopic observations of the sun to a lower wavelength limit of 2863 A,[22] astronomers have long been looking forward to the time when the unknown far-ultraviolet region could be observed. Even though balloons could reach altitudes of 30 km they were not quite able to pierce the ozone layer and, because of the ozone absorption band which lies just below 2900 A, the lower wavelength limit observed at 30 km was about the same as it was at sea level.[23]

A rocket which reached altitudes of 170 km and higher should prove very valuable in further solar spectral studies. To get such a spectrum and at the same time to get more constructive information on composition of the atmosphere, a special vacuum grating spectrograph, shown in figure 12, was designed to fit into the V-2.[6] Two small lithium fluoride beads are used for obtaining a wide angle of view so as to minimize the effect of roll and other movements of the missile. The image from this little bead is reflected to a grating and in turn to a 35 mm film on which the images from the two beads are recorded separately. The spectrograph was originally designed to fit in the nose of the warhead but, because of greater ease of recovery, it has been, in more recent flights, mounted in one of the tail fins. As pointed out previously, spectrographs have on several occasions been recovered in such good condition that they were capable of being used again.

Two successful experiments have been conducted to date in solar spectroscopy with the result that nearly 100 spectra have been obtained at various altitudes up to 160 km.[24,25] The spectrograph (similar ones were used in the two flights) was arranged to record only the wavelengths below 3400 A; in some of the spectra obtained at higher altitudes radiation was recorded down to 2100 A. Analysis of these spectra has produced the following results.

1. Solar Spectral Energy Distribution. The curve of average radiant energy as a function of wavelength—the so-called black-body curve of the sun—was extended from the previous limit of 2900 A to 2200 A shown in figure 13.

---

[22]Pettit, Edison, Measurements of ultra-violet solar radiations, Astrophys. Jour. 75: 185-221, 1932.

[23]Regener, E., and V. H. Regener, Aufnahmen des ultravioletten Sonnenspektrums in der Stratosphäre and vertikale Ozonverteilung, Phys. Ztschr. 35: 788-793, 1934; (See also references 4 and 5.)

[24]Baum, W. A., F. S. Johnson, J. J. Oberly, C. C. Rockwood, C. V. Strain, and R. Tousey, Solar ultraviolet spectrum to 88 kilometers, Phys. Rev. 70: 781, 1946.

[25]Durand, E., J. J. Oberly, and R. Tousey, Solar absorption lines between 2950 and 2200 angstroms, Phys. Rev. 71: 827-828, 1947.

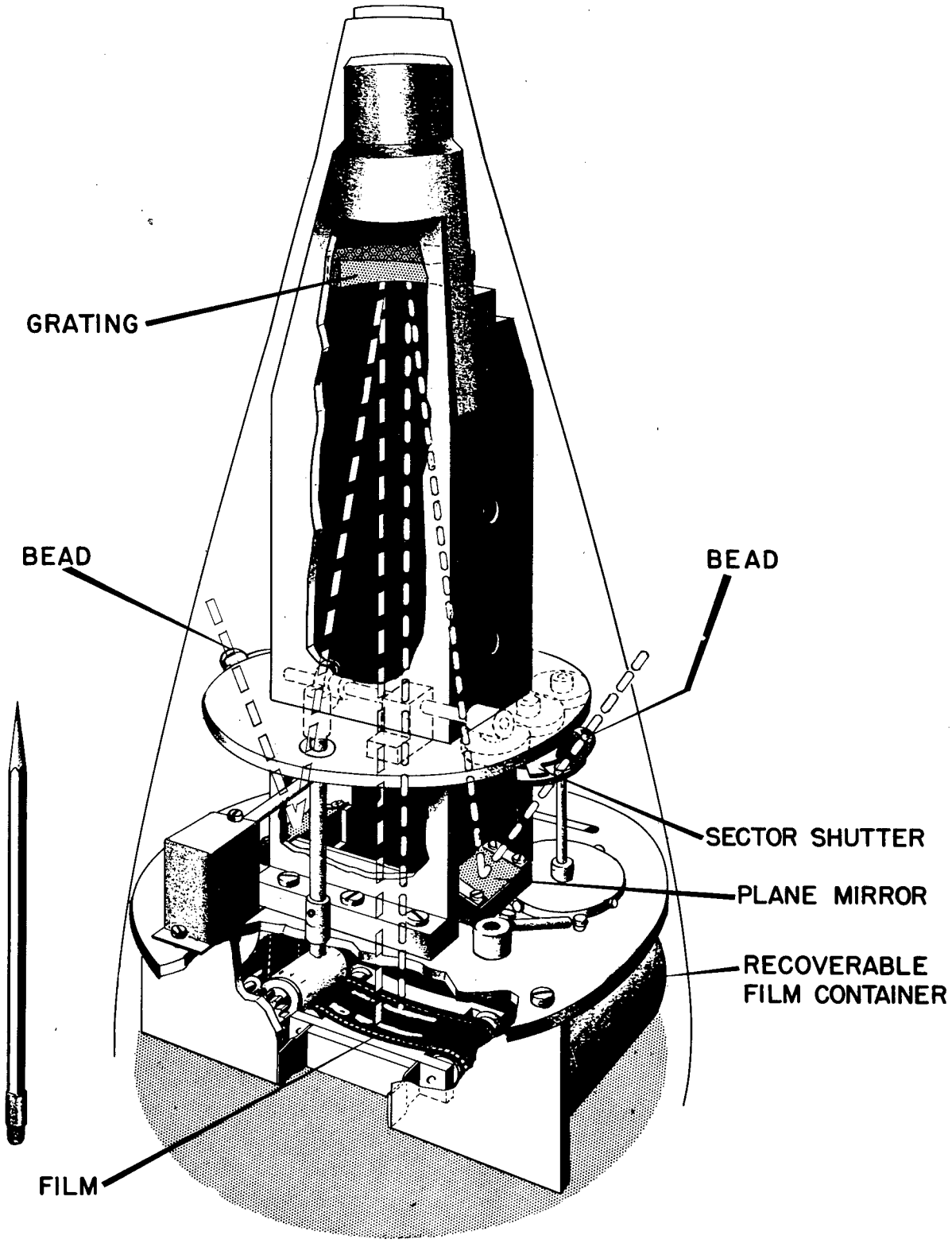

Fig. 12. Sketch of spectrograph designed for use in the V-2

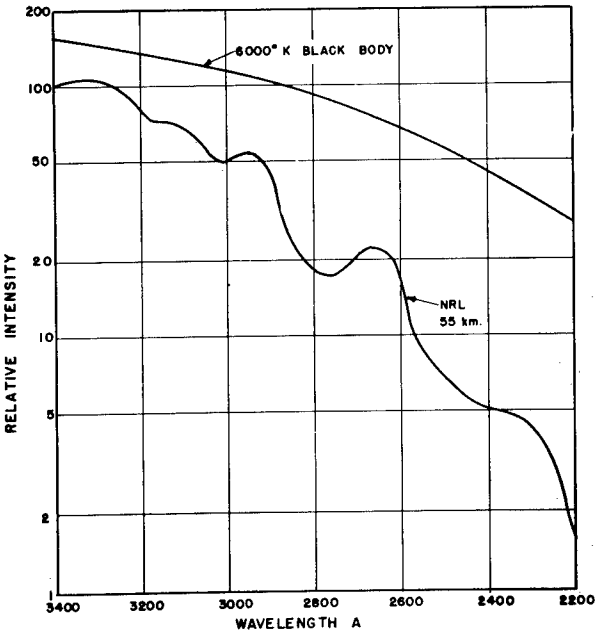

Fig. 13. Solar intensity distribution (preliminary) obtained from spectra of 10 October 1946

mation on this subject is contained in the spectra. Full analysis and evaluation of conditions in the sun will require another year or more of intensive work.

4. Ozone. The variations of the spectra with altitude for the 10 October flight are shown in figure 15. The effect of the absorption of ozone can be clearly seen by noting the absorption band in the region of 2300 to 2800 A below 55 km. The vertical distribution of ozone on this flight is shown in figure 16.[27] The results of the 1936 Explorer II balloon flight are shown for comparison.[5] The balloon data above 22 km are based on an indirect method and lack the inherent accuracy of the direct method employed

The ultraviolet intensities are much less than had been predicted.[26]

2. Fraunhofer Line Analysis. A large number of fully and partly resolved absorption minima were observed in the region between 2950 and 2300 A, as shown in figure 14. Nearly all observed minima are blends from two or more closely spaced lines, but the principal contributors have, in many cases, been identified. Of particular interest was the appearance of the Mg II doublet at 2795 and 2802 A as bright emission lines in the center of a broad absorption region created by the same pair.[25]

3. Line Shapes. Line widths and intensities are important in determining excitation conditions in the sun, and necessary to an understanding of the fundamental processes occurring there. Considerable infor-

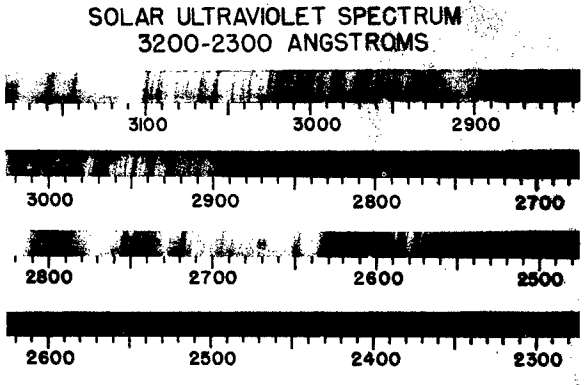

Fig. 14. Fraunhofer spectrum obtained in 7 March 1947 missile - first photograph with such high resolution in the region below 2900 A

---

[26]Durand, E., and R. Tousey, Upper atmosphere research report no. III, Chap. II, Naval Research Laboratory Report R-3120, 10, 1947.

[27]Ibid., 11.

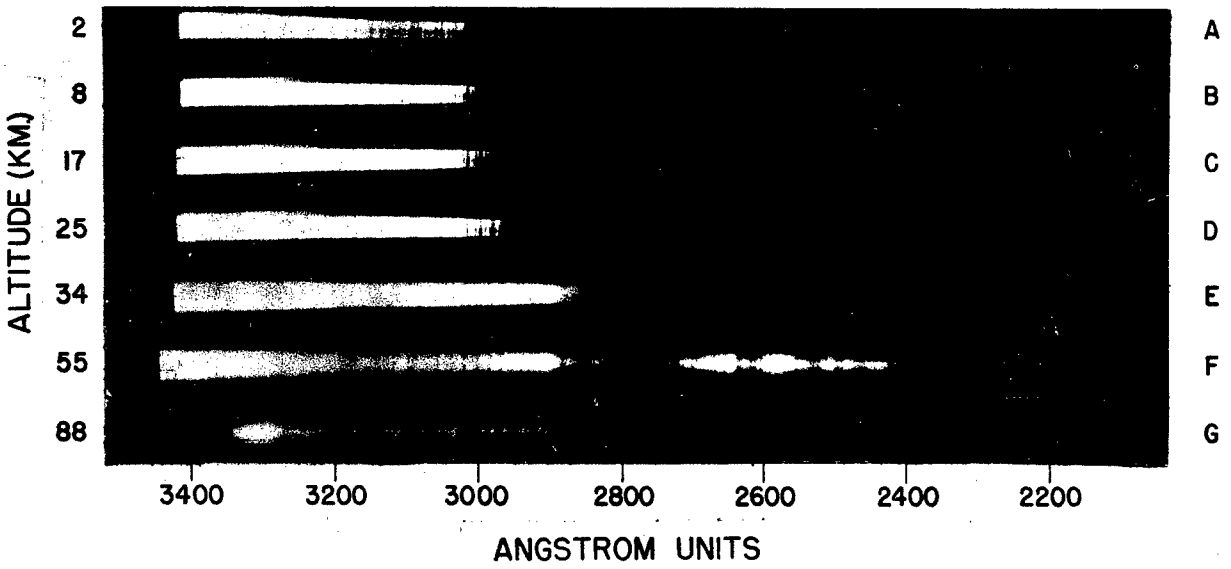

Fig. 15. Composite spectra showing ozone absorption band. The spectrum at 88 km actually extends as low in wavelength as at 55 km but because of lower intensity it did not reproduce in the print.

from the rocket. Further data are required to determine whether the disagreement at high altitudes is due to a real variation in the ozone or to experimental error. The lower maximum is known to be present on days when the total ozone content of the atmosphere is abnormally high.[28]

5. Sky Brightness. Some data in the ultraviolet are available. The experiments were not, however, designed particularly for this problem.

Future experiments in this field will aim at still lower wavelengths and greater resolution.

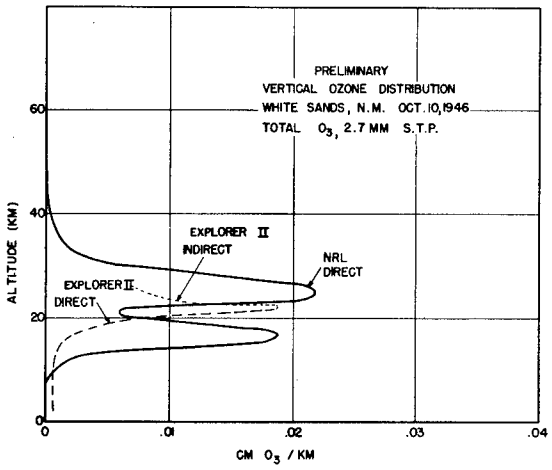

Fig. 16. Vertical ozone distribution. The double layer is rather unusual but has been reported previously.

[28] Götz, F. W. P., Der Stand des Ozonproblems, Vjs. Naturf., Ges. Zurich 89: 250, 1944.

PRESSURE AND TEMPERATURE EXPERIMENTS

Actual measurements of pressure and temperature in the upper atmosphere have been made for many years by various methods. Balloons regularly obtain this information up to 30 km. Above this altitude various indirect methods have been used, including measurements on meteors,[29] sound range measurements of large explosions,[30] and others.[2]

Although we have a vehicle which will carry us to an undreamed of altitude, the problem of measuring such basic quantities as pressure and temperature from a missile which is moving at a velocity of 1 mile a second is far from easy. This becomes clear when one calculates the adiabatic temperature rise on a thin piece of material placed on the nose of the V-2. For the velocities involved this temperature is higher than 1000° C.

Our attack on the problem to date has been to measure the so-called ram pressure at the nose of the missile and the pressure at a point on the side of the missile at which, according to wind tunnel tests, the pressure is within a very small percentage of ambient. Since a pressure range of 10^8 is covered in a normal flight, it is necessary to use various types of gauges. The range from atmospheric pressure down to about 1 cm of mercury is covered with a bellows gauge; the range of 2 cm mercury to 10^{-3} mm mercury is measured with Pirani gauges[31] while the region of 10^{-3} to 10^{-5} mm mercury is studied by means of Philips gauges[32] and ionization gauges.[33] The most complete measurements to date were obtained on flights in October 1946 and March 1947.[34,35]

---

[29]Whipple, Fred L., Meteors and the earth's upper atmosphere, Rev. Mod. Phys. 15: 246-264, 1943.

[30]Gutenberg, B., The velocity of sound waves and the temperature in the stratosphere in Southern California, Bull. Am. Met. Soc. 20: 192, 1939.

[31]Strong, J., Procedures in experimental physics, 145, New York, Prentice-Hall, 1944.

[32]Yarwood, J., High vacuum technique, 29, London, Chapman and Hall, 1945.

[33]Strong, op. cit., 143.

[34]Best, Nolan R., Eric Durand, Donald I. Gale, and Ralph J. Havens, Pressure and temperature measurements in the upper atmosphere, Phys. Rev. 70: 985, 1946.

[35]Best, N., R. Havens, and H. LaGow, Pressure and Temperature of the Atmosphere to 120 km, Phys. Rev. 71: (12), 915, 1947.

I would like to discuss briefly the March flight in which a total of 15 pressure and 2 skin temperature gauges were installed. Ambient pressures were measured up to about 80 km with gauges mounted on the side of the V-2, just forward of the tail section. Pirani gauges mounted in similar positions on opposite sides of the rocket gave readings which agree within experimental errors, indicating that no appreciable error was introduced by yaw of the missile up to this altitude. A single Philips gauge was mounted on the 15° cone of the warhead. The readings of this gauge, when reduced to ambient pressures by use of the theories of Taylor and Maccoll[36] gave values up to 120 km altitude. Pressure measurements obtained by these two methods are shown in figure 17.

Temperature measurements are of two types: (1) measurement of ambient temperatures and (2) measurement of skin temperatures and temperatures within the missile. The direct measurement of ambient temperatures from a rocket has not yet been successfully accomplished. The temperature of the atmosphere was calculated from the slope of the pressure vs. altitude curve and from the ratio of ram to ambient pressures. Pitot tube theory was used to obtain Mach number from the ratio of ram pressure to ambient pressure. The velocity of the rocket divided by Mach number gave the velocity of sound, from which temperature was calculated. Figure 18 is a plot of the temper-

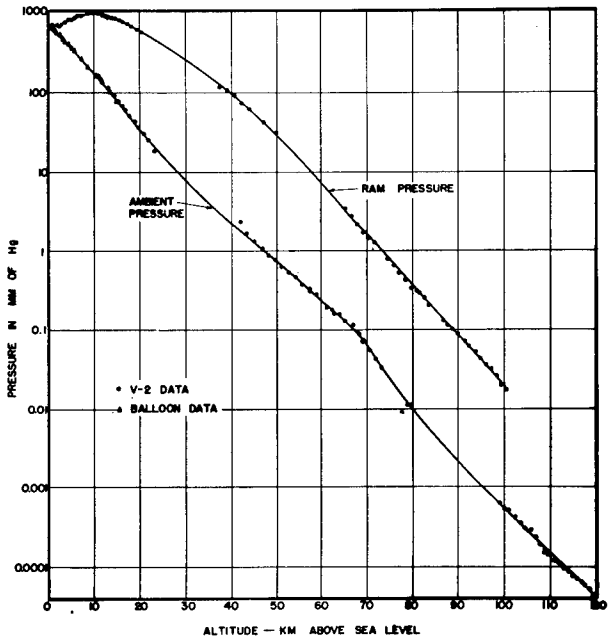

Fig. 17. Variation of pressure with altitude

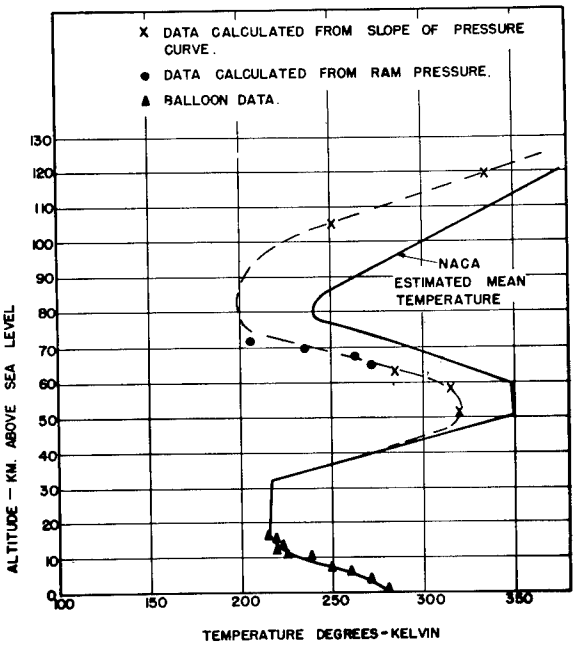

Fig. 18. Variation of temperature with altitude

[36]Taylor, G. I., and J. W. Maccoll, Proc. Roy. Soc. 139: 278, 1922.

atures derived by these methods. Shown also are the temperatures measured by means of a weather balloon released within an hour of the time of the rocket's flight. For comparison, the NACA estimated mean temperature[37] is included on the curve. Probable error is ±25° from 50 to 60 km, ±15° at 65 to 70 km, and ±20° at 72.5 km. The probable error above 100 km is ±40°. Temperatures calculated from ram pressures for altitudes between 10 and 20 km are 5 to 20° lower than the expected temperature. This discrepancy is possibly caused by errors in the velocities calculated from the poor radar data obtained during the first 20 km of the flight.

Two platinum resistance temperature gauges were installed to measure the temperature of sections of the 15° nose cone. The temperature rise on the 0.1 inch thick aluminum forward section of the nose was 120 ± 5° C. On the 0.1 inch steel section immediately behind the aluminum, the temperature rise was 85 ± 5° C.

IONOSPHERE

It is now possible to extend further our knowledge of the ionosphere[38] by utilizing rockets to make measurements within the ionized region of the upper atmosphere.

The value of experimental methods utilizing rockets may be shown by a consideration of the parameters involved in the simple approximate expression for the index of refraction in an ionized medium, neglecting the earth's magnetic field.

(1)
$$n = \sqrt{1 - \frac{4\pi N e^2}{w^2 m}}$$

n: Index of refraction
N: Ion density
e: Charge on the ion
m: Mass of ion
w: Angular frequency of radiation.

---

[37]Warfield, Calvin N., Tentative tables for the properties of the upper atmosphere, National Advisory Committee for Aeronautics, Technical Note 1200, 1947.

[38]Mimno, H. R., Rev. Mod. Phys. 9: 1, 1937.

Radio pulse ionosphere height-finding methods in wide use today[39] can at most measure directly the index of refraction at certain points, whereas rocket-borne experiments may be designed to measure directly both the index of refraction and the ion density N at all points reached by the rocket. The V-2 reaches altitudes corresponding to the top of the E layer. Since in the E layer there is at present ambiguity as to the ratio of free electrons to ions, rocket-borne experiments are the most direct way to determine whether the parameter on the right hand side of the expression should be in terms of electrons, ions, or both. A determination of data such as these will permit more accurate knowledge of many of the factors affecting long distance radio propagation, such as delay times, velocities of propagation, phase shifts, intensities and numbers of modes, direction of arrival of wave fronts, ducting, multipath phenomena, and the actual rapidity of variations of these quantities.

The method we are using for measuring the index of refraction consists of the transmission of two or more harmonically related crystal-controlled continuous wave radio frequency signals from the rocket to special receiving and recording equipment at suitable locations on the ground. These frequencies of transmission are so chosen that one is sufficiently high that its velocity of propagation is essentially unaffected by the ionosphere; that is, in the above equation, the index of refraction remains essentially unity. The other frequency is chosen to be slightly above the maximum critical frequency predicted for the regions which the rocket will penetrate. For the latter frequency, as may be seen from the equation, the index of refraction will approach zero, and as a result the velocity of propagation will be greatly affected. If one considers the phase relation between the two radio frequency signals as received on the ground, it may be shown, that for transmission from any point in the ionosphere, the rate of change of phase between the two signals as received on the ground is a function of the missile velocity and the index of refraction for the particular frequency at that point.[40] This allows the determination of the index of refraction for the low frequency as a function of altitude, with a suitable choice of the higher frequency.

The phase beat frequency experiment has successfully recorded continuous data up to an altitude of approximately 110 km and at several points above that up to 128 km.[41] Although the analysis of these data is very complex and although only a preliminary analysis has been made, I would like to

---

[39]Fleming, op. cit., ch. IX

[40]Seddon, J. C. and J. W. Siry, Upper atmosphere research report no. I, Theoretical discussion of the ionosphere experiment, Naval Research Laboratory Report R-2955: 49, 1946.

[41]Burnight, T. R., J. F. Clark, and J. C. Seddon, Upper atmosphere research report no. IV, Chap. VI, Ionosphere Research with the V-2, Naval Research Laboratory Report R-3171, 1947.

point out a few of the interesting results of this experiment. Figure 19 shows a series of curves of the received signal strength on the ground at one of the receiver stations versus the altitude of the missile. A similar set of curves was obtained at a second receiving station located about 30 miles from the first. The theoretical free-space signal strength at the receiver station should be a continuously decreasing function with altitude. The fluctuations in the curves are primarily due to ionospheric attenuation and the missile antenna patterns. The latter are being obtained from models, and the curves will be corrected accordingly. There is some reason to believe at this time that the sudden drop at 65 km is due to the presence of the D layer.

Figure 20 shows representative sections of the continuous film records obtained at one receiving station, and illustrates very clearly the different types of complex beats obtained. The phase beat frequency first became apparent at about 43 km altitude and remained at a low value up to about 84 km. This would imply that if a D layer exists in this region its effect on the 4.274 Mc signal was small below 84 km. The phase beat frequency increased rapidly at 84 km. At 111 km the beat frequency is lost owing to loss of the 4.274 Mc signal. Intensive analysis of the phase beat frequency data is continuing and it is hoped that a more definite report will be available in about six months.

Many experimental problems associated with the ionosphere work have been encountered and solved, and a great deal of invaluable experience as to a suitable instrumentation for rocket investigation has been acquired. It was soon found that the problem of developing suitable antennas for transmitting at low frequencies from the rocket was a major problem. Considerable theoretical and laboratory research has been carried out to establish a fundamental basis for the direct measurement of the electron and ion densities as a function of altitude. An experiment is virtually complete for inclusion in a July flight, which involves primarily a determination of the saturation current for electrons and positive ions.

MISCELLANEOUS

Cameras have been included in several flights and pictures obtained to altitudes of 160 km.[42] A composite of several such pictures is shown in Figure 21. The Gulf of California and surrounding terriority are clearly evident in the picture. Photographs of this type are very useful for meteorological cloud studies as well as for cartographic purposes.

On the night of December 17, 1946, the first night V-2 launching in this country was made for the purpose of conducting an experiment with artificial

---

[42]Bergstralh, T. A., Photography from the V-2 rocket at altitudes ranging up to 160 kilometers, Naval Research Laboratory Report R-3083, 1947.

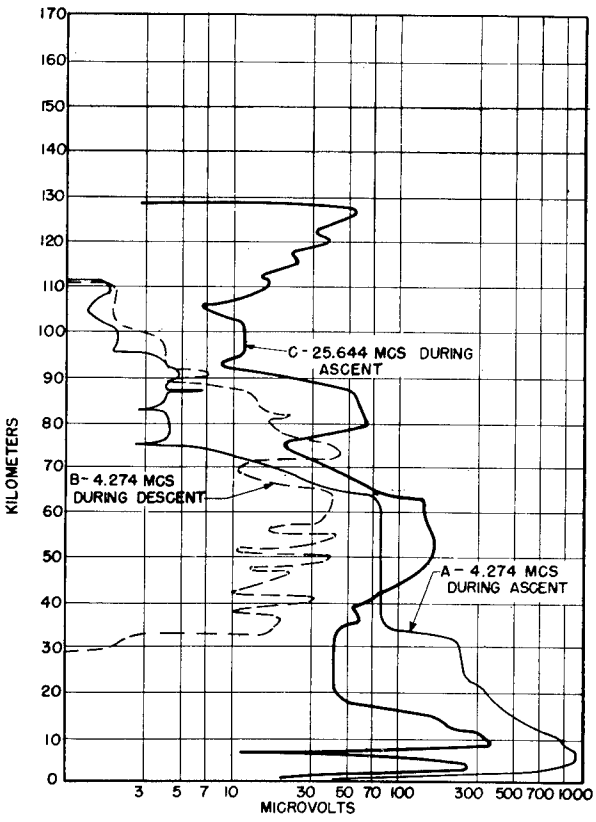

Fig. 19. Signal strength versus altitude as recorded at one of two ionosphere ground stations at White Sands, New Mexico, between 11:23 and 11:30 A.M. MST during the V-2 flight of 7 March 1947

A. Altitude 12 Km., 43 Seconds After Takeoff

B. Altitude 79 Km., 94 Seconds After Takeoff

C. Altitude 90 Km., 103 Seconds After Takeoff

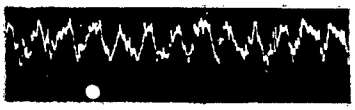

D. Altitude 100 Km., 113 Seconds After Takeoff

E. Altitude 111 Km., 123 Seconds After Takeoff

Fig. 20. Representative sections of the continuous film record showing beats of harmonically related frequencies. (a) Record obtained below the ionosphere (up to 43 km). (b) Slowly varying beat recorded at an altitude of 79 km. (c) Record at approximately 90 km showing a well defined wave form. (d) The beat above 100 km showing a more complex wave form. (e) The sudden cessation of the phase beat frequency at 111 km at which point the 4.274 mcs signal disappeared completely.

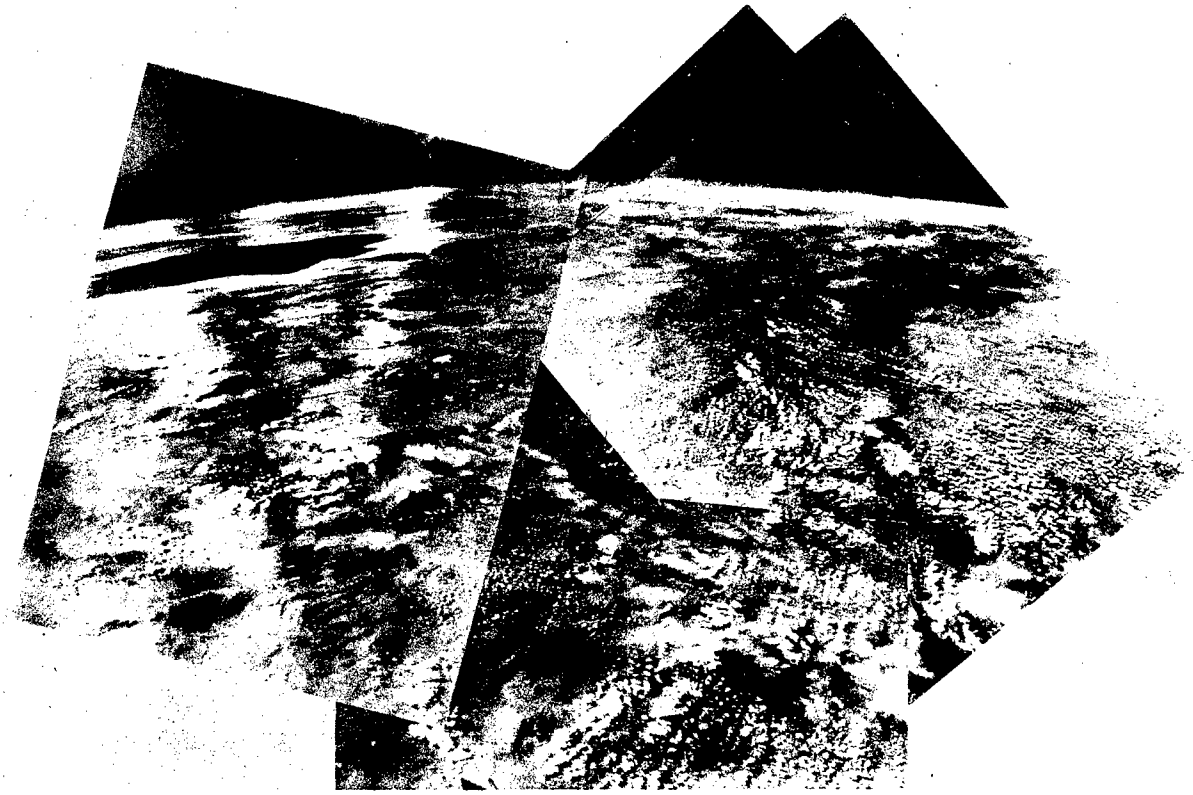

Fig. 21. A composite picture made up of three separate photographs taken at an altitude of 162 kilometers (101 miles). This picture covers approximately 500,000 square miles of southwestern United States and northern Mexico. The photographs do not match exactly owing to the varying camera angles.

meteorites. This experiment, conducted jointly by the Applied Physics Laboratory, the California Institute of Technology, and Harvard University, consisted of dropping out special charges, at intervals of about 20,000 feet, above 60,000 feet. The charges were to explode one or two seconds after leaving the missile. High velocity particles should then appear as artificial meteors and as a matter of fact in a few cases some of the particles might have enough velocity to escape the earth. This experiment was unsuccessful because of ejection difficulties but will be repeated sometime this fall.

On various flights special strains of rye seeds, corn seeds and fruit flies have been taken to altitudes of 170 km to determine whether radiation above the atmosphere might produce mutations. The order of magnitude of cosmic radiation was, of course, known and because of its low intensity very little or no effect was anticipated. However other less energetic radiation might exist at these altitudes which could possibly produce an effect. Analysis made by Harvard on recovered seeds and flies has shown that no detectable changes are produced by the radiation. These results are not yet conclusive because in most cases the seeds were shielded by metal (in order to facilitate recovery) so that only the higher energy radiation would have been effective. If recovery methods are improved, containers having very thin walls will be used to study the effects of the lower energy radiation.

In general the various laboratories involved are approaching the above problems in different ways. Numerous other experiments are being planned for the future, of which a few might be mentioned. The Applied Physics Laboratory and the Watson Laboratories are both planning different types of experiments to measure the intensity of the earth's magnetic field at different points in space. Three very interesting experiments—one to measure temperature, a second to take samples of the atmosphere, and a third to measure wind direction and velocity at various altitudes are to be conducted by the Signal Corps in a July firing. The measurement of temperature is to be accomplished by measuring the velocity of sound, generated by explosive charges detonated at various altitudes up to 60 km, between the rocket and the ground. Samples of the atmosphere are to be obtained at various altitudes up to 80 km by opening and sealing sample bottles at various altitudes. Wind velocities will be measured between the altitudes of 30 and 60 km by releasing smoke from a specially installed smoke generator after the rocket has reached approximately 30 km altitude. The smoke will then be tracked by optical instruments on the ground.

The next several years should see very interesting developments in the field of upper atmosphere research, now that the techniques and ground work therefor have been laid. At the present rate of firings there is a sufficient number of V-2's on hand to last for another two years. Because of this, numerous long range experiments are planned which are more complex than any that have been performed so far. The rocket has opened the door to vast regions of space which at present are known to us primarily through the astronomer's telescope. When one considers the large amount of work that has been done by the astronomers and the greater understanding of the universe that this work has given us, one cannot help being impressed by the research potentialities of this new field.

CHAPTER II

THE THIRD AND FOURTH CYCLES OF V-2 FIRINGS

by

J. W. Siry

As in earlier reports of this series it is convenient to regard the V-2 missiles fired by the Army Ordnance Department at White Sands as grouped into cycles. On this basis missiles 16 through 20 comprised what will be referred to as the third cycle of V-2 firings; missiles 21 through 24, the fourth cycle. Of these, the Naval Research Laboratory furnished the upper atmosphere research equipment for missiles 16, 18 and 21 which were fired on December 5, 1946, January 10, 1947 and March 7, 1947 respectively. The firing of the third cycle was accomplished during the period from December 5, 1946 to February 20, 1947; and the fourth cycle occurred in March and April of 1947. The important features of the flights in these two cycles are shown in Tables I and II.

The opening of cycle III stood in striking contrast to the first flight of the second cycle of V-2 firings. The firing of missile 16, which took place on December 5, 1946, was attended by a rare combination of mishaps. For the first time the rocket was successfully tracked by means of a telescope to the peak of its trajectory and during the descent until it disappeared behind a cloud after 330 seconds of flight. Immediately after Brennschluss it was seen to begin tumbling in end-over-end fashion. Presumably it continued to execute this motion throughout the remainder of the flight. This highly erratic performance precluded the possibility of obtaining useable information from the rocket. The observed tumbling of the December 5 missile immediately raised the question of whether earlier V-2's, which had not been followed successfully by optical means, also tumbled after Brennschluss. A review of the experimental data obtained on the earlier flights, however, showed no marked periodicity or fading which certainly would have been present had the rocket tumbled.

The missile rose to an altitude of 153 km (95 mi) and traveled 211 km (131 mi) horizontally. The impact area was located in the range of mountains to the north of White Sands. No parts of the wreckage were recovered.

The first V-2 to be fired in 1947, the eighteenth since the start of the program, took to the air on January 10 at 2:13 P.M., M.S.T. While a 7° tilt program was provided for, actually, the trajectory was inclined at an angle of about 5° to the vertical during the burning period. The fuel was spent 60 seconds after take-off, when the missile had an altitude

TABLE I

SUMMARY OF THE THIRD CYCLE OF V-2 FIRINGS

December 5, 1946 through February 20, 1947

Firing	Date	Research Agencies	Altitude Km.	Altitude Mi.	Range Km.	Range Mi.	Remarks
16	Dec. 5, 1946	Naval Research Laboratory	153	95	211	131	Rocket tilted at takeoff and tumbled throughout most of flight.
17	Dec. 17, 1946	Applied Physics Laboratory	183	114	31	19	Highest altitude attained to date.
18	Jan. 10, 1947	Naval Research Laboratory	119	74	40	25	Research facilities of this rocket devoted to cosmic ray studies. Air burst achieved and recovery effected.
19	Jan. 23, 1947	General Electric Company	47	29	26	16	Rocket spiraled during flight.
20	Feb. 20, 1947	Air Materiel Command	109	68	31	19	Air burst achieved.

TABLE II

SUMMARY OF THE FOURTH CYCLE OF V-2 FIRINGS

March 7, 1947 through April 17, 1947

Firing	Date	Research Agencies	Altitude Km.	Altitude Mi.	Range Km.	Range Mi.	Remarks
21	Mar. 7, 1947	Naval Research Laboratory	162	101	58	36	Improved telemetering antenna and warhead employed. Good results obtained spectroscopy, photography, and atmospheric pressure studies.
22	Apr. 1, 1947	Applied Physics Laboratory	121	75	43	27	Successful flight.
23	Apr. 8, 1947	Applied Physics Laboratory	103	64	31	19	Except for low altitude, normal flight.
24	Apr. 17, 1947	General Electric Company - Signal Corps	143	89	72	45	Normal flight, no recovery attempted.

of 32 km (20 mi). It reached the peak of its trajectory at 119 km (74 mi) above White Sands after 189 seconds of flight. The program timer[1] was preset to blow off the warhead 365 seconds after the V-2 left the ground, but was not relied upon since the rocket followed a lower trajectory than was expected. Instead, the signal to detonate the explosives was given by radio[1] 300 seconds after take-off. The missile broke up almost immediately, the parts falling to earth in an area whose center was approximately 25 miles north by west of the launching site.

The after part of the V-2 was the first section to be found. It is shown in figure 22. The cosmic ray recording camera,[2] which had been mounted in the tail section, was recovered. The warhead was located later. It had evidently landed in a horizontal position, for it was flattened by the impact, as can be seen from an inspection of figure 23. The Daughter ejection device was released 172 seconds after take-off, but landed in a morass and was not recovered.

Missile 21 took off at 11:23 A.M., M.S.T. on March 7, 1947. Brennschluss occurred 63 seconds after take-off. The V-2 had then attained its maximum velocity, 1,560 mps (5,120 fps), and was tilted toward the north with a zenith angle of 7°. The winds from the east then caused the missile to begin turning in that direction. This motion probably continued throughout the rest of the flight. At the peak of the trajectory, 162 km (101 mi) above White Sands, the rocket was inclined toward the northeast at a zenith angle of approximately 10°. The radio detonation signal was transmitted 330 seconds after take-off; the program timer had been set to detonate the explosive 3 seconds earlier. As on previous flights, actual breakup of the explosion-weakened rocket structure apparently occurred sometime after the blowoff signal was given, when the resistive forces offered by the denser atmosphere below became sufficiently great. In this case a complete breakup appears to have taken place 402 seconds after take-off. The parts fell to earth over a wide area of the white sands which give the region its name. The details of the flight are summarized schematically in the trajectory which is shown in figure 2.

The equipment to be recovered was well separated from the remainder of the rocket debris. Visibility in the white sands was unusually good, as can be seen from figure 24. This made recovery of equipment after the flight relatively easy.

---

[1] Naval Research Laboratory Report No. R-3030, Chapter II, Section B. (Unclassified)

[2] Op. cit., Chapter IV, Section D.

Fig. 22. V-2 engine as found after the January 10, 1947 flight

Fig. 23. Warhead recovered from the January 10, 1947 flight

Fig. 24. Parts of the V-2 as they were found in White Sands region after the March 7, 1947 flight

CHAPTER III

INSTRUMENTATION FOR THE THIRD AND FOURTH CYCLES OF V-2 FIRINGS

by

T. A. Bergstralh and C. P. Smith

A. Installations in the Rockets of the Third Cycle

The installations in the V-2 which was fired on December 5, 1946 were similar in general plan and arrangement to those employed in previous missiles and described in earlier reports of this series.[1] Three changes are worthy of note: 1) The successful attempts at recovery by means of rocket breakup led to the decision to discontinue the employment of ejection mechanisms and equipment. 2) A set of three photocells was installed. These were designed to furnish information concerning the aspect of the missile. 3) Two K-25 aircraft cameras were mounted in the midsection between the alcohol and oxygen tanks to photograph the earth and certain external installations on the missile. Previously, this function had been performed by 16 mm motion picture cameras installed in the tail ring of the V-2. All of these innovations continued in general use in the later V-2 firings discussed in this report. A typical night installation scene appears in figure 25.

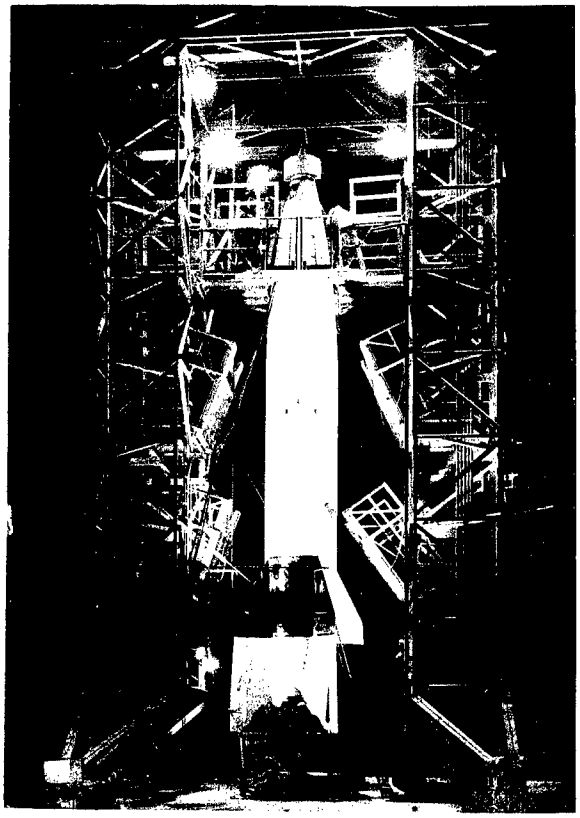

Fig. 25. Installing equipment in the V-2 fired on December 5, 1946

The January 10, 1947 rocket was unique in that it was devoted entirely to a single phase of upper atmosphere research: the study of cosmic radiation. Two separate installations were made, each designed to perform a complete experiment. A total of forty-nine Geiger-Mueller counter tubes were employed in the two telescopes. Each of these telescopes was served by its own electronic unit. A specially constructed thin-walled nose section was substituted for the usual cast steel spectrograph chamber in order to reduce the total mass present above the telescope. Three photocells and a gyroscope were installed to

[1] Upper Atmosphere Research Reports Nos. I, II, and III, (Naval Research Laboratory Reports Nos. R-2955, R-3030, and R-3120.

determine the aspect of the missile. The photocells were located at 120 degree intervals around the warhead. The telescope, the electronic units, and the locations of the photocells are shown in figures 26 and 27. A modified Schwein gyroscope was mounted in quadrant III of the control chamber. A cosmic ray recording camera was carried in a pressurized steel container which was installed in the tail section on the motor support frame just aft of the oxygen tank.

A block diagram of the missile wiring is given in figures 28 and 29. The entire warhead weighed 1,000 kg (2,200 lbs), 373 kg (823 lbs) of which consisted of steel and lead counterweights added to locate the center of gravity properly.

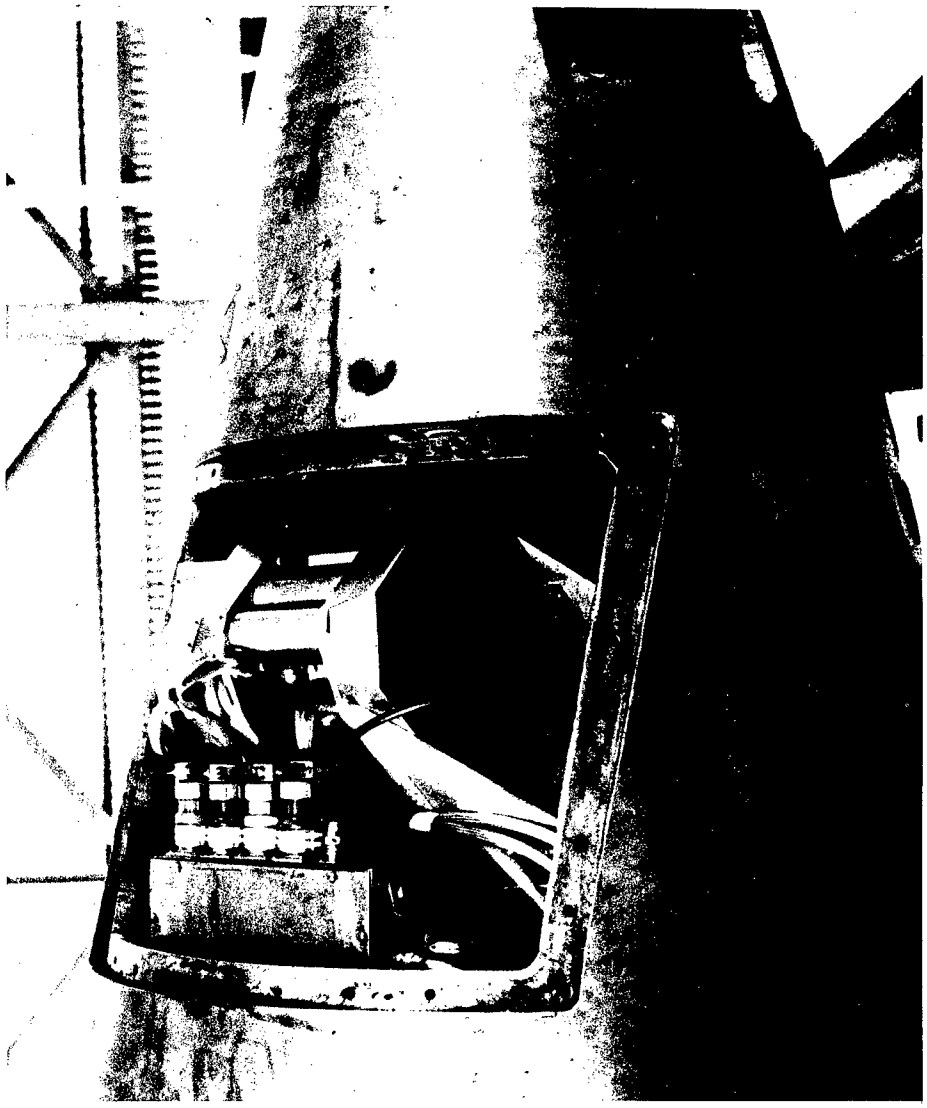

Fig. 26. A view of the January 10 warhead showing the locations of a cosmic ray telescope and two of the photoelectric cells

Fig. 27. Cosmic ray telescope and electronics mounted in the January 10 warhead

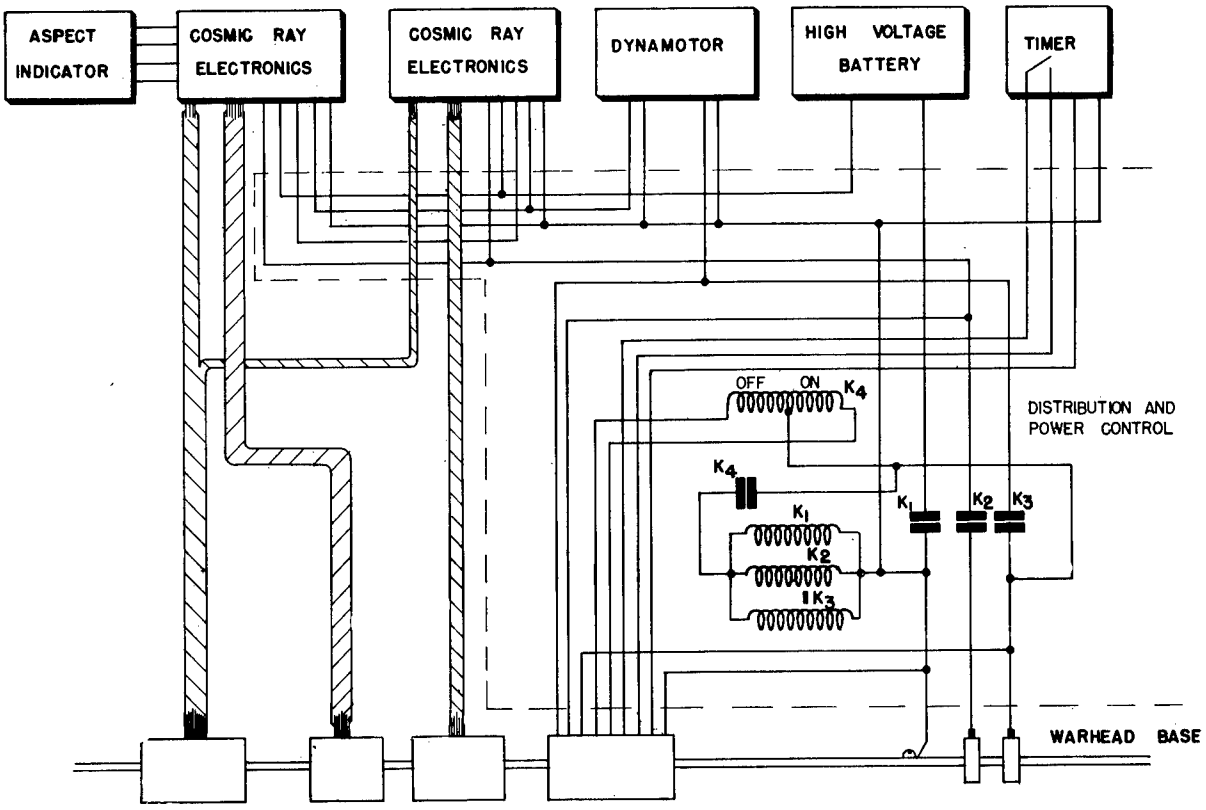

Fig. 28. Overall wiring diagram for the January 10 missile, part 1

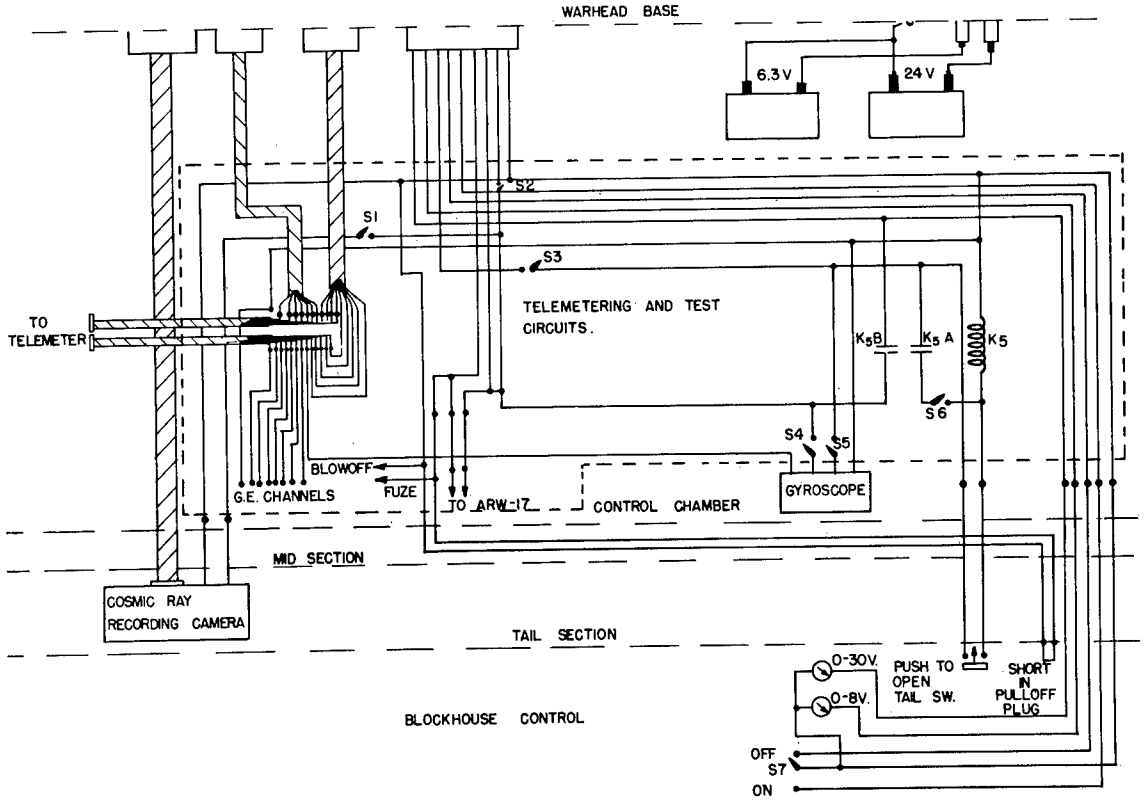

Fig. 29. Overall wiring diagram for the January 10 missile, part 2

B. Installations in the March 7 Rocket

The V-2 warhead designed by the Naval Research Laboratory for upper atmosphere research in the earlier flights contained a cast steel spectrograph chamber, which gave rise to a number of cosmic ray showers which in turn tended to obscure the results of the cosmic ray experiments. As a result, when the spectrograph was moved to its new location in fin II, a new type warhead was designed and constructed to eliminate some of the cosmic ray shower production.

The original warhead comprised three sections, a nose tip, a nose cone, and a main warhead body, each of which was made of 9.6 mm (0.375 in.) cast steel. For this flight the portion of the main warhead body forward of the lower access doors was removed and an upper base plate of 13 mm (0.5 in.) steel installed. This gave a main body 84 cm (33 in.) long with base diameters of 60.63 cm (23.84 in.) and 95.57 cm (37.625 in.). A nose cone 1.264 m (49.75 in.) long, with a base diameter of 60.63 cm (23.84 in.) was constructed to complete the warhead. The lower 64.8 cm (25.5 in.) of this cone was built of 2.6 mm (0.104 in.) steel, the forward section of the cone was fabricated from 1.6 mm (0.0625 in.) aluminum.

Thus the heavy rib construction associated with the upper base of the main warhead body and the lower base of the spectrograph chamber was eliminated. The warhead wall material was reduced in thickness and in atomic number. As a result, the probable number of cosmic ray showers produced in this portion of the warhead shell was reduced by at least an order of magnitude. In addition, the entire nose was removable from the lower section of the warhead to facilitate the mounting and testing of the cosmic ray equipment. The locations of the various experimental and service installations in the March 7 missile are given in figure 6. The modified warhead is shown assembled in figure 30, the main body appears in figure 31 and the nose cone in figure 32.

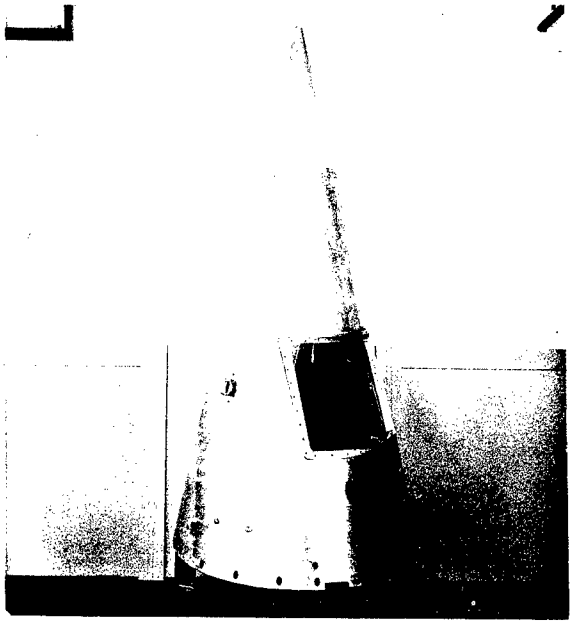

Fig. 30. The modified V-2 warhead used for the first time on March 7, 1947

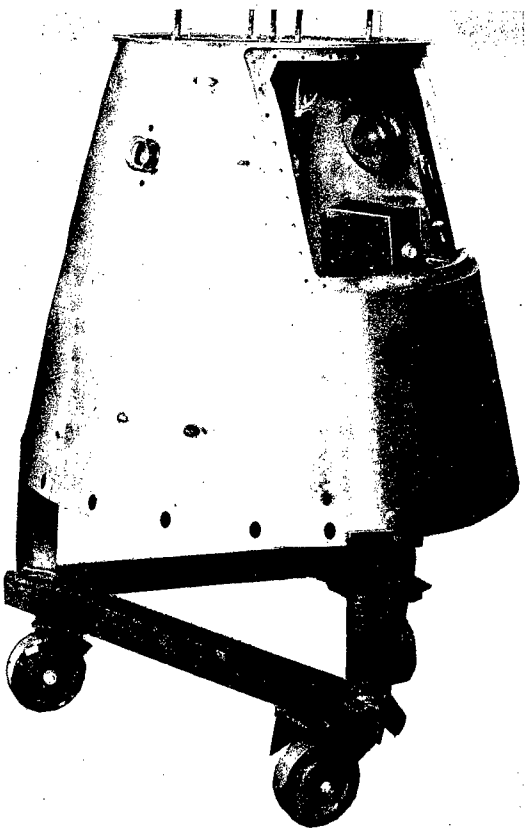

Fig. 31. The main body of the modified warhead

Fig. 32. The nose cone of the modified warhead

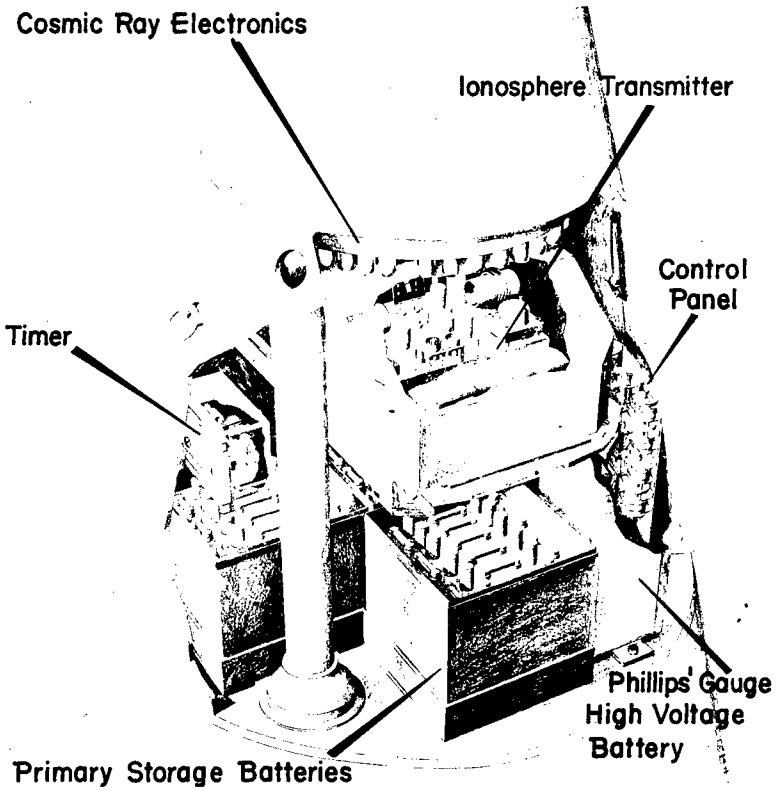

Fig. 33. Installations in the main body of the March 7 warhead

A wide variety of experimental equipment was installed in this warhead. The nose cone section was utilized to mount the following items, all of which are visible in figure 7.

(a) Pressure measuring apparatus consisting of a bellows gauge and four Pirani pressure gauges in the forward tip of the nose section. These covered the range of pressures from 10^3 mm Hg to 10^{-3} mm Hg.

(b) Two elements designed to measure the temperature of the aluminum and steel sections of the nose cone.

(c) A forty-five counter cosmic ray telescope mounted on the upper base plate of the main warhead section. The telescope, shielded by 454 kg (1,000 lb) of lead, occupied almost all of the forward nose section. It can be seen in figure 11. Two 150 watt space heaters were mounted on the lead shielding to maintain the temperature of the counters at the proper level during testing periods and at other times prior to flight.

The main warhead body carried the following equipment, as shown in figures 33 and 8.

(a) Ionosphere study equipment consisting of a double frequency transmitter unit in a 6.4 mm (0.25 in.) aluminum case. This was mounted upon two horizontal track members which spanned the warhead at the level of the lower edges of the main access doors.

(b) A Philips gauge and a Pirani gauge, both of which measured ambient pressure. These were located near the base of the warhead.

(c) An electronic system for the cosmic ray experiment. This unit was circular in form, of radius ten inches, and was suspended from the upper base plate of the main warhead body as shown in figure 11.

(d) A program timer which operated the cameras and provided for spectrograph film windup and missile breakup.

(e) Three vibration pickup units which measured vibration frequencies and amplitudes along three orthogonal axes.

(f) A distribution panel which supplied power to the various installations in the warhead, and combined the outputs of these equipments before they were fed to the telemetering transmitter.

(g) A commutator which was employed in connection with the temperature, pressure and ionosphere equipments. This unit subcommutated each of four telemetering channels into 14 sub-channels.

(h) Batteries, including a high voltage battery for the cosmic ray telescope, a 3000 volt battery to operate the Philips gauge, and batteries for primary power supply. One of the latter supplied -12 volts and -24 volts to the ionosphere transmitter, another provided the 24 volt power to the remainder of the experimental equipment, and the third was modified into a three section 8 volt battery for supplying filament requirements.

The instrumentation in the control chamber was as follows (cf. figure 9):

(a) The telemetering transmitter located in quadrant I, and the filament batteries for this transmitter in quadrant IV.

(b) The ARW-17 emergency cutoff receiver installed in quadrant II. This was the rocket-borne receiver of the system which provided remote control of the fuel cutoff and missile breakup circuits.

(c) A gyroscope measured the rate of rocket roll. This instrument, a modified Schwein gyroscope provided with a microtorque potentiometer, was mounted on the gyroscope plate in quadrant III.

(d) A telemetering and test switch junction box which facilitated the control and testing of all of the experimental installations in the rocket. This unit was installed in quadrant I.

(e) A Willard ER-8-30 30-volt storage battery, encased in a pressurized box, which provided power for the K-25 aircraft cameras.

Two K-25 aircraft cameras were mounted in the midsection of the missile to photograph the earth, and to provide information as to the motion of the rocket. The mounting of these cameras and the photographic results obtained are more completely described in Chapter IX.

The following experimental installations were made in the tail section:

(a) A spectrograph was mounted in fin II in a manner similar to that employed in the October 10 installation. A Pirani gauge was included in the spectrograph housing to measure the pressure. The entire fin was painted bright orange in order to facilitate the recovery of the spectrograph.

(b) One bellows gauge and six Pirani gauges were mounted on the skin of the rocket just forward of fins I and III. These gauges were designed to measure ambient pressure.

(c) An ionosphere antenna assembly, which comprised two L-type antennas, was mounted on the fins. Each antenna extended halfway around the rocket. The supporting stubs, of 32 mm (1.25 in.) outside diameter, were mounted 9.5 cm (3.75 in.) forward of the stabilizing vanes and projected 15 cm (6 in.) beyond the edge of each fin.

(d) A 19 channel cosmic ray recorder was mounted in a 6 mm (0.25 in.) steel container, which was attached to one of the rocket motor supports. This installation appears in figure 34.

The overall rocket wiring diagram is given in figures 35 and 36. This diagram shows all of the wiring for the experimental equipment installed in

Fig. 34. The cosmic ray recorder mounted in the March 7 V-2

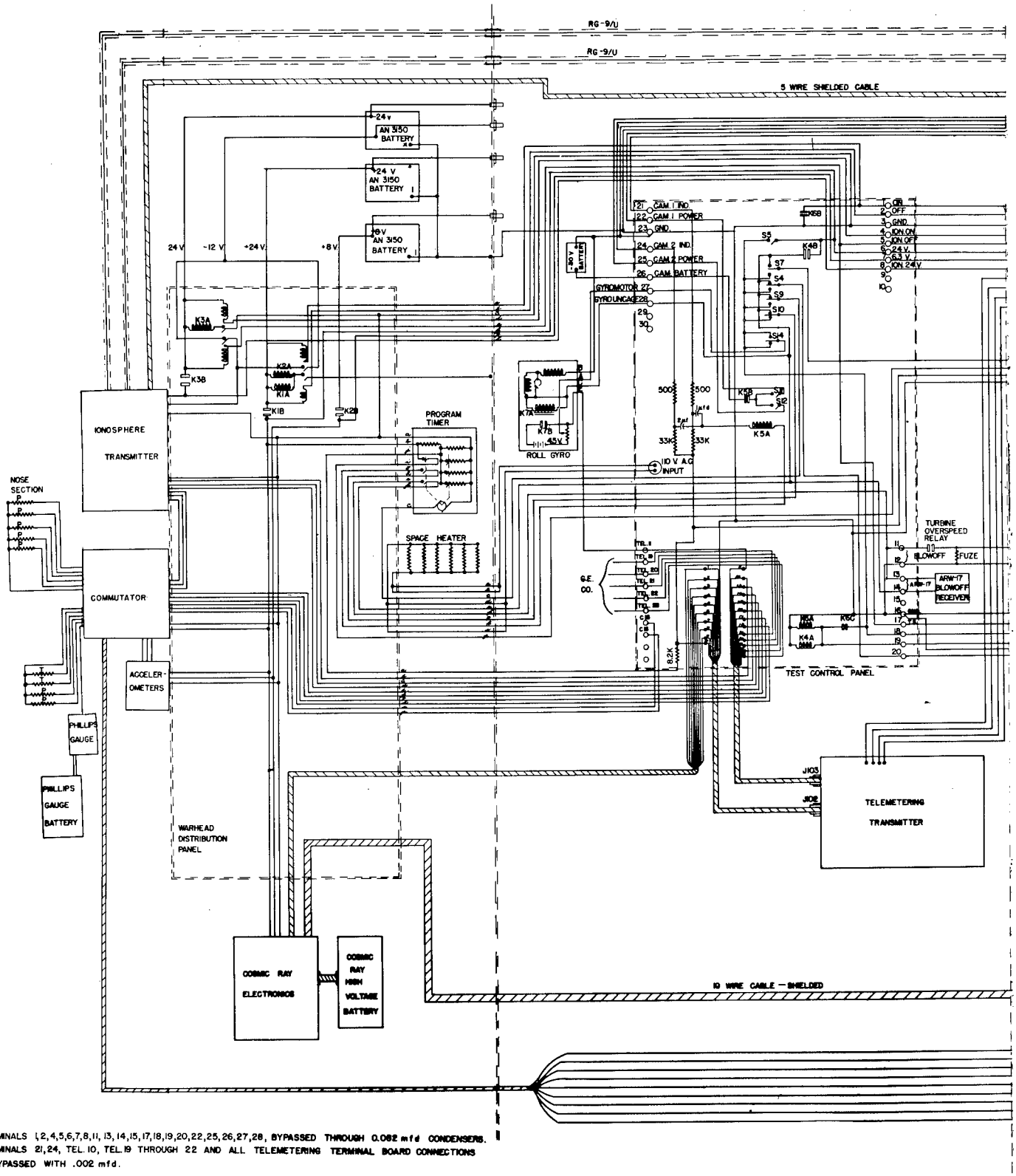

NOTE:
TERMINALS 1,2,4,5,6,7,8,11, 13, 14,15,17,18,19,20,22,25,26,27,28, BYPASSED THROUGH 0.082 mfd CONDENSERS.
TERMINALS 21,24, TEL. 10, TEL. 19 THROUGH 22 AND ALL TELEMETERING TERMINAL BOARD CONNECTIONS BYPASSED WITH .002 mfd.

Fig. 35. Overall rocket wiring diagram for the March 7 missile, part 1

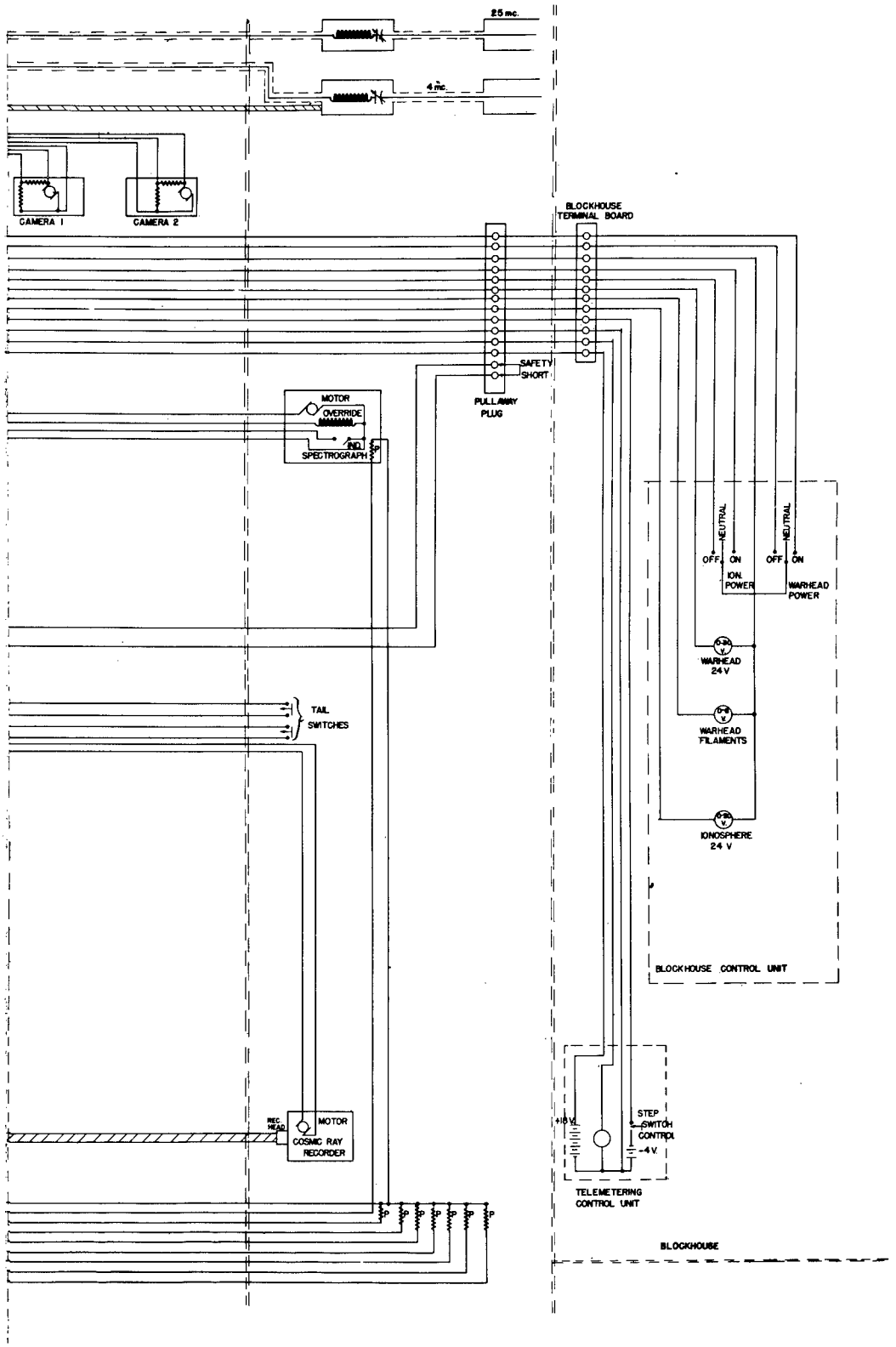

Fig. 36. Overall rocket wiring diagram for the March 7 missile, part 2

the missile by the Naval Research Laboratory. The cabling in the midsection of the rocket was installed at the White Sands Proving Grounds in accordance with the requirements of this Laboratory. The weight (1073 kg, or 2365 lb) of the completely equipped warhead, and the position of its center of gravity (51 cm, or 20 in., from the base), were such that no counterweights were required.

Previously, missile breakup had been accomplished by the detonation of TNT charges attached to each of the four structural members holding the warhead mounting ring. This arrangement was supplemented in the March 7 V-2 by a provision for separating the tail assembly. Five turns of primer cord were attached directly to the fuselage skin so as to encircle the rocket just aft of the point at which the tail assembly is bolted to the main frame of the missile. Provision was made to detonate all of these explosives simultaneously. The effort was successful, for the rocket broke up completely when it reached the denser atmosphere as it neared the end of its descent. Experimental equipment and rocket parts were found scattered over a large section of the white sands region. The items of interest were found well separated from the other rocket debris.

CHAPTER IV

COSMIC RAY RESEARCH ABOVE THE ATMOSPHERE

Introduction

Research into the nature and properties of the cosmic radiation as it exists above the earth's atmosphere received major emphasis in the third and fourth cycles of V-2 firings. Experiments were performed in the rockets fired on January 10, and March 7, 1947. The results obtained during these two flights were reported on in two letters to the Editor of The Physical Review[1], which are reproduced here in Sections A and B. The complex electronic circuitry which was employed to record these results is described in the next three sections. The basic methods developed are discussed in a paper which is currently appearing in The Review of Scientific Instruments[2], and is given here in Section C. The particular applications of, and modifications to, these methods which were incorporated in the January 10 and March 7 experiments are detailed in Section D. Two of the various means for determining missile aspect are also taken up in this Section.

A. Non-primary Cosmic-Ray Electrons above the Earth's Atmosphere

by

G. J. Perlow and J. D. Shipman, Jr.

In a V-2 rocket fired to a height of 70 miles on January 10 at White Sands, New Mexico, data were obtained on the penetration of cosmic rays through 2 and 4 cm of lead. In addition showers below each lead slab could be measured. The apparatus is diagrammed schematically in figure 37. Its axis was at 45° to that of the rocket and during flight it precessed about the latter. The rocket axis was a few degrees off vertical. The telescope pointed through a steel "window" 2.8 mm thick. Protection against warhead showers, found in this and each previous flight[3], was obtained by anti-coincidence counters (marked with crosses in the figure). The arrangement of the equipment in the warhead was such that a considerable amount of lead shielded most of the solid angle from below. The significance of this will be seen presently.

While a full account of the experiment awaits more detailed analysis, it seems desirable to report one interesting result at this time — namely,

---

[1] G. J. Perlow and J. D. Shipman, Jr., Phys. Rev. 71, 325 (1947); and S. E. Golian and E. H. Krause, Phys. Rev. 71, 918 (1947).

[2] B. Howland, C. A. Schroeder and J. D. Shipman, Jr., Rev. Sci. Inst. 18, No. 8 (1947).

[3] S. E. Golian, E. H. Krause, and G. J. Perlow, Phys. Rev. 70, 223 (1946) and 70, 776 (1946).

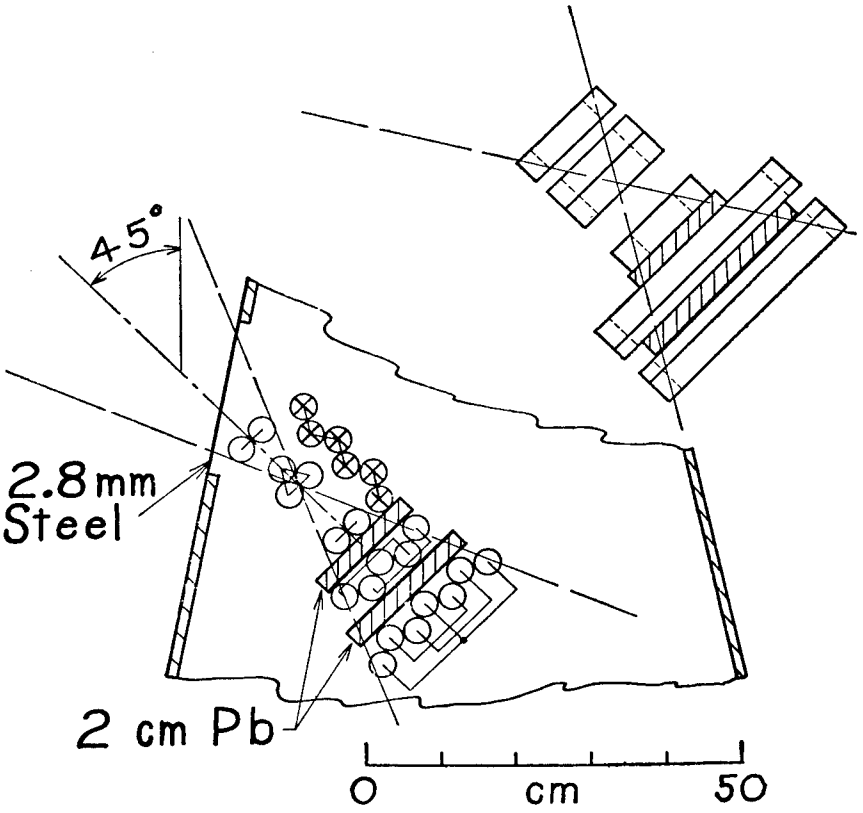

Fig. 37. Counter telescope in V-2 warhead

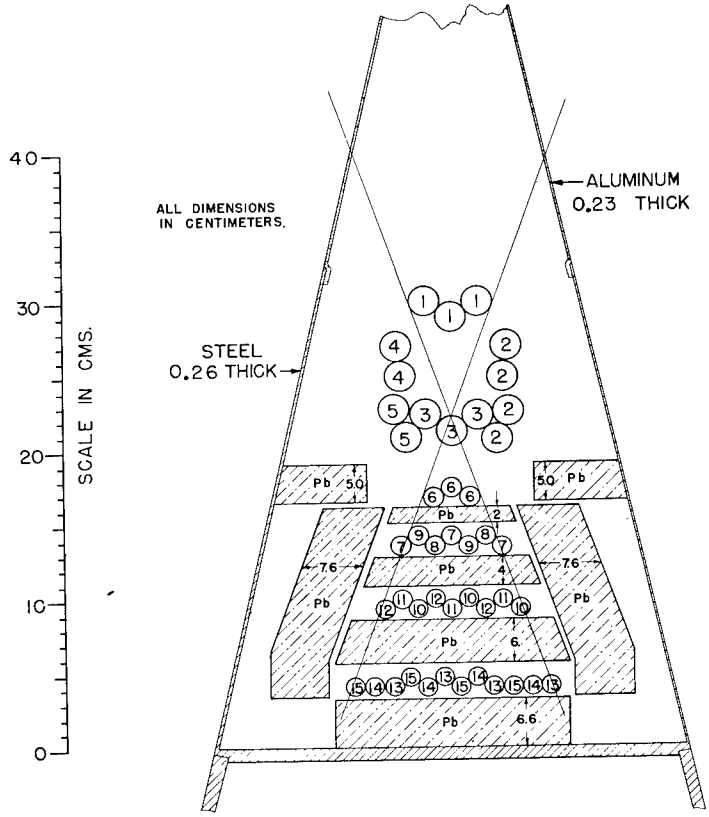

Fig. 38. Counter-tube telescope arrangement

the presence above the earth's atmosphere (<1 mm Hg) of relatively large numbers of particles absorbed in the lead. About 25 percent of the total ionizing component was stopped in the first 2 cm and 10 percent in the second. Of the latter group about 1 in 8 produced showers tripping at least 3 counters under the first slab. The number of particles stopping in 4 cm or less was about the same as the number which penetrated without multiplication. The remainder of the radiation penetrated 4 cm and produced showers either under 2 or 4 cm, or under both. The soft particles (range $\leqq 4$ cm) had an intensity in free space roughly 15 percent of the total intensity observed in the flight at the Pfotzer maximum.

It seems most reasonable to ascribe this soft radiation to electrons. On the basis of the cascade theory these will have energies $<5 \times 10^8$ ev for the most part. An extrapolation by Mr. Siry of this laboratory of the Lemaitre-Vallarta curves to 40° N geomagnetic latitude gives as the minimum energy for an extra-terrestrial electron $\sim 4 - 5 \times 10^9$ ev at 45° zenith angle. Thus the soft electrons appear to come as re-entrant particles generated in some atmospheric layer below.

The existence of such a component was suggested to the group at this laboratory by Professor J. A. Wheeler in a private communication some time ago. It was pointed out that the almost isotropic angular distribution of the decay electrons from low energy mesons would result in some vertical intensity upwards and that these would describe helical orbits about the magnetic field lines. It is possible that the soft particles observed are to be ascribed to this hypothesis.

If the downcoming soft particles observed arise from some atmospheric layer below, then an appreciable upward intensity must exist and it would appear that the results of certain types of balloon experiments reported in the literature might require some reinterpretation. A search will be made in a future rocket for an upward intensity.

B. Further Cosmic-Ray Experiments above the Atmosphere

by

S. E. Golian and E. H. Krause

Another in the series of experiments to determine the nature and reaction of the primary cosmic radiation above the atmosphere was performed in a V-2 fired on March 7, 1947 from the White Sands Proving Ground, New Mexico, to an altitude of 102 miles. A counter-tube telescope was arranged so that the percentage of particles penetrating 2 cm, 6 cm, and 12 cm of lead could be determined. The number of threefold showers under these same thicknesses was also measured.

The telescope was mounted vertically in a specially designed warhead so that it looked directly through the warhead nose as shown in figure 38.

The heavy lead shielding around the lower half of the telescope was in-

troduced in an attempt to reduce the number of rocket showers found in previous experiments.[4,5] This shielding in conjunction with the absorbing lead plates was sufficient to eliminate most of the registered rocket showers of primary or non-primary electronic origin. It was found that the number of rocket showers actually doubled over that of previous unshielded experiments. This would indicate that these showers must be of non-electronic origin. By the use of eight anticounters 2, 4, and 5 used in groups of 2, 4, 6, and 8 (quantity, not counter numbers) it was established that the policing efficiency was very good.

The information obtained included the following coincidences and anticoincidences: [1,3,6]; [1,3,6, -5]; [1,3,6, -2]; [1,3,6, -(2+4+5)]; [1,3,6, 7+8+9]; [1,3,6,10+11+12]; [1,3,6,13+14+15]; [1,3,6,13+14+15,-(2+4+5)]; [1,3, 6,7,8,9, -(2+4+5)]; [1,3,6,10,11,12, -(2+4+5)]; [1,3,6,13,14,15, -(2+4+5)]. Note: The negative sign in front of a symbol signifies anticoincidence. The data reported here were all obtained above the atmosphere (pressure less than 2 mm Hg). A total of 887 events were recorded of which 275 were events not involving rocket showers. Of the 275, it was found that above the atmosphere 25 percent were absorbed in 6 cm of lead. Although this is somewhat less than that reported by Perlow and Shipman[4] it is assumed to be the same type of non-primary electron component discussed by them. The different percentages in the two experiments are attributed to the variation of this component with zenith angle. A total of 59 percent of the particles penetrated 12 cm of lead. Of these, the most frequent single event penetrated without producing showers under the lead plates. About half the particles penetrating the 12 cm produced showers in one or more of the counter trays. The remaining 16 percent was absorbed in 12 cm. Here again the larger portion did not produce showers under the lead. Thus, primary electrons would be ruled out, since these would produce large showers under 2 and 4 cm. As a matter of fact, it is difficult to understand how any of this component could be due to primary particles, since the large energies associated with the primaries should produce some type of reaction below 12 cm of lead unless, of course, neutral particles are involved. Although it does not seem very probable, it is possible that this effect could be produced by neutral particles coming up from below due to nuclear explosions produced by the primaries in the lower part of the rocket.

If we assume that all of the radiation except that absorbed in 6 cm is primary, then we find that the electron component determined on the basis of shower production could not be more than a maximum of 14 percent of the primary; the non-electronic component absorbed in 12 cm is 18 percent of the primary, and the non-electronic component penetrating 12 cm is 68 percent of the primary.

---

[4]G. J. Perlow and J. D. Shipman, Jr., Phys. Rev. 71, 325 (1947).

[5]Golian, Krause and Perlow, op. cit., p. 776.

The ratio of the total radiation, determined by the events [1, 3, 6, -2(2+4+5)] , in free space to that at sea level was 11.5. The ratio of the hard component, determined by the events [1, 3, 6, 12, 14, 16, -(2+4+5)] , in free space to that at sea level was 9.0.

We wish to acknowledge the very helpful discussions and suggestions of J. A. Wheeler, N. Arley, and their associates at Princeton.

C. Electronics for Cosmic-Ray Experiments

by

B. Howland, C. A. Schroeder,
and J. D. Shipman, Jr.

A method is described for detecting coincidence between the discharges of Geiger counters. The basic circuit uses diodes as coincidence tubes. The output from a diode circuit is the same polarity pulse as the inputs, hence the output from one coincidence circuit can be used to generate more complex coincidences. An example is given of a typical counter-tube experiment utilizing the diode scheme. A formula is developed for the ratio of output for total and partial coincidence in terms of the pulse width and circuit parameters; in a practical case with a pulse width of 1 μ second a four fold to three fold output ratio of 40 is obtained. Mention is also made of a combination diode-pentode coincidence circuit.

Introduction

The continuing work at this laboratory and others on cosmic-ray experiments in rockets[6,7] has dictated the development of new electronic circuits for use with counter telescopes. In the German V-2 rocket thus far employed there has been no serious limitation on weight, but size and power consumption are constrained. On the other hand, the impossibility of repeating a flight with identical apparatus demands that as much data be obtained from a limited number of counters as the radio telemetering system is capable of transmitting[8]. It is therefore necessary for a given counter to figure in many coincidence circuits, in some of which it operates in parallel with other counters and in other circuits singly. A counter may also be required to cause anti-coincidence.

---

[6] Ibid., P. 223.

[7] Ibid., p. 776

[8] V. L. Heeren, C. H. Hoeppner, J. R. Kauke, S. W. Lichtman, and P. R. Shifflett, Electronics 20, No. 3, 100 (1947) and 20, No. 4, 124 (1947).

The scheme to be described performs these functions reliably and with a minimum of current drain. This has been done by the use of diodes as coincidence tubes.

Diode coincidence circuit

The basic diode coincidence circuit is shown in figure 39 (a) and (b). In circuit (a), positive pulses from several signal sources are applied to the cathodes of diodes D1, D2, ... Dn. The plates are connected to a positive supply +E volts by a resistor, R1, which is large compared to either a cathode resistor, R, or the resistance of a diode. The small current, I, through R1 will divide evenly among the n diodes. When the cathodes of several of the diodes are driven positive, the remaining diodes will carry the current I, which remains substantially constant, and the rise in plate voltage will be very small. When, however, all the cathodes are driven coincidently positive, the plates will rise in potential and a sizable output will be obtained. Figure 39 (b) is the corresponding circuit for negative pulses. Here the cathodes are connected together and grounded through a large resistor while the plates are connected to a positive supply by small resistors.

The diode circuit may be used to generate anticoincidences in a manner similar to that used by Herzog with the Rossi pentode coincidence circuit[9,10]. In figure 40, positive coincidence pulses are applied to the cathodes of diodes D1, D_2, and D_3. It is desired to prevent an output pulse at the diode plates whenever a given anticoincidence counter tube discharges. This is done by generating a negative pulse from the discharge of the counter and applying it to the cathode of D4. This cathode is biased and is effectively out of the circuit unless an anticoincidence pulse occurs. In such a case D_4 conducts, the plates are held negative, and no positive output will be obtained. If the output circuits should be sensitive to negative pulses, it is necessary to prevent the plates from going negative. This is accomplished by means of a clipping tube D_5.

It will be noticed that the output pulse from a diode coincidence circuit has the same polarity as an input. Thus the output from one coincidence circuit may be used to generate another more complex coincidence as shown in figure 41. Here we desire to obtain knowledge of two events; the first a coincidence 1, 2, 3, 4, and second a fivefold event 1, 2, 3, 4, 5. The former is first generated and the output is combined with five to form the latter, by use of two additional diodes.

It is sometimes desired to parallel the signals from several counters so that they will operate as a group in one coincidence while operating separately

---

[9]Rossi, Nature 125, 636 (1930).

[10]G. Herzog, Rev. Sci. Inst. 11, 84 (1940).

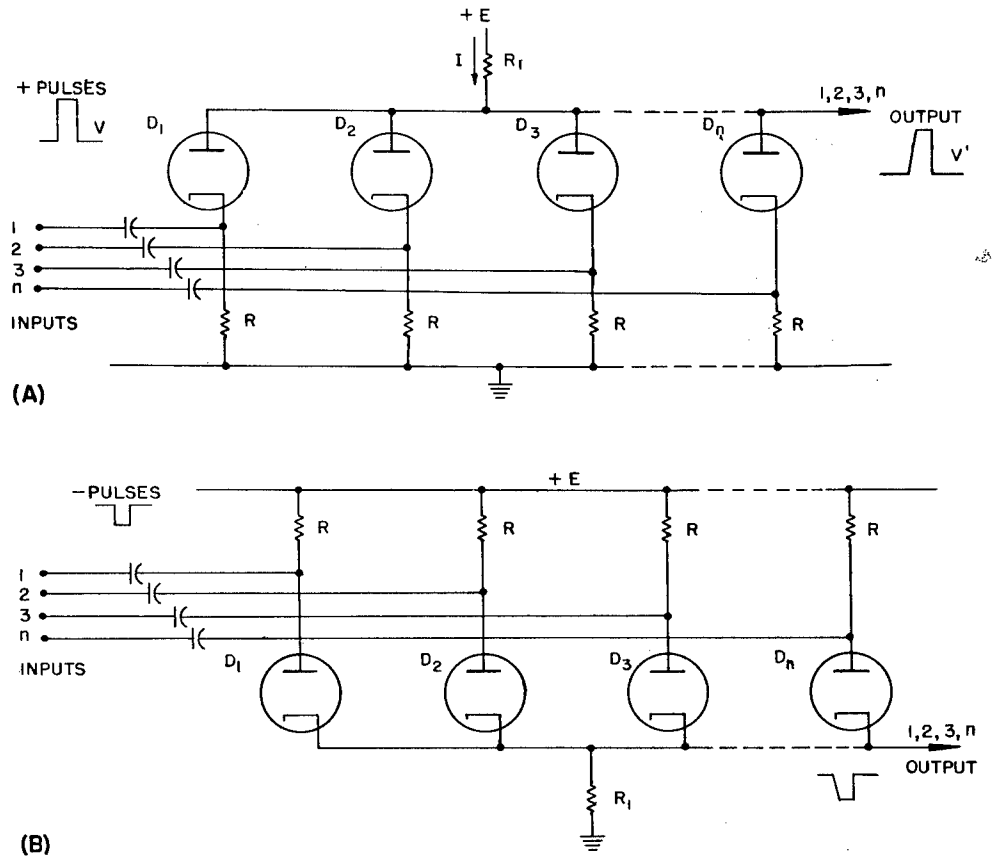

Fig. 39. Diode coincidence circuits. Typical values: $R_1 = 5 \times 10^5 \Omega$, R = 680Ω, E = 250 volts. Diodes are type 6AL5.

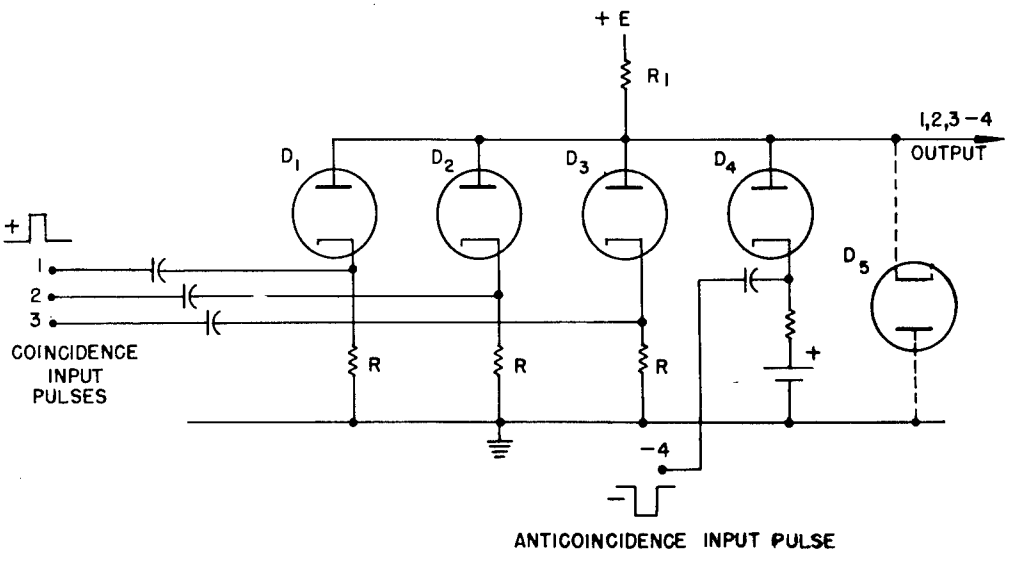

Fig. 40. Anticoincidence circuit

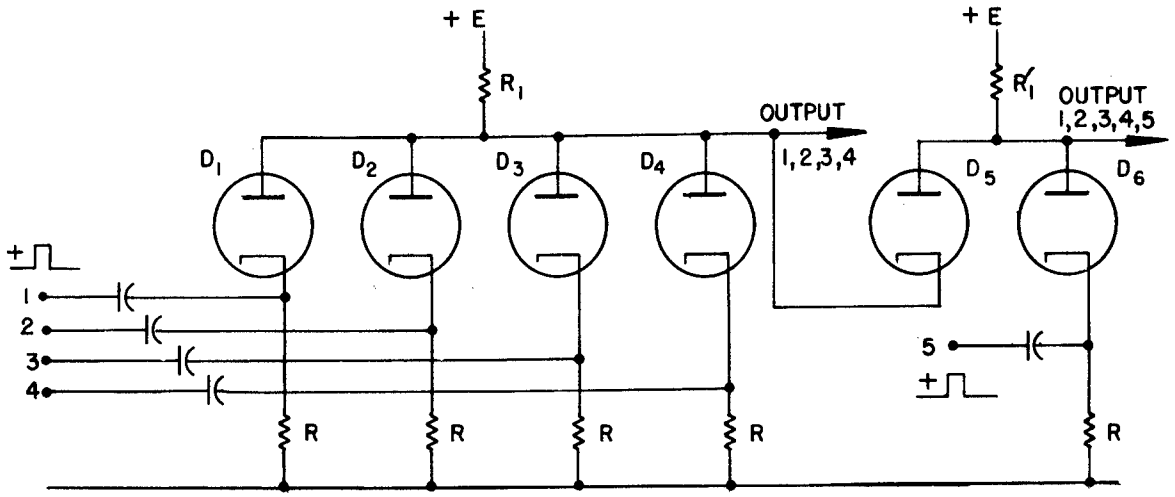

Fig. 41. Output of one coincidence circuit used as element in another coincidence

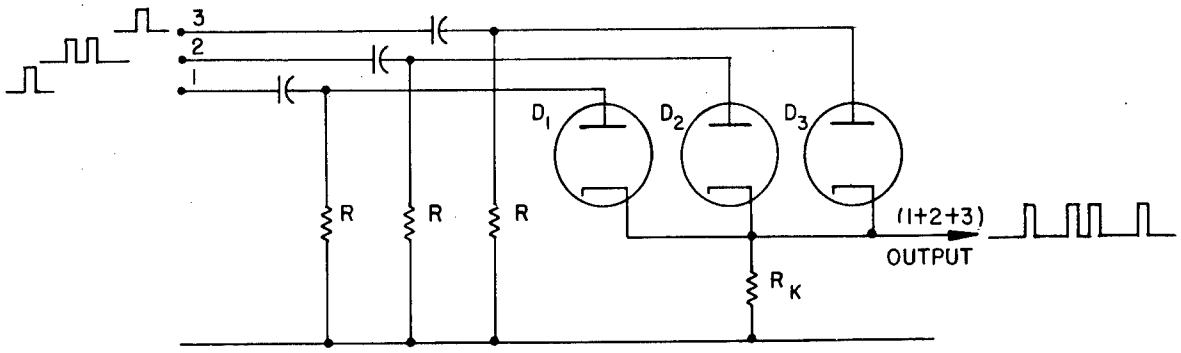

Fig. 42. Paralleling of several counter signals

elsewhere. This can be done with the simple diode circuit of figure 42. A positive pulse from either of signal sources 1,2, or 3 will give a positive output at the cathode. If the cathode resistor is several times the resistance of a signal source or a diode, the output signal, which we may write as (1+2+3), will be nearly as large as the output from any one signal source; however, the cathode resistor should still be small compared to the plate circuit resistor, R_1, in a coincidence circuit.

Design of diode coincidence circuits

It is instructive to calculate the output pulse amplitude from a diode coincidence circuit when a partial coincidence occurs. In the circuit of figure 39 (a) consider the worst case, a partial coincidence in which the cathodes of all the diodes except D_1 are driven V volts positive. The current, I, which previously divided among the n diodes will now flow through D_1 producing a small output pulse V', approximately equal to $I(R_c+R_d)\ (n-1)/n$, where

R_d is the d.c. resistance of a diode, and R_c is the combined impedance of the cathode resistor and the driving circuit measured from cathode to ground.

When a true coincidence occurs and all the cathodes are driven positive, V' will be very nearly equal to V, provided that the input pulse width is sufficient to permit the plate voltage to rise to this value. The ratio, ρ, of true coincidence pulse amplitude to largest false coincidence pulse amplitude, which may be considered a figure of merit for the circuit, will be:
Case 1. $V'=V$

$$\rho = \frac{V}{I(R_c+R_d)(n-1)/n} = \frac{V}{E}\left(\frac{R_1}{R_c+R_d}\right)\frac{n}{n-1} .$$

Thus, for greatest ρ the plate resistor R_1 should be made large compared to (R_c+R_d). As R_1 is increased, however, the speed of response of the plate circuit is decreased because of the shunting effect of stray capacitance, C_s, and a point will be reached where this rather than V determines the output pulse size, V'. In this case V' will be equal, approximately, to the product of the rate of rise of the plate voltage, I/C_s, and the input pulse width τ. The ratio ρ will then be given by:
Case 2. $V'=(I/C_s)\tau \leqq V$

$$\frac{(I/C_s)\tau}{I(R_c+R_d)(n-1)/n} = \frac{\tau}{(R_c+R_d)C_s}\cdot\left(\frac{n}{n-1}\right) .$$

This is only accurate if $C_s(R_c+R_d) \ll \tau \ll C_sR_1$.

The pulse width will in general be determined by the coincidence resolving time desired; and the stray capacitance, C_s, will depend upon the number of elements in the coincidence. In a practical case $n=4$, $R_c=680\Omega$, $R_D=300\Omega$, $C_s=35\mu\mu f$, and with $\tau=1\,\mu$sec., $\rho\sim40$. If a ρ of 10 were considered satisfactory, the pulse width could be decreased to 0.25 microsecond.

These calculations were made for a single n-fold coincidence circuit. In practice it is often desired to generate several coincidences using the same signal sources, in which case the partial coincidence pulses will tend to add together. This is seen if we consider, in the circuit of figure 41, the partial coincidence 2,3,4,5. The two d.c. currents through R_1 and R_1' will be switched through D_1 and R, producing a voltage of $2I(R_c+R_D)$ on the 1,2,3,4 output and $2I(R_c+R_D)+IR_D$ on the 1,2,3,4,5 output. In complex coincidence circuits with many different outputs, the partial coincidence pulses are important, and to minimize them it is necessary to use low resistance diodes and to feed the circuits from low resistance signal sources.

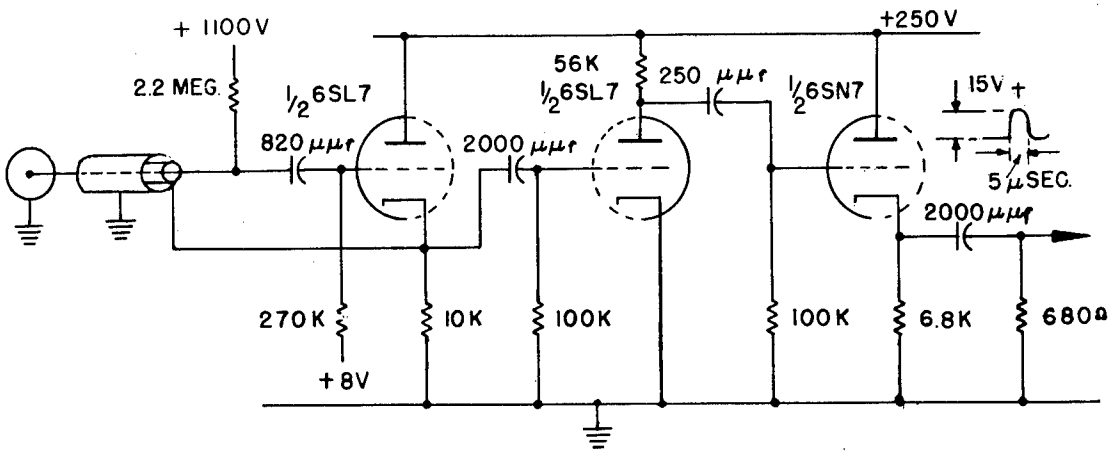

Fig. 43. Input circuit for coincidence counter

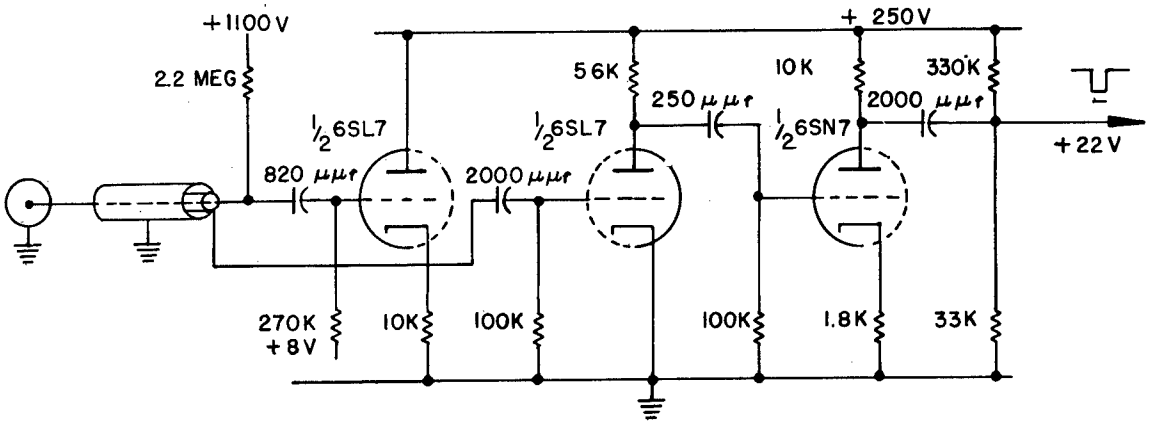

Fig. 44. Input circuit for anticoincidence counter

Input and output circuits

For experiments with Geiger counters, some form of input circuit is usually required to supply a low impedance signal to the diode coincidence circuit. Cathode followers have the desired input and output impedances and have been chosen for this purpose. In figure 43 is shown an input circuit used in recent experiments at this laboratory using argon-alcohol counters. It consists of an input cathode follower, an amplifier, a differentiating circuit, and an output cathode follower. The counter input cable is a type RG-59/U concentric cable shielded with an additional copper braid. This outer shield is grounded and the inner shield is connected to the cathode of the input cathode follower, thus minimizing by feedback the grid-circuit capacitance. This is important as a Geiger counter is a constant charge device, and the discharge pulse voltage is very much dependent on the shunt capacitance. The signal is amplified and differentiated to give a pulse of approximately 5-microseconds duration. The second cathode follower supplies

at low resistance a 15-volt positive pulse output to the diode coincidence circuit.

Figure 44 shows the corresponding anticoincidence input circuit which differs from the circuit of figure 43 only in the third triode stage. This circuit supplies a large negative pulse, 10 microseconds wide, to the coincidence circuit.

The coincidences are formed with 6AL5 miniature double diodes by proper interconnection of signals from the input circuits. (Crystal diodes could perhaps be used and would have advantages of low stray capacitance.) A typical experiment illustrating the method is shown in figure 45.[11] Here the signals from eight groups of counters are combined to form four coincidences and anticoincidences in the following way: First the signals 1,2, and 3 are combined to form the coincidence 1,2,3. This signal is then combined with the anticoincidence signals 4 and 5 to form the anticoincidence $1,2,3,-(4+5)$. This signal is then combined with 6,7, and 8 to form the eightfold anticoincidence $1,2,3,6,7,8-(4+5)$. The signals 6,7, and 8 are paralleled by diodes D_{11}, D_{12}, and D_{13}, and the signal $(6+7+8)$ is then combined with $1,2,3,-(4+5)$ to form $1,2,3,(6+7+8)-(4+5)$. The diode D_{16} prevents a negative output on the anticoincidence channels which might otherwise trigger the output circuits.

The output from the coincidence circuit is fed to a trigger tube and multivibrator. The cathode of the trigger tube is biased positively so that an 8-volt input pulse is required to trigger the multivibrator. Thus it is insured that the partial coincidence pulses, which are never larger than two volts, will not produce an output. The multivibrators are adjusted to give an output pulse of width suitable for transmission by the telemetering system.

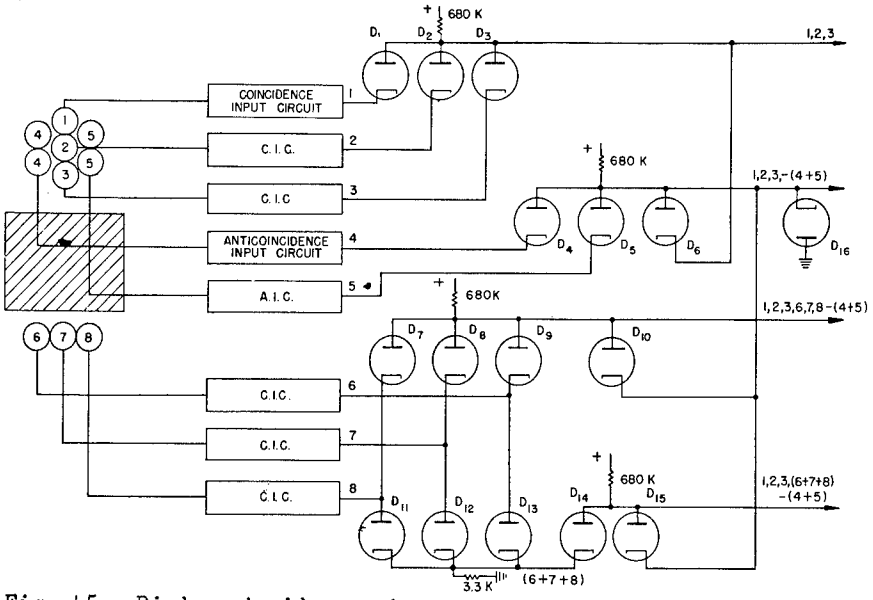

Fig. 45. Diode coincidence circuit for counter telescope experiment

[11] For a complete description of this experiment, see Phys. Rev., 70, p. 776 (1946).

Diode-pentode coincidence circuit

A combination diode and Rossi pentode coincidence circuit is shown in figure 46. Here it is desired to generate several related coincidences: 1,2,3;1,2,3,4,5, and 1,2,3 4,5-6. The first coincidence 1,2,3, is formed using pentodes P_1, P_2, and P_3 in a conventional Rossi circuit. This signal is coupled through diode D_1 to the plates of pentodes P_4 and P_5, from which point is taken the second output 1,2,3,4,5. The polarity of the diode is such that no positive output can occur at the plates of P_4 and P_5 unless the coincidence 1,2,3 occurs simultaneously with 4,5. The circuit is further extended to form the anticoincidence 1,2,3,4,5-6 by use of diode D_2 and pentode P_6.

It should be noted that when a partial coincidence of the type 2,3,4,5 occurs, the currents through all the plate load resistors will flow through pentode P_1. Pentodes with low internal resistances should, therefore, be used to insure small partial coincidence outputs.

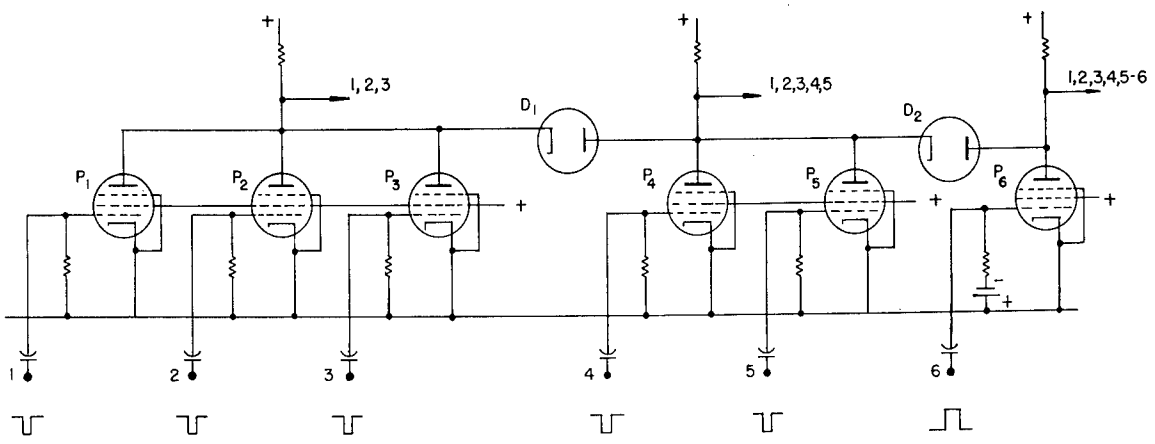

Fig. 46. Diode-pentode coincidence circuit

Acknowledgement

The writers wish to acknowledge the aid of their colleagues in the Rocket-Sonde Research Section of the Naval Research Laboratory, and are especially indebted to Messrs. S. E. Golian, E. H. Krause, and G. J. Perlow.

D. Electronic and Auxiliary Instrumentation for Specific Cosmic Ray Experiments

by

B. Howland, C. A. Schroeder,
and J. D. Shipman, Jr.

1. The January 10 Experiment

Two distinct experiments, each employing counter telescopes, were performed on January 10. Each of these telescopes was equipped with a complete electronic system. The basic circuits employed were described in the preceding section. The particular combinations of these which comprised the systems used on January 10 are given in the accompanying schematic diagrams, figures 47 and 48. The telescope and the electronic systems are seen in figures 26 and 27, as they appeared when mounted in the warhead.

Counter telescope A consisted of eight groups of Geiger counters. Five types of coincidence and anticoincidence were registered, as follows: 1,2,3; 1,2,3-(4+5); 1,2,3,(6+7+8)-(4+5); 1,2,3,(6+7+8); and 1,2,3,6,7,8. The pulses generated in the counters were amplified and shaped in the input circuits, and combined in a diode circuit of the type described in the previous section. Telescope B was somewhat more complex, containing an additional bank of three groups of counters. The electronic system was similar to that of the first telescope. In both cases the output multivibrators were adjusted to feed a 20 millisecond pulse to the telemetering system. This insured that each pulse was sampled at least three times. These wide pulses have the advantage of being distinguishable from noise pulses, but have the disadvantage of masking a proportionally greater number of events, since counter discharges are not registered if they occur during or shortly after the period of the output pulse. In all, twelve channels of the telemetering system were used to transmit cosmic ray information.

The greater part of this data was also recorded by a neon lamp camera recorder.[12] This recorder was housed in a pressurized steel container which was mounted in the tail section of the rocket. The unit was recovered intact, as shown in figure 49. A section of the recovered film is reproduced in figure 50. The time signal was recorded in the fourth channel (reading from the top). It was generated by a multivibrator having an accuracy of approximately 2 percent. This circuit is shown in figure 51.

The determination of the aspect of the rocket was accomplished in two

---

[12] Naval Research Laboratory Report No. R-3030, Chapter IV, Section D.

ways. A Schwein control gyroscope was modified by the addition of a potentiometer pick-off on the vertical axis. This arrangement generated a voltage which was a known function of the angle through which the rocket had rolled. This voltage was telemetered to earth.

Angular aspect with respect to the sun was determined by means of three photoelectric cells mounted at 120° intervals around the warhead. The locations of these may be seen in figures 26 and 27. The three outputs were each identified by a simple coding system. One of the anodes was connected to a positive voltage, the other two to the plates of an unbalanced multivibrator. The three signals were combined in a common cathode resistor and fed to the telemetering system. Figure 52 shows a typical section of the record. Cosmic ray pulses and the indications furnished by the gyroscope cells may be clearly seen.

The rate of rocket roll was unusually high on January 10, being approximately one revolution per second. Advantage was taken of this circumstance, and the fact that the instrumentation furnished accurate information as to aspect of the missile, to extract valuable information from the records concerning the variation of the cosmic radiation with azimuth.

2. The March 7 Experiment

The cosmic ray experiment performed on March 7 made use of a 45 counter telescope whose principal axis coincided with that of the rocket. This apparatus occupied the forward section of the warhead (cf. Chapter III, Section B). The new warhead design imposed severe space limitations upon the equipment in the remaining portion of the warhead. The elaborate telescope required a correspondingly complex electronic system. As a result of these two considerations, for the first time, a circular chassis was employed. It is shown in figures 53 and 54. It was mounted on the under side of the base plate which supported the counter telescope system. The telescope and the associated electronics thus virtually formed a single unit when mounted in the V-2. This can be seen in figure 11. This compact arrangement allowed the use of short input cables.

Fifteen groups of counters comprised the telescope. The following eleven types of coincidence and anticoincidence events were of primary interest (cf. Section B): A: 1,3,6; B: 1,3,6-5; C: 1,3,6-2; D: 1,3,6,-(2+4+5); E: 1,3,6(7+8+9); F: 1,3,6(10+11+12); G: 1,3,6,(13+14+15)-(2+4+5); H_1: 1,3,6,7,8,9,-(2+4+5); H_2: 1,3,6,10,11,12-(2+4+5); H_3: 1,3,6,13,14,15,-(2+4+5); I: 1,3,6,(13+14+15).

It is pointed out in Section C that some crosstalk is inherent in a diode coincidence circuit. The level of the crosstalk is proportional to the number of inputs firing during a partial coincidence. Inputs 1,3 and 6 appear in all telemetered events in this experiment, making it possible, under certain con-

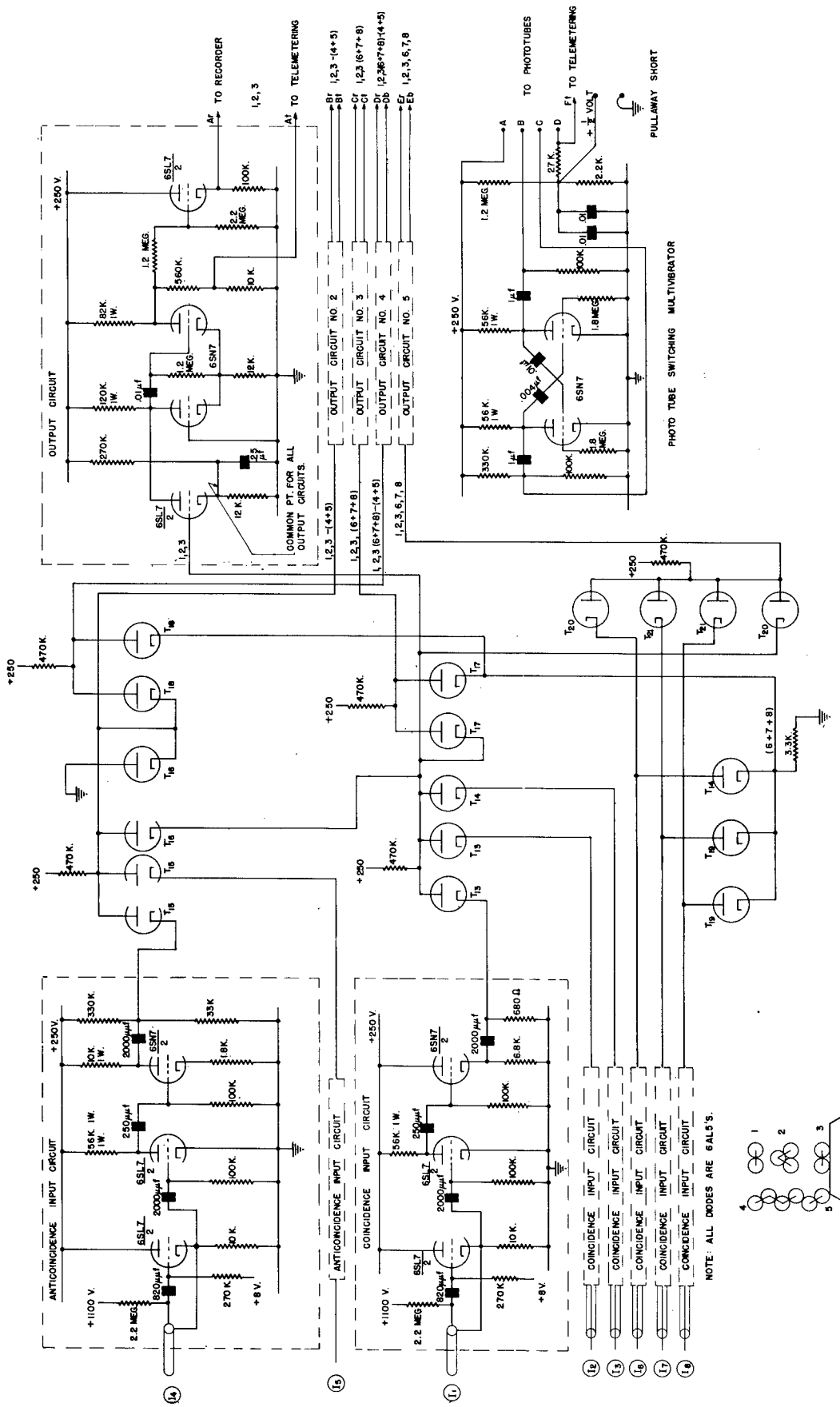

Fig. 47. Schematic diagram of the electronics associated with counter telescope **A** of the January 10, 1947 V-2

ditions, for the crosstalk to become excessive. Therefore, two diode feeding cathode followers were employed following the amplifiers of inputs 1,3 and 6. Six of the telemetered events were developed using 1_a,3_a and 6_a, and and five using 1_b, 3_b, and 6_b. With this arrangement the highest diode crosstalk voltage possible was approximately 25 percent of that necessary to actuate the output multivibrators. Since only nine telemetering channels were available three of the events, H_1, H_2, and H_3, were multiplexed on a single channel. This was accomplished by adding the outputs of the three output multivibrators in a common resistor. A coding device was again resorted to: the time constants of the multivibrators were adjusted to give pulses having distinctly different lengths. The output pulse lengths chosen were 20, 40 and 80 milliseconds, respectively. The use of pulses of this length should be confined to channels in which the counting rates are appropriately low.

A schematic diagram of the entire cosmic ray electronic system is given in figures 55, 56 and 57. An illustrative section of the telemetering record is reproduced in figure 58. The different pulse lengths may be clearly seen.

All of the information which was telemetered was also recorded on a 20 channel, neon-lamp, camera recorder. This instrument was similar to the one employed on January 10. A facsimile of the camera record of the events shown in figure 58 is given in figure 59. Here, again, the three distinctive pulse lengths employed in the multiplex channel are clearly visible. The events represented in channel three occupy different relative positions in the two records. This results from the physical arrangement of the neon lamps in the camera recorder.

For the first time, the data were read primarily from the record furnished by the camera. Previously the telemetering film was used as the principal working record in the tabulation of the various numbers and types of events.

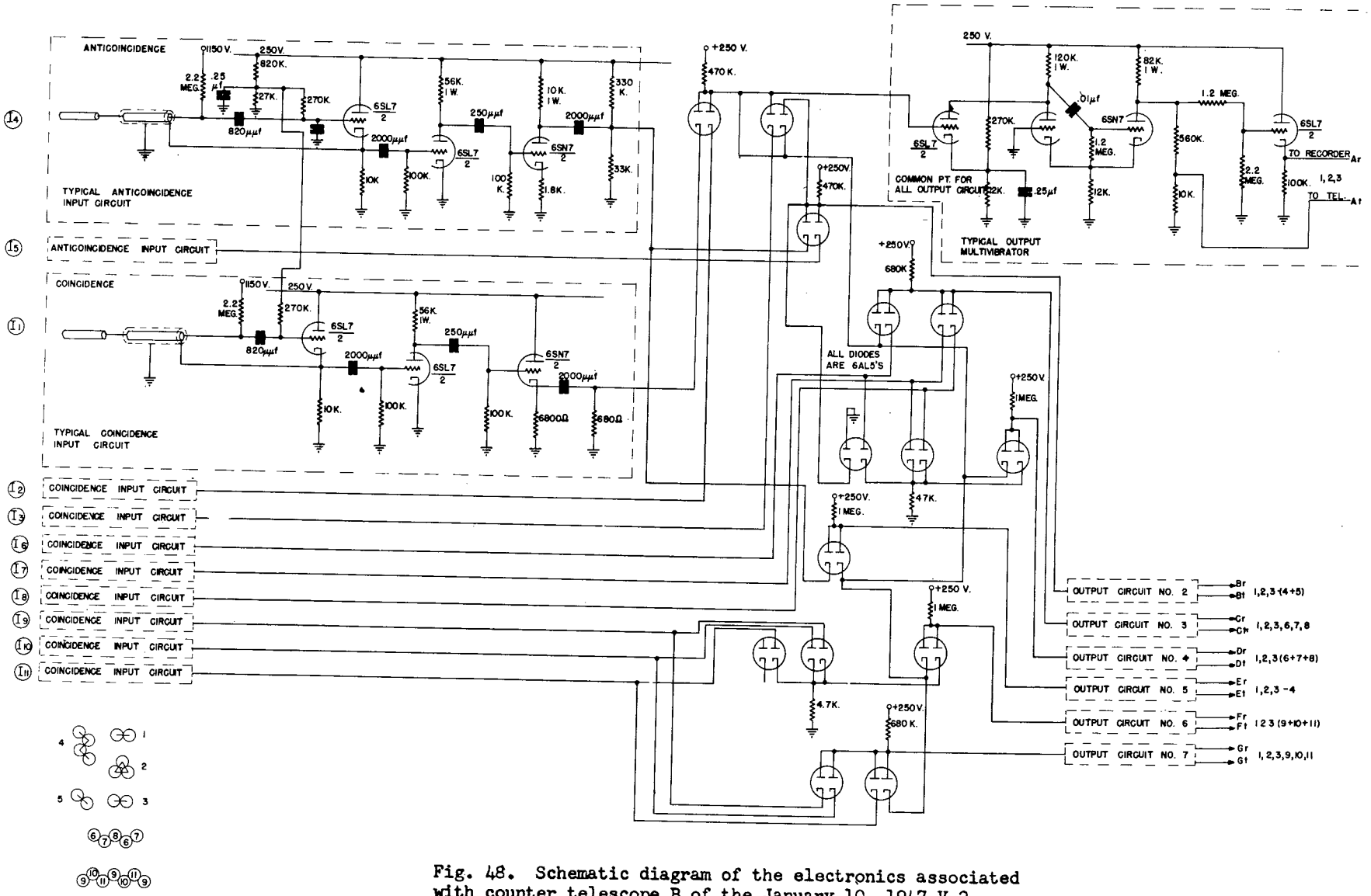

Fig. 48. Schematic diagram of the electronics associated with counter telescope B of the January 10, 1947 V-2

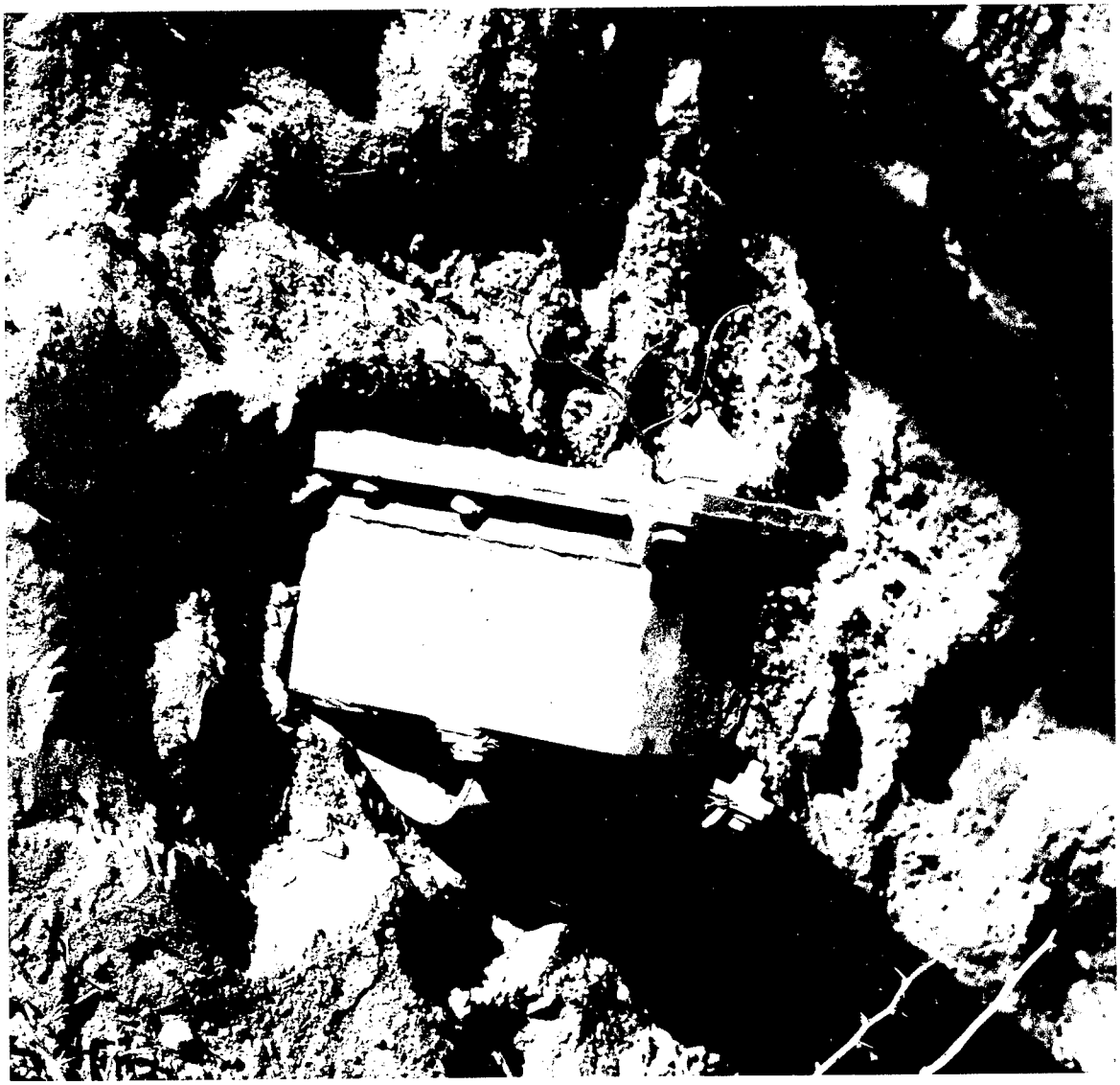

Fig. 49. The cosmic ray recorder as recovered after the January 10 flight

Fig. 50. A section of the film recovered from the cosmic ray recorder on January 10

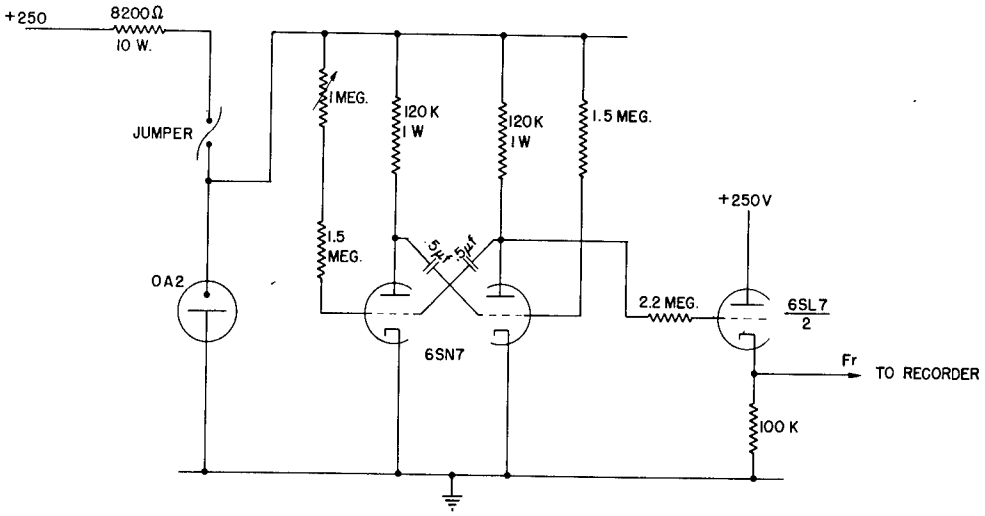

Fig. 51. The timing multivibrator employed on 10 January

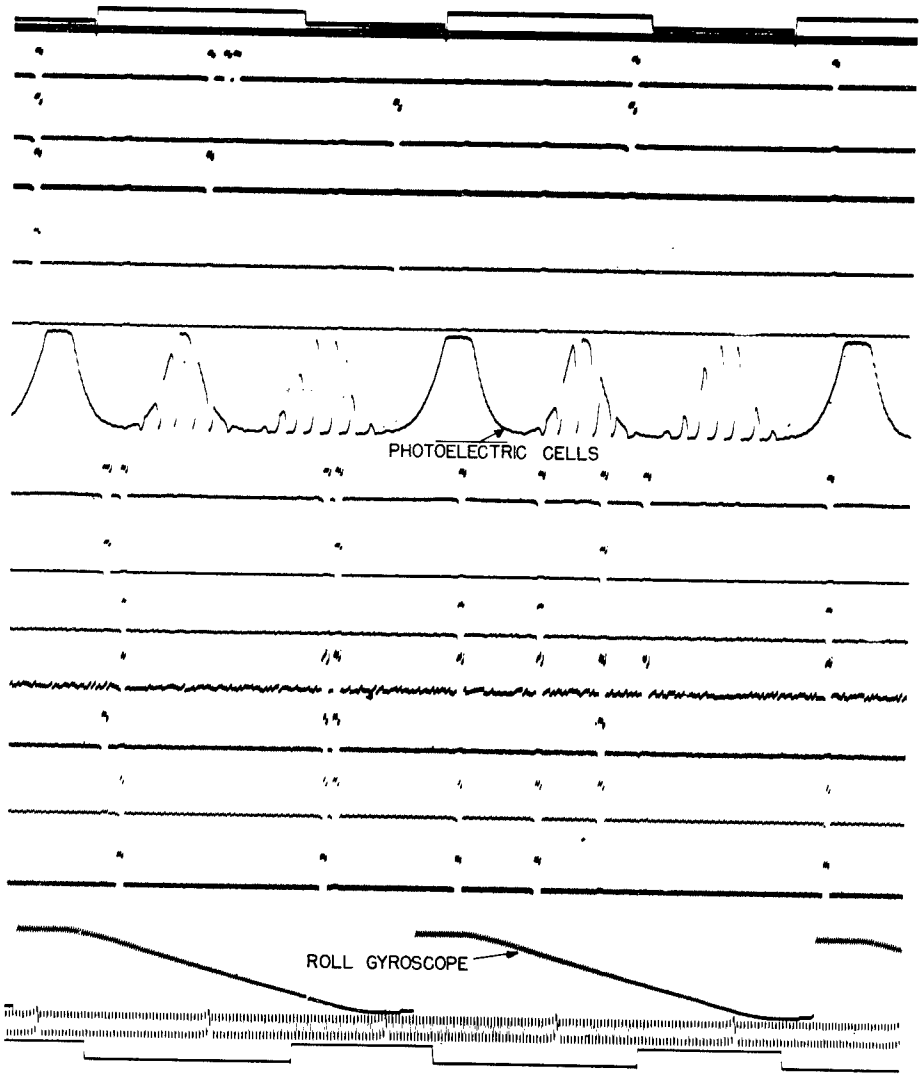

Fig. 52. A typical section of the telemetering record of the January 10 flight

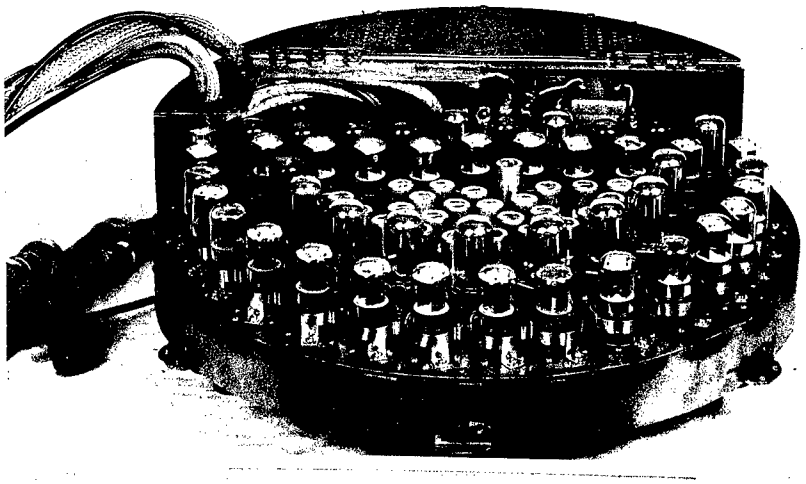

Fig. 53. The March 7, 1947 cosmic ray electronic system

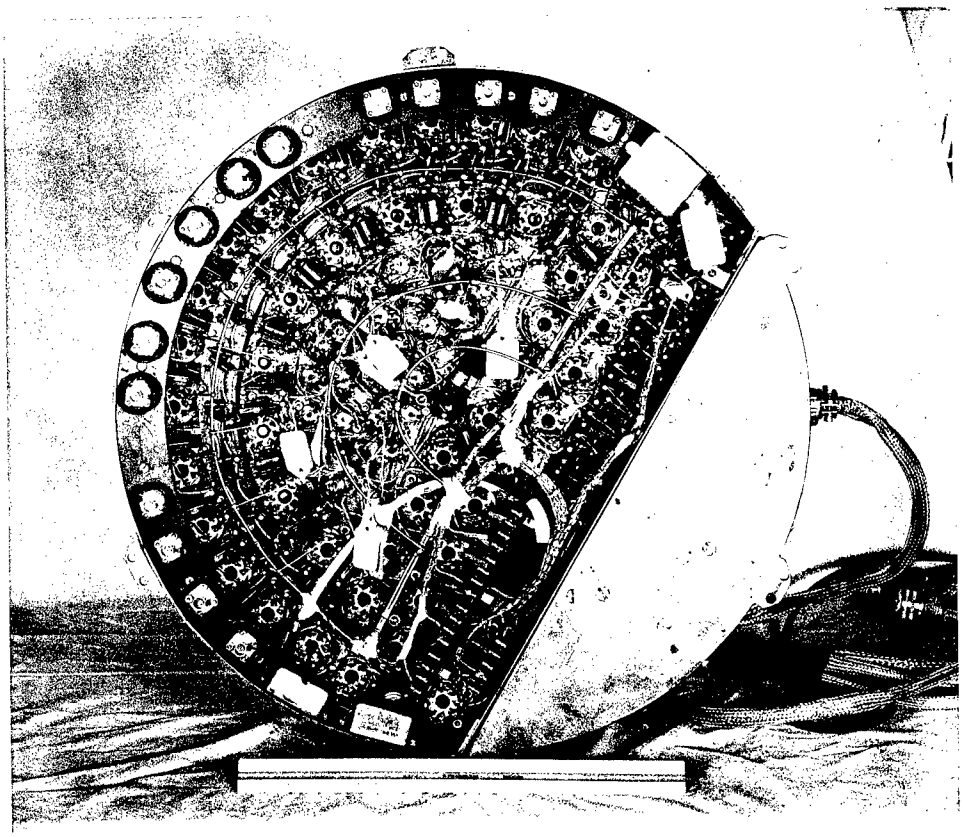

Fig. 54. Bottom view of the cosmic ray electronic system

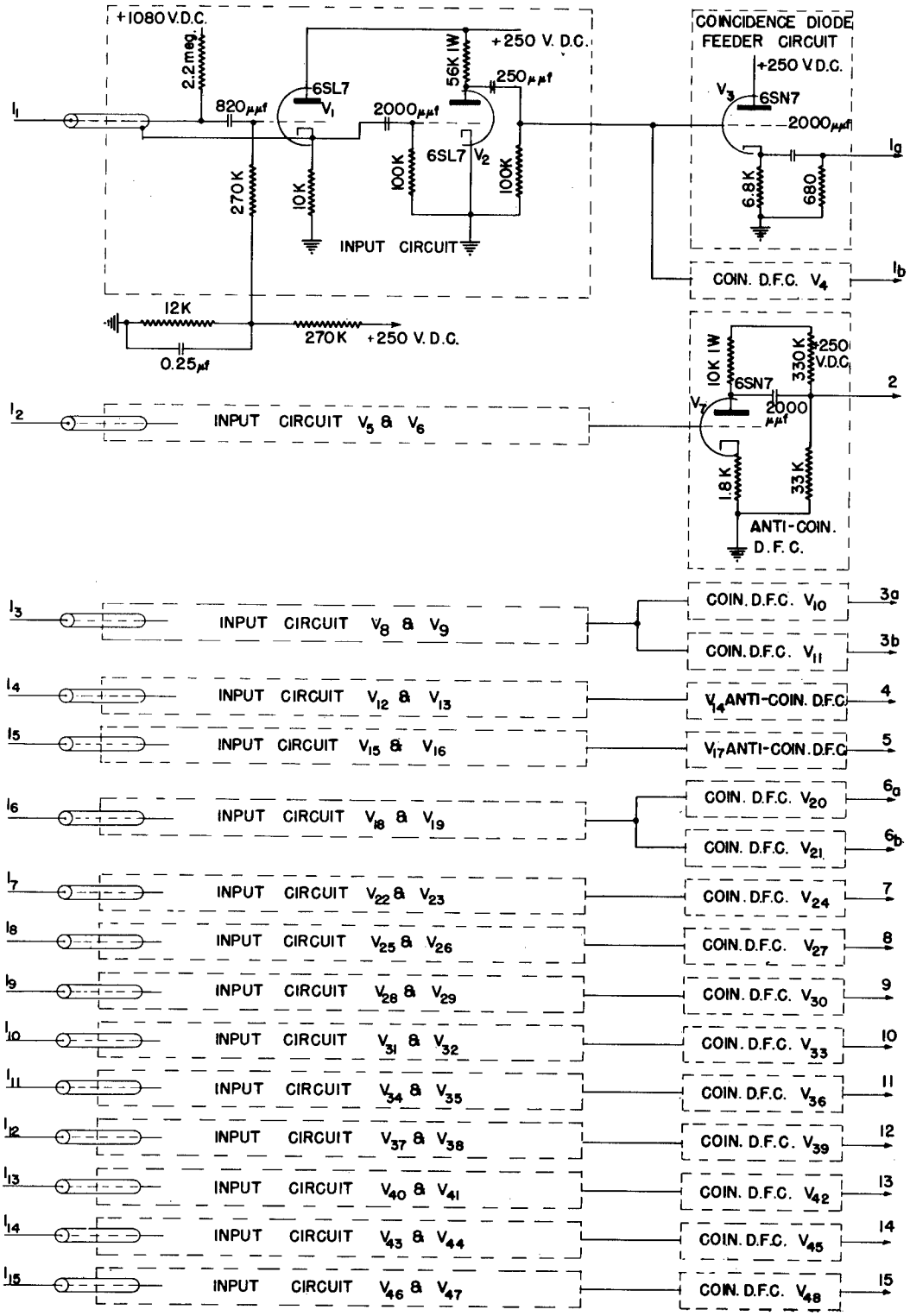

Fig. 55. Schematic diagram of the March 7 electronic system, Part 1

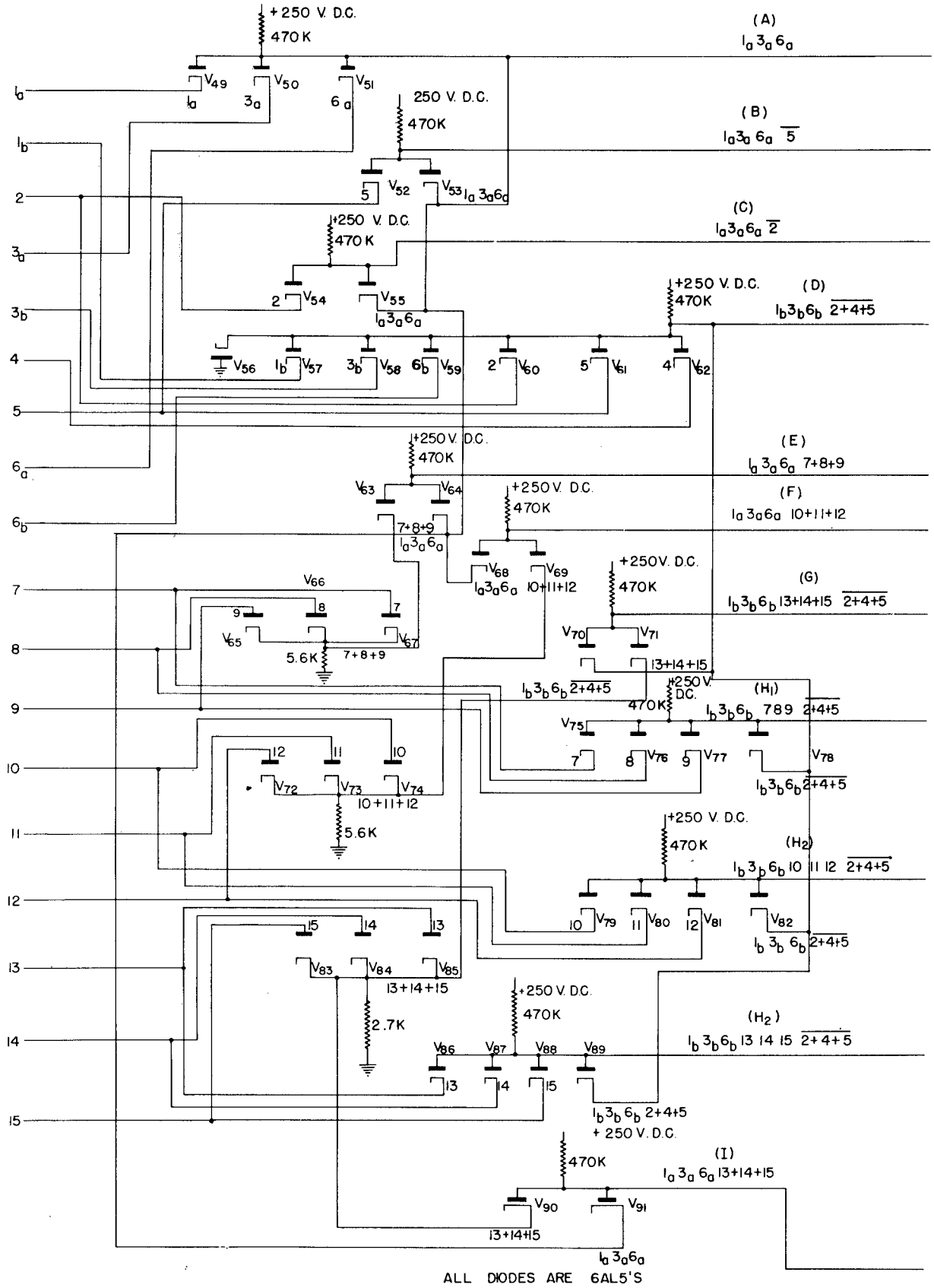

Fig. 56. Schematic diagram of the March 7 electronic system, Part 2

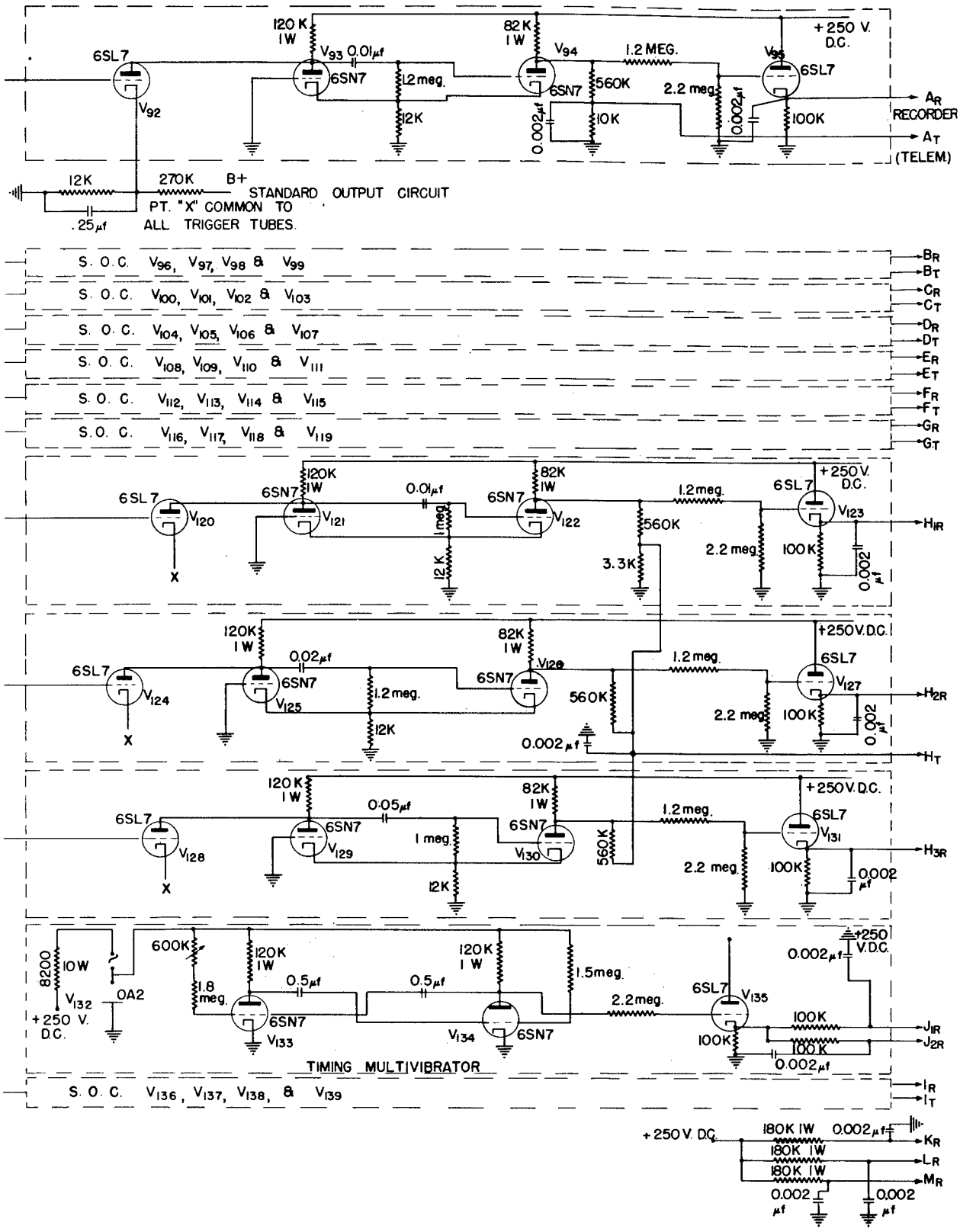

Fig. 57. Schematic diagram of the March 7 electronic system, Part 3

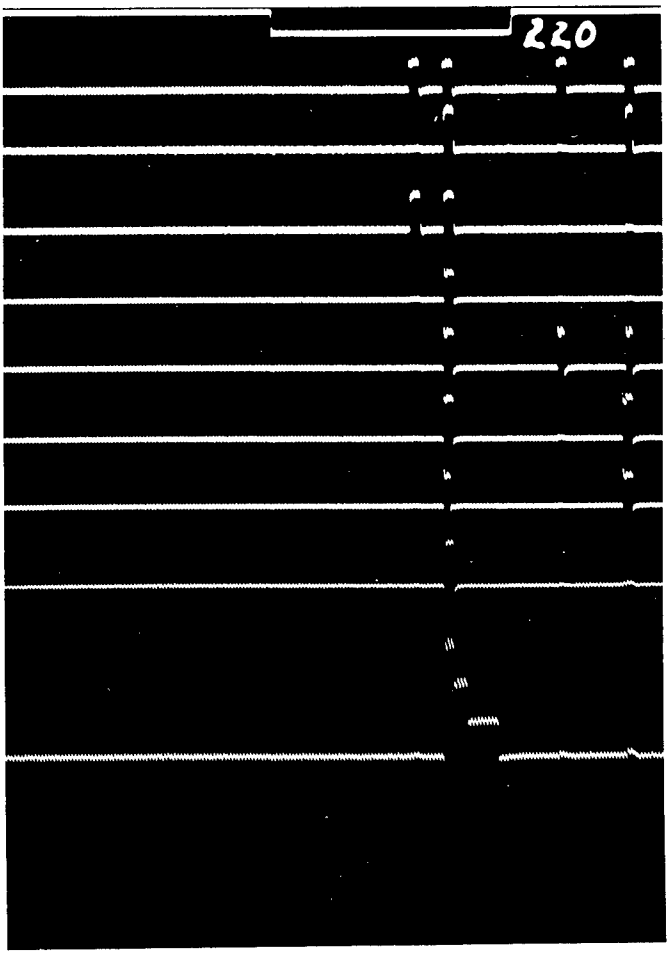

Fig. 58. A section of the telemetering record of the March 7, 1947 flight

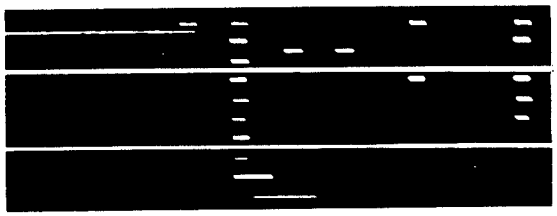

Fig. 59. The camera record of the events represented in Fig. 58

CHAPTER V

SPECTROSCOPY AT VERY HIGH ALTITUDES

Introduction

The analysis of the spectra obtained on October 10 has been continued. A study of the vertical distribution of ozone in the atmosphere, part of which was reported upon previously,[1] was carried out, and the significant results achieved up to the present time are given in Section A.

Solar spectrograms in the region below 3400 A were obtained to an altitude of 162 km (101 mi) during the V-2 flight of March 7. Sixty-six short exposures were made at various altitudes from 1 to 120 km (0.6 to 75 mi), and a single long exposure was made covering the range from 125 km (78 mi) to the top of the trajectory (162 km or 101 mi) and back to 140 km (87 mi). One spectrum was obtained at 75 km (47 mi) whose resolution was at least twice as high as that of the best of the October 10 spectra. The improvement resulted from the use of cylindrical mirrors which reduced astigmatism greatly, and thereby reduced smearing due to rocket roll. These results, together with those obtained on October 10, are being used as a basis for identifying the Fraunhofer lines in this portion of the spectrum of the sun. The preliminary results of this investigation were reported in a letter to the Editor of The Physical Review.[2] That letter is reproduced in Section B.

When the V-2 program was initiated, it was not known whether items such as spectrographic film could be recovered successfully. A photoelectric spectrometer was therefore designed and constructed so that spectroscopic studies could be carried out in the event that recovery efforts failed. The success which attended the recovery of film obviated the necessity for the use of this instrument. However, as it may have other research applications, it is described here in Section C.

---

[1] Naval Research Laboratory Report No. R-3030, Chapter IV, Section A, and Naval Research Laboratory Report No. R-3120, Chapter II, Section A.

[2] E. Durand, J. J. Oberly, and R. Tousey, Phys. Rev. 71, 827 (1947).

A. The Vertical Distribution of Ozone in the Atmosphere

by

E. Durand, F. S. Johnson,[3] J. J. Oberly
J. D. Purcell,[3] and R. Tousey[3]

The solar ultraviolet spectrum was obtained to an altitude of 88 km (55 mi) during the V-2 flight of October 10.[4] The spectrograms obtained were analyzed to determine the vertical distribution of ozone in the atmosphere above White Sands on that date. Provisional results of this study are presented here.

The quantity of ozone present between any two particular levels in the atmosphere was derived from a comparison of the spectra obtained at those heights. Exposures made at seventeen different altitudes, ranging from 8 to 67 km (5 to 42 mi), were employed in the analysis. The actual determinations of the quantities of ozone were made by means of photographic photometry. The values obtained are displayed in figure 60.

Two peaks in ozone concentration were found, at 17 km (11 mi) and 25 km (16 mi) altitude, respectively. Above 30 km (19 mi) the measured concentration decreased sharply, vanishing, within the experimental error, at 50 km (31 mi). From 50 km to 62 km (39 mi) there was no evidence of ozone. The upper limit to the quantity which might pass undetected appeared to be 0.0005 cm/km.[5] Between 62 and 67 km (42 mi) altitude, the highest region included in this study, there apparently existed a trace of ozone, the measured concentration being 0.0002 cm/km. This reading was probably the result of an experimental error. These spectra will be critically reexamined.

The total quantity of ozone in the atmosphere is given by the area under the curve of figure 60. Graphical integration gave a value of 2.7 mm. This is considerably above the 1.9 mm mean value for the same season found over California.[6] However, it is in good agreement with values of 2.5 and 2.7 mm measured the day before and the day after the flight, respectively, at the Observatory of the Smithsonian Institution on Table Mountain, Cali-

---

[3]Members of the Optics Division of the Naval Research Laboratory. These experiments are being carried out jointly by the Micron Waves Section, R. Tousey, Head, of the Optics Division, E. O. Hulburt, Superintendent; and the Rocket-Sonde Research Section, E. H. Krause, Head, of Radio Division I, J. M. Miller, Superintendent.

[4]Naval Research Laboratory Report R-3030, Chapter IV, Section A.

[5]1 cm/km=0.136 grains of O_3 per liter. This is equivalent to the pressure, in cm Hg, which is exerted by the O_3 contained in a vertical columm 1 km tall.

[6]F. W. Götz, Vierteljahrsschrift der Naturforschenden Gesellschaft in Zurich, pp. 250-264, 1944.

fornia.[7] The double-peaked distribution found in the rocket measurements is a most unusual one. It has been observed previously, however, by Götz[7a] in his study of the Umkehr Effekt. In that case, also, the total ozone content of the atmosphere was abnormally high, being 3.4 mm.

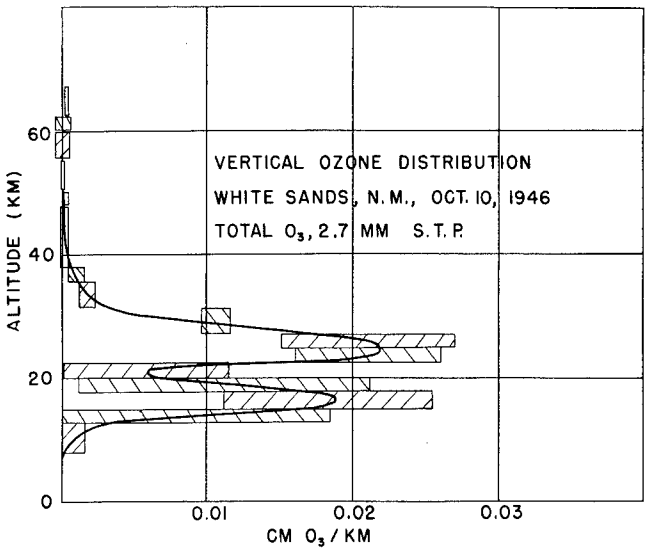

Fig. 60. Vertical ozone distribution

The concentration decreased somewhat more rapidly between 30 and 40 km (19 and 25 mi) altitude than in the instance reported by Götz. However, this aspect of the White Sands data was in good agreement with the theory of Wulf and Deming.[8] The fact that the concentrations above 50 km (31 mi) altitude were below the detectable limit, 0.0005 cm/km, also agrees with the theoretical calculations of Wulf and Deming, which predict values of less than 0.00005 cm/km for this region.

The shaded areas in figure 60 provide a rough indication of the magnitudes of the possible errors associated with the measurements. The experimental error was much smaller at the higher altitudes than at the intermediate levels. This was due to the fact that it was possible to make use of the shorter wavelength radiation which is absorbed much more rapidly by the ozone.

Efforts to increase the accuracy of these results will take two forms. Experiments are to be conducted when the sun has a large zenith angle, i.e., when it is in the vicinity of the horizon. This will provide a long light path through the absorbing layers, which should make it possible to detect very small amounts of ozone and, perhaps, of some of the other atmospheric constituents, such as the oxides of nitrogen. In addition, certain improvements have been made in the microdensitometer which will make possible the measurement of considerably higher values of density. This will increase the accuracy of the data obtained from the comparison of spectrograms. Plans for the future also include the remeasurement of the entire series of spectra obtained on October 10, and the corresponding recalculation of the distribution of atmospheric ozone.

---

[7] Private communication from Mr. L. B. Aldrich.

[7a] Götz. Op. Cit.

[8] O. R. Wulf and L. S. Deming, Terr. Mag. 41, 299 (1936).

B. Solar Absorption Lines between 2950 and 2200 Angstroms

by

E. Durand, J. J. Oberly, and R. Tousey

Solar spectrograms were taken by the Naval Research Laboratory on the V-2 rocket flights of October 10, 1946[9] and March 7, 1947. The spectra obtained at 55 km and 75 km on the respective dates have been studied to identify the Fraunhofer absorption lines in the region between 3000 and 2200 A. Some 300 observable absorption features were compared to a master finding list of 1100 of the principal classified lines of the arc and spark spectra of elements 1 to 30. The heavier elements will be added as time permits. The finding list was prepared in collaboration with Dr. Charlotte Moore-Sitterly, who generously made available the unpublished multiplet lists which are being compiled as an extension of the Revised Multiplet Table[10] to cover the rocket ultraviolet region. Entries included laboratory intensities, assigned multiplet numbers, and, in many cases her solar intensity predictions.

At the available resolution of about 1A, nearly every observed line is a blend; as many as 10 possible contributors to a single line have been found. Likely contributors have been assigned to nearly every observed feature, and work is under way to estimate their relative importance.

As in the previously known region, Fe I and Fe II are dominant and clearly contribute to a majority of the lines. In figure 61, the matching of many of the solar lines (indicated by dots) to the Fe arc spectrum is apparent. In the region just below 2750, 2630,2550 and 2490 A there is a piling up of intense iron lines. This causes the whole level of the solar radiation to fall off sharply as shown in figure 61. In addition, many strong single Fe lines are found throughout the spectrum.

The great Mg II lines at 2803 and 2796 A are of particular interest. They appear as two bright emission lines in the center of a great absorption band running from 2775 to 2825 A.

Dr. Menzel of the Harvard Observatory offered the above explanation of the observed spectra and suggested the following explanation: A strong eruption of hydrogen occurred about 1 hour before the rocket flight, and the Mg emission may have originated in the prominence. However, similar emission lines, unresolved, may be inferred from the October 10 spectra, at which time no important prominences are known to have occurred.

---

[9] W. A. Baum, F. S. Johnson, J. J. Oberly, C. C. Rockwood, C. V. Strain, and R. Tousey, Phys. Rev. 70, 781 (1946).

[10] Charlotte E. Moore, "A revised multiplet table of astrophysical interest," Princeton Observatory.

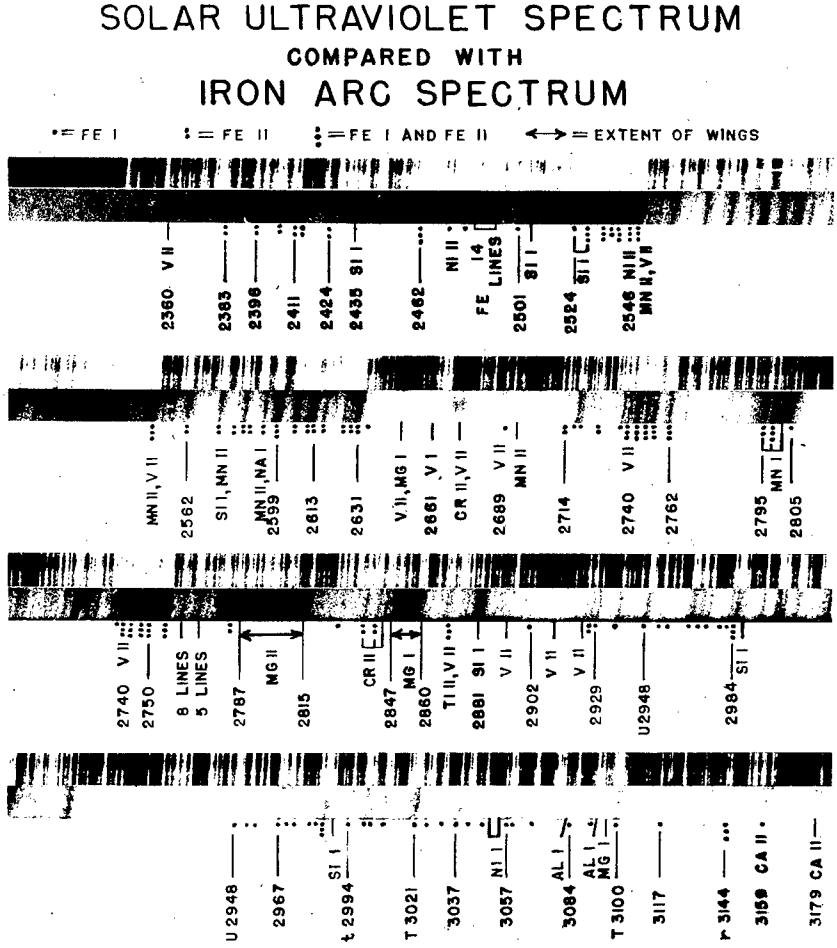

Fig. 61. Solar ultraviolet spectrum compared with iron arc spectrum

Twelve lines of Si I of great intensity were found. The one at 2882 and the group between 2507 and 2529 A showed strong wings. The existence of wings on the group between 2208 and 2219 A could not be proved. A strong line of C I was found at 2478 A.

In addition to the above elements one or more lines have been assigned as follows: definite, V I, V II, Cr II, Mn II, Co I, and Al II; probable, Na I, Ni I, Ni II, Cr I, Co II, Be I, and Al I; possible, P I, and Cu I. More definite asignment will be made taking into account multiplet intensity and the relative abundances of the elements.

There appear to be regions of general absorption between 2886 and 2893 A and between 2442 and 2472 A. The finding list contains few lines in these regions; the absorption may, therefore, be molecular.

A complete report of the analysis will be published later.

C. The Photoelectric Spectrometer

by

M. L. Greenough, J. J. Oberly, and C. C. Rockwood

At the outset of the Upper Atmosphere Research Program it was not known whether the recovery of exposed photographic film would be possible. An effort was made therefore, to develop a spectrometer which would record spectral intensities in selected wavelength regions in such a manner that these values could be telemetered during flight. An instrument of this type was actually built and was nearly ready for installation when a series of successful recoveries, which began with the recovery of the complete afterbody of the July 30 rocket, eliminated the original necessity for the project. Since that time the use of photographic spectrographs has occupied the central position in the program of experimental spectroscopy. The tests of the photoelectric spectrometer were therefore not completed, and it is not likely that it will ever be installed in a rocket. However, since its design features, including particularly the logarithmic multiplier phototube circuit, may have laboratory applications, its plan, construction and mode of operation are presented here.

Two alternative methods of accomplishing the desired results were considered. A scanning mechanism might be employed to cover all wavelengths, or a continuous record of two selected wavelength regions could be made. The latter course was chosen. The first region was centered at 2900 A, near the edge of the great Hartley absorption band of ozone. A continuous record of intensities in this zone would furnish the information from which the vertical distribution of ozone in the atmosphere could be deduced. The second wavelength selected for study was 1216A, the Lyman α line in the emission spectrum of hydrogen. In addition, for control purposes, a continuous record of the undispersed light reflected by the grating at zero order is obtained. This provides a means for correcting for loss of light when the sun is off the optical axis.

Figure 62 is a photograph of the instrument, with the covers removed. The optical and mechanical arrangements are shown schematically in figure 63. Radiation enters the instrument through a 2 mm spherical lithium fluoride bead, which is identical with those used in the photographic spectrographs now employed in the rocket studies.[11] A small image of the sun, 0.012 mm (0.0005 in.) in diameter, is formed behind the bead. This image serves in place of the more conventional entrance slit. From the bead, the radiation travels through a set of optical baffles to a concave grating similar to the one mounted in the photographic spectrograph.[12] It is made of aluminized

---

[11] Naval Research Laboratory Report No. R-2955, Chapter III, Section H.

[12] Loc. Cit.

glass, has a 40 cm (15.75 in.) radius of curvature, and is ruled with 15,000 lines per inch. After it leaves the grating, the light is dispersed, and comes to a focus on the Rowland circle, where three slits are mounted. These slits select the desired wavelengths, and allow the radiation to pass through three windows into a pressurized chamber. The chamber contains two multiplier phototubes and a photoelectric cell, each of a type appropriate to the radiation it is to receive.

The first slit transmits the central or zero order image. The radiation passes through a quartz window into the pressurized chamber, where it is reflected by a small mirror to the sensitized surface of a type 929 phototube. The window behind the second slit is covered with a fluorescent coating of type P5 blue phosphor. This coating converts any radiation of wavelength near 1216 A to radiation of a longer wavelength. The latter is capable of penetrating the air in the chamber and actuating the type 931-A multiplier phototube. The window behind the third slit, which admits the 2900 A band, is also of quartz. Radiation transmitted by this slit is incident upon the type 1P28 multiplier phototube. This slit, which is adjustable, is set so as to transmit a 200 A band, centered near 2900 A. The solar intensity at the earth's surface falls off very rapidly between 3000 and 2950 A, due to the ozone absorption. Therefore, a small displacement of the long wavelength edge of this slit results in a large change in the amount of energy transmitted. Advantage is taken of this effect to adjust the phototube current obtained from the solar radiation at sea-level to a value slightly in excess of the normal dark current. Calculations, based on the assumption that the sun acts as a black body at 6,000° C in the region below 2900 A, predict that the total energy transmitted by the slit should increase by a factor of 10^3 passing entirely through the ozone layer. The multiplier phototube circuit is designed to cover this range of intensities logarithmically. The circuit details are given below.

The use of a lithium fluoride bead in place of a conventional entrance slit created one new problem which seriously complicated the task of arranging the exit slits. As was pointed out above, the effective entrance slit for the system is the small image of the sun formed behind the bead. After

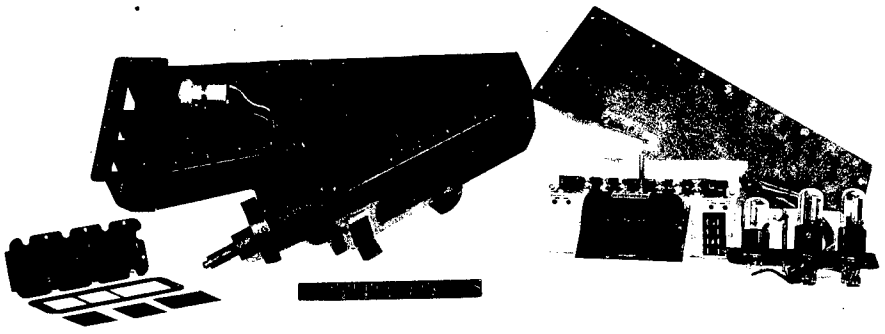

Fig. 62. The photoelectric spectrometer

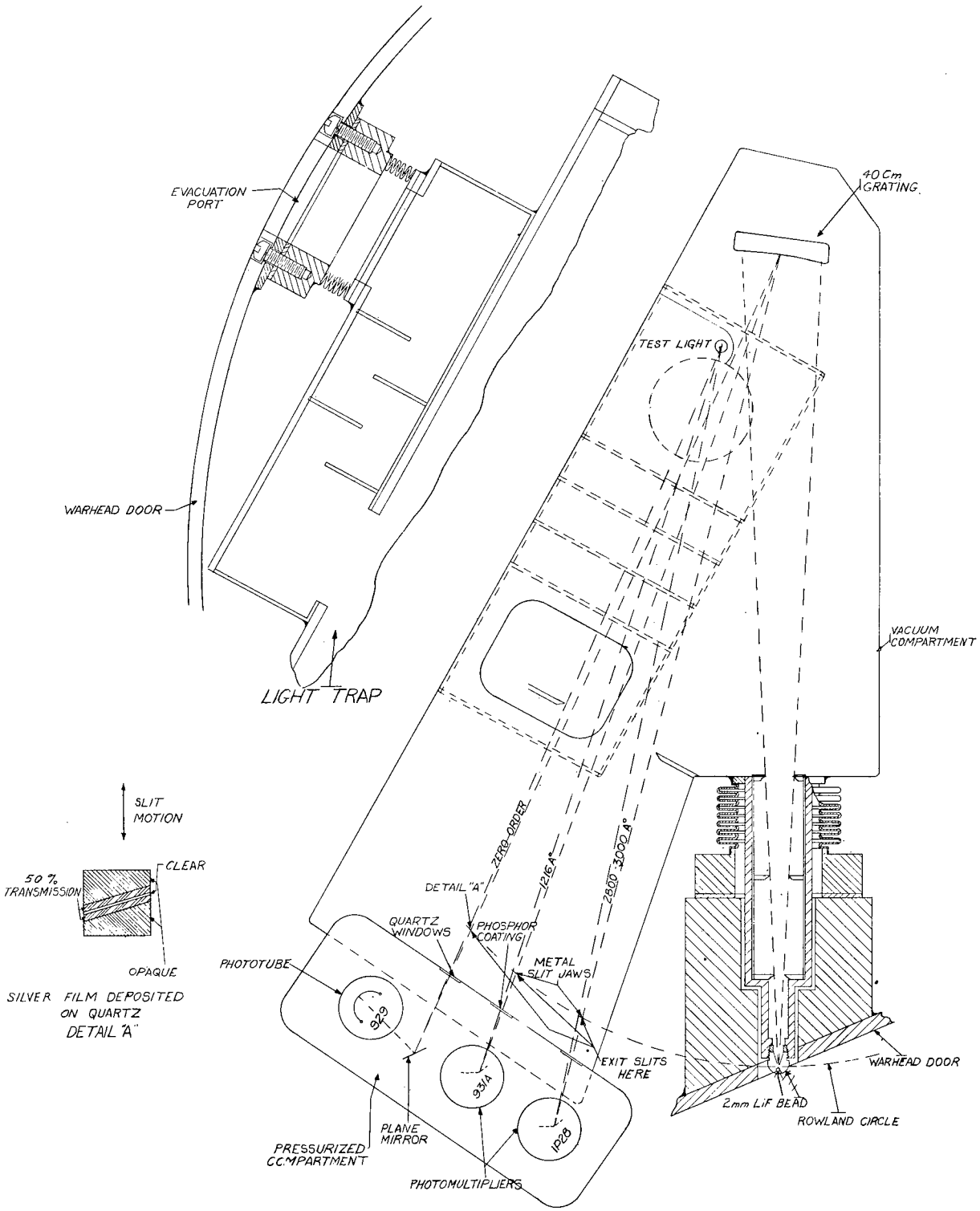

Fig. 63. Functional sketch of solar spectrometer

Brennschluss the rocket's tendency to roll, pitch, etc. is unchecked. Such motions cause changes in the angle which the entering solar radiation makes with the optical axis through the bead. The corresponding changes in the position of the image result in displacements of the spectral lines. These displacements may each be resolved into three mutually perpendicular components, two lying in, and one normal, to the plane of the slits. The latter translation is not serious since it produces only a slight defocusing at the slits. The effect of the component perpendicular to the dispersion in the plane of the slits is also unimportant, since the exit slits are made long enough to allow for the greatest possible displacement in this direction. The effect of the component in the direction of the dispersion is to change the wavelength bands transmitted by the slits. Thus, a fixed slit system would be virtually useless. The usual changes in the direction of the rocket axis due to roll, etc. will displace the 1216 A line, and the central image by an amount sufficient to carry them out of the acceptance areas of the corresponding slits. To circumvent this difficulty the two slits are therefore mounted on a carriage, which is mechanically driven back and forth over a range which is slightly greater than the maximum possible displacement of the images. Hence, corresponding to any given position of the sun which is within the acceptance angle of the lithium fluoride bead, there will be two moments during each scanning cycle when both the central image and the 1216 A line will fall on their respective slits. The scanning cycle is coded by using different speeds for the forward and the backward traverses. The start of each cycle is marked on the telemetering record, so that, by measuring the time interval between the start and the momentary appearance of the central image signal on the record, the amount of spectral displacement can be calculated. Knowledge of the scanning motion then allows precise determination of the wavelengths entering the two slits. The slit assembly and the scanning mechanism are shown in figure 64.

The zero order slit consists of a clear region 0.1 mm wide flanked on either side by 1.5 mm regions which transmit half of the energy incident upon them. Thus, a continuous record of the central image intensity may be obtained without interfering with the wavelength determination measurements. The semi-transparent zones also allow the study of higher intensities, since

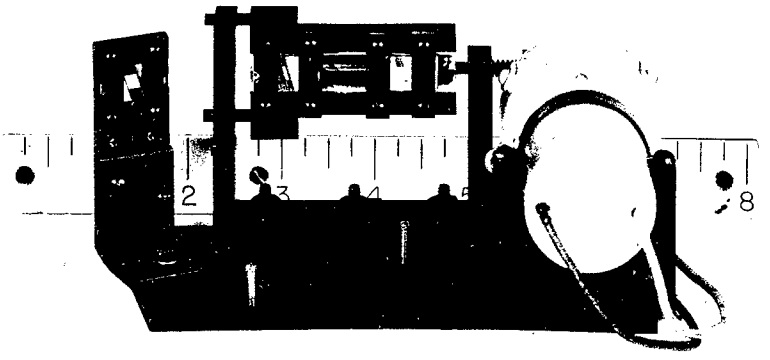

Fig. 64. The slit assembly showing the scanning mechanism

the limiting factor is the point at which the amplifier saturates. In order to meet rigid mounting requirements, the lithium fluoride bead was placed below the Rowland circle, and the slits above this circle. Consequently, the astigmatic images formed by the grating are not normal to the Rowland circle. The slits are made parallel to the images, as shown in detailing "A" of figure 63. During flight air is evacuated from the optical paths inside the instrument through a vent which leads from the body of the instrument to the exterior of the rocket. The vent is equipped with light baffles which appear in the drawing at the top of figure 63. A small test lamp is mounted inside the instrument so as to be able to illuminate all three phototubes simultaneously. This lamp, shown in figure 63, can be used as a secondary standard to check the operation of the phototubes and the electronics.

The instrument is designed to be mounted in the rocket so that the lines ruled on the grating are normal to the axis of the rocket. With this arrangement, the motion of the solar image which occurs when the rocket rolls is, primarily, parallel to the slits. This orientation was chosen because it was believed that roll was more probable than pitch or yaw, and because image motion parallel to the slits introduces the fewest difficulties. The optical

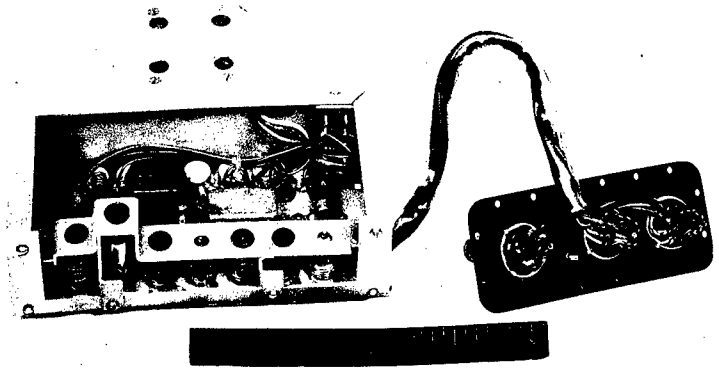

Fig. 65. The spectrometer electronics

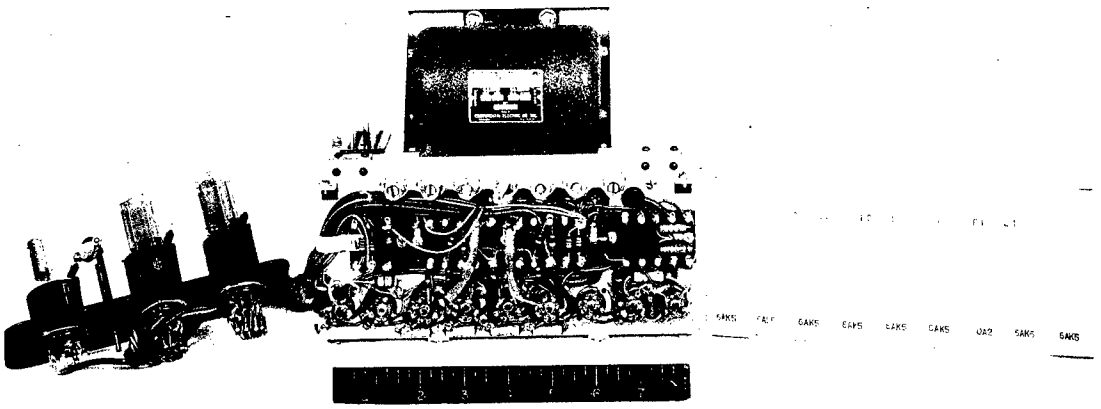

Fig. 66. The spectrometer electronics, bottom view

axis through the bead was to make an angle of 55° with the principal axis of the rocket. A reasonably high intensity is obtained with this view during the stabilized portion of the flight.

The electronic equipment in the spectrometer proper consists of three phototubes which are shown on the right of figure 65, and on the left of figure 66. The other items are mounted on a small chassis which may be located at a distance from the main instrument. It is shown in figures 65 and 66. The heaters are operated from a 6 volt storage battery. All other voltages are obtained from the dynamotor, which is powered by the main 24 volt supply. The dynamotor output is regulated by means of an OA2 tube. The high voltage needed for the multipliers is had by rectifying the pulses appearing across an inductance in the plate circuit of one tube of the 2,000 cycle multivibrator, shown in figure 67. This supply will deliver 1,250 volts at about 0.5 milliamperes.

The circuit which was designed to obtain a logarithmic output from the phototubes is also shown in figure 67. This type of response is obtained by varying the d-c voltage applied to the phototube in such a way as to maintain its output current at an approximately constant value. A fraction of this d-c voltage is then applied to the telemetering channel to give the required logarithmic measure of the incident intensity. The details of operation are as follows. The 6AK5 regulator tube acts as a variable efficiency peak rectifier. In the absence of radiation, the multiplier phototube output is small, the 6AK5 control grid voltage is accordingly positive and the rectification efficiency of the 6AK5 is high. As the radiation intensity is increased the voltage at the control grid of the 6AK5 decreases, and the rectification efficiency drops, reducing the d-c voltage across the phototube. Thus the circuit stabilizes, with the phototube anode current maintained approximately constant. A characteristic curve of the output voltage plotted as a function of the intensity of the radiation incident upon the phototube is given in figure 68.

The resistance connected to the plate of the 6AK5 regulator tube, and the capacity in parallel with the phototube voltage divider, form a filter which eliminates the 2,000 cycle ripple voltage. However, the time constant is kept small enough to allow a sufficiently rapid response to the anticipated changes in, and rates of change of, the radiation intensity.

It is believed that the instrument described here is capable, when installed in a V-2 rocket, of obtaining a useful record of solar intensity in the band centered at 2900 A. It is doubtful whether any record would be obtained at 1216 A, unless the solar intensity in that region, as measured above the earth's atmosphere, is very great.

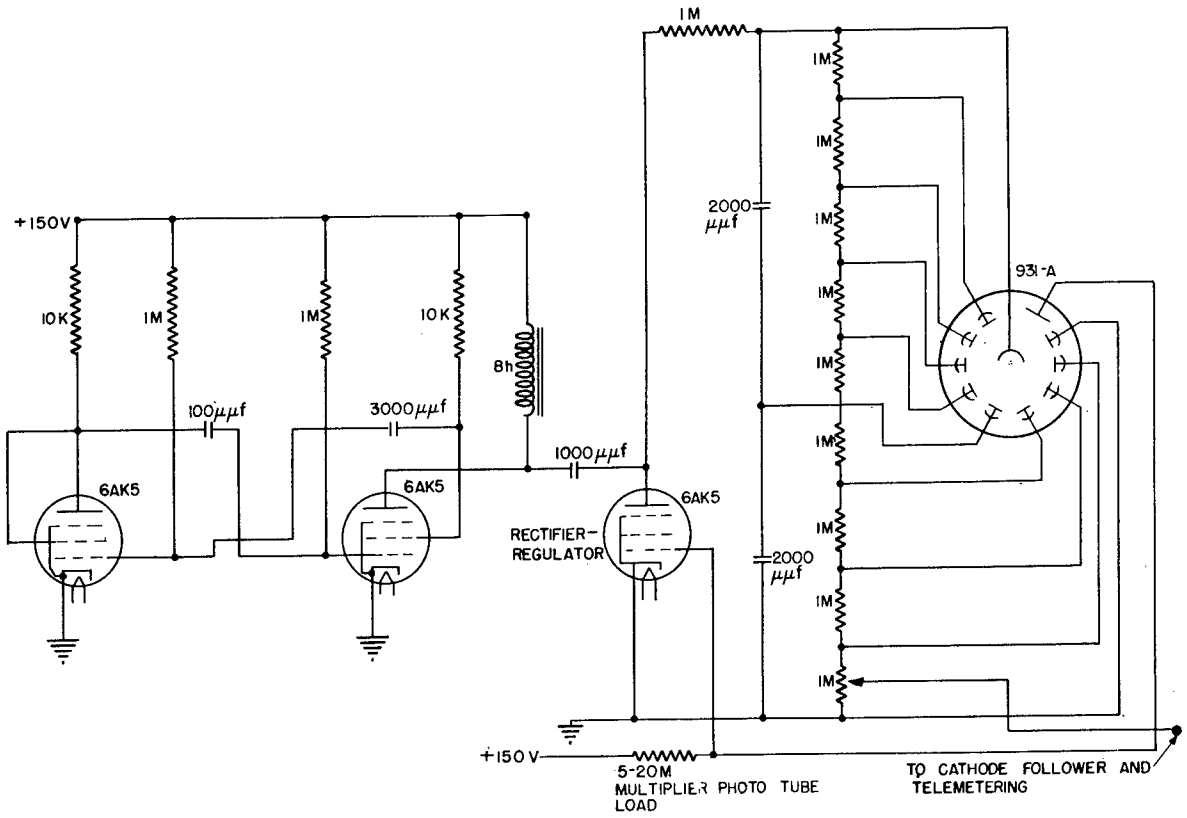

Fig. 67. Schematic diagram of the logarithmic multiplier phototube circuit

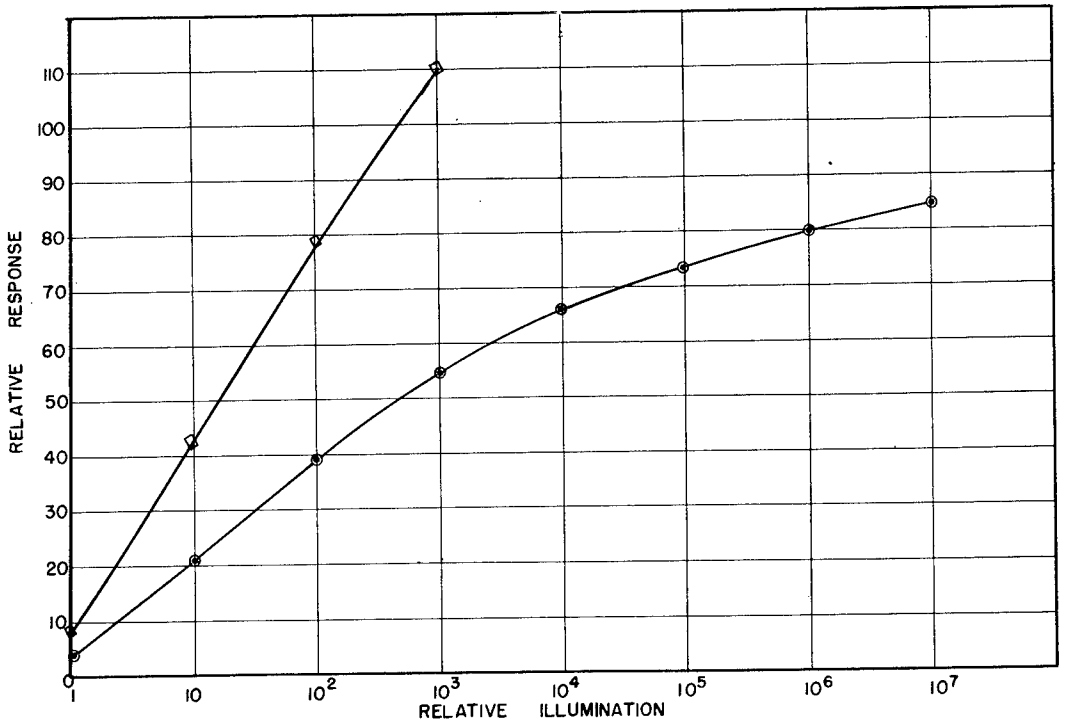

Fig. 68. Typical response curves for the logarithmic multiplier phototube circuit

CHAPTER VI

IONOSPHERE RESEARCH WITH THE V-2

Introduction

The V-2 flight of March 7, 1947 marked the first occasion on which measurements of ion density were made from vantage points within the ionosphere itself. The theory of the experiment performed during that flight is discussed in earlier reports of this series,[1] as is the previous progress made in the development of equipment and techniques.[2] The experimental results obtained on March 7 are discussed in Section A of this chapter The rocket-borne transmitter and antennas are described in Sections B and C respectively. Finally, the receiving and recording systems located at the two ionosphere ground stations are detailed in Section D.

A. The March 7 Ionosphere Experiment

by

T. R. Burnight, J. F. Clark, Jr.
and J. C. Seddon

Experimental data concerning the ion density in the ionosphere were obtained during the V-2 flight of March 7. Signals were recorded at both ground stations during the first 402 seconds. This covered the period from take-off to approximately the time at which the rocket broke up.

Ground Station I was located 14 km (9 mi) from the launching site bearing 7° west of north. Ground Station II was situated 74 km (46 mi) north northeast of the firing area. The same types of data were recorded at each of these stations. Electromagnetic radiation at the crystal-controlled frequencies of 4.274 mc and 25.644 mc was transmitted from the rocket. These two signals were received at the ground stations and the rate of change of the phase difference between them was recorded as a phase beat frequency. The

---

[1] Naval Research Laboratory Report No. R-2955, Chapter III, Section F, and Naval Research Laboratory Report No. R-3120, Chapter II, Section C.

[2] Naval Research Laboratory Report No.R-2955, Chapter II, Section G, and Naval Research Laboratory Report No. R-3030, Chapter IV, Section E.

received signal strength was also measured. In addition, several quantities were measured in the rocket, and the values were transmitted to earth via the telemeter. In this way, voltages proportional to the cathode currents of the two output amplifiers were recorded, as were the r-f voltages at two points, approximately one-quarter wavelength apart, in both the 4.274 mc and the 25.644-mc transmitter output coaxial cables.

Take-off time, 11:23:29 a.m. M.S.T., was determined by correlating the timing signal furnished by the Ballistic Research Laboratories with the time reference broadcast by Station WWV. The 25.644-mc transmitter operated properly during the first 142 seconds of flight, and, intermittently, for short intervals thereafter. The 4.274-mc signal was transmitted throughout the 402 seconds of flight from take-off to rocket breakup.

The strengths of the signals as received at the two ground stations are plotted in figure 69 and figure 19. The variations in transmitter output, the antenna pattern, the aspect of the rocket, and the possible existence of corona discharge at the antennas, all can effect the received signal strength. The results shown in the two figures have not been normalized with respect to these parameters. This reduction is being carried out where possible, and will be reported upon subsequently.

Several relevant ionospheric phenomena were observed at the time of the firing. The fading of radio signals which occurred in various parts of the world indicated the presence of disturbances in the ionosphere. The National Bureau of Standards recorded an abnormally high value of attenuation at 4.274 mc at its station near Washington, D. C. This agency also operates an ionosphere height finding station at the site of Naval Research Laboratory Ionosphere Ground Station I at White Sands. Readings obtained there immediately before and after the flight also attested to the severe ionospheric absorption. Thus, a highly attenuating layer at the lower edge of the E layer, often referred to as the D layer, was evidently present during the experiment.

Serious interference was caused, after 128 seconds of flight (i.e., above 117 km, or 73 mi, altitude), by a c-w communication signal. This factor complicated the analysis of the data.

As can be seen in figure 19 the 4.274 mc signal disappeared in receiver noise at an altitude of approximately 111 km (69 mi) during the ascent, and it reappeared at the same altitude on the downward leg of the flight. Station II did not record this effect, since its receivers were less sensitive, and had a higher background noise level. The telemetering record of the r-f voltages measured in the rocket shows that the transmitting system continued to operate in the region above 111 km. Thus it appears that the loss of the low-frequency signal was due to the disturbed condition of the ionosphere.

The measurements at the two ground stations definitely correspond as to evidence for the presence of the D layer. A sharp drop in received sig-

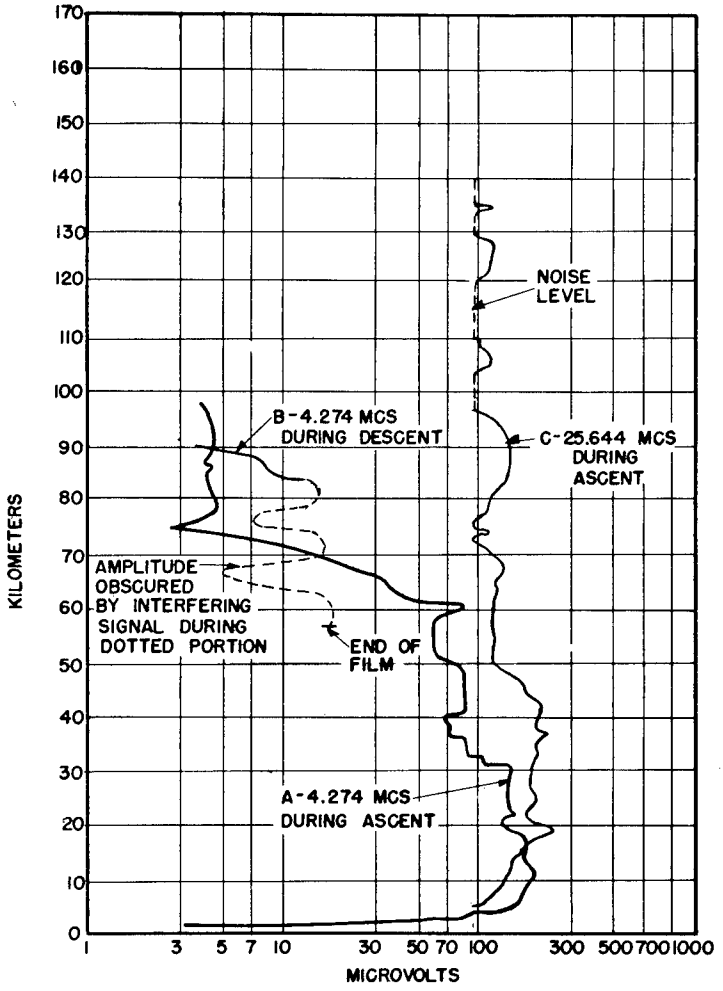

Fig. 69. Received signal strength against altitude as received at Station II White Sands, between 11:23 and 11:30 A.M., M.S.T. on March 7, 1947

nal level began just above 60 km altitude in both cases. This altitude is in general agreement with previous estimates of the location of the D layer.

The features of the phase beat frequency data which are of immediate interest are the altitude at which the beat frequency commenced and the manner in which it varied with the height of the rocket. The phase beat frequency first became apparent at about 43 km (27 mi) altitude. It remained at a low value up to 84 km (52 mi). Above 84 km the phase beat frequency increased, and above 91 km (57 mi) it increased rapidly. At 111 km (69 mi) it ceased, due to the fact that the 4.274-mc radiation was no longer received.

Representative sections of the continuous film record taken at Ground Station I are displayed in figure 20. The characteristic trace obtained when both signals were well above the limiting level is shown in section A of the film. Section B shows a portion of a beat recorded when the V-2 was 79 km (49 mi) over White Sands. The well-defined waveform seen in Section C corresponds to an altitude of 90 km (56 mi). A more complex waveform is

reproduced in Section D, and the sudden cessation of the beat frequency at 111 km (69 mi) altitude is clearly visible in Section E.

The analysis of these data continues, and future reports of this series will contain the further results.

B. The Ionosphere Transmitter

by

J. F. Clark, Jr. and G. Van Sickle

An improved transmitter was designed for the March 7 ionosphere experiment. It represented an advance over the equipment employed in the firing on October 10, 1946. Since it was intended to serve in addition as a prototype for future work, it was designed to be not only physically rugged and electrically stable but also to be readily adaptable to use over a wide range of frequencies without the necessity for any substantial changes in the basic plan.

Previous experience led to the decision to obtain a minimum of 50 watts of r-f output power from the transmitter at each of the two operating frequencies, which, in this experiment, were 4.274 and 25.644 mc. The 829-B dual beam tetrode was then selected for use in the power amplifier stages because of superior mechanical characteristics[3] (cf. figure 70). Trials demonstrated that the 6V6 beam tetrode, when operated as a frequency doubler, had a power output which was more than adequate to provide the excitation necesary for the power amplifiers.

To increase stability, the crystal oscillator was operated at half the frequency of the low frequency power amplifier. A low temperature coefficient AT-cut crystal was incorporated in a 6V6 tetrode circuit. The tube (labelled V1 in figure 70) was operated with a low screen grid voltage and minimum feedback in order to reduce frequency drift as much as possible. As shown in figure 71, all resistors and fixed condensers in each stage of the exciter were mounted on a cylindrical terminal board directly beneath the tube socket. A small change of frequency was had by tuning the variable condensers; a large change by replacing the separately mounted coils.

The low frequency doubler stage (V2 in figure 70) employed another 6V6 beam tetrode. Each 6V6 exciter tube was operated with low screen grid voltage in order to permit an indefinite period of detuned operation without exceeding the dissipation rating of the tube. The operating conditions of the tripler (V5) and high frequency doubler (V6) were similar to those of the

---

[3]For example, the 4D22 proved to be mechanically unsatisfactory.

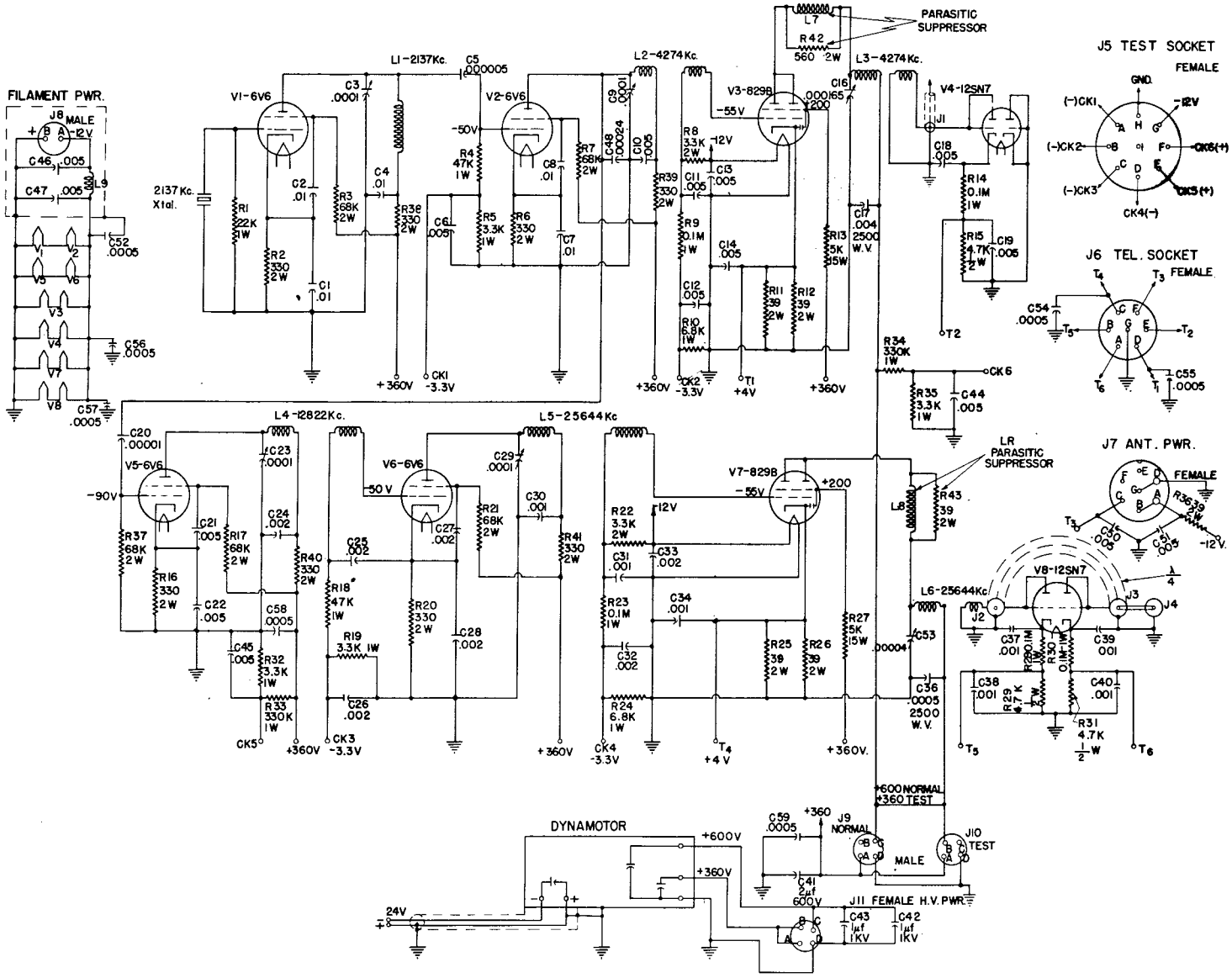

Fig. 70. Schematic diagram of ionosphere transmitter

low frequency doubler, the exception being that the tripler was operated with approximately 75 volts of bias as compared to about 50 volts in the case of the doublers. The tuning of each exciter stage was accomplished by observing the grid bias developed in the following stage at the check points which were provided for this purpose. These are labelled CK1, CK2, CK3, and CK4 in figure 70. Check points 5 and 6 provided a measure of the exciter and power amplifier plate supply voltages, respectively. Check point 7 permitted the measurement of the filament supply voltage.

The two power amplifiers (V3 and V7) were similar in operation. Each 829-B dual beam tetrode was operated as an amplifier rather than as a frequency multiplier in order to obtain better efficiency, and to minimize any harmonic output which might cause interference in other experiments. After careful stability checks, the two halves of each dual power amplifier tube were operated in parallel, without neutralization. This was done in order to simplify adjustment and the excitation requirements, to allow frequency changes to be made without reneutralizing, and to obtain an r-f output voltage unbalanced-to-ground without disturbing a balanced push-pull amplifier. An inductively-coupled low-impedance grid circuit was employed. Throughout the transmitter, the use of r-f chokes was avoided in order to prevent low-frequency parasitic oscillations. Regeneration at the operating frequency was prevented by means of thorough shielding between the input and output circuits of the power amplifiers. This shielding included the use of bypass condensers which were built into all of the output amplifier tube socket terminals except those connected to control grids. Very-high-frequency parasit-

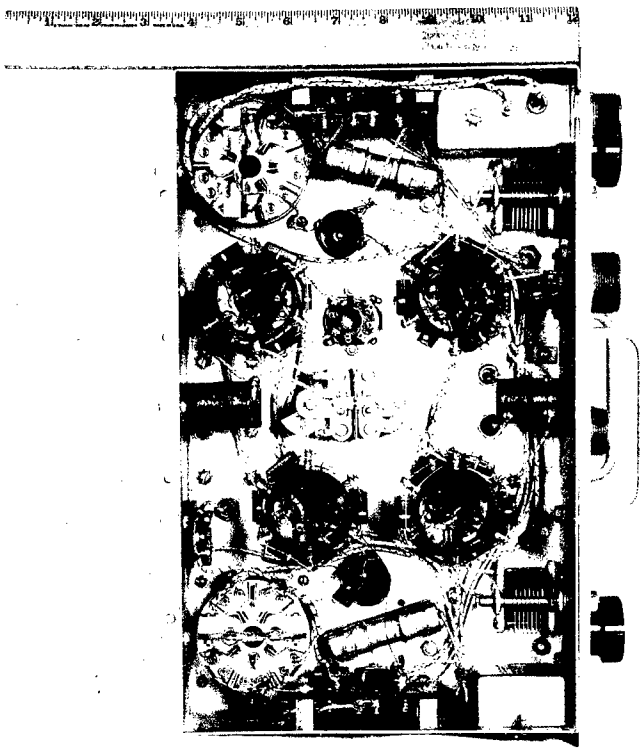

Fig. 71. The ionosphere transmitter, bottom view

ics were prevented through the use of a small inductance in parallel with a resistance, such a pair being placed in series with each 829-B plate lead. Increased stability was also obtained by operating all variable condenser rotors at ground potential. This also made it possible to mount these condensers more ruggedly. Each variable condenser was provided with a rotor lock to prevent any changes in setting which might be caused by the vibrations and shocks incident to the firing and flight of the V-2.

The control grids of the power amplifiers were returned to the negative terminal of the 12 volt filament battery in order to prevent these tubes from conducting an excessive amount of plate current in the absence of excitation. The 5,000 ohm screen grid dropping resistors (R13 and R27) prevented the screen grids from exceeding their dissipation ratings under any conditions of operation, including operation with the plate disconnected. Subsequent experience has pointed to the desirability of increasing these resistance values to 10,000 ohms in order to limit the off-resonance plate current, which occurs when the antennas are detuned, to a value which is more consistent with safety of operation. The voltage drops across the 19.5 ohm cathode resistors (R11, R12 and R25, R26) were telemetered to earth. These furnished a measure of the total cathode current in each power amplifier tube.

The r-f voltage appearing across each output transmission line was measured by means of 12SN7-GT dual triodes (V4 and V8), which were connected as diodes. These voltages were read at the output coupling loops and a quarter wavelength away, in the transmission lines. In the case of the low-frequency line the wavelength requirement located the second diode in the tail of the V-2. Filament power and telemetering connections for this diode were provided through socket J7. In the case of the high frequency however, both second diodes were located in the transmitter case, with a quarter wavelength of transmission line connected between J2 and J3. The diode voltages were telemetered from cathode voltage dividers of the type exemplified by R14 and R15.

In order to prevent interference in other experiments, many precautions were taken to avoid the leakage of r-f energy from the transmitter case. All test and telemetering leads were bypassed inside the case and carried in shielded cables. The filament power was taken through a shielded low-pass pi-section filter (C46, C47 and L9). As seen in figure 72, the lead which carried 24 volt primary power to the generator was shielded up to the internal dynamotor bypass condenser, and, in fact, did not terminate within the radio-frequency region of the transmitter. A cover plate was provided to shield test jack J5 when it was not in use.

As shown in figures 73, 74, and 75, all components, including the dynamotor and the transmitter chassis, were rigidly mounted on a 6 mm (0.25 in.) steel base plate. Figure 76 illustrates the clamps which secure this plate to the warhead mounting rails. The rails provided additional protection against lateral motion. The plate extended through the rear of the transmitter case and was secured to the rails adjacent to the warhead door. Thus,

when the unit was in position in the warhead, it was free to move only in the forward direction. Clamps were then affixed to secure it completely. The aluminum case was used primarily to provide rigidity and shielding. Since all electrical connections and removable mechanical fittings were accessible from the front (cf. figure 76), it was possible to remove the transmitter through that single access door. The complete transmitter weighed 32 kg (70 lb).

A special voltmeter was provided for transmitter adjustment and testing. The use of 15 m (50 ft) of shielded fourteen-conductor cable enabled this voltmeter to monitor the seven transmitter check points and the six telemetered voltages from the base of the V-2 when it was erected on the firing platform. This greatly facilitated the adjustment of the antennas.

Initial alignment of the transmitter was readily accomplished. For maximum stability, the crystal oscillator tuning condenser was adjusted so that the voltage at check point 1 had 80 percent of its maximum value. The lower capacity point was used for this setting. The low-frequency doubler, the tripler, and the high-frequency doubler tuning condensers were then adjusted in turn so as to maximize the voltages at check points 2, 3 and 4, respectively. When properly adjusted, check points 1, 2, 3, and 4 all indicated approximately 3 volts on the test meter, which corresponded to 45 volts of bias in each stage. The final amplifier stages were tuned to resonance by minimizing their respective cathode currents, which were read via telemetering channels 1 and 4.

Power requirements for the transmitter were -12 volts at 3.9 amperes for the filaments, and -24 volts at approximately 20 amperes. The latter figure was a function of the antenna loading. Dynamotor efficiency was approximately 50 percent. The efficiency of the power amplifier circuits, including the effect of r-f losses in the output coupling and diode circuits, was measured and found to be greater than 60 percent for an r-f power output of 60 watts at each of the two operating frequencies.

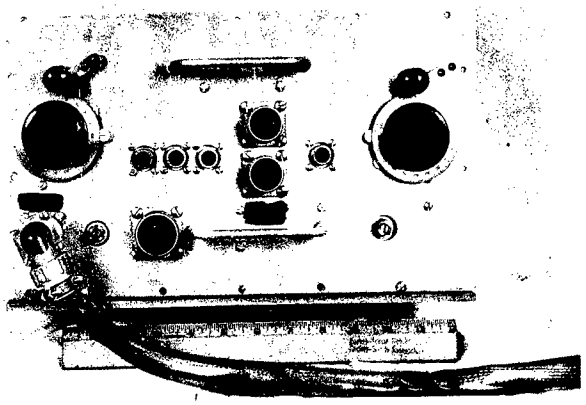

Fig. 72. The ionosphere transmitter, front view

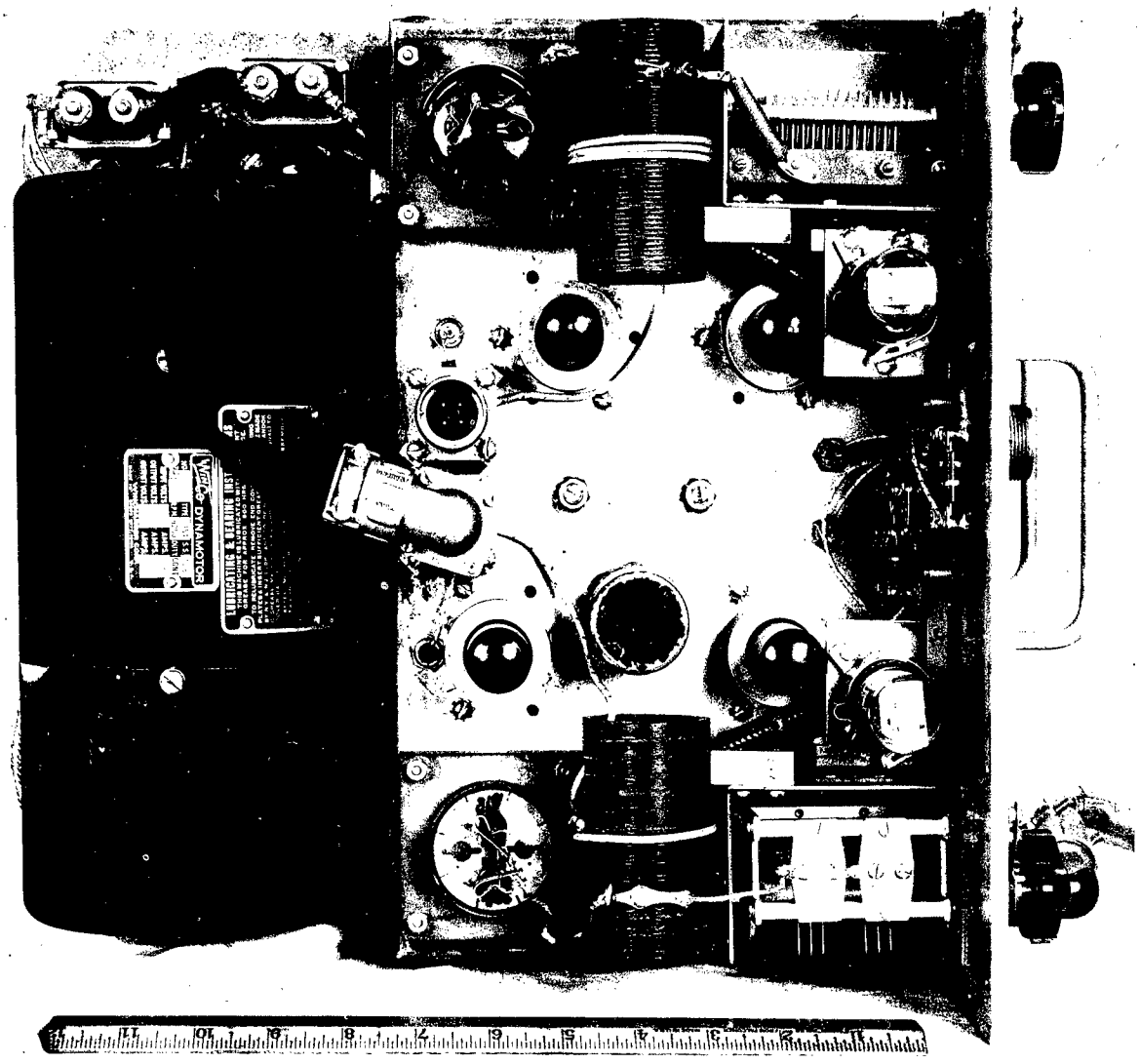

Fig. 73. The ionosphere transmitter, top view

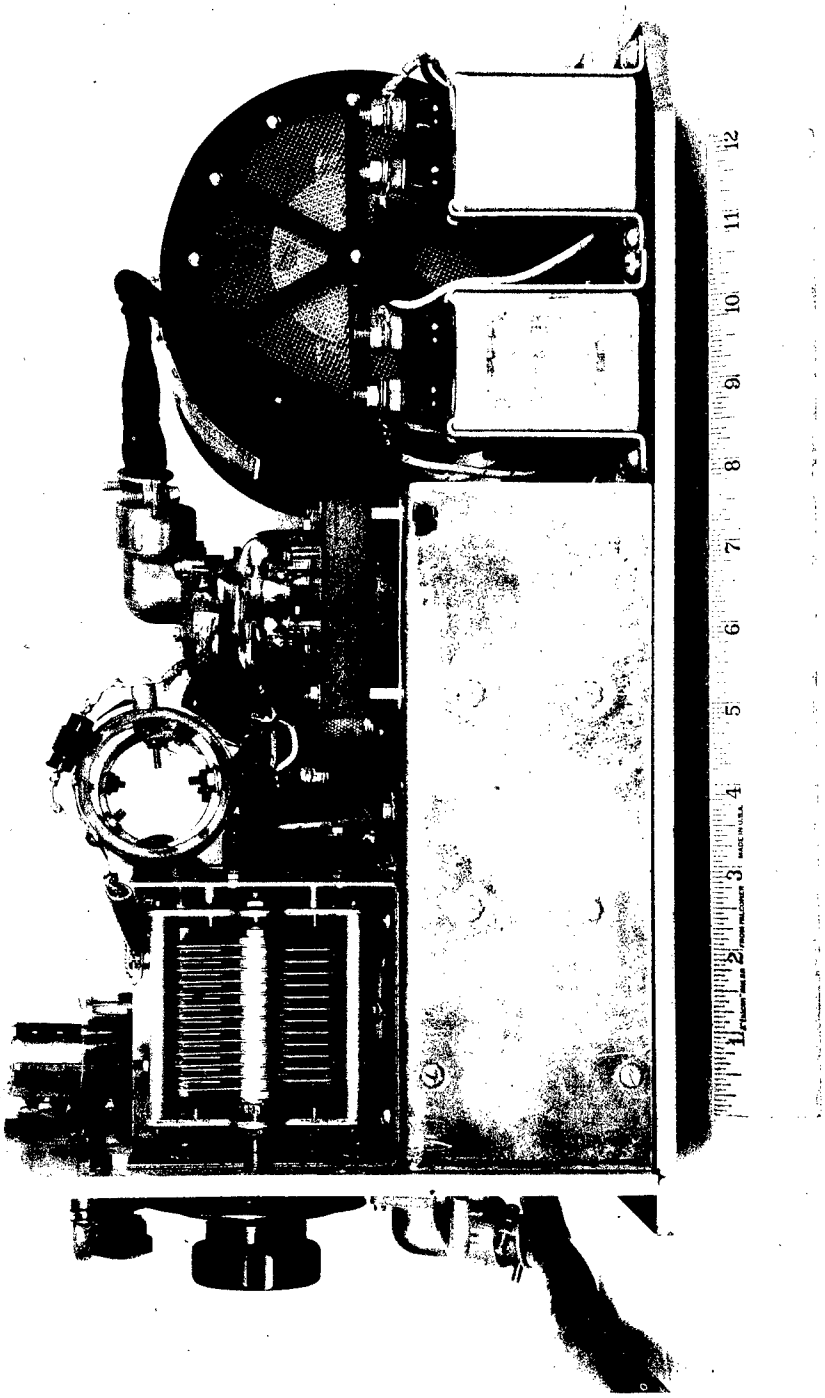

Fig. 74. The ionosphere transmitter, side view

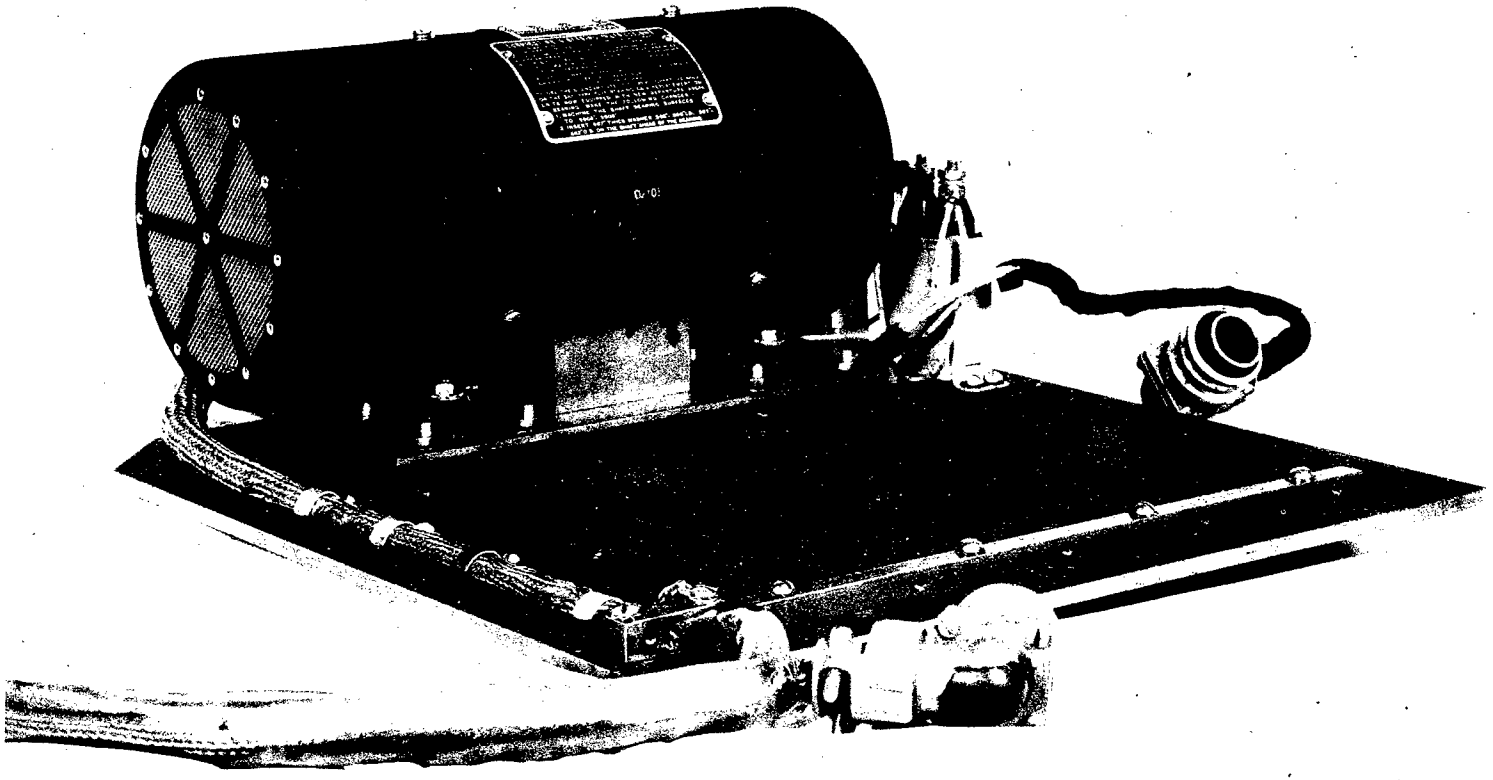

Fig. 75. The dynamotor mounted on the base plate of the ionosphere transmitter

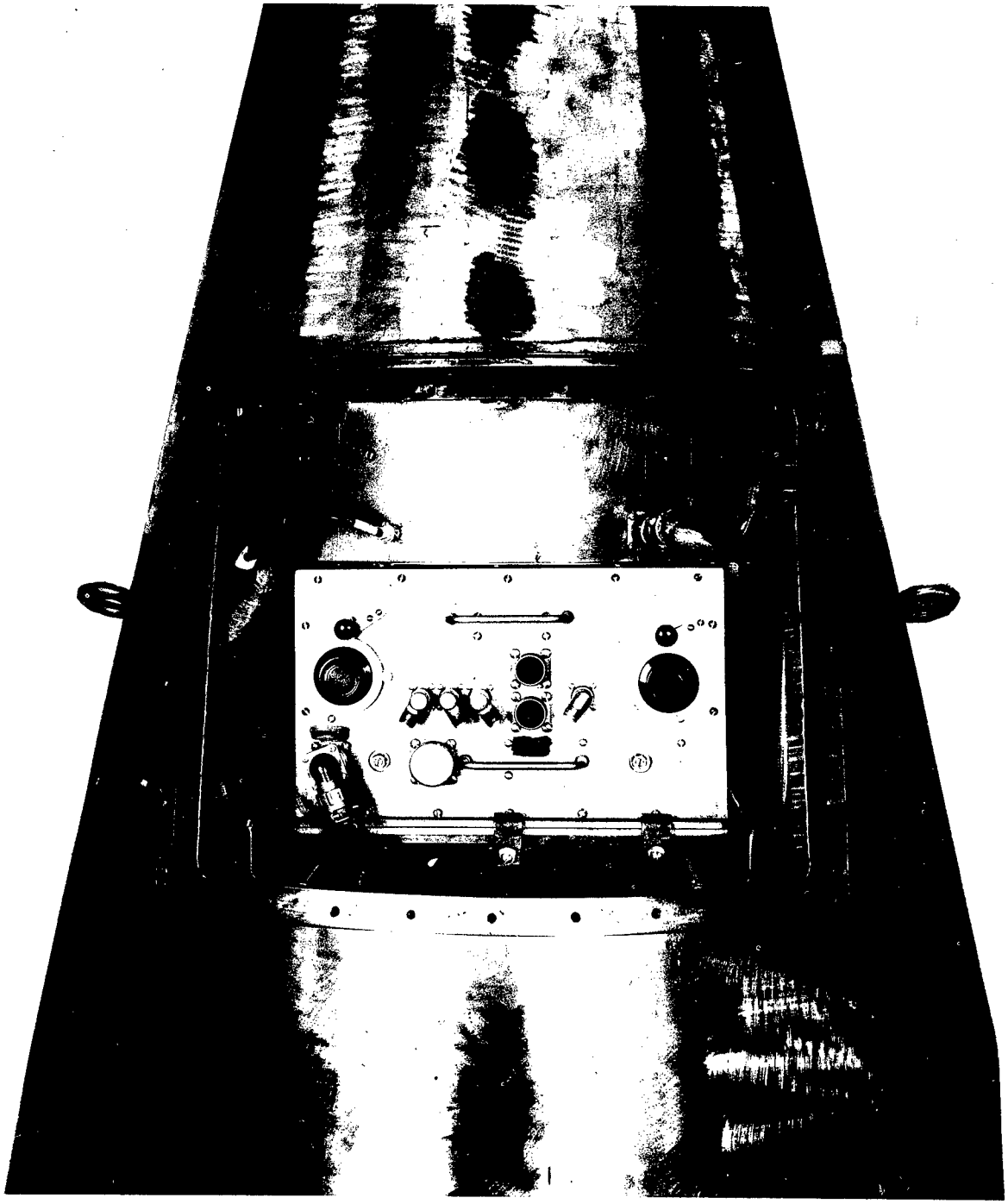

Fig. 76. The ionosphere transmitter mounted in the warhead of the March 7, 1947 V-2

C. Rocket Antennas for Ionosphere Research

by

T. R. Burnight, W. F. Fry,
and J. C. Seddon

The problem of constructing suitable antennas has been one of the most difficult to arise in connection with the ionosphere measurements. The side antennas used in early flights[4] were difficult to install. The trailing wire antennas employed later did not have satisfactory patterns. Therefore a new type of antenna was installed on the V-2 which flew on March 7.

The antennas consisted of wires which went around the tail structure of the rocket near its base. The wires were supported by means of four bakelite insulators which extended 15 cm (6 in.) beyond the edge of each fin, and lay in a plane normal to the missile axis. As before, a certain amount of slack was allowed in each wire in order to decrease the stresses imposed by the supersonic velocity with which the V-2 travels. Figures 77 and 78 illustrate the method of mounting.

The 25.644 mc antenna was a balanced dipole which was fed at fin I. The 4.274 mc antenna was bottom loaded and fed at fin II. It was supported at fin III and extended to fin IV. The two matching transformers were mounted in fins I and IV. Each was connected to its antenna by 76 cm (30 in.) of shielded cable.

The determination of the impedances which these matching units should present was a particularly difficult phase of the antenna problem. The antenna impedances were first measured with the radiators mounted on a V-2 tail section which stood on a roof. The high and low-frequency antenna impedances were there seen to be 50+j270 ohms and 14-j570 ohms, respectively. The matching units were constructed accordingly, due consideration being given in each case to the 76 cm (30 in.) of feeder cable and the 50 ohm impedance of the transmission line which led to the transmitter.

The impedances were determined several times while the rocket was in the launching area. When the missile was mounted on the Meillerwagen horizontally, impedances of 55+j6 and 64+j5 ohms were measured at the transmitter panel for the high and low frequencies, respectively. With the rocket standing alone in firing position, impedance values of 35+j0 and 50+j12 ohms were found. These latter measurements were made with the aid of temporary cable lengths which were equivalent to the transmission lines mounted in the rocket between the transmitter in the warhead and the antennas at the tail. Finally, when the Gantry crane was brought up to the rocket and the various testing cables were connected, the impedances changed radically.

---

[4] Naval Research Laboratory Report No. R-2955, Chapter III, Section G.

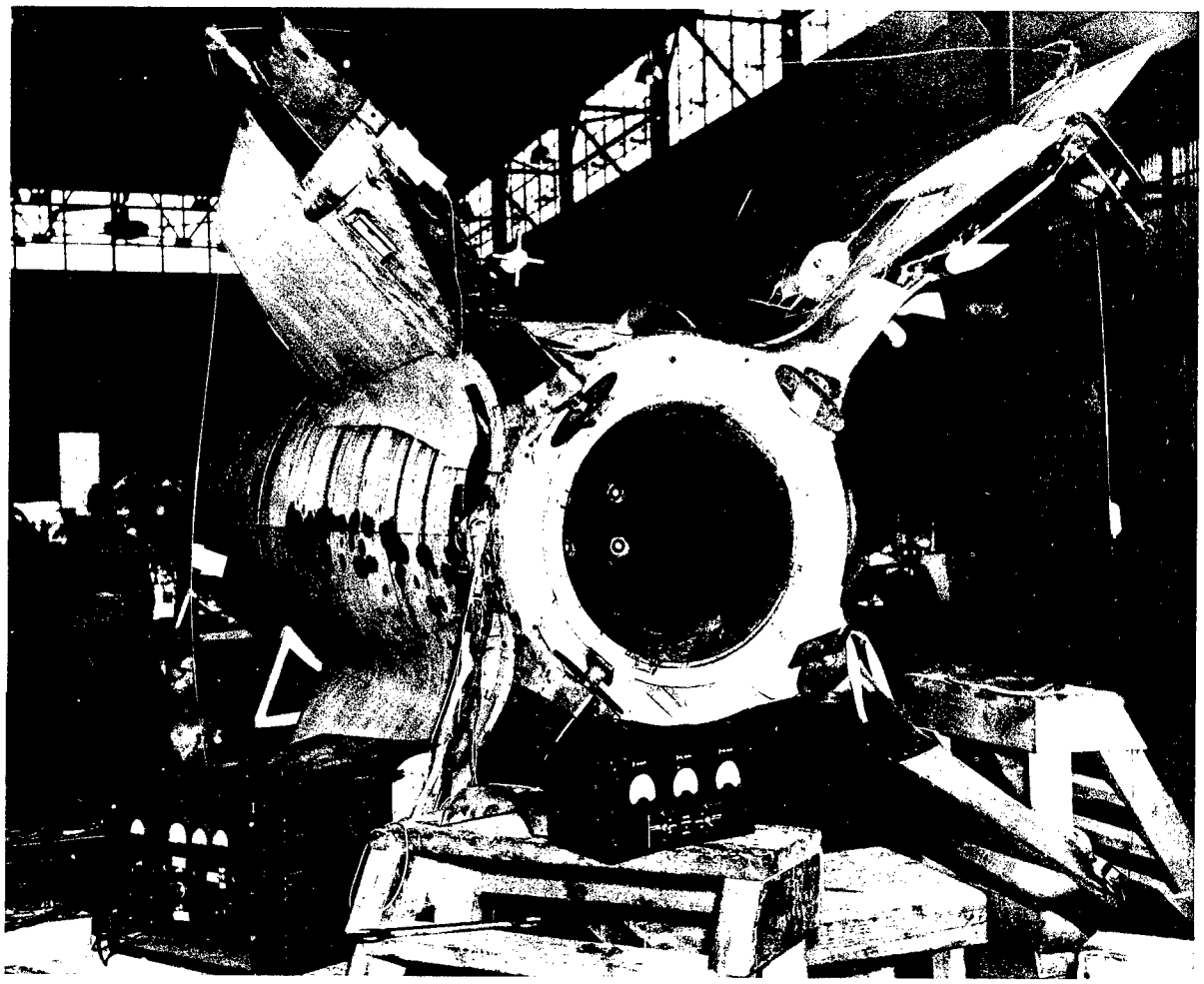

Fig. 77. Ionosphere antennas mounted on the V-2 tail structure

The last values given here were taken to be the most representative of flight conditions, and antenna tuning was accomplished on this basis. The presence of the platform upon which the V-2 stood (cf. figure 79) undoubtedly affected the impedances, however, no better method of tuning was available at the time.

At the ground stations, half-wave horizontal dipoles served to receive the high-frequency radiation. In each case the low-frequency antenna comprised a half-wavelength horizontal section with a quarter-wavelength vertical lead and a half-wavelength reflector which was positioned a quarter-wavelength below the horizontal element.

As noted in Section A, signals were received at both ground stations during much of the flight. The variations in the strengths of these signals indicated either that the antenna patterns were not suitable, or that the transmitters were not properly matched to the antennas after the V-2 left the ground, or both.

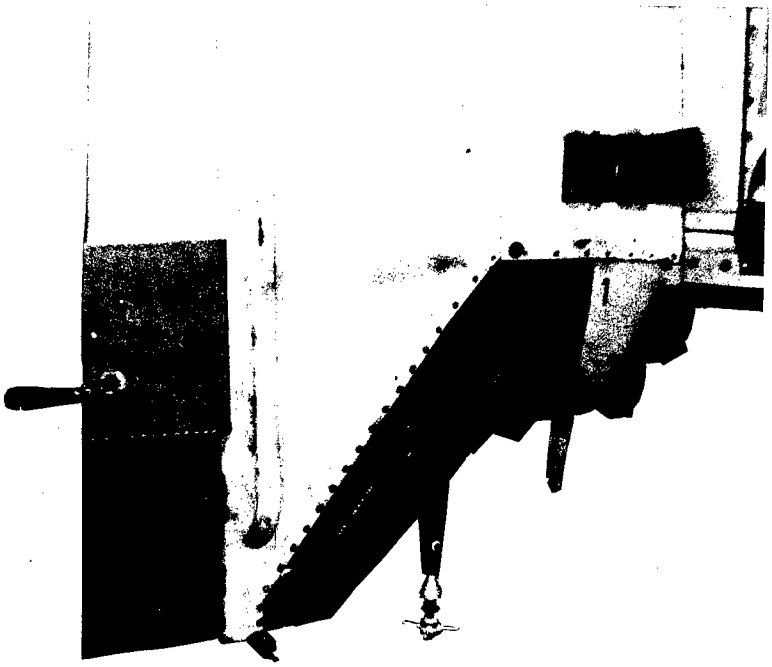

Fig. 78. Ionosphere antenna mounting insulator. The telemetering turnstile transmitting antenna is also visible.

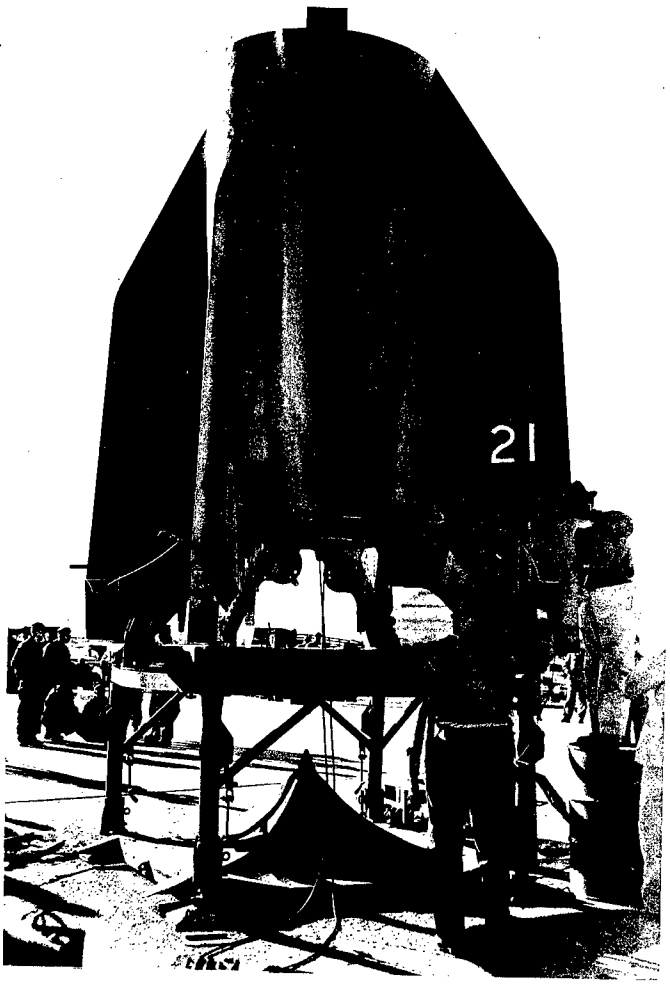

Fig. 79. Mounting ionosphere antennas on the V-2

At the present time several methods of meeting the radiation problem are being investigated. Antenna impedances have been measured on a rocket mounted nose down. Antenna patterns are also being measured with the aid of models. The use of an automatic tuning device is also under consideration.

D. The Ionosphere Receiving and Recording System

by

J. F. Clark, Jr., C. W. Miller
and G. H. Spaid

A receiving and recording system of improved design was employed in the March 7 ionosphere experiment. A brief description of this system, together with a short history of its evolution, is presented here. A more complete discussion of the theoretical design considerations will appear in a future report of this series.

The two receiving and recording stations are located so as to be approximately beneath the points at which the rocket penetrates the E layer of the ionosphere on a normal flight. Two types of data were to be gathered at these stations: (1) equivalent electron density as a function of altitude, and (2) the attenuation of each signal, also taken as a function of altitude. In addition, long range propagation data were to be obtained over paths between the rocket-borne transmitters and the many receiving stations scattered throughout the world which were manned by cooperating agencies.

Basically, as shown in figure 80, the original receiving and recording system was comprised of two receivers tuned to harmonically related frequencies, a unit designed to multiply the frequency of the amplified low frequency signal to that of the high frequency radiation, and a mixer, amplifier, and recorder which compared the phase of the two resulting signals. The rate of change of the phase difference was capable of being used to determine the refractive index at the lower of the two frequencies, and equivalent electron densities, in the strata of the ionosphere. Signal levels were measured to provide attenuation data. Timing markers were also recorded with the data, in order to correlate ion density with altitude.

In the first experiments, three radio frequencies were employed. Since the first cycle of V-2 firings, however, only two frequencies (4.274 and 25.644 mc) have been used. Nevertheless the present system was designed so as to permit the use of a third frequency simply by adding another receiver and the associated mixing and recording equipment.

In all of the previous experiments, tuned radio frequency receivers were used. They were selected primarily because they were simple to design and construct. The use of these receivers revealed a number of disadvantages, including inadequate sensitivity and selectivity, and excessive vari-

able phase shift. Variable phase or frequency shift occurring within either receiver may have the same appearance, when recorded, as the phase beat frequency data. Such a phase shift may be caused by the Miller effect in those stages which employ automatic volume control. This effect is essentially a detuning which is caused by variation in the effective shunt capacitance of the control grid of the tube. This in turn is due to the change in amplification factor caused by the application of avc voltage. Consequently, the design of a more acceptable system was undertaken for use in the March 7 and subsequent firings.

If an ordinary superheterodyne receiver were used, local oscillator frequency drift would also introduce errors. A change in amplitude of either signal, when applied to the mixer, also has an effect on the oscilloscope trace which is similar in appearance to the phase beat frequency indication. Thus, it is necessary to limit the amplitude of each signal before it is fed to the mixer. However, should another signal appear, comparable in amplitude and frequency to the signal under study, the limiting process might introduce additional frequencies by a phase modulation process. These frequencies would differ from the one being studied by integral multiples of the difference frequency. Their presence would considerably complicate the analysis. If the received signal drops below the limiting amplitude, the level of the output voltage of the mixer will depend upon the received signal strength, as well as upon the phase difference. These considerations imposed strict design requirements on the receivers. These may be summarized as follows. Variations in the phase shift introduced by the receivers had to be kept to a minimum. The total gain of the receivers had to be sufficient to secure limiting with very low input signal levels. Signal-to-noise sensitivity had to be optimum in order to ex-

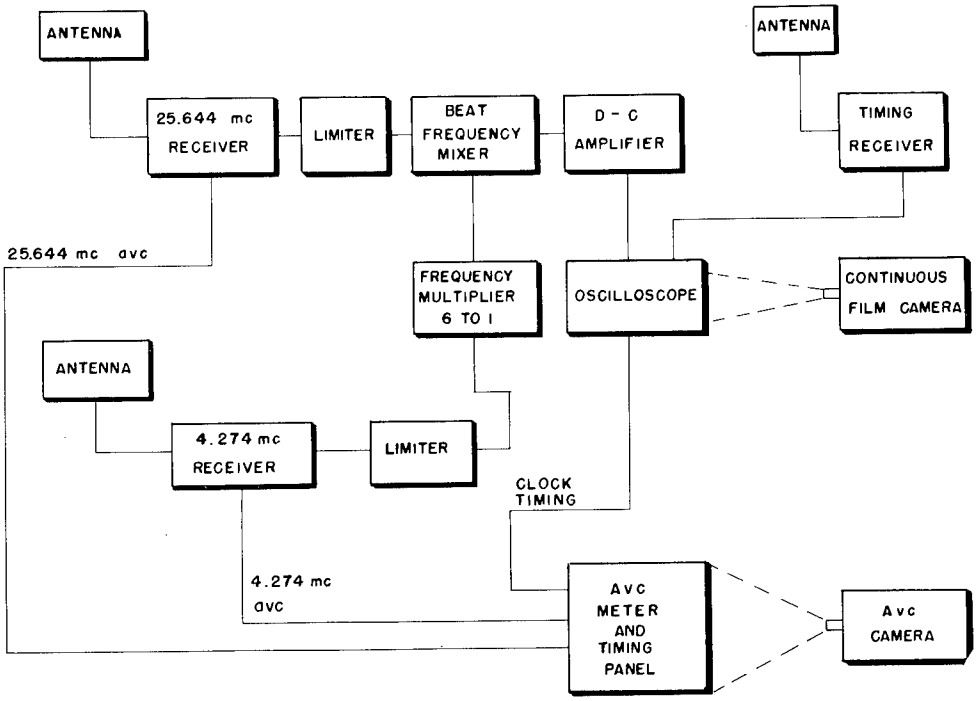

Fig. 80. Basic ionosphere receiving and recording system

clude noise from the data when received signal levels were low. High selectivity was essential due to the prevalence of excessive atmospheric noise, and the frequent occurrence, at White Sands, of interfering signals having frequencies close to the experimental frequencies.

The first type of receiver which was considered for the new design was a system which would eliminate the error introduced by local oscillator drift, while retaining the numerous advantages of the superheterodyne principle. Such a receiver is illustrated schematically in figure 81. It converts the input frequency to an intermediate frequency, amplifies the latter, and reconverts it, using the same local oscillator, to the original input frequency. This system may be used with only one receiver if desired. However, it is diffucult to obtain sufficient gain without introducing the instability caused by feedback from the high level output stages to the low level input stages.

The equipment which was actually employed on March 7 is diagrammed in figures 82, 83, 84 and 85. It consisted essentially of two superheterodyne receivers with harmonically related local oscillators which were controlled by a single crystal. This system, which must include both receivers, has the further requirement that the intermediate amplifier and local oscillator frequencies have the same ratio as the original transmitted frequencies. With this arrangement, the limited output from the i-f amplifier of the low frequency receiver may be multiplied and mixed directly with the output from the i-f amplifier of the high frequency receiver. This affords the advantage of amplifying at two frequencies in each receiver, permitting a higher overall gain without loss of stability. The high frequency receiver includes a separate local oscillator. This allows it to be tested independently of the low frequency receiver. The system is also flexible enough to permit considerable changes in the operating frequencies. Such changes may be accomplished through the use of different local oscillator crystals and the adjustment of the tuned circuits preceding the intermediate frequency amplifiers.

In order to correlate the photographic data with missile position, timing pulses starting at take-off were transmitted from the launching site and recorded on each data film. These pulses occurred each half-second. Every twentieth pulse was omitted. The amplified pulses flashed neon bulbs which were in the fields of view of the continuous cameras. In addition, each ground station had an independent timing system referred to a chronometer. It could be used to ascertain the instant of take-off with reference to the time standard furnished by WWV. It was also capable of providing accurate time intervals in the event of a failure in the main timing system.

A photograph of the present ionosphere receiving and recording system appears in figure 86. The top panel includes the transformers which match the impedances of the antennas to the 50 ohm unbalanced receiver input terminals. The third shelf contains the high frequency receiver and the output mixer circuit. On the fourth shelf is mounted the low frequency receiver. The second shelf contains the timing and recording circuits. These include a direct coupled amplifier for the display of mixer phase difference

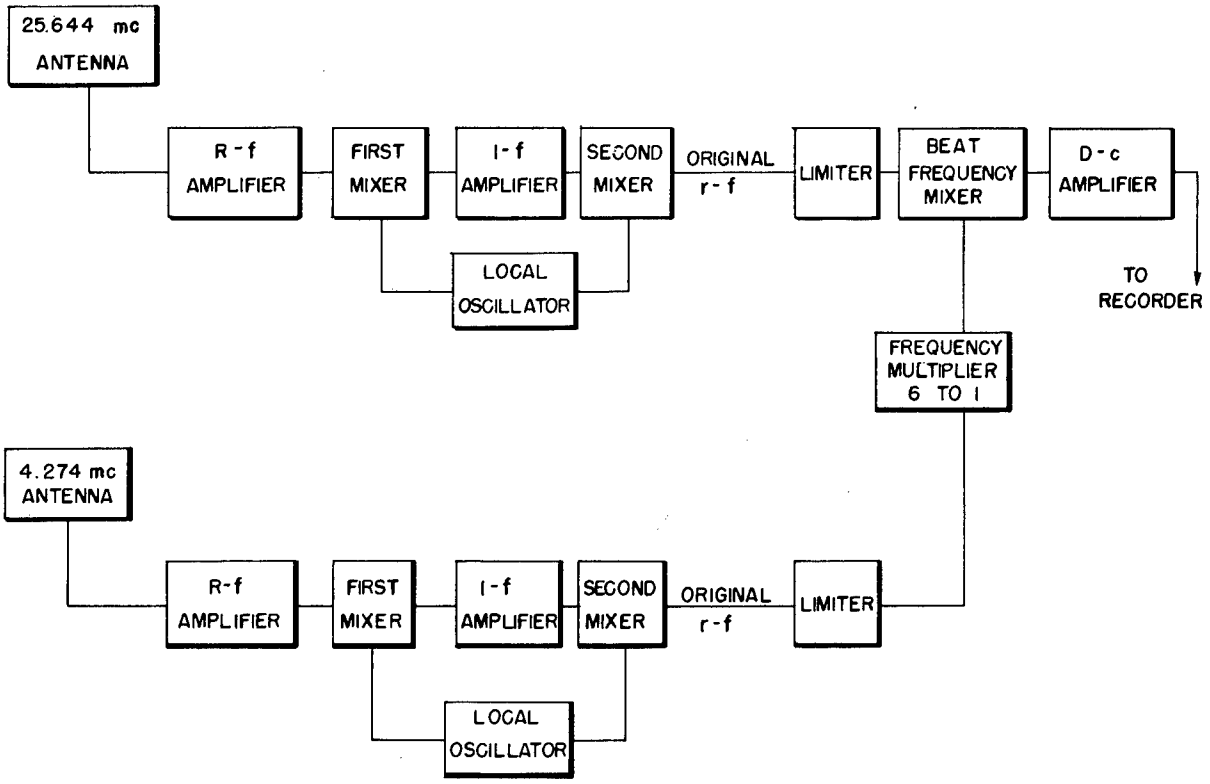

Fig. 81. Double conversion superheterodyne system

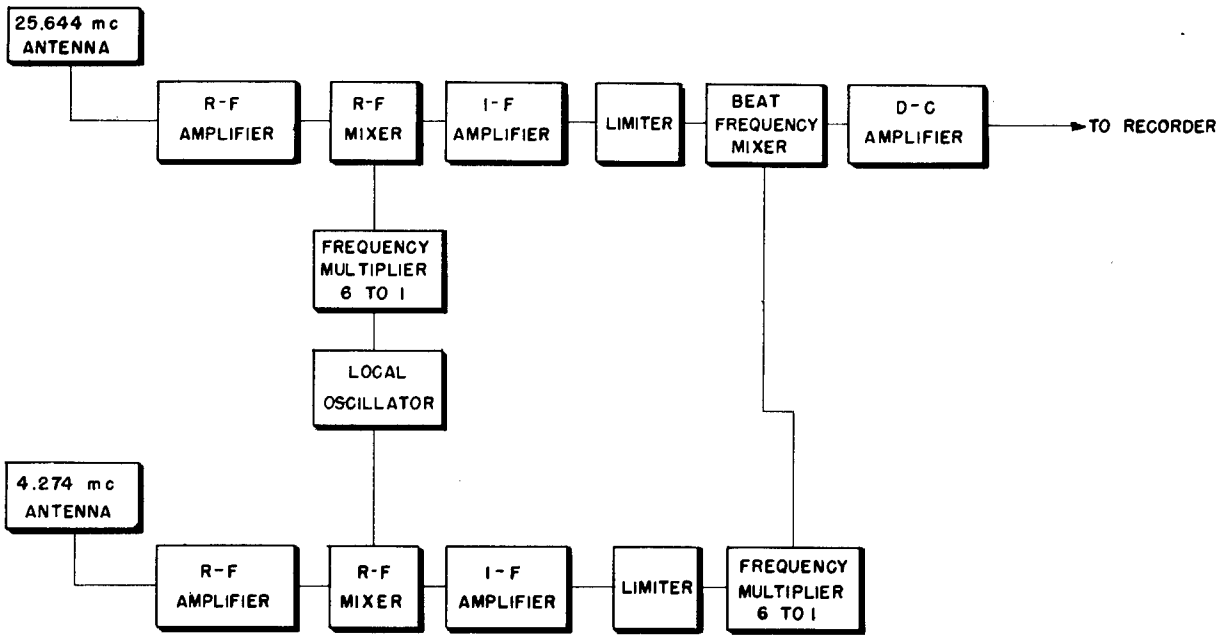

Fig. 82. Common local oscillator superheterodyne system

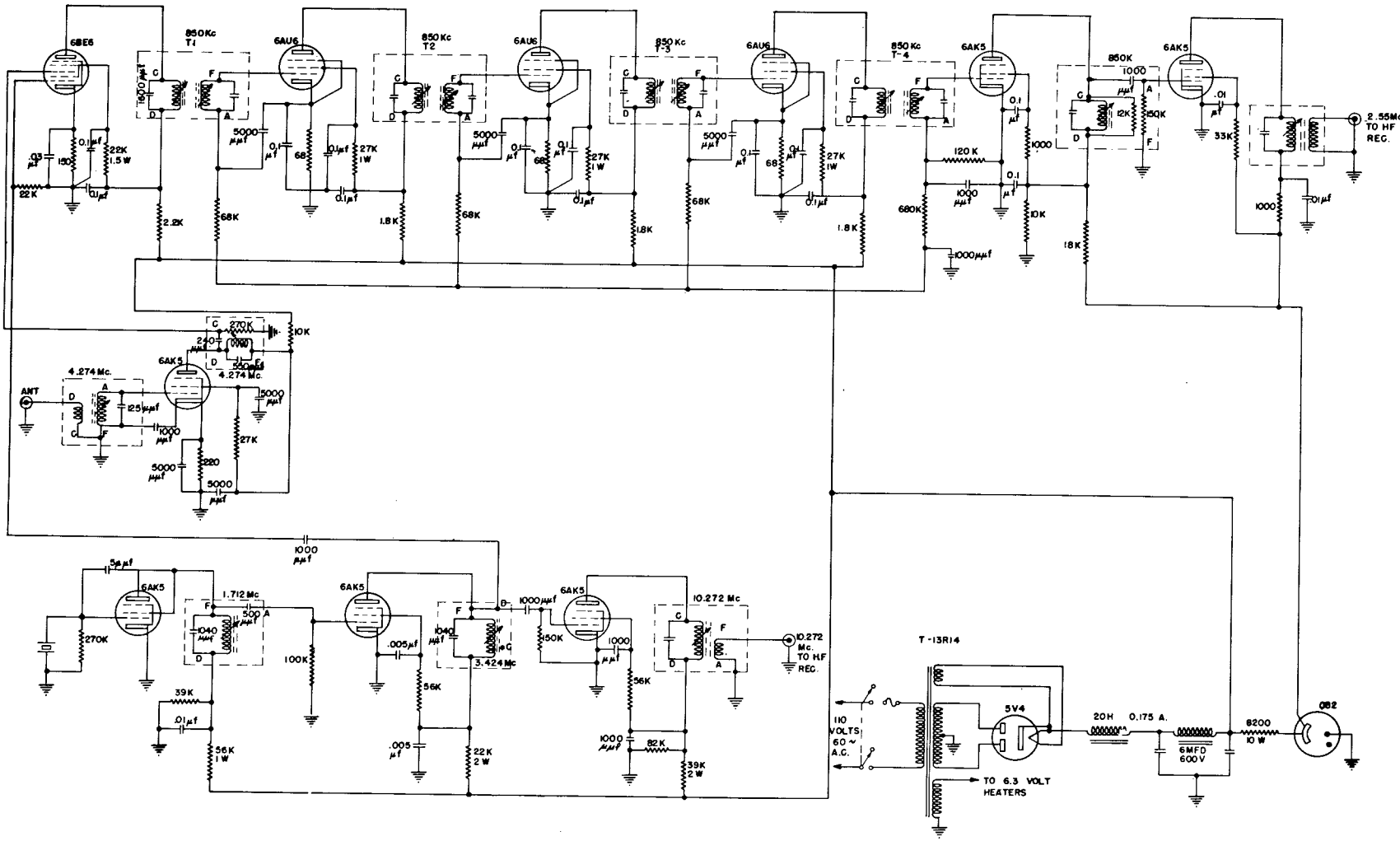

Fig. 83. 4.274-mc receiver for ionosphere measurements

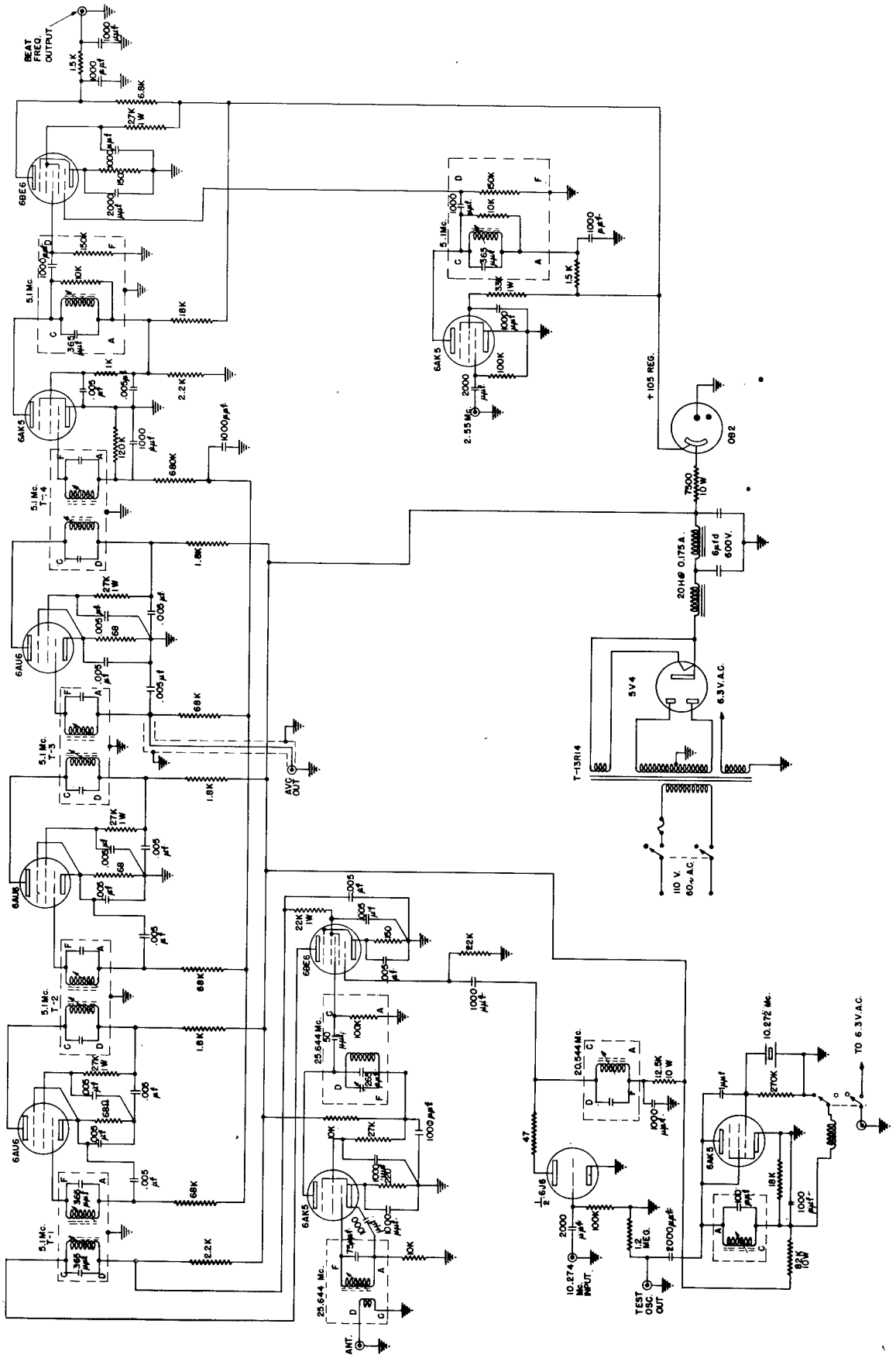

Fig. 84. 25.644-mc receiver for ionosphere measurements

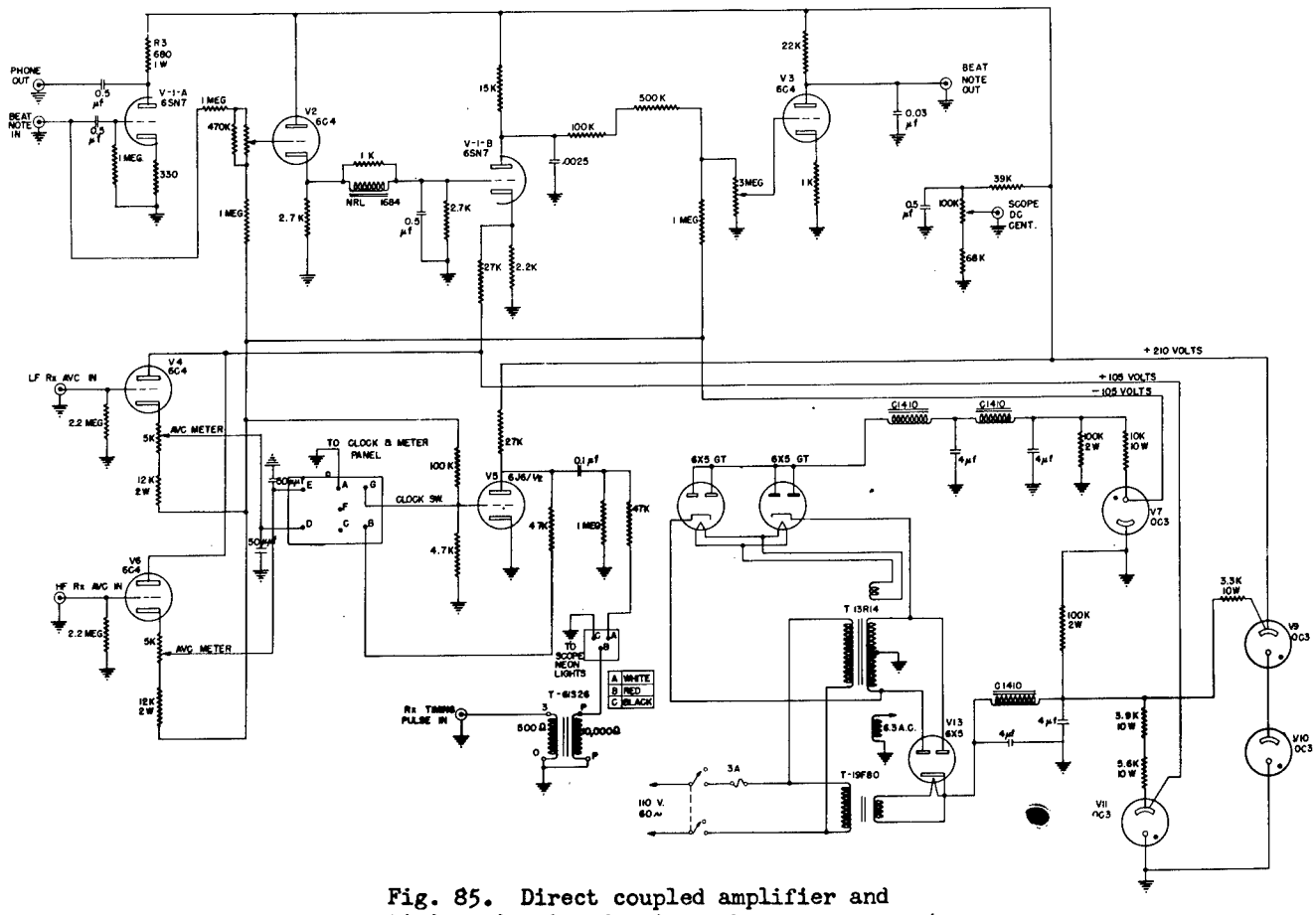

Fig. 85. Direct coupled amplifier and timing circuits for ionosphere measurements

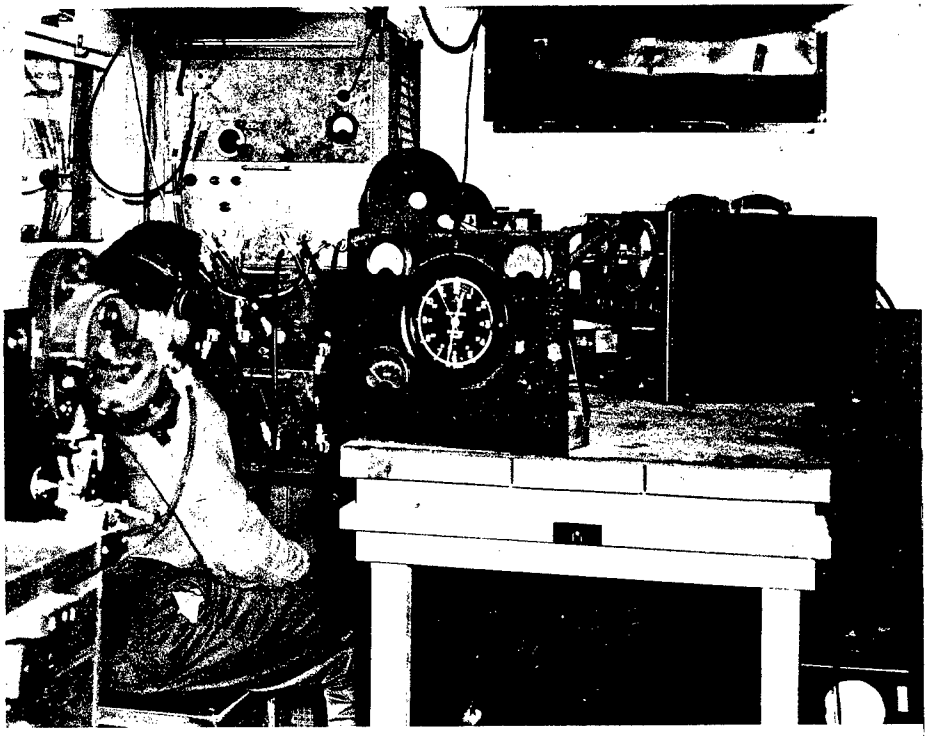

Fig. 86. Ionosphere receiver and recorder on mobile trailer I

on an oscilloscope, and cathode followers used to present signal level data on low impedance meters. The direct coupled amplifier has two output terminals. The first provides a capacity coupled unfiltered output useful for aural monitoring and for wire tape recording purposes. The phase beat frequency signal is filtered in a low pass unit which has a cutoff frequency of approximately 150 cycles. This serves to minimize the beat frequencies generated by interfering signals and the signal under study. The filtered phase beat frequency appears at the second output terminal.

The phase beat frequency data are recorded by means of continuous film cameras which are focused on the oscilloscope screens. The signal level data are recorded by means of a framing camera which is focused on the avc meter dial.

Tests showed commercial intermediate frequency amplifiers to be unsuitable, particularly with regard to the dependence of phase shift upon signal level. Accordingly, a high frequency receiver was designed which introduced less than 20 degrees of phase shift per stage for the maximum possible variation in signal level. This gave a maximum total phase shift of 60 degrees for the three i-f amplifier stages. The low frequency receiver called for less than 5 degrees per stage, or 15 degrees maximum total phase shift. This shift is still less than 90 degrees after the intermediate frequency has been multiplied to the high frequency i-f level. Preliminary checks of the receivers indicated that their performance was within these limits. Selectivity curves for both receivers are given in figures 87 and 88. The bandwidth measured at the half-power points was approximately 0.2 percent of the input frequency in each case. Sensitivity was essentially the same for both receivers, with two microvolts being required to obtain a fully limited signal. Ordinarily, 0.5 microvolts were required for a two-to-one signal-to-noise ratio in each receiver. Curves of avc voltage vs. signal input in microvolts for the two receivers are presented in figures 89 and 90. The avc time constant of each receiver was approximately 0.01 second. This short duration was chosen to minimize the loss of data which occurs when bursts of noise block the receiver.

As can be seen from an inspection of figure 19, a sharp drop occurred in the level of the 25.644 mc signal received at ground station I when the V-2 reached an altitude of 5 km. This was not accompanied by any shift in phase. The performance of the receiving system in this instance served to demonstrate that the present design has mitigated some of the undesirable effects associated with changes in received signal amplitude.

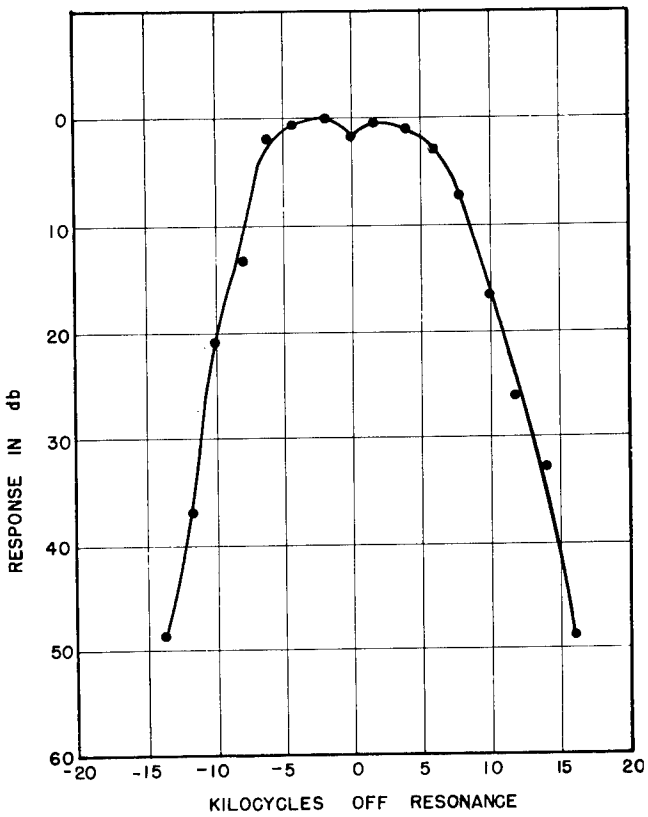

Fig. 87. Selectivity curve for 4.274-mc ionosphere receiver

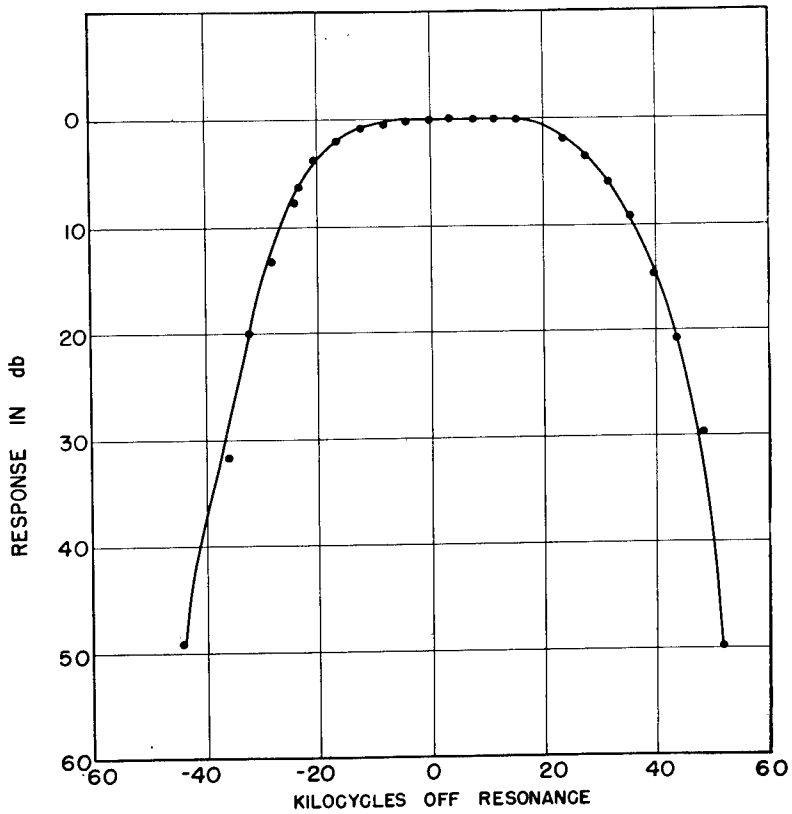

Fig. 88. Selectivity curve for 25.644-mc ionosphere receiver

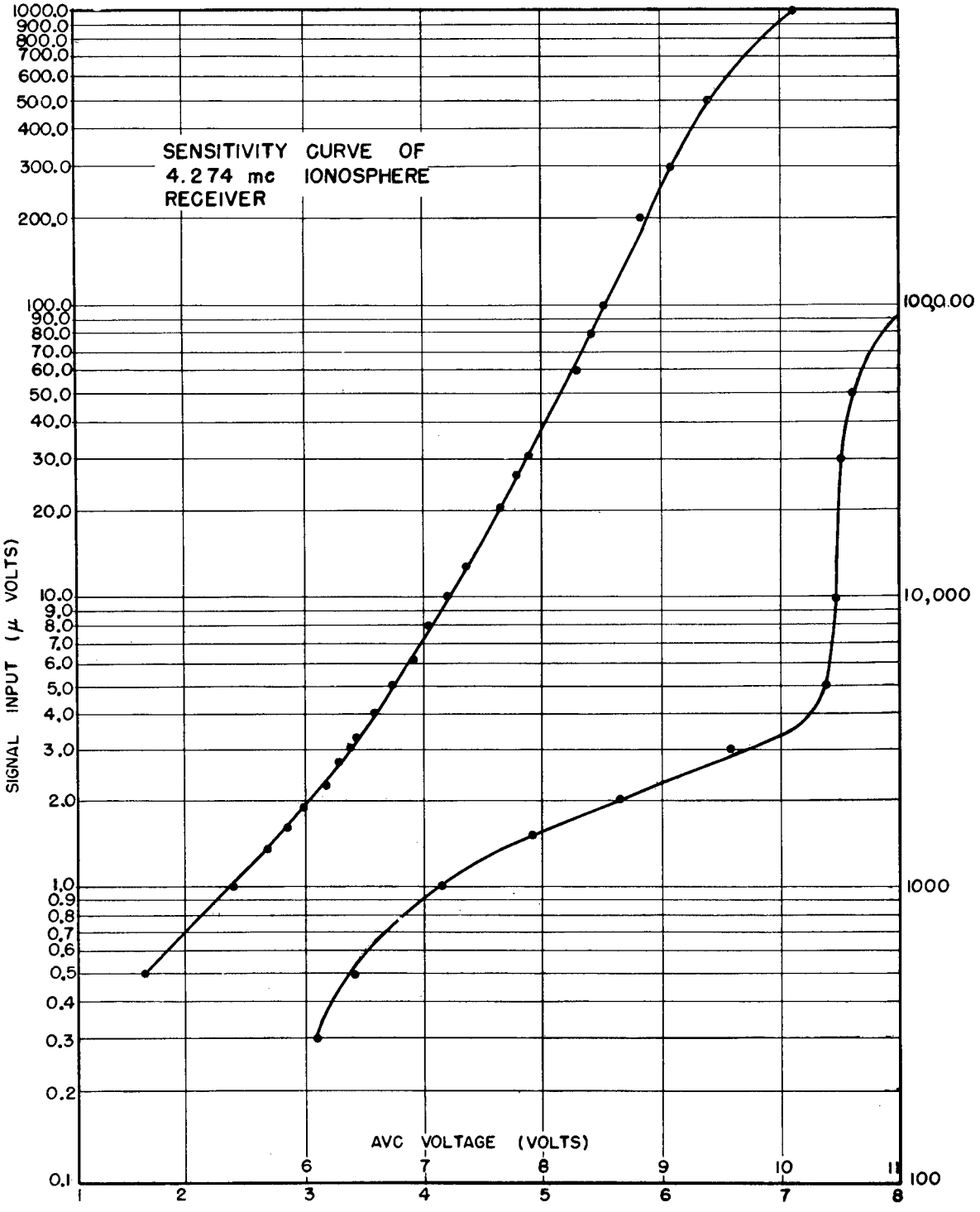

Fig. 89. Sensitivity curve of 4.274 mc ionosphere receiver

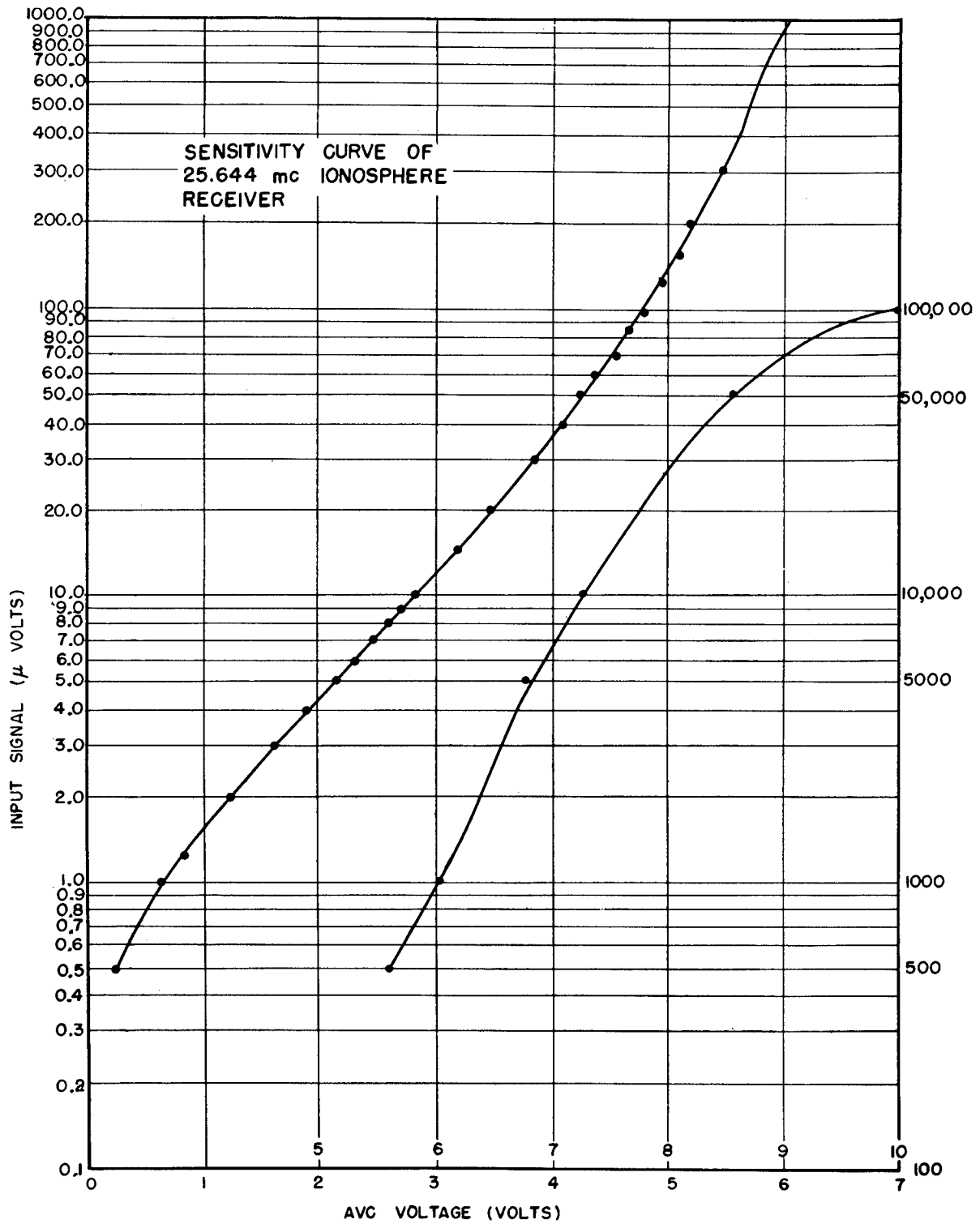

Fig. 90. Sensitivity curve of 25.644 mc ionosphere receiver

CHAPTER VII

THE PRESSURE AND TEMPERATURE OF THE UPPER ATMOSPHERE

by

N. Best, R. Havens
and H. LaGow

A study of the pressure and temperature of the atmosphere was carried out at very high altitudes during the V-2 flight of March 7. This work was a continuation of the measurements which were begun earlier in the Rocket-Sonde Research Program.[1] The physical and electrical arrangements of the various equipments are discussed in Section B of Chapter III, and illustrated in figures 6, 7, 8, 35 and 36. The results of the experiments are contained in a letter to the Editor of The Physical Review,[2] which appears below.

Pressure and Temperature of the Atmosphere to 120 Km

Pressures and temperatures of the atmosphere up to 120 km were determined from data taken on the V-2 rocket fired at White Sands, New Mexico on March 7, 1947. The methods used in obtaining these data were similar to those used in a previous flight.[3] The pressure measurements were made with bellows gauges for pressures between 1000 mm Hg and 10 mm Hg. For pressures between 2 mm Hg and 10^{-2} mm Hg, tungsten and platinum wire Pirani gauges were used. A Philips gauge was used for pressures between 10^{-3} and 10^{-5} mm Hg.

Ambient pressures shown in figure 91 were measured up to about 80 km with gauges

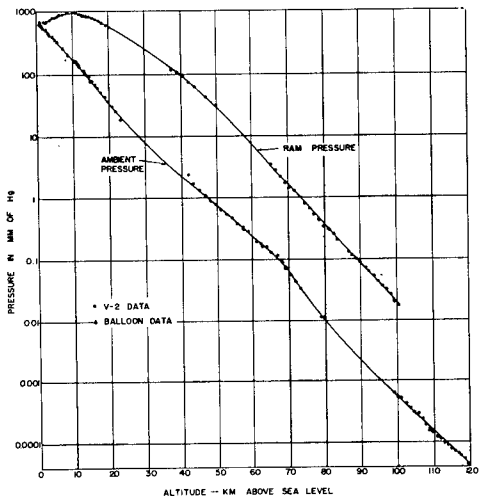

Fig. 91. Ambient and ram pressures as a function of altitude

[1] Cf. Naval Research Laboratory Report No. R-2955, Chapter III, Sections D and E, and Naval Research Laboratory Report No. R-3030, Chapter IV, Section B.

[2] N. Best, R. Havens and H. LaGow, Phys. Rev. 71, 915 (1947).

[3] Best, Durand, Gale and Havens, Phys. Rev. 70, 985 (1946).

mounted on the side of the V-2, just forward of the tail section. Pirani gauges, mounted in similar positions on opposite sides of the rocket, gave readings which agree within experimental errors, indicating that no appreciable error was introduced by yaw of the missile up to this altitude. A single Philips gauge was mounted on the 15° cone of the warhead. The readings of this gauge were reduced to ambient pressures by use of theories of Taylor and Maccoll.[4] Photographs of the earth made from the missile and gyroscope data indicated a yaw of about 15° at 110 km and a roll period of 40 seconds. From the above data it has been calculated that at 110 km the aspect of the rocket was such that the Taylor and Maccoll corrections used were valid (Figure 91). However, at 100 km the pressure shown is probably too high, while at 120 km it is too low, in each case by a factor of less than two.

The temperature of the atmosphere was calculated from the slope of the pressure vs. altitude curve and from the ratio of ram to ambient pressures. Figure 92 is a plot of the temperature derived by this method. Also shown are the temperatures measured by means of a weather balloon released within an hour of the time of the rocket's flight. For comparison, the NACA estimated mean temperature[5] is included on the curve. The probable error is ±25° from 50 to 60 km., ±15° at 65 to 70 km, and ± 20° at 72.5 km. The probable error above 100 km is ± 40°. Temperatures calculated from ram pressures for altitudes between 10 and 20 km are 5 to 20° lower than the expected temperatures. This discrepancy is possibly caused by errors in the velocities calculated from the poor radar data obtained during the first 20 km of the flight.

Pitot tube theory was used to obtain Mach number from the ratio of ram pressure to ambient pressure. The velocity of the rocket divided by Mach number gave the velocity of sound from which the temperature was calculated.

It has been found necessary to apply corrections in the readings of the Pirani gauges to allow for their time constants. This effect resulted in a 1.5-second lag in the gauge used in October, corresponding to 2 km at altitudes between 60 and 80 km. When the October data were recalculated to allow for the lag, they were found to agree with the March data at 60 km, but to be higher that the March data at 80 km. This difference may be a seasonal effect and not experimental error. To establish the seasonal effect definitely, accurate data are needed between 75 and 100 km.

Two platinum resistance temperature gauges were installed to measure temperature of sections of the 15° nose cone. The temperature rise on the 0.1-inch thick aluminum forward section of the nose was 120° ± 5° C. On the 0.1-inch steel section immediately behind the aluminum, the temperature rise was 85° ± 5° C.

****

---

[4]G. I. Taylor and J. W. Maccoll, Proc. Roy. Soc. 139, 278 (1922).

[5]National Advisory Committee for Aeronautics, TN 1200 "Tentative Tables for the Properties of the Upper Atmosphere" (1947).

The information contained in the preceding letter is presented in greater detail in the tables which follow. Table III provides ambient pressure data, and Table IV gives the temperatures measured at two points on the warhead as functions of time and pressure. Figure 93 shows the points at which these readings were taken. Further analysis of the data showed that the warhead temperature rise had the values 135° ± 10° C on the aluminum forward section, and 95° ± 10° C on the steel section, rather than those given in the letter above. For comparison, the results of similar measurements made on October 10, 1946 are given in Table V. The temperatures shown were measured on the 0.5 mm steel skin of the V-2 control chamber. This surface made an angle of 9° with the rocket axis.

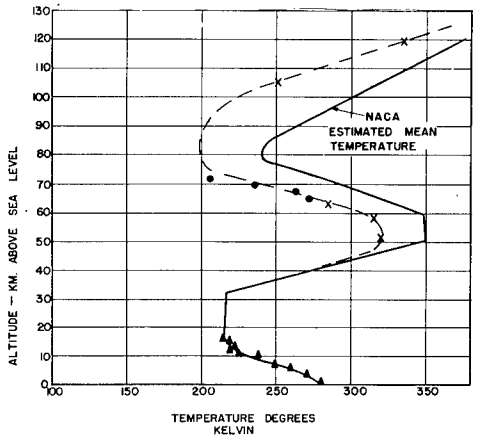

Fig. 92. Temperature as a function of altitude. The crosses indicate data calculated from slope of pressure curve; the black circles, data calculated from ram pressure; the triangles represent balloon data.

TABLE III

Ambient Pressures Observed on March 7, 1947*

Altitude in Km	Pressure in mm Hg as Measured from a- Balloon	V-2	Altitude in Km	Pressure in mm Hg	Altitude in Km	Pressure x 10^4 in mm Hg#
1.2	657		45.0	1.3	106.6	1.7
1.5	638		46.7	1.05	107.7	1.4
2.4	571		48.2	0.86	108.7	1.2
3.0	527		49.6	0.74	109.7	1.1
4.3	447		51.0	0.60	110.8	1.0
5.5	375		52.6	0.52	111.8	0.85
7.6	268		54.1	0.45	112.8	0.85
9.1	312		55.5	0.36	114.0	0.75
10.7	166	175	57.1	0.32	115.0	0.70
11.3		158	58.4	0.27	116.0	0.65
11.9		145	61.3	0.19	116.8	0.60
12.2	141		62.4	0.170	117.7	0.50
12.6		130	63.8	0.154	118.5	0.40
13.3		116	65.2	0.124	119.5	0.40
13.7	107		66.7	0.106	120.6	0.40
14.0		102	68.1	0.086	122.5	0.35
14.8		91	69.3	0.071	125.1	0.30
15.2	86		70.6	0.054	126.0	0.25
15.6		76	72.0	0.042		
16.4		67	73.3	0.032		
17.3		60	97.8	0.00058#		
18.2		51	98.9	0.00051#		
19.2		43	100.0	0.00049#		
20.2		36	101.2	0.00041#		
21.2		29	102.3	0.00036#		
22.2		25	103.4	0.00028#		
42.0		2.3	104.5	0.00028#		
43.5		1.6	105.6	0.00023#		

* Except where noted otherwise, these measurements were made from the V-2.
\# These values were calculated from measurements made on a 26° cone using methods developed by Taylor and Maccoll. [Cf. Proc. Roy. Soc. 139: 278 (1922).]

TABLE IV

V-2 Warhead Skin Temperatures Measured on March 7, 1947

Time in Seconds After Take-off	Velocity in Meters per Second	Altitude* in Km	Pressure in mm Hg	Skin Temperature# in °C at Point - 1	2
0	0	1.2	660	22	30
10	109	1.7	630	22	30
20	260	3.5	495	22	30
25	348	5.0	410	22	30
30	438	7.0	300	25	30
35	530	9.4	210	35	31
40	646	12.3	130	45	40
45	810	15.9	76	62	55
47.5	900	18.0	52	77	65
50	995	20.4	33	87	75
52.5	1090	23.0	23	97	84
55	1200	25.9	14.5	108	92
57.5	1305	29.0	9.6	118	98
60	1420	32.4	5.8	124	105
65	1540	39.9	2.3	135	116
70	1490	47.5	.95	142	122
75	1440	54.8	.40	147	122
80	1390	61.8	.18	156	125
100	1200	87.5	.003	160	-

*To within ± 0.5 km
#To within ± 10°C

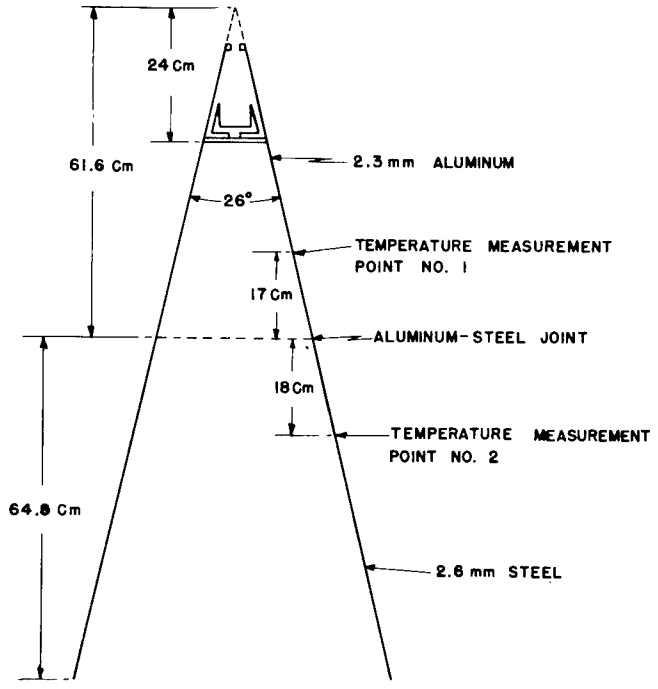

Fig. 93. The locations of the skin temperature measurement points on the warhead of the March 7, 1947 V-2

TABLE V

V-2 Control Chamber Skin Temperatures Measured on October 10, 1946*

Time in Seconds After Take-off	Velocity in Meters per Second	Pressure in mm Hg	Skin Temperatures# in °C as Measured With a Thermistor
-10.0	0	660	21
- 4.0	0	660	23
3.5	26	640	21
11.9	125	620	20
19.1	222	510	23
23.0	291	460	28
26.7	354	390	35
29.4	409	340	37
32.2	450	275	43
35.9	520	210	51
37.8	552	180	60
40.6	625	145	68
44.2	705	97	81
45.8	730	75	89
46.9	790	67	92
51.8	916	36	118
52.8	955	28	128
56.1	1065	18	132
58.9	1175	10.2	140

Time in Seconds After Take-off	Velocity in Meters per Second	Pressure in mm Hg	Skin Temperatures in °C as Measured With a Pt Resistance†
0	0	660	12
19.1	224	510	10
21.6	268	480	18
26.2	348	390	25
30.8	430	300	36
35.4	512	210	58
41.1	630	115	82
43.6	700	100	90
44.7	722	89	100
46.9	790	67	108
57.2	1090	15	162

*These temperatures were measured on a 0.5 mm steel surface which made an angle of 9° with the rocket axis.

#The error in relative temperature is about 3° C. However, a 10° C error in absolute temperature is possible due to the shifting of the calibration curves.

†To within ± 10° C, except for the last value given. The resistance thermometer was becoming a pressure gauge in this region; as a result the error at this point was ± 20° C.

CHAPTER VIII

VIBRATION MEASUREMENTS IN THE V-2

by

C. B. Cunningham[1] and C. P. Smith

The nature of the vibrations which are developed in the V-2 during flight was studied experimentally for the first time on March 7, 1947. Theoretical calculations might have predicted the frequencies of vibration, but such quantities as amplitude and acceleration were best determined by direct measurement. Accordingly, the design and construction of a suitable apparatus was undertaken as part of the preparation for this flight.

It was decided not to employ electronic amplification, since the vibrations might generate microphonic noise in the necessary equipment. Such noise would tend to mask the effect being studied. A self-generating type of instrument was therefore preferred for this application. As there were no actual data which could be used in determining the sensitivity requirement, it was arbitrarily assumed that the V-2 vibrations were similar in character to those encountered in ships and aircraft. These considerations led to the choice of the type 4-102 vibration velocity pickup which is manufactured by the Consolidated Engineering Corporation. This is a self-generating unit which faithfully amplifies those types of vibrations which were expected to occur during the flight. It is shown in figure 94.

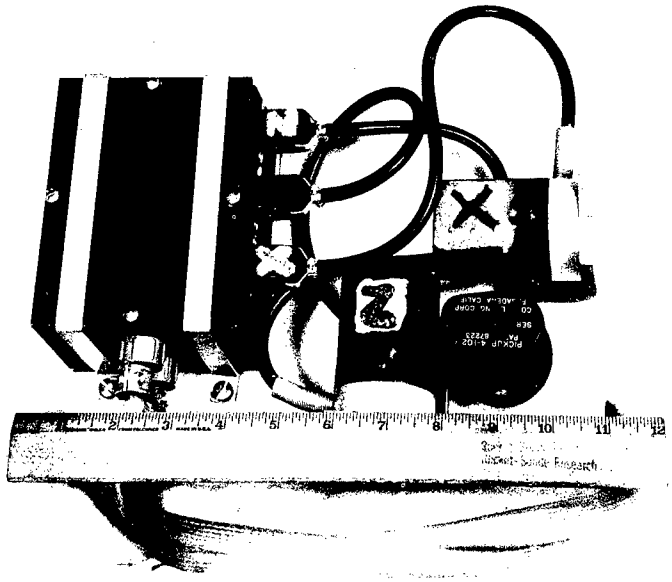

Fig. 94. The vibration-measuring equipment

[1]Member of the Sound Division of the Naval Research Laboratory. The vibration measurements have been carried on as a joint project by the Shock and Vibration Research and Evaluation Section and the Rocket-Sonde Research Section.

Since the instrument has a sine wave output, and since the telemeter accepts only positive voltages, a 3-volt bias was employed. Diode limiting was also used to prevent the signal level from exceeding the range of voltages accepted by the telemeter. A schematic diagram of the installation is given in figure 95. Three pickups were installed. Their outputs were combined in a single telemetering channel by means of a commutator.

The pickups were mounted on a plate which was fastened to the base of the warhead. The location of the assembly in the main warhead body is shown in figure 8. One of the units had its axis parallel to the principal axis of the missile, while the axes of the other two were parallel to the fin planes and lay normal to the rocket's longitudinal axis.

Vibrations in the plane normal to the missile's main axis had amplitudes which were too small to be measured by this installation. Vibrations along the principal rocket axis were recorded. The frequencies ranged from 42 to 57 cps. The peak vibrational velocities varied between 2.7 and 4.6 cm (1.06 and 1.82 in.) per second. The amplitude measurements were not very accurate, however, this quantity was calculated by integrating the velocity. In this way it was estimated that the total excursion varied between the extreme values of 0.17 and 0.29 mm (0.0068 and 0.0116 in.).

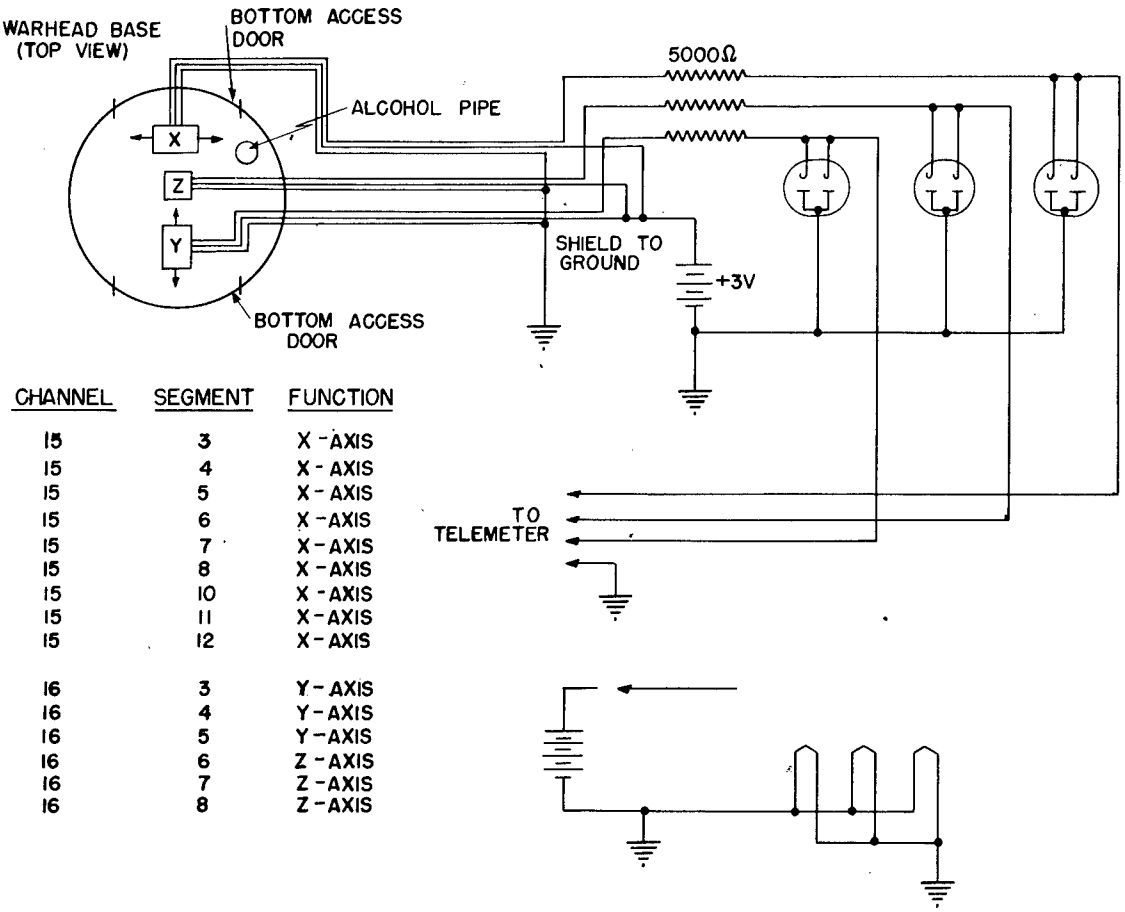

CHANNEL	SEGMENT	FUNCTION
15	3	X-AXIS
15	4	X-AXIS
15	5	X-AXIS
15	6	X-AXIS
15	7	X-AXIS
15	8	X-AXIS
15	10	X-AXIS
15	11	X-AXIS
15	12	X-AXIS
16	3	Y-AXIS
16	4	Y-AXIS
16	5	Y-AXIS
16	6	Z-AXIS
16	7	Z-AXIS
16	8	Z-AXIS

Fig. 95. Schematic diagram of the vibration-measuring installation

The vibration was not continuous. Its intermittent character suggested that it might be due to shocks which originated in the rocket motor and were transmitted through the missile structure. These shocks may have been caused by uneven burning of the fuel. All the measured vibrations ceased at Brennschluss. The propulsion unit, therefore, is considered to have been the source of the disturbances. The vibrations were undoubtedly more intense in the tail section. This structure was closer to the V-2 engine, had a smaller mass and a more extensive configuration than the warhead.

A more sensitive instrument will be installed in the warhead, and additional measurements will be made at other locations in future rockets. Particular interest attaches to the observations which will be made with these refinements during the period of transonic flight.

CHAPTER IX

PHOTOGRAPHY FROM THE V-2 AT ALTITUDES RANGING UP TO 160 KILOMETERS

by

T. A. Bergstralh

On March 7, 1947 the twentieth[1] V-2 to be launched in America took to the air from the Army Ordnance Proving Grounds at White Sands, New Mexico. As on several of the previous flights, an attempt was made to obtain photographs of certain rocket installations, and of the earth. In this attempt the effort met with considerable success. Included among the group of pictures obtained are the first ever to be taken from altitudes greater than 160 kilometers (100 miles). The quality of the photographs is fairly good. For the first time in pictures taken at such high altitudes, it is possible to identify many geographical features. In addition, the cameras recorded numerous cloud formations and other information of meteorological value.

The appearance of the earth is unquestionably the most striking feature of the photographs. The Colorado River, the Gulf of California, the peninsula of Lower California, and the Pacific Ocean beyond are all clearly discernible in the Frontispiece which was taken as the rocket reached the peak of its trajectory. More than 500,000 square kilometers (200,000 square miles) of the United States and Mexico are visible between the bottom of the picture below the rocket and the curved horizon 1,450 kilometers (900 miles) to the west. If the V-2 had risen in another part of North America, a similar photograph could easily have included both New York and Chicago. Many lesser lakes, rivers, dry lakes, etc. have been identified. Their locations are indicated in the Frontispiece.

One of the primary purposes of the photographic program was to acquire a better knowledge of various motions executed by the missile in going through the upper atmosphere. It was also desired to obtain accurate information concerning existence of corona discharge at the radiating elements, and the relative positions of the antennas and the jet exhaust flame of the rocket, in order to assess the performance of these components. Important information in these matters was obtained from the photographs taken on March 7.

When the rocket takes off, it can be controlled by the action of its carbon vanes in the jet exhaust and the stabilizing action of the air vanes on its fins. These restoring forces also can prevent rolling. However, after the end of powered flight, this source of correction is, for all prac-

[1]Missile No. 21. Missile No. 1 was expended in a static firing test.

tical purposes, no longer available. There is no jet, and the drag of the atmosphere on the air vanes is negligible. Thus, if the rocket possesses a residual roll at this time, the mechanism orders constantly increasing amounts of correction in vain; i.e., the air vanes are turned to their extreme positions, nevertheless the rocket continues to roll. The film furnished positive evidence that this rolling actually does take place. The turning of one of the vanes and the rolling of the rocket are both clearly visible in the complete sequence of photographs. These also show that the flame came between an antenna and the ground station during a portion of the flight.

The photographs were made with two K-25 aircraft cameras one of which is shown in figure 96. These cameras employed 24 volt power and operated automatically. They were mounted symmetrically in opposite sides of the midsection of the rocket. Each was equipped with a right angle prism and in both cases the field of view was directed toward the tail at an angle of 20° to the missile axis. Each roll of film provided for fifty-five 10.2 cm x 12.7 cm (4 in. x 5 in.) negatives. A 1/500th second exposure time, an f/11 lens setting, K-25 infrared reconnaissance base film, and a Wratten 25A red filter were used. This combination had an exposure index of 50. The recovered film was found to be slightly underexposed. Experience gained on this flight indicates that f/8 is nearer the optimum lens setting for the conditions experienced.

The V-2 rose vertically from the launching site, tilting gradually toward the north during the burning period. At the point at which the fuel was spent, 63 seconds after take-off, it had a zenith angle of 7°. The winds from the east then caused the missile to begin turning in that direction. This motion probably continued throughout the remainder of the flight. The last six pictures given here were made while the V-2 was inclined toward the northeast at a zenith angle of approximately 10°. Explosive charges at the base of the warhead and the junction of the midsection and tail were detonated 330 seconds after take-off. The rocket broke up shortly afterward as it entered the denser portions of the atmosphere. The parts fell to earth over a wide area of the white sands which gave the region its name. Both cameras were recovered on the following day. One of these was partially destroyed upon impact, allowing light to enter. As a result some of the pictures taken during the latter part of the flight were partially fogged.

The following pages contain a selection of nine photographs, figures 97-105 which, together with the Frontispiece and figure 21 are representative of those taken during the V-2 flight of March 7. They are indicative of the results which may be obtained by means of photography at very high altitudes.

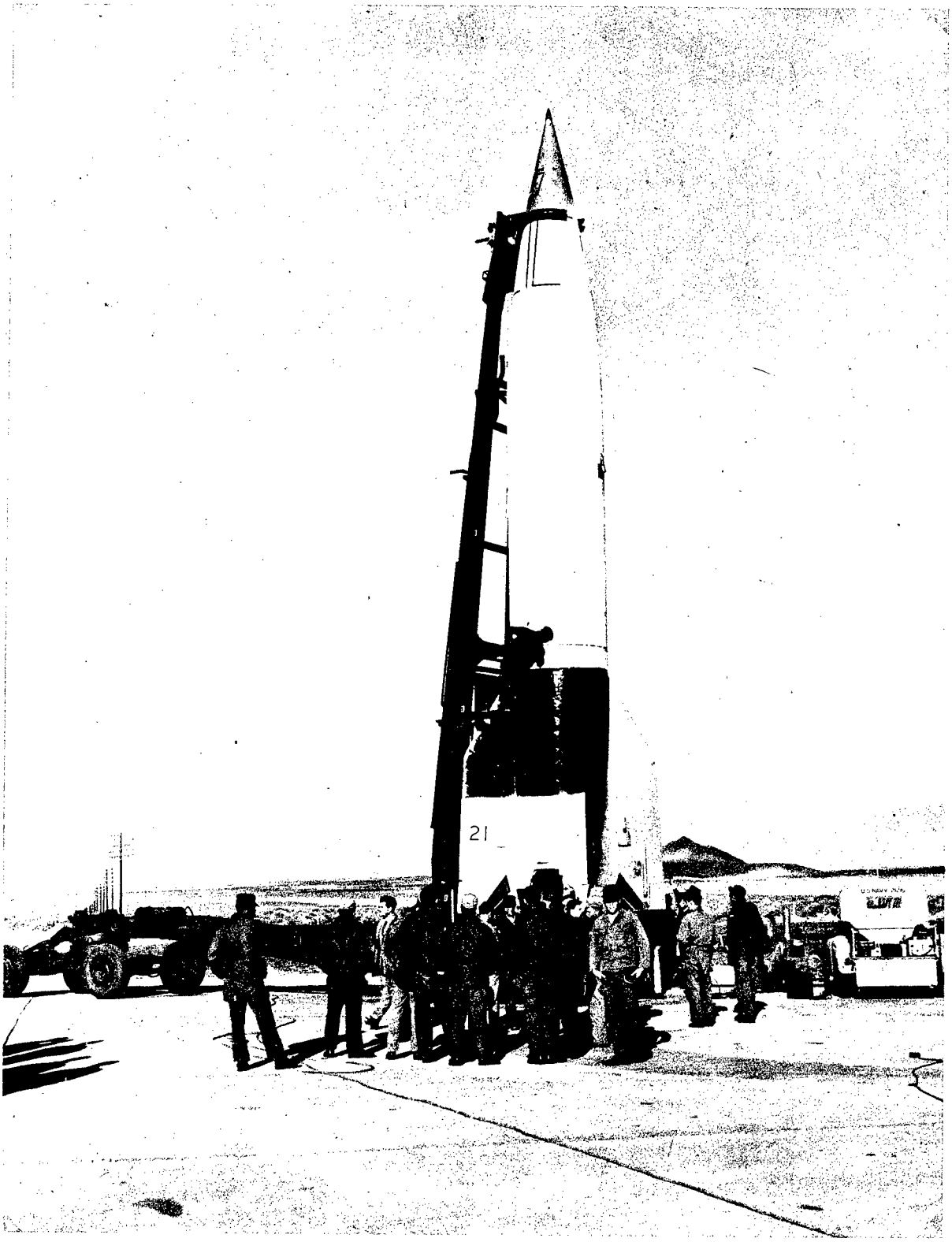

Fig. 96. V-2 rocket No. 21 on its launching platform, showing one of the cameras mounted in the midsection

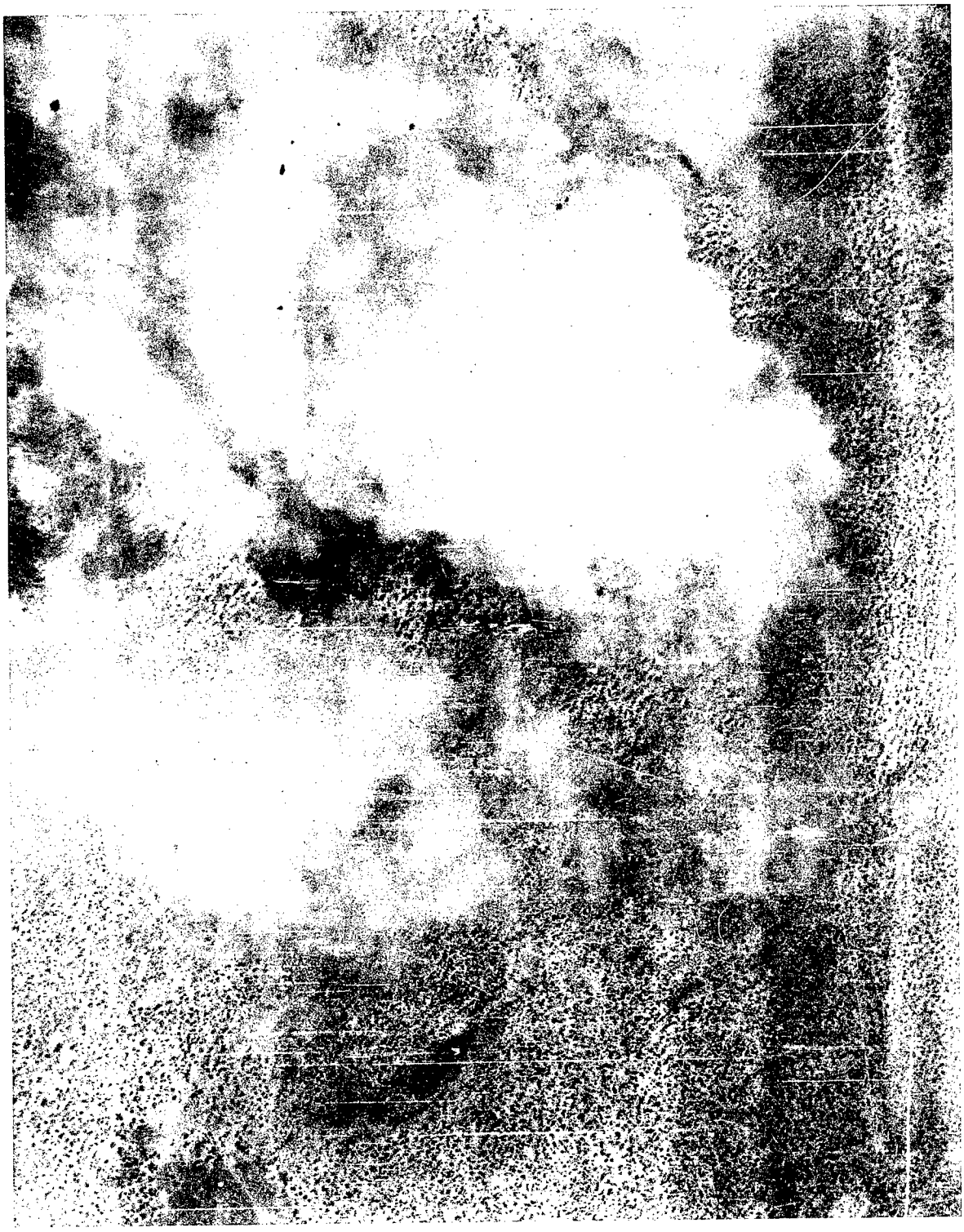

Fig. 97. A photograph taken 7 seconds after takeoff at an altitude of 225 meters (750 feet). The camera was pointed southeast. Desert scrub bushes can be seen.

Fig. 98. A photograph taken 43 seconds after takeoff at an altitude of 12 kilometers (7 miles). The camera was pointed southeast.

Fig. 99. A photograph taken 63 seconds after takeoff at an altitude of 34 kilometers (21 miles). The camera was pointed southeast.

Fig. 100. A photograph taken 81 seconds after takeoff at an altitude of 60 kilometers (37 miles). The camera was pointed west. Part of White Sands area shown in lower left. (Fig.103 shows same area at a higher altitude.)

Fig. 101. A photograph was taken 100 seconds after takeoff at an altitude of 85 kilometers (53 miles). The camera was pointed northeast.

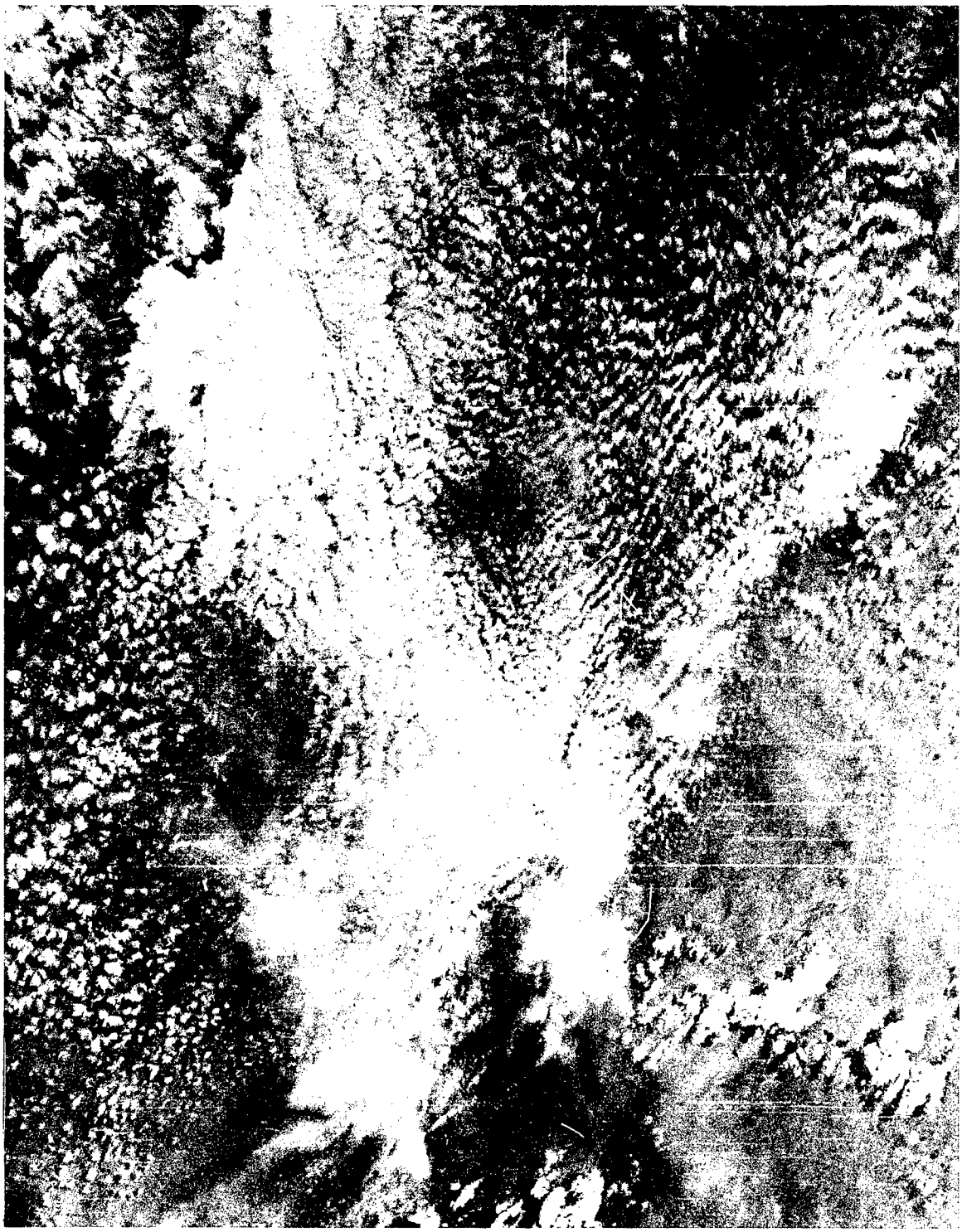

Fig. 102. A photograph taken 136 seconds after takeoff at an altitude of 123 kilometers (76 miles). The camera was pointed north northeast. A portion of the lake formed by Caballo Dam on the Rio Grande River is visible in the lower left hand corner.

Fig. 103. A photograph taken 155 seconds after takeoff at an altitude of 137 kilometers (85 miles). The camera was pointed southwest. The White Sands region appears between the clouds in the right center. The rocket came to earth in this area.

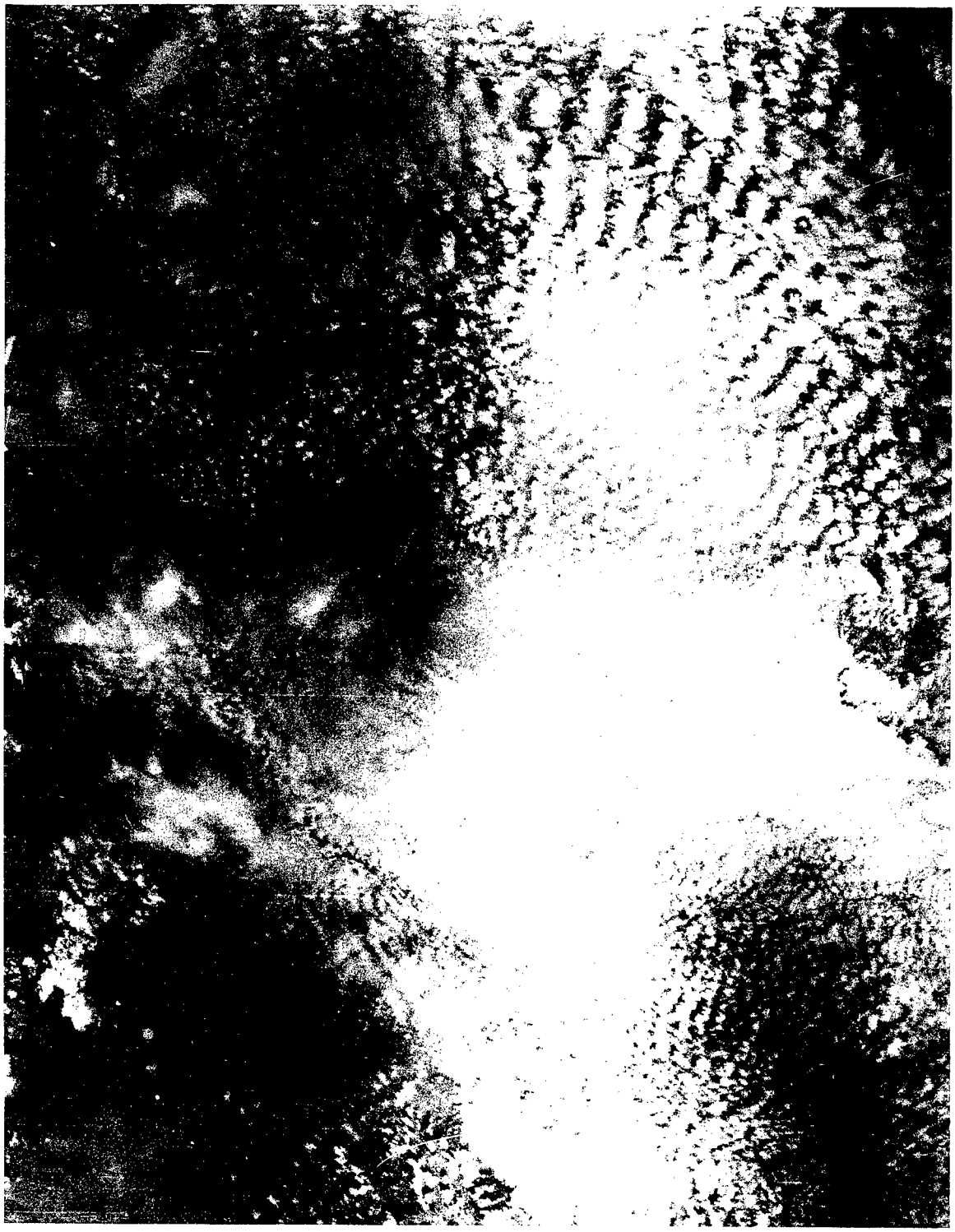

Fig. 104. A photograph taken 190 seconds after takeoff at an altitude of 156 kilometers (97 miles). The camera was pointed southwest. Caballo Dam Lake, the lower end of Elephant Butte Dam Lake and the Rio Grande River between are all discernible in the upper left hand corner.

Fig. 105. A photograph taken 209 seconds after takeoff at an altitude of 161 kilometers (100 miles). The curvature of the earth may be clearly seen. The camera was pointed toward the northwest.

CHAPTER X

AN ANALYTICAL BASIS FOR DETERMINING THE ATTITUDE OF A SPINNING MISSILE AFTER FUEL CUTOFF

by

H. E. Newell, Jr.

INTRODUCTION

A knowledge of missile attitude as a function of time is an important factor in the interpretation of many of the upper atmosphere measurements made from the V-2. Since the rocket is stabilized prior to fuel burnout, the motion of the missile through the denser portions of the air is predetermined. It is the rocket behavior after full cutoff which is open to question, and which will be investigated below.

Once the rocket attains the free fall portion of its trajectory, the effect of air resistance is presumably negligible and will not be considered in the discussion. The influence of the motions of the rocket's turbine and of any residual alcohol or oxygen in the fuel tanks will also be neglected. The problem, then, is that of determining the motion of a freely falling rigid rocket, upon which no torques are acting, the angular momentum of which, therefore, remains constant.

The Equations of Motion.

The axes of figure 106 are thought of as attached to the center of mass $O:(\bar{\xi},\bar{\eta},\bar{\zeta})$ of a rocket. The (X, Y, Z)-axes move with the rocket, but remain fixed in orientation, the Z-axis being vertical. The (x, y, z)-axes, on the other hand, are fixed within the rocket as shown in figure 107, and alter in orientation as the rocket attitude changes. The parameters θ, ϕ, ψ shown in

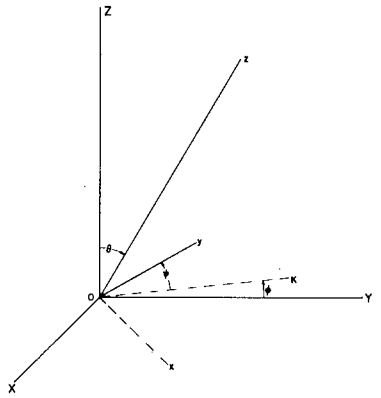

Fig. 106. Diagram showing the relationship between a fixed set of axes and the Eulerian angles

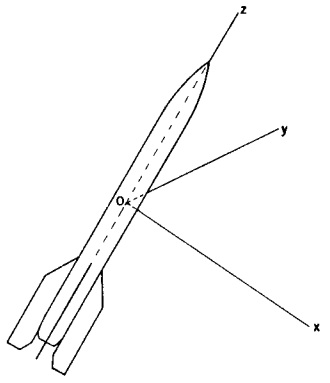

Fig. 107. Diagram illustrating the position of the moving axes of Fig. 106 as they appear fixed in the rocket

figure 106 are the Eulerian angles relating the (x, y, z)-axes to the (X, Y, Z)-axes.

Let ω_x, ω_y, ω_z be the components of the angular velocity of the rocket referred to the (x, y, z)-axes. Then

$$\omega_x = \dot{\theta} \sin \psi - \dot{\phi} \sin \theta \cos \psi$$
$$\omega_y = \dot{\theta} \cos \psi + \dot{\phi} \sin \theta \sin \psi$$
$$\omega_z = \dot{\psi} + \dot{\phi} \cos \theta.$$

The kinetic energy of the rocket is given by

$$T = \tfrac{1}{2}M(\dot{\bar{\xi}}^2 + \dot{\bar{\eta}}^2 \dot{\bar{\zeta}}^2) + \tfrac{1}{2}(I_x \omega_x^2 + I_y \omega_y^2 + I_z \omega_z^2),$$

where M is the mass of the rocket, and I_x, I_y, I_z are the moments of inertia. The potential energy is given by

$$V = Mg \sqrt{\bar{\xi}^2 + \bar{\eta}^2 \bar{\zeta}^2}.$$

Hence the Lagrangian function L is of the form

$$L = \tfrac{1}{2}\left(I_x \omega_x^2 + I_y \omega_y^2 + I_z \omega_z^2\right) + f\left(\bar{\xi}, \bar{\eta}, \bar{\zeta}; \dot{\bar{\xi}}, \dot{\bar{\eta}}, \dot{\bar{\zeta}}\right),$$

where F does not involve the Eulerian angles.

Set $I_x = I_y = a$, $I_z = c$. Then

$$L = \tfrac{1}{2}\left[a(\dot{\theta}^2 + \dot{\phi}^2 \sin^2 \theta) + c(\dot{\psi} + \dot{\phi} \cos \theta)^2\right] + f.$$

Substituting into Lagrange's equation

$$\frac{d}{dt}\left(\frac{\partial L}{\partial \dot{q}}\right) - \frac{\partial L}{\partial q} = 0,$$

where q is any one of θ, ϕ, ψ, one obtains, after some simplification, including two immediate integrations:

1a.) $\ddot{\theta} - \dot{\phi}^2 \sin \theta \cos \theta + \beta \Omega_z \dot{\phi} \sin \theta = 0$

1b.) $\dot{\phi} \sin^2 \theta + \beta \Omega_z \cos \theta = h$

1c.) $\dot{\psi} + \dot{\phi} \cos \theta = \Omega_z$.

Here $\beta = \frac{c}{a}$ and h and Ω_z are constants of integration.

The equation 1c.) states simply that the rate of spin of the rocket about the z-axis remains constant at its initial value Ω_z, which is assumed throughout to be not zero.

Integration of the equations of motion.

Case 1. θ never vanishes.

Suppose first of all that the rocket is never vertical, so that θ never vanishes. From 1b.)

$$\dot{\phi} = \frac{h - \beta\Omega_z \cos\theta}{\sin^2\theta} .$$

Using this in 1a.):

$$\ddot{\theta} = (h^2 + \beta^2\Omega_z^2)\frac{\cos\theta}{\sin^3\theta} - \frac{2h\beta\Omega_z}{\sin^3\theta} + \frac{h\beta\Omega_z}{\sin\theta} .$$

Multiplying through the last equation by $2\dot{\theta}$ and integrating:

$$\dot{\theta}^2 = A^2 - \frac{h^2 + \beta^2\Omega_z^2 - 2h\beta\Omega_z\cos\theta}{\sin^2\theta} ,$$

where

$$A^2 = \Omega_\theta^2 + \frac{h^2 + \beta^2\Omega_z^2 - 2h\beta\Omega_z\cos\theta_o}{\sin^2\theta_o} ,$$

and $\Omega_\theta = \dot{\theta}(0)$, $\theta_o = \theta(0)$.

This reduces to

$$\dot{\theta}\sin\theta = \pm\left[B^2 - A^2\left(\frac{h\beta\Omega_z}{A^2} - \cos\theta\right)^2\right]^{\frac{1}{2}} ,$$

where

$$B^2 = A^2 - (h^2 + \beta^2\Omega_z^2) + \frac{h^2\beta^2\Omega_z^2}{A^2} .$$

Integrating:

$$\arcsin\frac{h\beta\Omega_z - A^2\cos\theta}{AB} = \gamma \pm At,$$

where

$$\gamma = \arcsin \frac{h\beta\Omega_z - A^2 \cos\theta_o}{AB} .$$

Solving for cos θ:

2.) $$\cos\theta = \frac{h\beta\Omega_z}{A^2} - \frac{B}{A} \sin(\gamma \pm At) .$$

The azimuth angle ∅ can now be obtained as follows. From 1b.):

$$\dot{\phi} = \frac{h - \beta\Omega_z \cos\theta}{\sin^2\theta} = \frac{d\phi}{d\theta}\dot{\theta} .$$

Using the expression derived earlier for $\dot{\theta}\sin\theta$, this becomes

$$\frac{d\phi}{d\theta} = \frac{h - \beta\Omega_z \cos\theta}{\pm \sin\theta \left[B^2 - A^2\left(\frac{h\beta\Omega_z}{A^2} - \cos\theta\right)^2\right]^{\frac{1}{2}}} .$$

Upon integration

3.) $$\phi - \phi_o = \pm\left[\arctan \frac{\beta\Omega_z - h\cos\theta}{\left[B^2 - A^2\left(\frac{h\beta\Omega_z}{A^2} - \cos\theta\right)2\right]^{\frac{1}{2}}} - \arctan \frac{\beta\Omega_z - h\cos\theta_o}{\left[B^2 - A^2\left(\frac{h\beta\Omega_z}{A^2} - \cos\theta_o\right)2\right]^{\frac{1}{2}}}\right.$$

or

3'.) $$\phi - \phi_o = \arctan \frac{\beta\Omega_z - h\cos\theta}{\dot{\theta}\sin\theta} - \arctan \frac{\beta\Omega_z - h\cos\theta_o}{\Omega_\theta \sin\theta_o} .$$

Also, using 2.) and

$$\dot{\theta}\sin\theta = \pm B\cos(\gamma \pm At),$$

3''.) $$\phi - \phi_o = \arctan \frac{\beta\Omega_z (A^2 - h^2) + h\,AB\sin(\gamma \pm At)}{\pm A^2 B\cos(\gamma \pm At)} - \arctan \frac{\beta\Omega_z - h\cos\theta_o}{\Omega_\theta \sin\theta_o} .$$

Finally, from 1c.)

$$\dot{\psi} = \Omega_z - \dot{\phi} \cos \theta$$

$$\dot{\psi} = \Omega_z - \frac{h \cos \theta - \beta \Omega_z \cos^2 \theta}{1 - \cos^2 \theta}$$

$$\dot{\psi} = (1 - \beta)\ \Omega_z + \left[\frac{\beta \Omega_z - h \cos \theta}{1 - \cos^2 \theta} + \dot{\phi}\right] - \dot{\phi}$$

$$\dot{\psi} = (1 - \beta)\, \Omega_z - \dot{\phi} + \frac{h + \beta \Omega_z}{1 + \cos \theta} \quad .$$

4.) $$\psi - \psi_o = (1 - \beta)\Omega_z t - (\phi - \phi_o) \pm 2 \left[\arctan \frac{(A^2 + h\beta\Omega_z) \tan \frac{1}{2}(\gamma \pm At) - AB}{A\,(h + \beta \Omega_z)} \right.$$

$$\left. - \arctan \frac{(A^2 + h\beta\Omega_z) \tan \frac{1}{2} \gamma - AB}{A\,(h + \beta \Omega_z)} \right] .$$

Integration of the equations of motion.

Case 2. θ assumes zero values.

The integration of equations 1.) is somewhat simpler in the case in which the rocket becomes vertical at times during its motion. In such a case, setting $\theta = 0$ in 1b.) yields

$$\beta \Omega_z = h,$$

whence

$$\dot{\phi} = \frac{\beta \Omega_z (1 - \cos \theta)}{\sin^2 \theta} = \frac{\beta \Omega_z}{1 + \cos \theta} \quad .$$

Equation 1a.) becomes

$$\ddot{\theta} = - \frac{\beta^2 \Omega_z^2 (1 - \cos \theta)^2}{\sin^3 \theta} \quad .$$

Integrating, and assuming that $\theta(0) = 0$:

$$\dot{\theta}^2 = \Omega_\theta^2 - \beta^2 \Omega_z^2 \left[\frac{1 - \cos\theta}{1 + \cos\theta}\right] .$$

This can be put in the form

$$\dot{\theta} = \pm \frac{\Omega_\theta}{\cos\frac{\theta}{2}} \left[1 - \frac{\Omega_\theta^2 + \beta^2 \Omega_z^2}{\Omega_\theta^2} \sin^2\frac{\theta}{2}\right]^{\frac{1}{2}} .$$

Thus

5.) $$\sin\frac{\theta}{2} = \frac{\Omega_\theta}{\sqrt{\Omega_\theta^2 + \beta^2 \Omega_z^2}} \sin\tfrac{1}{2}\sqrt{\Omega_\theta^2 + \beta^2 \Omega_z^2}\ t .$$

It is now a simple matter to obtain

6.) $$\tan(\phi - \phi_0) = \frac{\beta \Omega_z}{\sqrt{\Omega_\theta^2 + \beta^2 \Omega_z^2}} \tan\tfrac{1}{2}\sqrt{\Omega_\theta^2 + \beta^2 \Omega_z^2}\ t ,$$

and

7.) $$\psi - \psi_0 = (1 - \beta)\,\Omega_z\, t + \phi - \phi_0 .$$

General discussion of the motion. The zenith angle θ has an extremum when $\dot{\theta}$ vanishes; that is, when $B = 0$ or when

$$\cos(\gamma \pm At) = 0$$

$$\gamma \pm At = \frac{\pi}{2} + \nu\pi ,$$

where ν is an integer. Assume for the moment that $B \neq 0$. Then from 2.) it is apparent that

$$\cos\theta_M = \frac{h\beta\Omega_z}{A^2} - \frac{B}{A} , \quad \gamma \pm At = \frac{\pi}{2} + 2\mu\pi$$

$$\text{Cos } \theta_m = \frac{h\beta\Omega_z}{A^2} + \frac{B}{A} \quad , \quad \gamma \pm At = \frac{\pi}{2} + (2\mu + 1)\pi \quad ,$$

where θ_M and θ_m are the maximum and minimum values of θ respectively.

Using 3'.) and 3''.) it is easily shown that $\beta\Omega_z - h \cos\theta \neq 0$ when $\dot{\theta}$ vanishes, unless $A = h$, in which case $B = 0$. Under the assumption, then, that $B \neq 0$, it can be seen from 3'.) that the azimuths ϕ corresponding to the various times when θ assumes its extreme values, differ among themselves only by multiples of π.

Figure 108 is a schematic drawing of the trace of the z -axis on a unit sphere about the origin. $\angle$ Z0 P_M and $\angle$ Z0 P_m are θ_M and θ_m respectively. Let Z be moved along the great circle arc $P_m \overset{\frown}{Z} P_M$ to a new position Z'. Let $\angle$ Z'Oz be denoted by θ', and $\angle$ZOZ' by α. Then if z is close to, but not coincident with, P_M:

$$\left| \theta - \theta' \right| \angle \alpha \ ,$$

whereas if z coincides with P_M:

$$\left| \theta - \theta' \right| = \alpha \ .$$

Thus $\theta - \theta'$ has an extremum when z coincides with P_M, and $\dot{\theta} - \dot{\theta}'$ vanishes. Since at this point $\dot{\theta}$ also vanishes, it is clear that $\dot{\theta}' = 0$, and that θ' has an extremum.

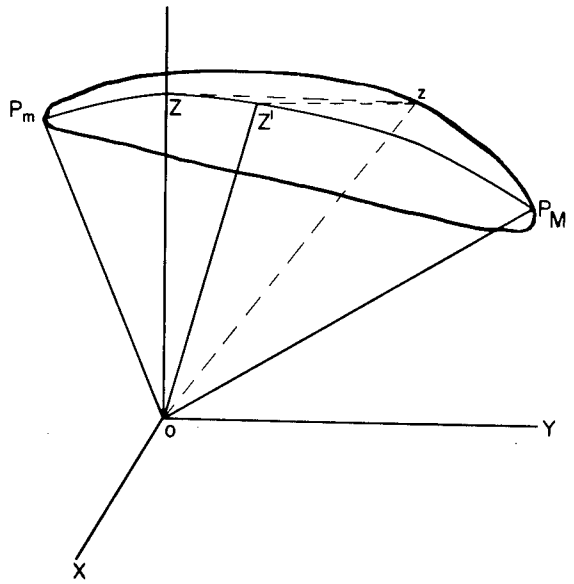

Fig. 108. A schematic diagram of the curve traced by the precessing of the missile axis

Similarly θ' has an extremum when z coincides with P_m.

Obviously, changing the axes of reference has no effect on the actual path of the z-axis in space. Suppose, then, that Z be moved along $P_m \overset{\frown}{Z} P_M$ to the point midway between P_m and P_M. Then as Z approaches its new position, θ_M and θ_m approach a common value, and $B \to 0$. Thus if the (X, Y, Z)-axes be chosen with the new orientation, $B = 0$, and

$$\dot{\theta}' \equiv 0 \ ,$$

or θ' is constant:

$$\theta' \equiv \theta_o' \quad .$$

The prime superscript will be used consistently to denote quantities referred to the new (X, Y, Z)-axes.

Equation 1a.) becomes:

$$-\dot{\phi}' \sin\theta' \,(\dot{\phi}' \cos\theta' - \beta\Omega_z) = 0 \quad .$$

The case in which $\dot{\phi}' \sin\theta' = 0$ is that in which the direction of the z-axis is fixed, and the rocket merely spins about this axis. Otherwise

$$\dot{\phi}' = \frac{\beta\Omega_z}{\cos\theta'} \quad .$$

Then from 1b.):

$$\beta\Omega_z = h' \cos\theta' \quad ,$$

and

$$\dot{\phi}' = h' = \Omega_{\phi'} \quad ,$$

where $\Omega_{\phi'} = \dot{\phi}'(0)$.

$$\phi' - \phi_o' = \Omega_{\phi'}\, t \quad .$$

Also

$$\dot{\psi}' + h' \cos\theta' = \Omega_z$$
$$\dot{\psi}' = (1 - \beta)\,\Omega_z$$
$$\psi' - \psi_o' = (1 - \beta)\,\Omega_z\, t \quad .$$

Collecting formulas

8.)
$$\begin{cases} \theta' = \arccos \dfrac{\beta \Omega_z}{h'} \\ \phi' - \phi_o' = \Omega_{\phi'} t \\ \psi - \psi_o' = (1 - \beta)\, \Omega_z\, t. \end{cases}$$

These relations show that, relative to its center of mass, the motion of a rocket spinning about its longitudinal axis, consists of the spin alone, the rate of which remains constant; or consists of the spin plus a precession of the spin axis at a constant rate about a fixed direction in space, the inclination of the spin axis to the precessional axis remaining constant.

The actual determination of rocket aspect. The discussion above can be made the basis of a means for determining the aspect of the rocket at each moment during the free fall portion of its flight above the atmosphere. It is sufficient to determine the angle θ as a function of the time, and to measure $\Omega_z t$. This can be done by means of gyroscopes suitably mounted in the rocket.

From such data one immediately obtains Ω_z, θ_m, and θ_M. Then

$$\frac{h\beta\Omega_z}{A^2} = \tfrac{1}{2} (\cos \theta_m + \cos \theta_M)$$

$$\frac{B}{A} = \tfrac{1}{2} (\cos \theta_m - \cos \theta_M)$$

$$A = \left| \frac{\dot{\theta} \sin \theta}{\left[\frac{B^2}{A^2} - \left(\frac{h\beta\Omega_z}{A^2} - \cos \theta \right)^2 \right]^{\frac{1}{2}}} \right|$$

$$B = \frac{B}{A} \cdot A$$

$$h = \frac{h\beta\Omega_z}{A^2} \cdot \frac{A^2}{\beta\Omega_z} .$$

The constant γ can now be determined, and $\phi - \phi_o$ and $\psi - \psi_o$ can be obtained from 3'.) and 4.).

If $\beta\Omega_z - h \cos \theta$ never vanishes, the zenith angle of the axis of precession is given by $\frac{1}{2}(\theta_M + \theta_m)$, and the inclination of the spin axis to the precessional axis is $\frac{1}{2}(\theta_M - \theta_m)$. On the other hand, if $\beta k - h \cos \theta$ changes sign as θ varies, then the zenith angle of the precessional axis is $\frac{1}{2}(\theta_M - \theta_m)$, and the inclination of the precessional axis thereto is $\frac{1}{2}(\theta_M + \theta_m)$.

CHAPTER XI

THE TELEMETERING SYSTEM

by

S. W. Lichtman, J. T. Mengel and C. H. Smith, Jr.[1]

INTRODUCTION

The March 7 V-2 firing was the eighteenth in which the Naval Research Laboratory telemetering system was used. The system, designed, installed and operated by the Laboratory specifically for use in the upper atmosphere research program, was also employed in all seventeen of those previous flights in which telemetering played a part. An account of the progress made in the early stages of the program was given in earlier reports of this series.[2]

Since the last report, a considerable advance has been made toward improving the performance of the telemetering system, including the establishment of a permanent telemetering ground station, and the development of an automatic pre-flight calibrator. Design changes in the present system include the use of circular polarization, and of a turnstile antenna. In addition, a new system employing pulse matrix principles has been designed and is now under construction. It is anticipated that it will be ready for use in April 1948.

The telemetering ground station is described in Section A of this chapter. The preflight calibration procedure is detailed in Section B and the receivers and servo-controlled receiving antennas are taken up in Section C. A discussion of the recent improvements in the rocket-borne transmitting antennas is contained in Section D. An operational report on the firings from December 5, 1946 through March 7, 1947 is given in Section E. The improvements contemplated for the remainder of 1947 are discussed in Section F, and a general description of the new pulse matrix telemetering system is presented in Section G.

---

[1]The accomplishments and developments described in this chapter are the result of the combined efforts of the members of the Electronic Instrumentation Subsection of the Rocket-Sonde Research Section. The authors wish to mention particularly Messrs. V. L. Heeren, P. R. Shifflett, K. M. Uglow and J. Y. Yuen for their contributions to the ground station developments; Mr. R. E. Taylor for his work on the rocket-borne antennas; Mr. D. G. Mazur and Mr. H. A. Strothers for their assistance in the design of the new pulse matrix system; and Mr. J. R. Kauke for his part in establishing the present ground station in a permanent building and in solving many of the operational problems encountered at the White Sands Proving Grounds.

[2]Naval Research Laboratory Report No. R-2955, Chapter II, Section C
Naval Research Laboratory Report No. R-3030, Chapter III, and
Naval Research Laboratory Report No. R-3120, Chapter III, Section B.

A. The Ground Station

The telemetering ground station at White Sands, formerly mounted in mobile trailers, is now housed in a permanent concrete block building. This structure, shown in figure 109, is situated on a rise of land which is 9 km (6 mi) and 5° west of north from the launching site. It contains two complete telemetering stations, radio communication facilities, a darkroom for film processing, a working area, and storage cabinets. Two telemetering receiving antennas using four foot paraboloids mounted on servo-controlled pedestals are mounted on the south side of the roof in a position affording an unobstructed view of the launching area.

A third station is housed in a K-65 trailer on a rise of land about 800 meters (0.5 mile) to the north of the telemetering building. It is used chiefly for the training of personnel in the operation of the tracking antennas, receivers, decoders and recording units. In this manner trainees obtain complete operational experience during an actual flight without endangering the recording of data at the master telemetering stations.

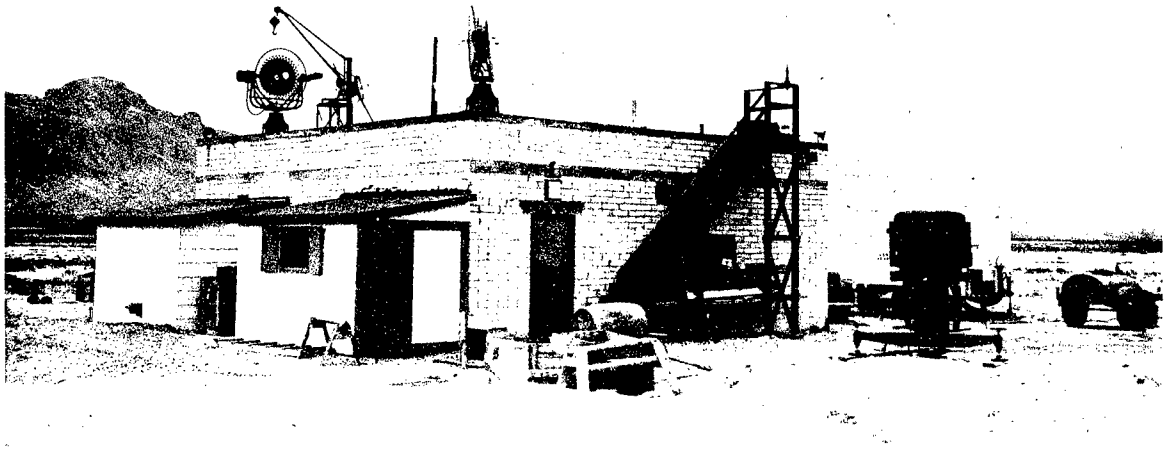

Fig. 109. The permanent telemetering ground station building at the White Sands Proving Grounds

The interior arrangement of the telemetering house appears in figure 110, and the disposition of equipment on the roof is illustrated in figure 111. The decoders, receivers, video amplifiers and monitoring oscilloscopes for stations I-A and I-B are located together at positions A and B, respectively. The string oscillograph recorders are mounted on a bench along the south wall. Two of these, labelled R_1 and R_4, are twenty-four channel Hathaway units equipped with fifteen galvanometers and two side-marking solenoids. Recorders R_2 and R_3 are similar, but with twelve channels and twelve galvanometers. The fifth instrument was built by the General Electric Company. Its six channels record information pertaining to rocket propulsion and control. The side marker solenoids on the Hathaway recorders are used to record one second intervals marked by a Navy chronometer. Take-off time and elapsed flight time are recorded from the blockhouse master time signal on one of the galvanometers in each recorder. Figures 112 and 113 are photographs of stations I-A and I-B respectively, while figure 114 shows the arrangement of the recorders. The ground station circuitry is essentially the same as that described in the previous reports of this series.[3]

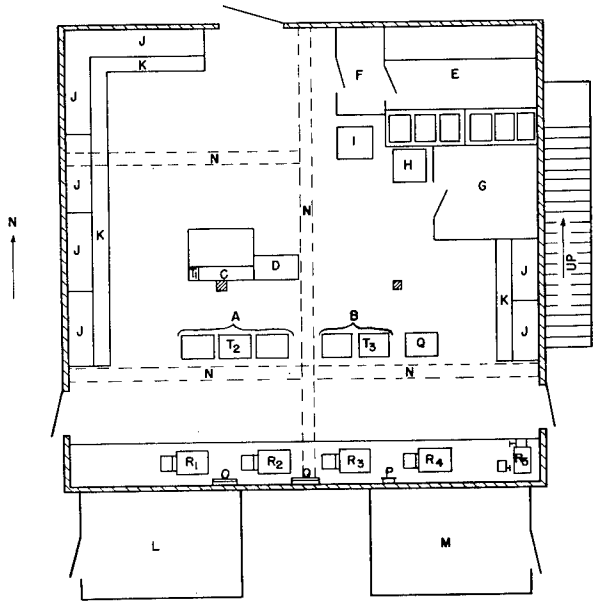

Fig. 110. The interior arrangement of the telemetering building

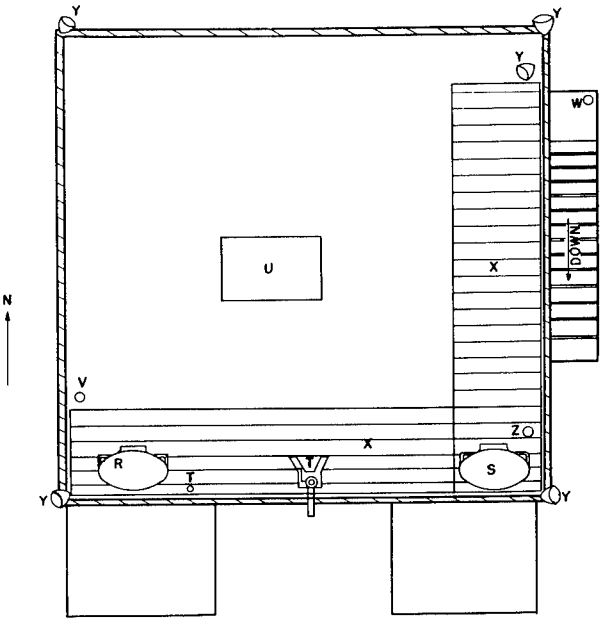

Fig. 111. Disposition of equipment on the roof of telemetering building

3 Naval Research Laboratory Report No. R-2955, Chapter II, Section C and Naval Research Laboratory Report No. R-3030, Chapter III.

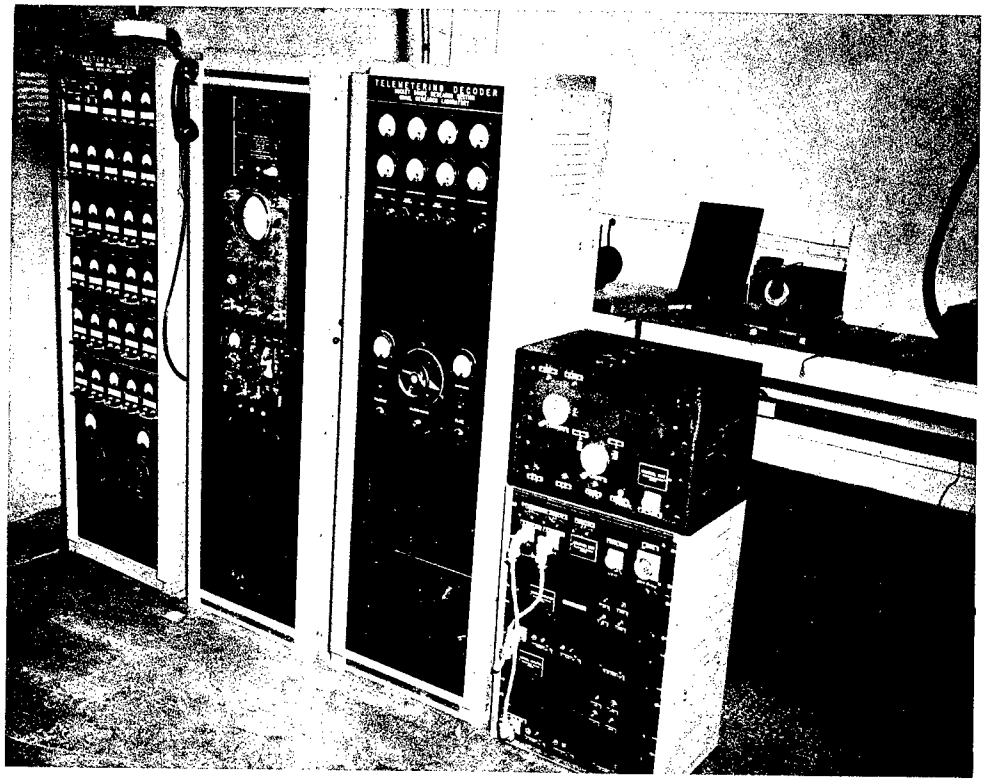

Fig. 112. Telemetering ground station I-A

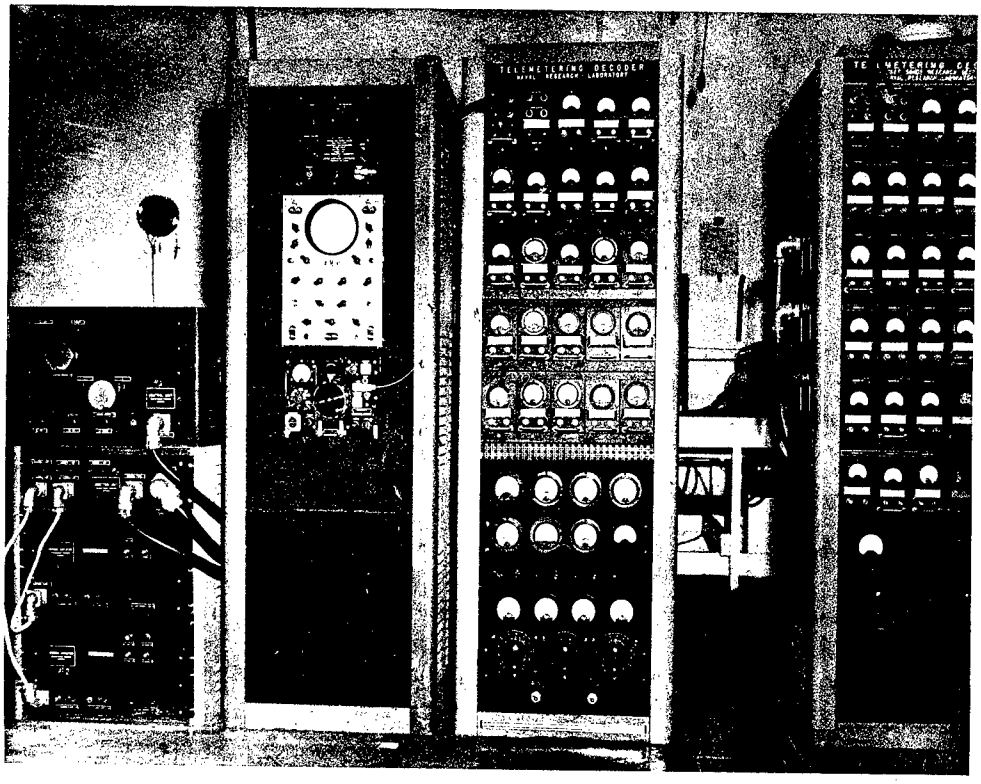

Fig. 113. Telemetering ground station I-B

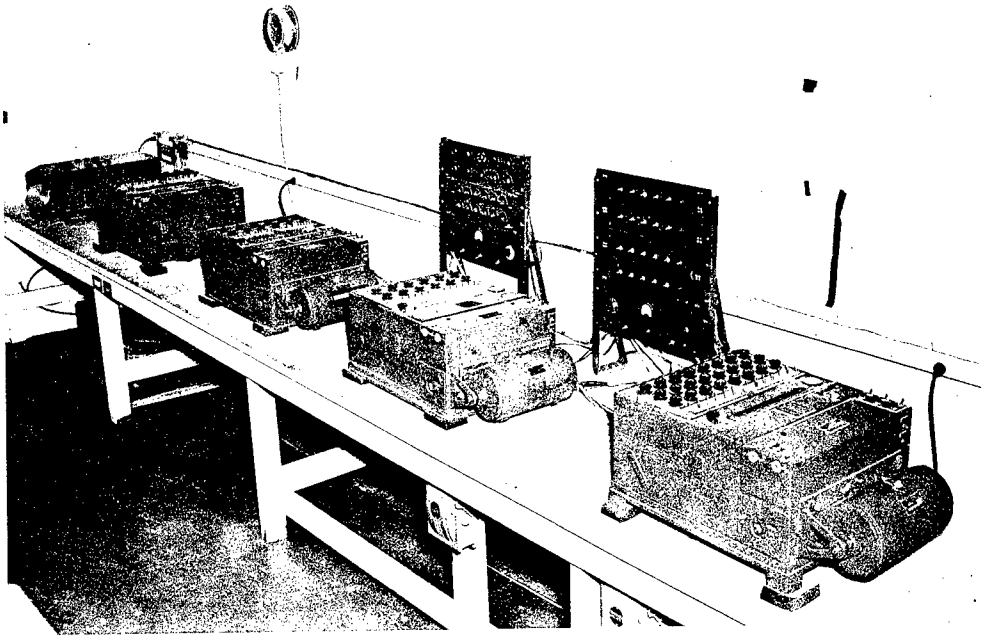

Fig. 114. The film recorders installed in the telemetering building

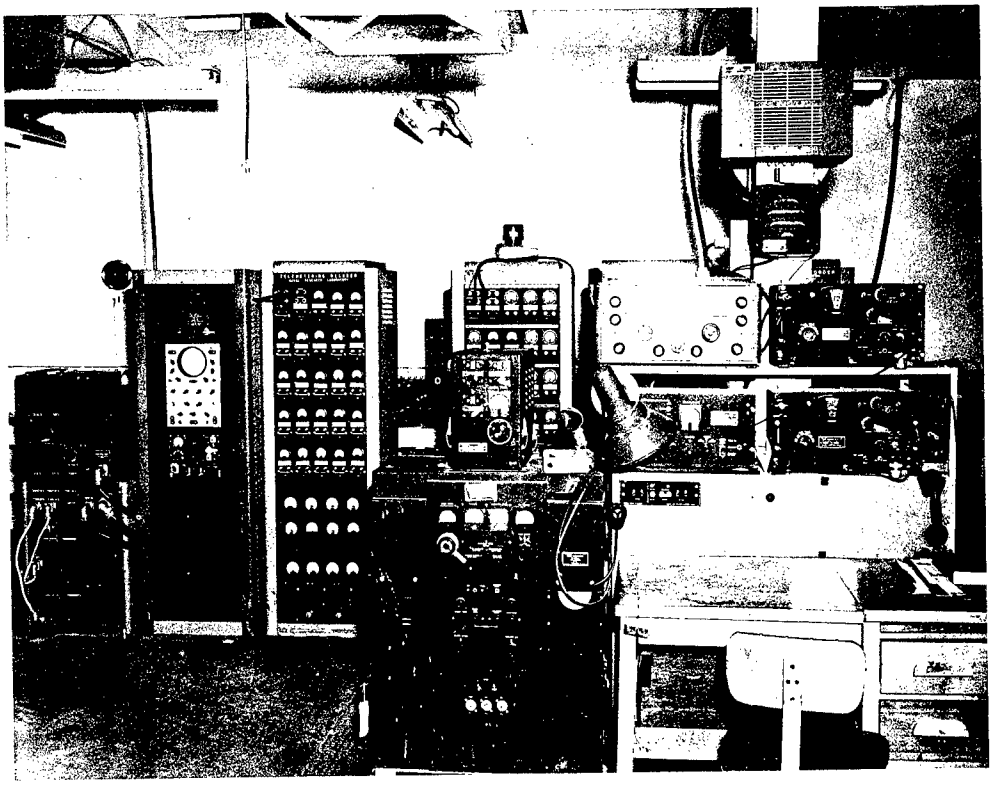

Fig. 115. The radio communication station located in the telemetering building. Parts of the two ground stations may be seen in the background

In addition to the two telemetering receiving stations, a complete radio communication station is housed in the building. It is located at positions C and D in figure 110, and is shown in detail in figure 115. This service is used during telemetering test periods for communication with headquarters and test aircraft, and for relaying information to other Naval Research Laboratory sites farther up the firing range. A similar communication station is mounted in the trailer which houses the third telemetering ground station.

The telemetering record is made on film which is developed and processed by the New Mexico College of Agriculture and Mechanic Arts, under a contract with the Office of Naval Research. The college maintains a master storage file of all film records of the various flights. Prints of these are furnished upon request to any participating agency concerned. A file of record prints and analyses is also maintained at the Naval Research Laboratory.

The success of the firing is determined, in part, by the quality of the telemetering records. Complete operational testing of the telemetering system before each firing therefore includes the making of sample records. It is necessary that these be developed and processed as rapidly as possible, so that a check on overall system performance can be made immediately before the flight. Accordingly, complete developing and processing facilities are provided in the telemetering ground station building. The darkroom appears at E in figure 110. It is equipped with Smith developing tanks, means for mixing developer and fixer, and special equipment for the development of 24 cm (9.5 in.) film in lengths up to 60 m (200 ft). A normal pre-flight test involves the use of 150 m (500 ft) of film.

Power is supplied by an M-18 motor generator unit capable of delivering 10 kva of 110 volt, 60 cycle a-c power. A similar unit is maintained as an alternate, to serve in case of a failure of the main supply.

During the first two cycles of V-2 firings, several auxiliary methods of recording telemetered data were employed. These included a camera which photographed the meter panel, a continuous film camera which recorded the video presentation on a cathode ray tube, and a wire recorder which made a record of the video output.

However, satisfactory records were furnished by the Hathaway instruments during each of the flights in that series. This form of record was also the most suitable for purposes of analysis. Its dependability and superior reading characteristics led to the decision to dispense with the alternative recording methods. Accordingly, beginning with the third cycle of V-2 firings, only the primary recording system was employed.

B. The Calibration Procedure

The telemetering system must be calibrated before each V-2 flight. Each link which transmits data voltages must be checked. The data voltages themselves must be calibrated with respect to the quantities under study, and calibration curves must be drawn for each measuring instrument. This part of the procedure is conducted by the interested agency, and is independent of the calibration of the telemetering link. Telemetered data are represented on the final record by lateral deflections of lines which run the length of the film. The amount of deflection must be calibrated against the original data voltage which it represents. The data voltages change form several times in the telemetering process, hence the system must be adjusted at each point of change in order to insure that all voltages remain within the acceptance ranges of the various components, and to make the operation of the system as nearly linear as possible. The large number of telemetering channels multiply the number of adjustments which must be made. To make adjustments and calibrations as accurately and rapidly as possible special methods were developed, and special equipment was designed and constructed. A typical calibration is described below.

The pulse spacings of the time modulation in the airborne transmitter are adjusted so that 50 and 200 microsecond intervals correspond to data voltages of 0 and 5 volts, respectively. The two extreme voltages are applied alternately to each channel, and adjustments are made until the correct pulse spacings are obtained. These adjustments are performed in sequence from channel 1 through channel 23.

The next operation in calibration is to adjust the channel outputs from the ground station decoder to vary from 2 to 27 volts as the data voltages vary from 0 to 5 volts. The minimum value of 2 volts was chosen in preference to the 0 volt level in order to allow for drift. This is necessary because negative voltage outputs are clipped, and the corresponding information is lost.

When adjustments are completed, the Hathaway recorder in the ground station is operated, and calibrated voltage levels are inserted into each channel of the airborne transmitter in 0.5 volt steps from 0 to 5 volts. In this way a check is made on the linearity of each channel. During an actual flight, an absolute voltage calibration is obtained by alternately applying two known voltages to each channel at intervals of approximately 10 seconds. These voltages afford a measure of any slow drift in the system, and provide a true voltage calibration throughout the transmission.

In order to obtain a more accurate and rapid means of calibrating each channel in the overall system, a preflight calibrator was constructed. A circuit diagram of this device is shown in figure 116. The connections to the telemetering channels are made through two AN-3108-20-IP connectors which are attached to the airborne unit in place of the leads from the measuring instruments. Calibration voltages are inserted into each of the channels in 0.5 volt steps from 0 to 5 volts, each half volt step being adjustable. The adjustability makes it possible to compensate for variations in the supply voltage, which ranges from 5 to 7 volts.

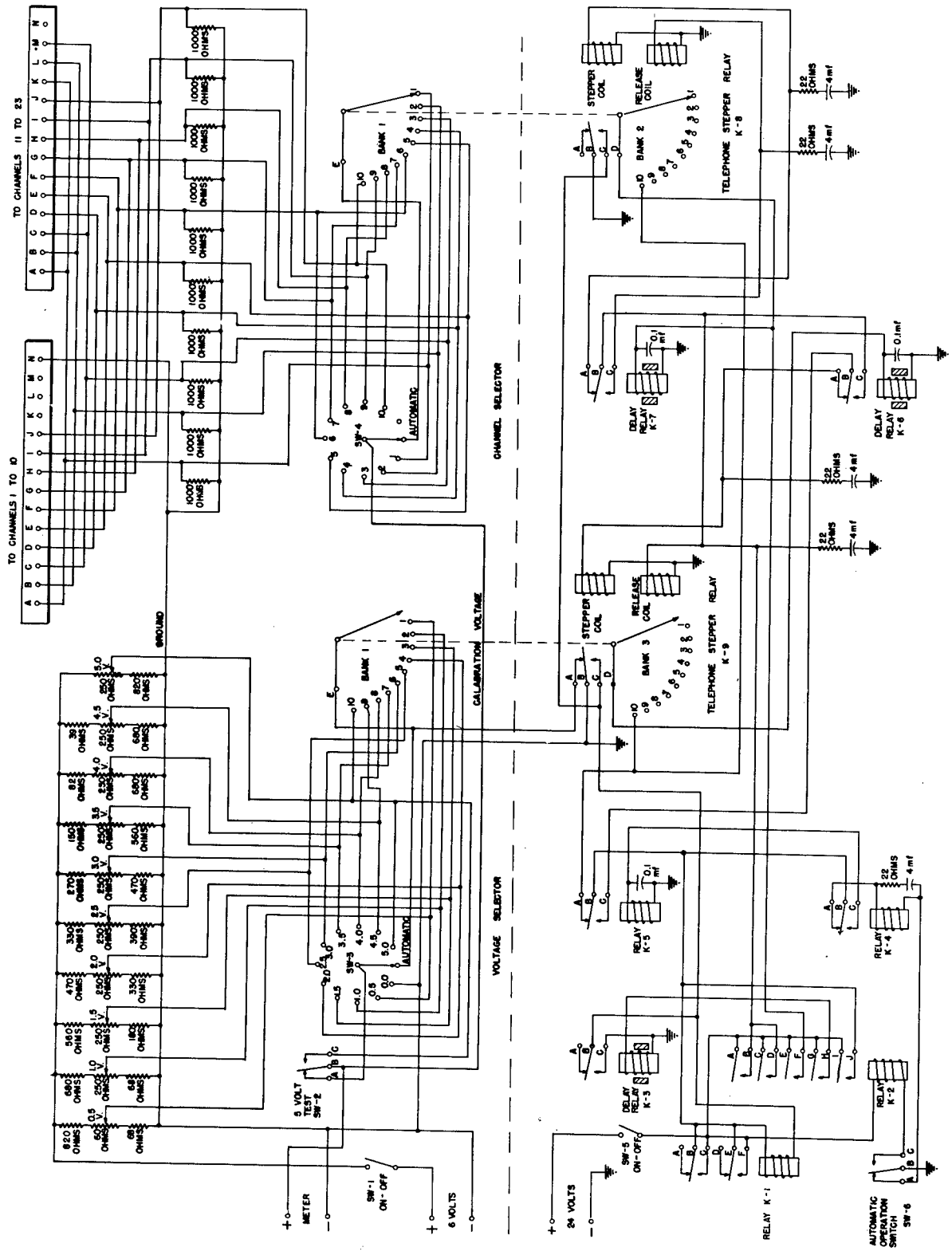

Fig. 116. Schematic diagram of the preflight calibrator

Manual selection of the voltages is made by means of the selector switch, SW-3, and manual selection of the channel to be calibrated by SW-4. A 0-to 5-volt precision d-c meter, having an impedance of at least 200 ohms per volt, is connected to the meter terminals to indicate the voltage selected by SW-3. The impedance of the meter does not affect the calibration, provided it remains the same from the time the voltages are adjusted until after the calibration is completed. SW-2 is a microswitch for measuring the supply voltage at the 5 volt tap point. It is also used in making those telemetering system adjustments which require the alternate application of 0 and 5 volts.

All telemetering channels are not calibrated simultaneously due to the presence of cross-talk. The interference is most severe between adjacent channels. The channels are therefore calibrated in groups of two or three, as shown in figure 116. Those within any one group are separated from each other by at least nine intervening channels. A 1000 ohm shunting resistor is employed to reduce any error which may be due to differences in the channel input impedances. The maximum possible error is = 0.5%, a negligible quantity in this operation. Since it is proportional to the calibration voltage amplitude, its effect is further reduced by the two reference voltages which are transmitted periodically during each flight.

When switches SW-3 and SW-4 are in the automatic position, the operation of switch SW-6 causes the two telephone stepper relays K-8 and K-9 to make proper voltage and channel selections. Relay K-9 makes the voltage selections, and relay K-8 makes the channel selections. When K-9 is in starting position, terminal A is grounded through terminal B, providing a zero calibration point. When the selector arms of K-9 advance to step 1, terminals A and B open, and the selector arm of the first bank of contacts chooses the 0.5 volt calibration voltage. As the arm advances from step to step, the calibration voltage increases in steps until the 5 volt point is reached. The contacts of the first bank of F-8 are connected to the ten groups of channels, respectively. The starting position for K-8 is position 1. This insures that at least two channels will be connected at all times and, therefore, that a more nearly constant impedance will be presented to the voltage source. During the calibration process, the selector arm of K-9 passes over all positions for each setting of K-8. This gives an eleven-point calibration for each group of channels. When the calibration of all channels is completed, the action of the relays stops automatically.

Certain features have been incorporated in the automatic drive to make the operation of the system more convenient. When the 24-volt power is connected and switch SW-5 is turned on, all the actions follow automatically after switch SW-6 is pressed and released once. The stepper relays first are released to the starting positions, and then are advanced through the set of operating positions. The action of the network then performs the desired calibrations. When these are completed, the action of the relays ceases automatically. The timing of the relay actions is a very important factor in the process. The actions of the relays during and after the times at which switch SW-6 is depressed and released will now be described in the

same sequence in which they occur. Throughout the discussion, reference is made to figure 116.

Action 1. The pressing of switch SW-6 causes terminal C of that switch to be grounded through terminal B. This, in turn, grounds one terminal of the coil of relay K-2, closes the relay, and supplies 24-volt power through all five pairs of terminals. Terminal F of K-2 supplies power to relay K-7, closing it. Power is applied through terminals B and D of K-2 to the release coil of K-9, and through terminals B and C of K-7 to the release coil of K-8. The selector arms of both stepper relays are released and returned to their starting positions from whatever random positions they may be occupying. The starting position for K-9 is below step 1, while the starting position for K-8 is at step 1. When the selector arms are in the starting positions, terminals A and B of both stepper relays make contact, and terminals B and C break contact. This disconnects the ground return of relay K-1, which had been made through those contacts. However, terminal A of K-2 supplies power to K-3, closing it, and causing terminals B and C to make contact. This provides an alternative ground connection for the coil of K-1. Terminal J of K-2 supplies 24-volt power to the other side of coil K-1, and K-1 closes. Terminal J also supplies 24-volt power through A and B of K-5 to position 10 in each stepper relay, and, through terminals A and B of K-4, to the coil of that relay. The ground side of K-4 is disconnected because SW-6 is not in its normal position.

Action 2. Switch SW-6 is released, breaking the ground connection to K-2, thus allowing this relay to open. Power is disconnected from the release coils of the stepper relays, making them ready for the stepping action. Power is also disconnected from the coils of K-3 and K-7, however, because of their delayed opening characteristic, they remain closed until shortly after action 2 is completed. The ground connection of K-1 remains closed, and 24-volt power is supplied to the coil of K-1 through its terminals B, C, E, and F. All 24-volt power passes through these terminals during each of the subsequent actions, due to the fact that relay K-2 remains open. The releasing of SW-6 also restores the ground return of the coil of K-4. The 4 μf condenser in parallel with K-4 charges, causing this relay to close. The 24-volt connection through its terminals A and B is broken, but K-4 receives power from the condenser until it is discharged. Terminals B and C of K-4 make contact and relay K-5 is closed. Terminals B and C of K-5 make contact, and power flows from terminal C of this relay, through B and A of K-6 to the stepper coil of K-9. The selector arm is advanced to step 1, and terminals B and C of K-9 make contact, providing another ground return for K-1.

Action 3. Relay K-3, having been held closed since action 1 by its delay characteristic now opens, breaking the first ground return of K-1. The second ground return is still maintained through terminals B and C of K-9. This action occurs one-quarter of a second after action 2. Relay K-7 opens a half second after action 2.

Action 4. The condenser in parallel with the coil of relay K-4 becomes effectively discharged about one-third of a second after the relay closes. This allows K-4 to open. Power is disconnected from K-5 and this relay opens. The condenser in parallel with the coil of K-5 prevents sparking at the B-C contact point in relay K-4, however, its capacitance is too small to delay ap-

preciably the opening of K-5. Power is disconnected from the K-9 stepper coil, and the stepper lever relaxes. The condenser across K-9 prevents sparking at the B-C contact point in relay K-5.

Action 5. When K-4 opens, the 24-volt power again charges the condenser in parallel with its coil, in approximately one-tenth of a second, whereupon the relay closes. Power is again supplied to K-5, and it closes and allows power to flow through terminals B and A of relay K-6 to the stepper coil of K-9. The selector arm of K-9 advances to the next step. K-4 opens and closes at the rate described in actions 4 and 5 until the entire calibration has been completed.

Action 6. Actions 4 and 5 are repeated alternately until the selector arm of K-9 reaches step 10 in the course of one of the executions of action 5.

Action 7. As in action 4, relay K-4 opens, allowing relay K-5 to open. The stepper lever of K-9 then relaxes. When K-5 opens in action 7, however, 24-volt power passes through its contacts B and A to position 10 of K-9, and thence through the selector arm to the coil of K-6, closing that relay.

Action 8. As in action 5, relay K-4 closes, closing K-5. Power is disconnected from K-6, but its delay characteristic keeps it closed for an additional one-quarter second period. When K-5 closes, power flows through its contacts B and C, thence through contacts B and C of K-6 to the release coil of K-9. It then passes through contacts A and B of K-7 to the stepper coil of relay K-8. The selector arm of K-9 is released to the starting position, and the selector arm of K-8 is advanced to the next step. To prevent sparking, condensers are placed in parallel with all stepper and release coils of relays K-8 and K-9. Although the ground return of K-1 which passes through B and C of K-9 is now broken, another ground return is completed through contacts B and C of K-8 because the selector arm of the latter relay has advanced out of the starting position. Relay K-6 opens one-quarter of a second after action 8 begins.

Action 9. The sequence of actions 4, 5, 6, 7 and 8 is repeated until the selector arm of K-8 reaches position 10 in the course of one of the executions of action 8. At this point the selector arm of K-9 is in the starting position.

Action 10. As in action 7, relay K-4 opens, allowing K-5 to open. The release lever of K-9 and the stepper lever of K-8 then relax. When K-5 opens, power flows through its terminals B and A through position 10 of K-8, to relay K-7, which is thereby closed.

Action 11. An action 5 follows action 10, thereupon actions 4 and 5 occur alternately until the selector arm of K-9 reaches position 10. Action 11 is similar to action 6, except that each time K-5 opens, power flows to K-7, holding it closed. The amount of time by which the opening of K-7 is delayed is greater than the interval during which power is disconnected from it, therefore, this relay remains closed during action 11.

Action 12. Relays K-4 and K-5 open as in action 7 and power flows through terminals B and A of K-5, through the selector arms of K-8 and K-9, closing K-6 and holding K-7 closed.

Action 13. Relays K-4 and K-5 close, allowing power to flow through contacts B and C of K-5 to the release coil of K-9, and thence through contacts B and C of K-7 to the release coil of K-8. The selector arms of both stepper relays are then released to their respective starting positions. Terminals B and C of both K-8 and K-9 separate, breaking all ground connections to relay K-1. The latter then opens, disconnecting the 24-volt supply from all relay circuits. This ends the complete calibration action.

C. The Receiving System

The telemetering receiving antennas employ circularly polarized parabolic reflectors mounted on two-axis, servo-driven pedestals. These may be remotely controlled by means of a manual tracking unit, an optical director, or an electronic tracking system which trains the antenna on the maximum of the received signal. The antenna system is shown in figure 117. It consists of a 122 cm (48 in.) paraboloid, energized by a three-phase circularly polarized element.

The antenna is driven in both azimuth and elevation by two-phase a-c servo motors of the low-inertia type. They are Navy type 211515, and have a

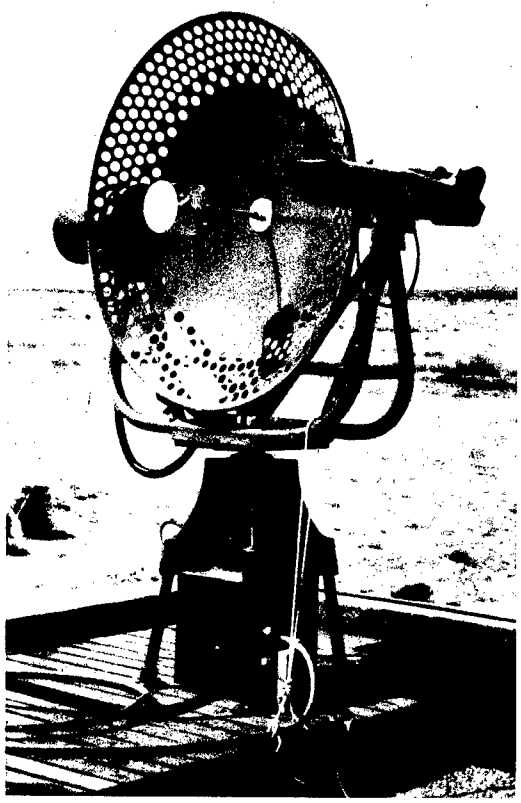

Fig. 117. The telemetering receiving antenna mounted on the roof of the telemetering building at the White Sands Proving Grounds

power output of 50 watts. The gear ratios in both azimuth and elevation are about 250 to 1. The full speed tracking rates are 60° per second. One-speed synchro gearing provides sufficient accuracy for the antenna beam-width employed. A coaxial contact-type rotary joint allows rotation in azimuth, and a length of flexible coaxial line permits rotation in the vertical plane.

The servo system is a conventional a-c control unit. The synchro error signal is amplified, shifted in phase by 90°, and applied to one winding of the two-phase servo motor. The other winding is connected to the same 115-volt source as the synchro generator rotor. Under these conditions the motor will always run in such a direction as to reduce the error signal. As a result, the antenna follows the director synchro generator. A schematic diagram of the system is given in figure 118.

The system is stabilized by the antihunt circuit shown in figure 119. This is a modified, bridged-T, band-elimination network which rejects the error signal frequency of 60 cycles. Its bandwidth is variable. Control resistor R-222 is adjusted so that the quadrature component of the filter output is zero at the fundamental frequency. Potentiometer R-221 controls the bandwidth and maximum rejections of the filter, determining the amount of in-phase component added in series by transformer T-201. The setting of R-222 is fixed for a given a-c line frequency, while the setting of R-221 depends upon the characteristics of the servo system, and particularly upon the inertia presented to the driving motor. Thus, in general, the setting of R-221 will depend upon whether the amplifier is used for azimuth or for elevation control. The filter attenuates the fundamental of an error signal of varying amplitude to a much greater degree than it does the sidebands. Thus,

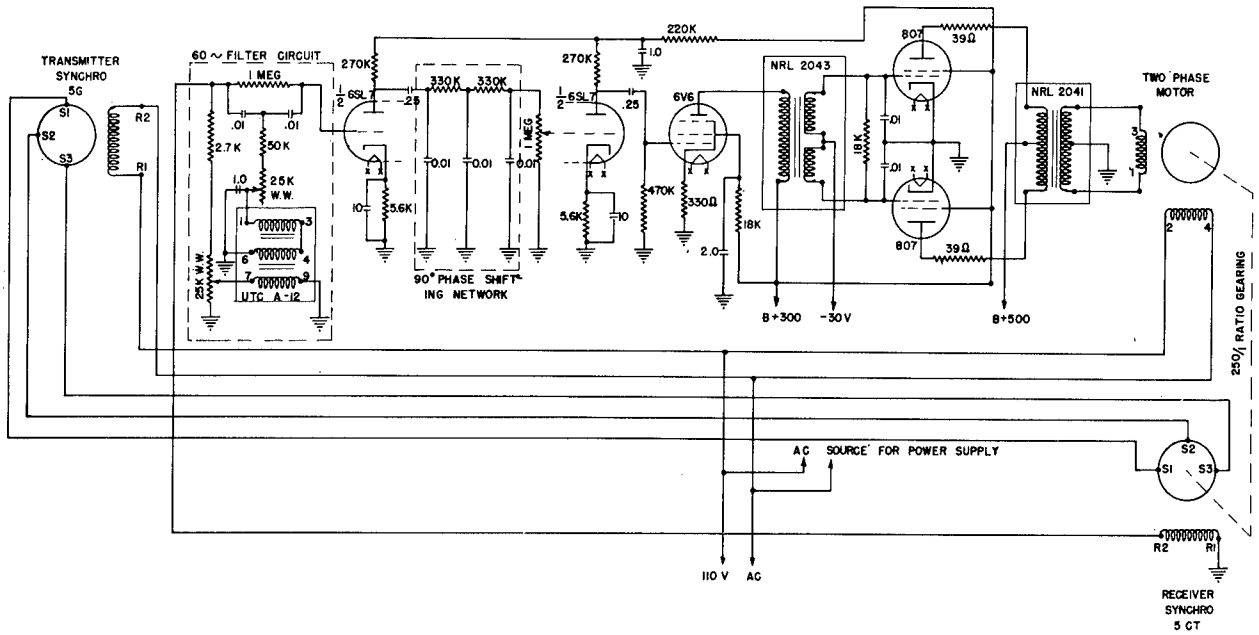

Fig. 118. Schematic diagram of servo control amplifier

the latter combine in the output to give a 60 cycle voltage whose amplitude is proportional to the rate of change of the error signal amplitude, and to the small amount of fundamental frequency remaining. In this action the circuit is analogous to the differentiating circuits employed to stabilize d-c control servo systems. The differentiation allows the drive motor to be controlled by changes in the amplitude of the synchro error signal. Thus, a decreasing signal causes reverse voltage to be applied to the motor, braking it and reducing or preventing the overshoot and the hunting oscillations which are due to inertia.

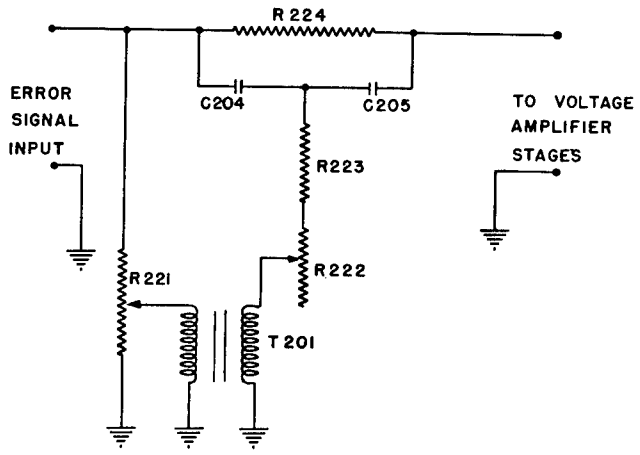

Fig. 119. Servo antihunt network

Following the antihunt circuit is a two stage voltage amplifier. This compensates for the large attenuation which occurs in the antihunt network. The network between the two halves of the 6SL7 serves to attenuate those harmonics of the synchro output which have been emphasized by the antihunt network. It also shifts the phase of the amplifier output by 90° to operate the two-phase servo motor. Following the voltage amplifiers is a 6V6 power amplifier which drives a pair of 807 type tubes in class AB_2 operation. About 80 watts of output power is supplied to operate the servo drive motor.

The receiving antennas are controlled by an Army Ordnance M-2 Tracker[4], which is installed at the telemetering ground station. The M-2 is a fire-control tracking unit equipped with eight-power telescopes. It can be operated by one man, however, a better performance is obtained with two operators. The eight power telescopes are to be replaced by twenty power units as soon as these can be procured. The azimuth data are furnished by a one-speed synchro generator which controls the antennas. Elevation data are normally supplied by a four-speed synchro generator, but such a system could not be used with the one-speed antenna control system. Instead, the one-speed synchro repeater provided in the director is used as a generator simply by locking its dial mechanically to the coarse elevation indicator dial.

The M-2 tracker provides optional aided-tracking operation. In this type of operation, the tracker is moved by slewing motors, while the handwheels serve only to correct the present position of the director. The amount and rate of correction added by the handwheels are integrated and the resulting quantities are used to govern the speeds of the slewing motors. These will thus maintain constant angular tracking rates unless and until

---

[4]Cf. War Dept. TM9-2300 "Standard Artillery and Fire Control Material" 7 Feb. 1944 and TM9-1671-B "Ordnance Maintenance, Directors M9, etc." 13 July 1944.

corrections are introduced as a result of the integration process. Thus, if the angular velocities vary, the handwheels are turned, and the slewing motor speeds change. This type of tracking is considerably smoother and more accurate than position tracking, in which the handwheels control the tracking angles directly. It also has the advantage of keeping the target within the field of view of the telescope even though it may be concealed for short periods by small clouds. The director was first used to control the telemetering antenna during the March 7 firing. It proved fairly successful, in spite of a layer of high, scattered clouds.

An improved telemetering receiver for the V-2 program is under development. It will provide both audio and video outputs, and employ automatic gain control capable of handling the wide range of signal strengths received from the rockets. It is designed to have an overall effective bandwidth of 4 megacycles and a noise figure of less than 10 db, which corresponds to an r-f sensitivity of 3 microvolts at a 50 ohm input impedance level.

The receiver employs an input tuning cavity with a bandwidth of 10 megacycles, a tuning range of 950 to 1,150 mc, and an insertion loss of less than 1 db. This unit can be switched in or out of the circuit. The crystal mixer is fixed-tuned over the range from 950 to 1,150 mc. Fixed local oscillator coupling is used. Local oscillator power is controlled by the operating voltage of this component. A transit-time local oscillator with a single tuning cavity is employed. The oscillator tube is a 2C46 lighthouse triode, developed especially for transit-time applications.

The intermediate frequency amplifier obtains a low noise figure through the use of a two-triode input circuit. The first stage uses a 6AK5 grounded cathode which drives a 6J6 grounded grid amplifier. This is followed by four 6AK5 stages arranged in two stagger-tuned pairs.

The output of the video amplifier supplies about 1.5 volts to a 93 ohm line, and 50 volts at a high impedance level. A pulse automatic gain control system is incorporated to regulate the i-f stages. It also furnishes a current which is a function of received signal strength to one of the Hathaway recorders. A diode pulse stretcher and amplifier supply the audio output.

An experimental model has been completed, and extensive tests of the components are now underway.

D. The Rocket-Borne Transmitting Antennas

The various motions executed by the V-2 during flight impose definite restrictions upon the types of antennas which may be used to radiate the telemetering signal. During an average flight, the missile rolls, pitches and yaws. Of these, the most troublesome motion is roll. The rocket does not tumble in the course of a normal flight. Hence, antennas with hemispherical coverage mounted at the tail are adequate.

The problem of providing complete hemispherical coverage with an antenna mounted on a rotating rocket falls naturally into two parts. First, circular polarization must be employed if the received signal is not to be characterized by the presence of periodic nulls, which are a function of the configuration of the antenna and the angle through which the rocket has rotated. Second, the radiation pattern itself must be reasonably isotropic in the plane plane of the elements, otherwise nulls will appear which are simultaneously a function of the antenna pattern and the amount of roll.

The first of these problems was solved by the use of the three-phase, circularly polarized antenna which is described in an earlier report of this series.[5] The three-phase antenna, which replaced the original dipole installation, was employed during the third cycle of V-2 firings. Its pattern was characterized by the existence of three main lobes and three rather sharp nulls. This radiator was an interim device, relied upon to improve the performance of the telemetering system until the present antenna could be brought into play.

The turnstile antenna effectively solves both of these problems. It was employed for the first time in the V-2 firing of March 7, and its use was continued in the flights which followed. According to present plans, it will be installed on all future V-2's. This antenna is plane polarized in the plane of the elements, and circularly polarized in the direction normal to

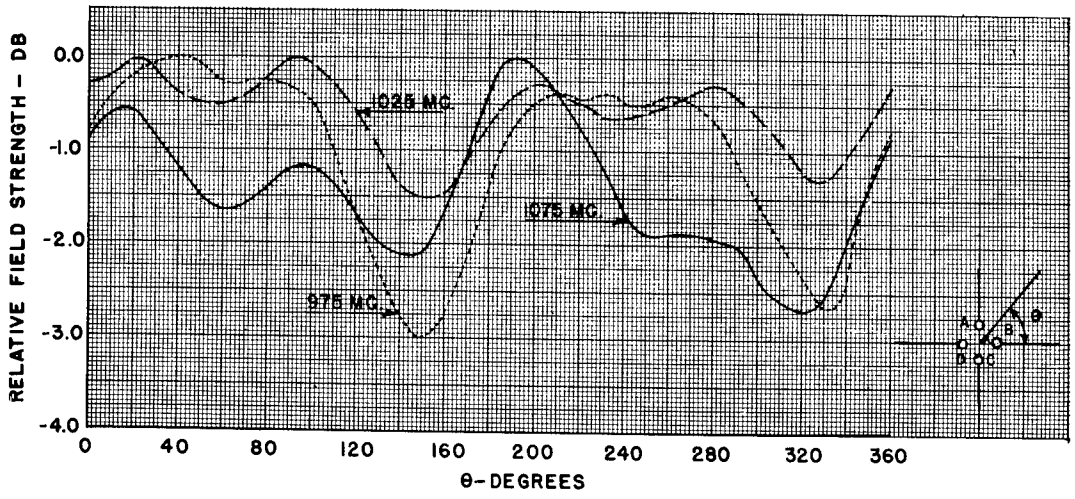

Fig. 120. The turnstile airborne transmitting antenna plane polarized radiation pattern in the plane of elements

[5] Naval Research Laboratory Report No. R-3030, Chapter III, Section A.

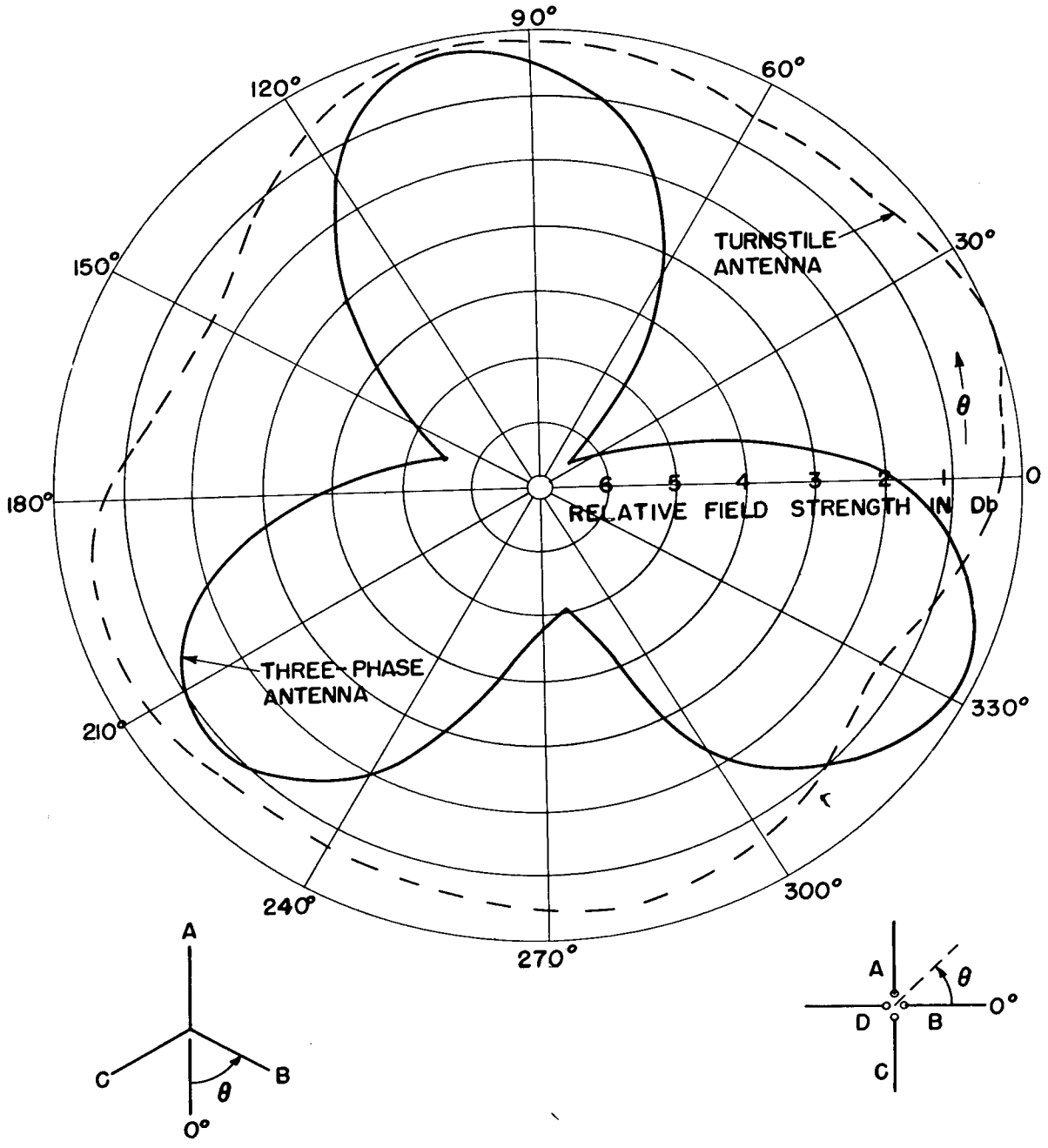

Fig. 121. Comparison of the radiation patterns of the turnstile and three-phase transmitting antennas

this plane. The pattern in the plane of the elements is nearly circular. It is plotted in figures 120 and 121.

The improvement is shown in figure 121 which compares the radiation patterns of the two antennas. The interim antenna had nulls which were 7 db down from the maxima at 1025 mc, while the corresponding figure for the turnstile is 1.5 db.

The newly-designed antenna consists of two half-wave coplanar dipoles mounted normally to each other. The unit is illustrated in figures 122 and 123. The two crossed dipoles are fed with equal currents which are phased 90° apart in time. The radiation field may be made to rotate in either direction, simply by causing the current in AC to lead or to lag the current in BD. Rotation in the direction of increasing azimuth angle was chosen for both the transmitting and receiving antennas. The turnstile's polarization eccentricity in the direction normal to the plane of its elements is never greater than 3 db in the range from 975 to 1125 mc.

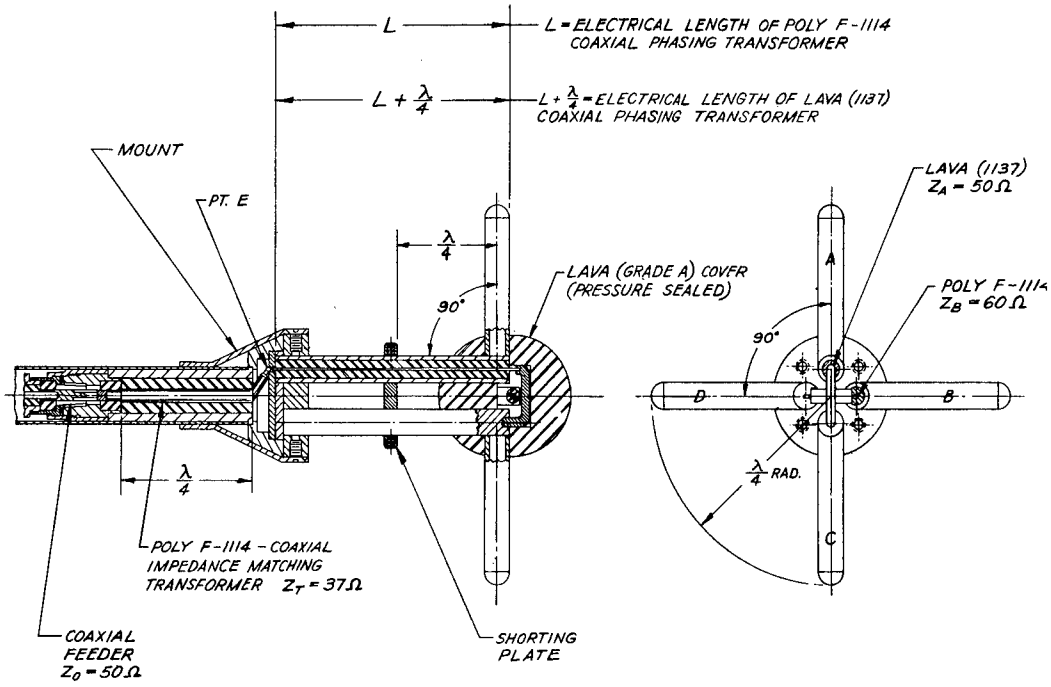

Fig. 122. Drawing of the turnstile transmitting antenna

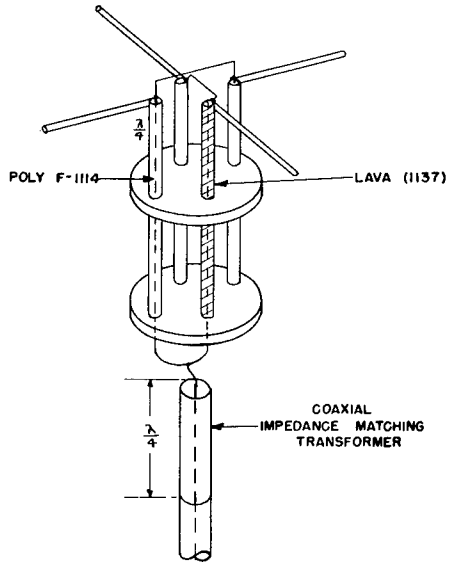

Fig. 123. Schematic diagram of the turnstile transmitting antenna →

The turnstile antenna may be considered as essentially comprising four identical, symmetrically-spaced elements, with terminals at the points labeled A,B, C and D in figure 124(a). The relative magnitudes and phases of the various currents can then be represented by means of the vector diagram of figure 124(b). The current I_A leads the current I_D by 90°. Similarly, I_C lags I_D, I_B lags I_C, and I_A lags I_B, in each case by 90°. Both dipoles are resonant, hence, the current and voltage into each element are in phase. The impedances Z_3 and Z_4 are those presented by the dipoles. The coupling between adjacent elements is negligible.

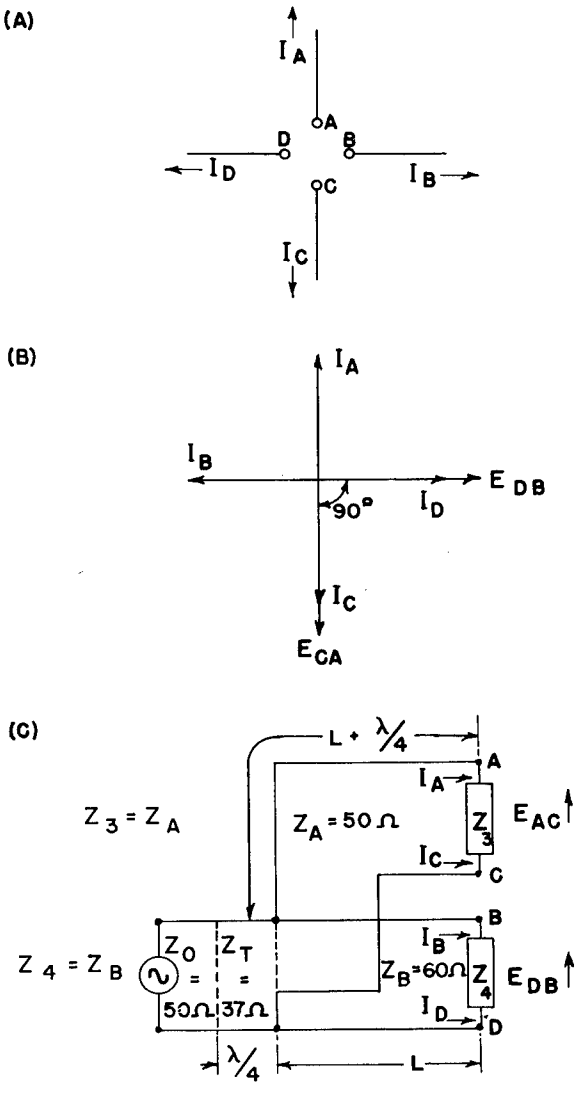

Fig. 124. Equivalent circuit diagram of the circularly-polarized turnstile transmitting antenna

Phasing is accomplished by feeding the dipoles with separated coaxial feeders having physical lengths which are equal, and electrical lengths which differ by a quarter-wavelength. This is achieved by employing different dielectric materials in the lines. Lava 1137 (dielectric constant: $C_A = 4.6$) and Poly F-1114 (dielectric constant: $C_B = 2.1$) are used. These dielectric constants should not vary by more than .05 in either case. The physical length is given by the relation:

$$\lambda_p = \frac{\lambda}{4[\sqrt{(C_A)} - \sqrt{(C_B)}]}$$

where λ is the wavelength in free space.

There are no appreciable standing waves on the dipole feeders. The characteristic impedances of the feeders, Z_A and Z_B, are matched by dipole resistances of 50 and 60 ohms, respectively. The center conductors of these feeders loop together at the point labelled E in figure 122. A series quarter-wavelength transformer matches the impedance at the point E to the 50 ohm characteristic impedance of the RG-9/U feeder cable. The voltage standing wave ratio is 1.3:1, or less, from 920 to 1115 mc. These measurements are plotted in figure 125. Antenna currents are prevented from flowing on the outside of the RG-9/U cable by means of a balanced-to-unbalanced transformer, consisting of a high impedance, quarter-wavelength, shorted section of balanced transmission line. This section also serves as a mechanical support for the dipoles in

the manner illustrated in figure 122. The precautions taken to prevent arc over in the transmission line will be continued. These include the use of pressurized fittings and Dow Corning No. 4 ignition sealing compound. The turnstile antenna is mounted on fin I of the V-2 in the same way as was the three-phase antenna.

An equivalent circuit diagram of the feed system is presented in figure 124(c). L, in this case, represents the electrical length of the Poly F-1114 phasing transformer, and $L + \lambda/4$, the electrical length of the Lava 1137 phasing transformer. Figure 126 is a photograph of the airborne turnstile mounted on a fin of the V-2.

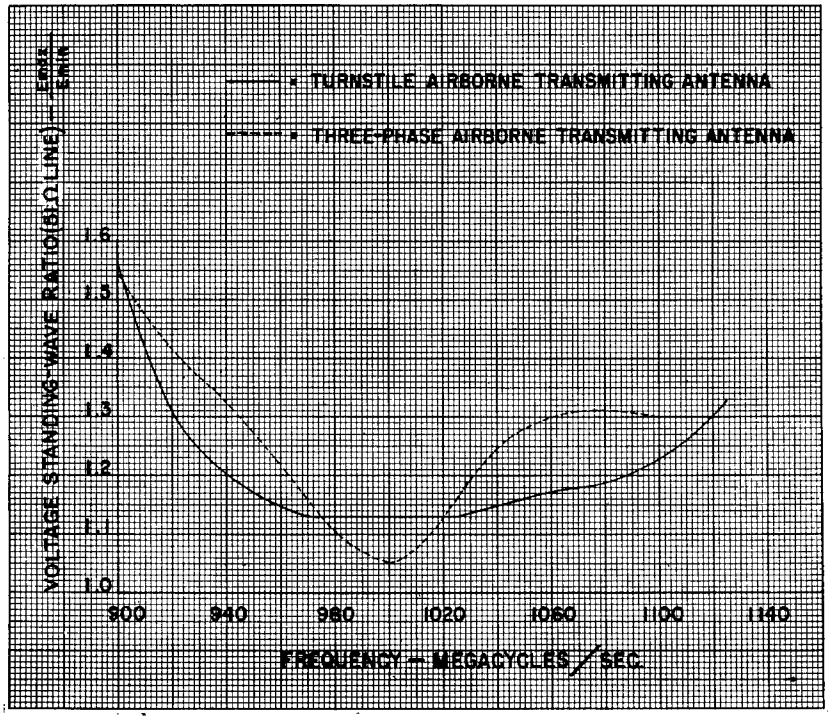

Fig. 125. Graph of voltage standing-wave ratio vs frequency for the turnstile and three-phase airborne transmitting antennas

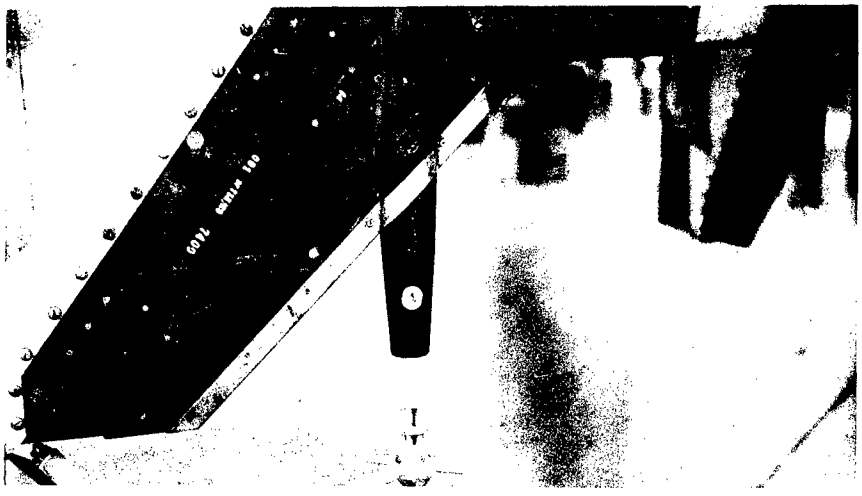

Fig. 126. The turnstile transmitting antenna mounted on a fin of the V-2.

E. An Operational Report on the Firings From December 5, 1946 Through March 7, 1947

Six V-2 firings occurred during the period from December 5, 1946 through March 7, 1947. They are reviewed here to furnish an indication of the performance of the telemetering system and to exemplify several of the situations dealt with elsewhere in this chapter.

Certain improvements incorporated in the equipment during this period resulted in better system performance. Among these, three changes were most important: the use of a circularly polarized antenna on the rocket, the use of a circularly polarized receiving antenna with a servo-operated parabolic reflector, and a rearrangement of the ground station together with an accompanying revision of the operating procedures.

Table VI summarizes the results obtained at each receiving station during the six firings. The time shown in column 3 nearly always corresponds to the time of impact, warhead blow-off, or the disappearance of the missile behind concealing terrain.

TABLE VI

SUMMARY OF THE PERFORMANCE OF THE TELEMETERING SYSTEM DURING THE PERIOD FROM DECEMBER 5, 1946 THROUGH MARCH 7, 1947

Firing	Date	The time, in seconds, after take-off at which the last readable record was obtained	The percentage of the time shown in column 3 during which a satisfactory record was obtained at station -		
			I-A	I-B	II
16	December 5, 1946	311	62.4	78.4	50.8
17	December 17, 1946	360	56.6	*8.1	17.7
18	January 10, 1947	300	93.4	95.7	*29.6
19	January 23, 1947	238	53.8	43.0	52.6
20	February 20, 1947	287	99.6	78.0	73.0
21	March 7, 1947	360	76.7	*	#

*Ground equipment failure

#Operating personnel inexperienced.

December 5, 1946 marked the first occasion upon which circularly polarized antennas were used at both the airborne and the ground stations. Stations I-A and I-B were fitted with the new equipment, while station II had the plane polarized antenna of the first system. The value of the change is apparent. The difference in performance between stations I-A and I-B is a reflection of the difference in the amount of experience of the operating personnel. The total amount of record obtained on this flight was exceptional, in view of the highly erratic performance of the rocket. During the portion of the flight above the atmosphere, the missile executed violent end-over-end tumbling. This caused the path between transmitting and receiving antennas to be blocked periodically by the main body of the rocket which, in turn, resulted in complete loss of the signal. The receiving system did not employ automatic gain control. Therefore, the sudden disappearance and reappearance of the signal made the task of the operating crews unusually difficult.

Missile 17 was fired at night on December 17, 1946. It reached a record altitude of 183 km (114 mi). Antenna tracking was hampered by the fact that the missile was not visible beyond Brennschluss. The operating personnel who manned the equipment during the flight were relatively inexperienced. These two factors were probable causes of the rather low level of performance during this flight.

The telemetering record made during the flight of January 10, 1947 was one of the best ever obtained. Station I-B recorded continuously from Brennschluss until 300 seconds after take-off when the warhead was blown off. The rocket control system did not operate properly after the first 40 seconds of the burning period. As a result, during the next 260 seconds of flight, the missile rolled with a period of approximately one second. The rocket engine was operating during the first 20 seconds of this period and the record showed that the signal was lost each time the flame came between the transmitting and receiving antennas. It was also clear from the record that the fraction of time during which the signal was received decreased as the rocket ascended. The spinning of the rocket tended to prevent tumbling and thus made it less likely that the transmitting antenna would be shielded by any parts of the V-2.

The normal preflight procedure includes the preparation of a spare transmitter. A type of periodic interference developed in the system shortly before firing time on January 10. The reserve transmitter was installed, but the difficulty persisted. The rocket was fired, after some improvements were made, and it was noticed that the interference disappeared completely after take-off. Subsequent analysis of the record indicated that the interference was caused by one of the rocket inverters.

The flight of missile 19 (January 23, 1947) was unusually erratic. Evidence for this is seen in the telemetering record, which showed that the plate voltage in the gyroscope computing unit dropped to zero 9.5 seconds after take-off. This probably contributed to the uncommon performance. Since the missile was visible during the entire flight, optical antenna tracking was employed. This increased the amount of record obtained.

Missile 20 (February 20, 1947) performed in much the same manner as did missile 18, (January 10, 1947) except that the period of rotation was much longer. An excellent record was obtained because of the stability imparted to the rocket by spin.

A good record was obtained from rocket 21 (March 7, 1947) until 225 seconds after take-off when the V-2 was 162 km (101 mi) above the earth. The signal was sporadic from this time on, as the rocket descended. A possible explanation for the fairly sudden drop in received signal level is that the air pressure in the coaxial cable feeding the antenna gradually decreased during the ascent due to a split in the outer covering. One such fissure was detected before take-off and repaired, but it is possible that others may have occurred if the low temperatures at high altitudes caused the covering to harden and thereby become susceptible of splitting.

Experience has shown that several factors can cause a hiatus in the telemetering record. These include equipment failure, insufficient transmitted signal strength, errors in antenna training, an automatic gain control which does not have a sufficiently rapid response, and the interruption of the radiation path by parts of the rocket.

Equipment failures may be kept to a minimum in the usual ways. Restrictions on the size, weight and radiated power of the transmitter are imposed by the limitations of the V-2. Recent efforts had the complementary objective of increasing receiver sensitivity. The results are described in Section C. It is estimated that they are equivalent to a ten-fold increase in transmitted power.

The antenna at station II has a broader radiation pattern than those at the other two stations. On several occasions the latter have lost the signal for short periods, while station II continued to receive it. Thus, it is seen that tracking errors still occur. They are being eliminated through the continued training of operating personnel.

An automatic gain control with a rapid response is helpful to the telemetering operators, as well as to the antenna trainers. Such a control has been incorporated in the receiver, and is described in Section C.

The rocket-borne antenna was located at a position outboard of fin I in an effort to minimize the probability that other parts of the rocket would intersect the transmission path. This change has overcome the difficulty to some extent.

F. Improvements in the Installations and Equipment

The experience acquired during the past eighteen months has indicated the desirability of making a number of improvements in the telemetering ground station installations. These changes have been initiated, and it is anticipated that they will be completed during the current year. They include the following:

(a) The introduction of commercial, 108-220 volt, three-phase power to the telemetering building. The commercially supplied power will be transmitted via standard high-voltage poles to a position 300 meters (1000 feet) from the building, where it will be transformed to 108-220 volt, three-phase power in a concrete vault structure. It will then be fed to the house by means of underground lines.

(b) The installation of twenty-eight pairs of telephone lines connecting the house to the base camp, the Army blockhouse, and the Navy blockhouse. These lines will be laid underground from the house to a point 300 meters (1000 feet) east, and carried on standard poles from there to the Army blockhouse where distribution to the other points will be effected.

(c) The installation of a complete hot water heating system and an automatic air conditioning-ventilating unit at the house. This unit will make it possible to keep out the fine sand which now infiltrates through the ventilating system into the building.

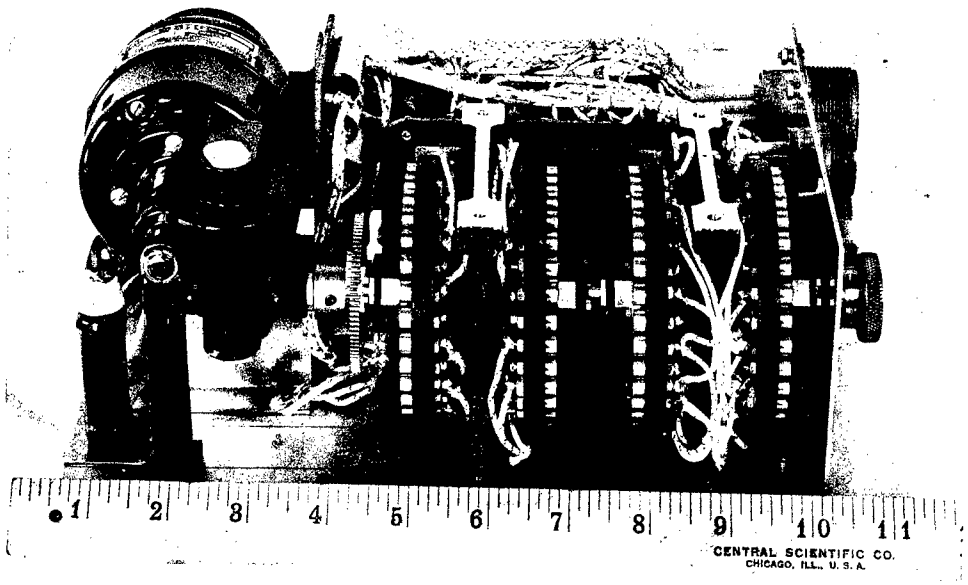

Fig. 127. Commutator used with the telemetering system

The accompanying modifications will include the installation of a vestibule gas-lock at the east door, the sealing of the west door, and the fitting of the north door with dust-gaskets.

(d) The installation of poles at each side of the building for the mounting of communication antennas. This will improve the reliability of radio communication to the camp and to the more distant Naval Research Laboratory field sites farther up the firing range. The antenna poles will be located so as not to cause interference with the telemetering system.

In addition to these improvements to the buildings and facilities at the telemetering site, the following improvements to the present telemetering equipment are being initiated:

(a) The modification of the Army M-2 optical tracker as a director for the servo-controlled antennas. The tracker will be used to provide continuous motion in elevation through the full 180°. The M-17 telescopes in this unit will also be modified to provide 20-power magnification. This will make it easier to track the missile at the peak of the trajectory.

(b) The construction of a video amplifier providing automatic gain control for the i-f stages of the receiver. This unit will also provide a recorder output to monitor the absolute level of the received telemetering signal.

(c) The use of two additional 24-channel Hathaway recorders at stations I-A and I-B to obtain greater flexibility of operation and increased deflection amplitudes. A completely flexible patch board for the recorder inputs will also be installed at the same time so that any of the recorders can be fed from either of these two telemetering stations.

(d) The development of an automatic tracker-director, operating on the lobe-switching principle, capable of keeping the antennas directed toward the maximum of the received telemetering signal.

The use of subcommutating devices as adjuncts to the telemetering system has been described in a previous report of this series.[6] These instruments, capable of combining as many as 14 sub-channels in a single telemetering channel, were designed, built, and used by the Rocket-Sonde Research Section in connection with four V-2 firings. Good results were obtained. The section has continued and expanded the program by procuring ten commutators from the Hathaway Instrument Company. These are sixty sub-channel units which feed four telemetering channels simultaneously. A photograph of one of these commutators appears in figure 127.

---

[6] Naval Research Laboratory Report No. R-2955, Chapter II, Section C.

G. A General Description of the New Naval Research Laboratory Pulse Matrix Telemetering System

The present telemetering system was developed within a period of three months at the outset of the Rocket Sonde Research Program in order to make the service available for the first V-2 firings at White Sands Proving Grounds. That this equipment included various undesirable features was recognized from the beginning. Accordingly, a new telemetering system possessing superior characteristics has been under development in the Rocket-Sonde Research Section since the summer of 1946.

This system is a pulse matrix type, employing pulse time modulation. It provides thirty channels and a sampling rate of 312 cycles per second. The airborne unit has a minimum peak r-f output power of three kw at 1000 megacycles.

The system differs from the one now in use in that equally spaced time reference pulses are used for the initiation of each channel sampling interval, rather than a pulse derived from the end of the previous sampling interval. The modulation intelligence consists of the series of equally spaced marker pulses interleaved with a succession of channel information pulses. Channel intelligence is contained in the time spacing between a channel information pulse and its corresponding time reference marker. All marker pulses are supressed during transmission with the exception of one during each sampling period. This is a triple pulse, suitably coded in time spacing so as to distinguish it from the channel information pulses, which furnishes the basis for synchronization of the ground station.

A schematic diagram of the airborne unit, including the multiplex modulator, is shown in figure 128. The corresponding ground station is represented in block diagram form in figure 129.

The multiplex modulator of the rocket-borne transmitter utilizes a series of triggering pulses which are initiated by a 10 kc oscillator and shaped in pulse forming tubes, labelled T-1, T-2, and T-3 in figure 128. The pulses are injected successively into the screen grid elements of 32 thyratron tubes which form a closed chain. In the process, the 10 kc oscillator controls the tubes labelled T-4 through T-35, so that they fire in succession at precisely 100 microsecond intervals. Each tube remains conducting for at least 100 microseconds during each group period. The exact time duration is made as close as possible to 100 microseconds by choosing the tube and circuit constants properly.

The first tube in the chain is free running, with a period exceeding the group sampling time. This makes the chain self-starting. Since the group periods and the channel firing periods are both controlled by the 10 kc oscillator, they are uniform in length. When T-4 fires, a saw-tooth voltage wave is generated in its cathode circuit, R-1, C-1. This voltage is coupled through condenser C-4 to the control grid of the next tube in the chain. The

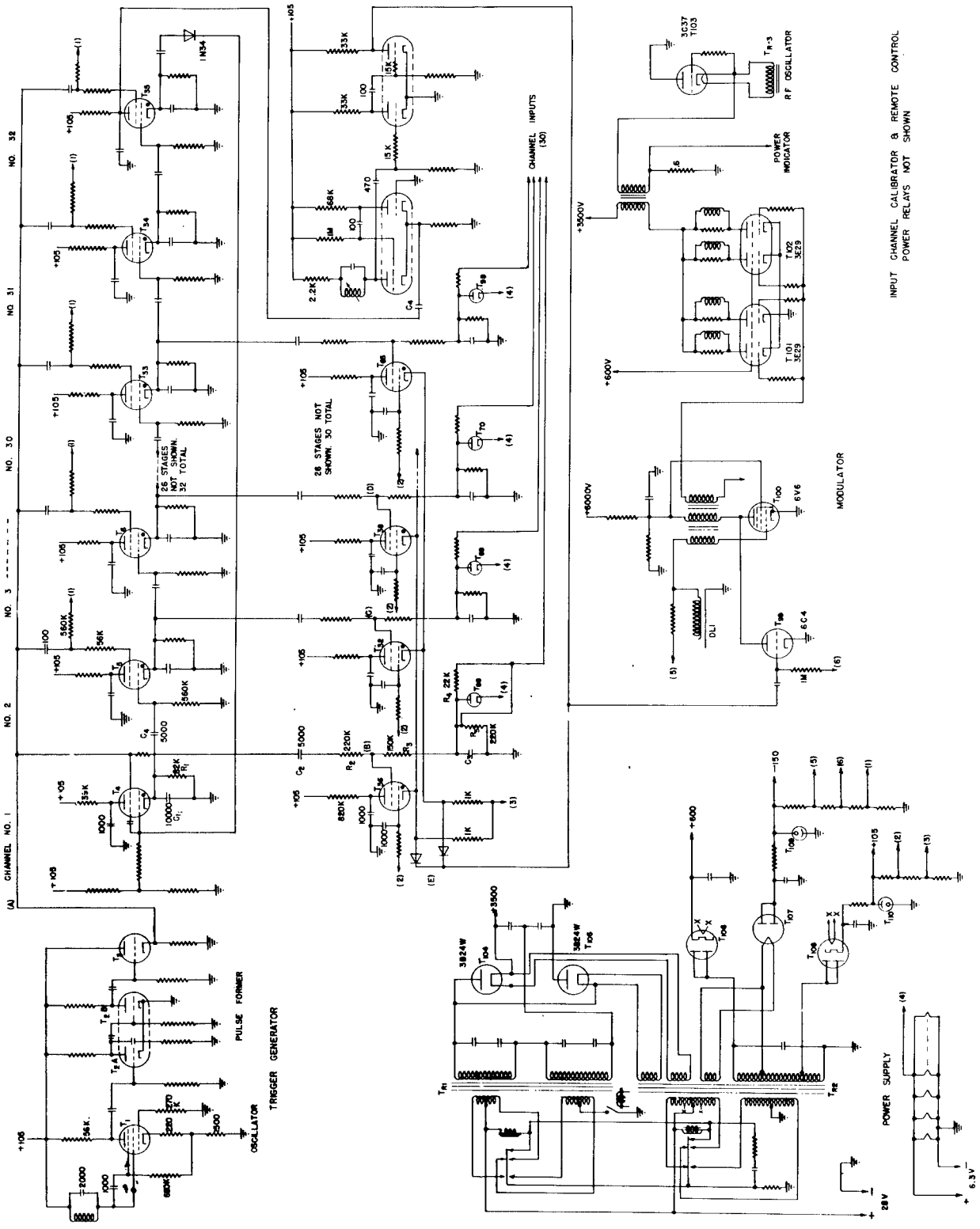

Fig. 128. Schematic diagram of the rocket-borne unit of the pulse matrix telemetering system

tube is then primed, i.e., it will fire upon the arrival of the next triggering pulse from the oscillator. The process then repeats itself, travelling from one tube to the next, until it has run the entire length of the chain. No tube in the chain can fire unless the priming voltage obtained from the previous tube and the triggering pulse from the 10 kc oscillator are simultaneously impressed on its control and screen grids, respectively. The final tube, T-35, furnishes the priming voltage for T-4, the first tube in the chain, enabling it to fire upon the arrival of the next oscillator triggering pulse. The chain is therefore closed. In this manner the chain tubes are flashed in succession by the 10 kc triggering pulses, and a sequence of 100 microsecond saw-tooth voltages are generated.

The saw-tooth voltage developed in the cathode circuit of each chain tube is applied through a coupling circuit, e.g., C-2 and R-2 in the circuit of T-4, to a grid element of one of the pickoff tubes in a second bank of thyratrons. The tubes in this group are labelled T-36 through T-65, respectively, one being used in each channel. The data voltage is applied to the same grid element of the pickoff tube for example, through network R-3, R-4, R-5 and C-3 in the case of tube T-36. Thus, a thyratron in the second bank conducts, for a brief period, whenever the sum of the data and saw-tooth voltages reaches the firing potential. This action causes a narrow pulse to be developed in the cathode circuit. A change in the amplitude of a data voltage causes a proportional change in the amount of time which elapses before the corresponding pulse appears. Data voltage amplitudes are thus represented by time intervals at this point in the telemetering system. The sampling rate for 30 channels, spaced by a 10 kc oscillator, is 312 cycles per second.

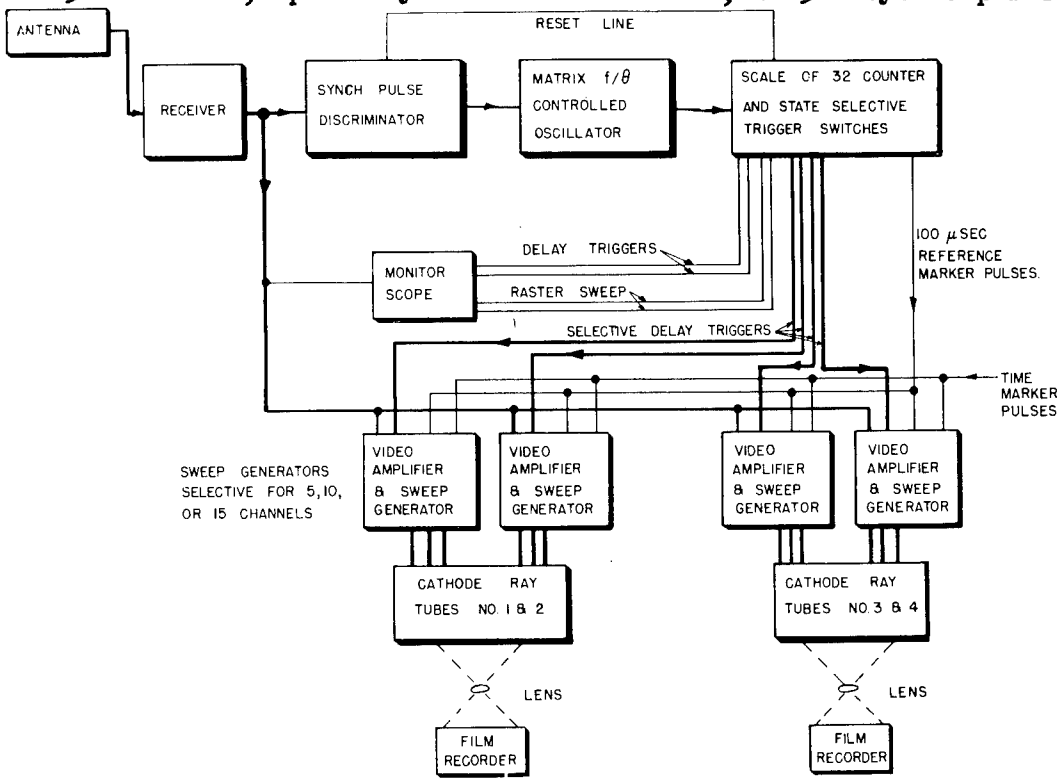

Fig. 129. Block diagram of the ground station of the pulse matrix telemetering system

Diodes T-68 through T-98 are provided in the input circuits of all channels to furnish protection against positive voltages greater than 6 volts. The input terminal board also provides space for similar diodes which may be connected oppositely to provide protection against negative input voltages.

The ground station is synchronized with the rocket transmitter by means of a triple pulse which is generated once during each group sampling period. A one-shot multivibrator, T-66, having an LC circuit in the plate of the normally non-conducting tube serves as the pulse generator. It is triggered from the plate circuit of T-35, the last tube in the primary chain, through coupling condenser C-4. The recovery time of the multivibrator is chosen to allow 2.5 cycles of oscillation to take place in the LC circuit. The output is clipped and differentiated in tube T-67, and the circuits associated with it, to produce three equally spaced, one microsecond, pulses. The interval between the first and last pulses may be varied from 10 to 15 microseconds by adjusting the inductance, L. These synchronizing pulses and the cathode pulses generated in the thirty pickoff tubes are collected at point E of figure 128 and fed to a blocking oscillator, T-99 and T-100. A series of output pulses is obtained whose widths may be varied from 0.8 to 1.2 microseconds by adjusting the delay line, DL-1. The output of the blocking oscillator is fed to two 3E29 modulator tubes (T-101 and T-102) connected in parallel, and finally to the 3C37 r-f oscillator tube, T-103.

Typical waveforms produced in this sequence are illustrated in figure 130. Only the data pulses and the triple, coded synchronization pulse group are transmitted in this system. The reference pulses which mark the 100 microsecond intervals are not transmitted. The leading edge of the last pulse of the group of three bears a fixed time relation (in this case it occurs 85 microseconds earlier) to the time at which the complete thirty-channel group begins. It initiates the synchronizing pulse in the ground station. The synchronizing pulse is used for initiating directly, or through a delay unit, precision x-axis sweep voltages for one or more cathode ray record tubes. The delay unit consists of a scale-of-32 counter driven by a frequency and phase controlled oscillator synchronized with the reference pulse, and a state selector which can be manually set by means of tap switches to give any delay which is an integral multiple of 100 microseconds, the maximum delay being 3,000 microseconds. The video output of the receiver is amplified and impressed on the intensity grids of the same cathode ray record tubes. Thus the original data voltages are represented by spots on the screen of the tube. The x coordinates of these spots are functions of the data voltages. Continuous film cameras, in which the film moves in a direction normal to the sweep, record these oscilloscope presentations as an unbroken line of dots. The resulting records are nearly identical in appearance to those now obtained with the Hathaway recorders. Provision is included for recording on either 35 mm (1.38 in.) or 9.5 in. (24 cm) film.

The data may also be presented on meters and observed visually in a manner similar to that employed in the present system. For this purpose an

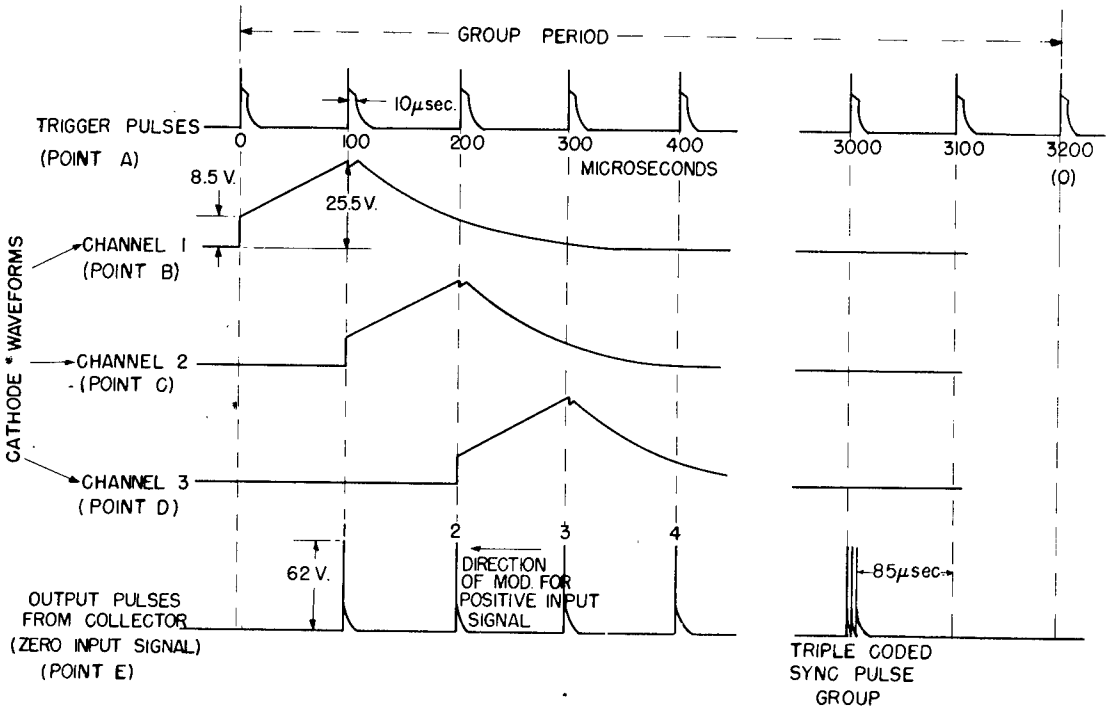

Fig. 130. A sequence of waveforms typical of those produced in the matrix multiplex modulator

automatic frequency and phase controlled oscillator is used to feed a scale of-32 counting circuit which is synchronized with the triple pulse group. Metering circuits of the type now in use[7] are turned on in succession by the state selector tubes, which are controlled from the scale-of-32 counter. They are turned off by the video signal. The information contained in the different channels is thus separated and converted to the form in which it was delivered to the telemetering system.

The new pulse matrix telemetering system has many advantages over the one now in use. These may be summarized as follows:

(a) Simpler and more reliable recording at the ground station. This is had by using cathode-ray tube camera recording directly from the output of the video amplifiers. The new method eliminates the need for the many decoding units which are required in the present system.

(b) Superior weak-signal operation. This is due to the use of synchronization which depends solely upon the reception of a triple coded pulse. A noise pulse will therefore affect only the channel being transmitted at that instant. It will have no effect upon subsequent channels in the group. Signal noise pulses will appear on the photographic record as random spots occurring in addition

---

[7] Cf. Naval Research Laboratory Report No. R-2955, Chapter II, Section C.

to the normal channel information. On the other hand, if a noise burst occurs in the present system, it destroys the channel synchronization from that instant until the group ends, and it deletes all the associated channel information signals in the process. The new system employs a positive synchronizing signal, the triple coded pulse, while the old system synchronized with a gap. The new method is more effective in working through noise.

(c) Lower inherent crosstalk. This is due to the fact that each channel sampling period is initiated at a time which is fixed with respect to the group reference, rather than at a time which depends upon the status of the previous channel.

(d) Greater inherent accuracy (better than 1%). This is due to the use of multiple point calibration voltages, the elimination of multivibrators in the airborne unit, and the matrix type of multiplexing.

(e) Improved stability of operation and simplified transmitter maintenance. These advantages result from the elimination of unstable multivibrator circuits in the multiplex modulator. These circuits frequently made it necessary to hand tailor individual channels. They are replaced by a multiplexing system in which the channels are automatically spaced and distributed by means of a single freely running oscillator.

(f) Higher peak r-f output power. The unit will deliver more than 3 kw.

(g) Simplified installation and greater safety during servicing. These benefits are due to the use of vibrator power supplies for all high voltage requirements in the rocket-borne unit. These supplies require only one low-voltage, primary storage battery.

The first three advantages listed accrue directly from the use of the new pulse matrix design. The last two have no special connection with this design, and would have been incorporated in the original system. The remaining advantages are due, in part, to the pulse matrix system, and, in part, to the general improvement program which is continually in progress.

At the present time, the airborne transmitter unit has been completely designed, and a contract for the construction of seventy of these units has been let with the Hazeltine Electronics Corporation. The ground station for this installation will be made by the Rocket-Sonde Research Section, as was done in the case of the present system. It is anticipated that the pulse matrix telemetering system will be ready for overall testing at the White Sands Proving Grounds by January 1948, and that it will be ready for use by all participants in the V-2 Program by April 1948.

TITLE: Upper Atmosphere Research Report No. IV

AUTHOR(S): Newell, H. E.; Siry, J. W.
ORIGINATING AGENCY: Office of Naval Research, Washington, D. C.
PUBLISHED BY: (Same)

ATI- 24526
REVISION: (None)
ORIG. AGENCY NO.: R-3171
PUBLISHING AGENCY NO.: (Same)

DATE	DOC. CLASS.	COUNTRY	LANGUAGE	PAGES	ILLUSTRATIONS
Oct'47	Unclass.	U.S.	Eng.	180	photos, tables, diagrs, graphs

ABSTRACT:

This document describes the Rocket-Sonde Research Program during the period of the third and fourth cycles of V-2 firings at White Sands. Results in cosmic ray research, high altitude spectroscopy, the investigation of the ionosphere, and atmospheric pressure and temperature studies are given. Photography at very high altitudes is discussed. An analytical basis for determining the altitude of a spinning missile after a fuel cutoff is presented. Finally, there are discussions of continued progress in telemetering, including a description of the new Naval Research Laboratory pulse matrix telemetering sysiem.

DISTRIBUTION: Copies of this report obtainable from Air Documents Division; Attn: MCIDXD

DIVISION: Meteorology (30)
SECTION: Upper Air Research (3)

ATI SHEET NO.: R-30-3-13

SUBJECT HEADINGS: Meteorology, Upper air (62000); Meteorology - Research (61815); Cosmic rays (27800); Ionosphere - Observations (53310)

Air Documents Division, Intelligence Department
Air Materiel Command

AIR TECHNICAL INDEX

Wright-Patterson Air Force Base
Dayton, Ohio

AD-B955 509

Recd 10/27/2000

Naval Research Laboratory
Technical Library
Research Reports Section

DATE: October 20, 2000

FROM: Mary Templeman, Code 5227

TO: **Code 7600 Dr Gursky**

CC: Tina Smallwood, Code 1221.1 to

SUBJ: Review of NRL Reports

Dear Sir/Madam:

1. Please review NRL Reports R-3171 for:

☑ Possible Distribution Statement
☐ Possible Change in Classification

Thank you,

Mary Templeman

Mary Templeman
(202)767-3425
maryt@library.nrl.navy.mil

The subject report can be:

☒ Changed to Distribution A (Unlimited)
☐ Changed to Classification _____
☐ Other:

Signature 23 Oct 00 Date